# NEUTROPHIL CHARACTERIZATION FOR THE DEVELOPMENT OF NOVEL COMBINATION THERAPY IN A MURINE MODEL OF INFLUENZA PNEUMONIA WITH SECONDARY PNEUMOCOCCAL COINFECTION

By

Jennifer Rudd

Bachelor of Science in Biomedical Sciences
Oklahoma State University
Stillwater, OK
2008

Doctor of Veterinary Medicine
Oklahoma State University
Stillwater, OK
2011

Submitted to the Faculty of the
Graduate College of the
Oklahoma State University
in partial fulfillment of
the requirements for
the Degree of
DOCTOR OF PHILOSOPHY
May, 2018

NEUTROPHIL CHARACTERIZATION FOR THE DEVELOPMENT OF NOVEL COMBINATION THERAPY IN A MURINE MODEL OF INFLUENZA PNEUMONIA WITH SECONDARY PNEUMOCOCCAL COINFECTION

Dissertation Approved:

Dr. Narasaraju Teluguakula

Dissertation Adviser

Dr. Keith Bailey

Dr. Shitao Li

Dr. Jennifer Shaw

# ACKNOWLEDGEMENTS

This work would not have been possible without the financial support of the Center for Veterinary Health Sciences at Oklahoma State University, the National Institutes of Health, and generous donors who have supported me through the Robberson Fellowship, Distinguished Graduate Fellowship, and various other scholarships. I am especially grateful to Dr. Raju for his dedication to my success as a student and researcher throughout my time in his lab. In addition, I would like to thank all the support staff and faculty who have contributed to this project: In particular, Marie Montelongo, Jerry Ritchey, Todd Jackson and his amazing team with lab animal resources, and Tim Snider, as well as my committee members who have all shown extra effort to ensure my success.

I am blessed to be surrounded with people who have not only taught me what it is to be a researcher, but also an effective teacher, collaborator, and leader as well. Jill Akkerman, Gina Morris, Kristi Dickey – your encouragement, support and expert advice has shaped me into who I am today and will continue to inspire me in the future.

Most importantly, I am indebted to my family for the commitment they have shown to this degree and my career. I have a village of family and friends without which none of this would be possible. Benton, you are a marvel and the best man. To my sons who are my constant inspiration – Harrison and Calvin, I hope that I can always be a role model for you and I love you both more than words can express.

Name: Jennifer Rudd

Date of Degree: MAY 11, 2018

Title of Study: NEUTROPHIL CHARACTERIZATION FOR THE DEVELOPMENT OF NOVEL COMBINATION THERAPY IN A MURINE MODEL OF INFLUENZA PNEUMONIA WITH SECONDARY PNEUMOCOCCAL COINFECTION

Major Field: VETERINARY BIOMEDICAL SCIENCES

Abstract: Pneumococcal coinfection is a critical complication of influenza pneumonia and has played a vital role in the lethal synergism seen in influenza pandemics throughout the last century. This project focuses on identifying novel combination therapy which targets the excessive innate immune response in addition to the pathogens involved to improve clinical outcome. In order to develop this therapy model, a consistent and appropriate murine model for dual infection is established and the availability of chemokine receptors as potential targets is evaluated. Finally, a CXCR2 antagonist, Sch527123, is tested in combination therapy in this model and shows promise when used in combination and when administered near the start of clinical disease. This research provides the foundation for the exciting potential of innate immune targets to treat pneumococcal coinfection in pandemics.

TABLE OF CONTENTS

Chapter Page

LIST OF TABLES

Table Page

LIST OF FIGURES

Figure Page

Figure Page

# CHAPTER I

# **THE COMPLEXITY OF COINFECTION**:

A Literature Review of the History, Pathogenesis, and Therapeutic Options in Influenza Pneumonia with Secondary Bacterial Infections

## ***1. Pandemic Coinfection: A History of Influenza Pandemics and Secondary Bacterial Pneumonia***

Beginning in 1918, as World War I was coming to a close, an influenza pandemic occurred resulting in an estimated 50 million deaths worldwide [1-4]. The pandemic had killed well over double the number of people who had died due to World War I. Termed the "Spanish Flu", this pandemic resulted in excessive mortality well beyond the expected seasonal influenza and targeted young, otherwise healthy adults with a swiftly deadly disease course [1, 5]. Based on preserved lung tissue sections and analysis of thousands of autopsies, over 95% of these deaths were due to bacterial superinfections, primarily with pneumococcal pneumonia [5, 6]. In addition, over 70% were also bacteremic [6] and widespread pulmonary thrombi were noted on postmortem histopathology and examination [7]. Since 1918, several influenza pandemics have occurred. The "Asian Flu" pandemic (1957-1958) caused by the H2N2 virus affected primarily the young and elderly, resulting in an estimated 1.1 million excess deaths [8]. In 1968, the Hong

Kong Flu hit the world in two waves – the first causing excessive mortality in North America, and the second wave affecting Europe, Asia and Africa much worse than the first, coinciding with a drift in the neuraminidase antigen between 1968 and 1970 [9]. More recently, in 2009, the triple reassortment H1N1 virus, termed the "Swine Flu", had killed roughly 285,400 people worldwide by its completion in 2010 [2, 5]. Throughout all these pandemics, bacterial coinfections continued to play key role in lethality, making it crucial to consider these bacterial co-pathogens when planning for a pandemic [10, 11].

In an extensive review of influenza and bacterial coinfections from the 20$^{th}$ century, several more common pathogens were identified including *Streptococcus pneumoniae (S. pneumoniae)*, *Haemophilus influenzae*, *Staphylococcus spp*. (in particular *S. aureus*), and other *Streptococcus spp.* [12]. Beyond the threat of high rates co-infections in pandemics, bacterial-superinfections also contribute to about 65,000 deaths by seasonal influenza virus infections every year in the United States [2, 12], although the rates of bacterial coinfections were found to be considerably higher during a pandemic than during the seasonal influenza period – of those bacterial coinfections, 41% were identified as *S. pneumoniae*, followed by 25% *Staphylococcus spp.*, 16% other *Streptococcus spp.*, and about 13% *H. influenza*e. [12]. During the 1957 pandemic outbreak *S. aureus* was identified as most predominant bacteria in superinfections [13]. By the following pandemic in the late 1960's, *S. pneumoniae* had again emerged as the predominant bacterial co-pathogen. Although coinfections are more frequently seen in pandemic outbreaks, they are also well documented in seasonal outbreaks. An estimated 28% of all seasonal influenza deaths are co-infected [14], and *S. pneumoniae* continues to be the most common single pathogen identified in 16.6% of co-infected cases [12].

***1.2.*** *The association of S. pneumoniae in secondary bacterial complications following influenza.*

*S. pneumoniae*, also termed pneumococcus, is a gram-positive diplococci that commonly colonize the upper respiratory tract of 20-50% of healthy children and 8-30% of healthy adults [15]. Although generally asymptomatic when colonizing the nasopharynx, pneumococcus is also the most frequently seen bacterial agent in bacterial meningitis, otitis media, sepsis and all community-acquired pneumonia [15] and is correlated with an increase in intensive care unit hospitalizations and death [2]. Pneumococcal disease is difficult to classify because of the diverse nature of its various strains and serotypes which affect disease outcomes, coinfection models and transmission [16]. Pneumococci can express one of over 90 capsule types which greatly alters their pathogenicity, and makes development of effective vaccines and therapies difficult [16-18]. Diagnosis is also quite difficult, as many of the bacterial pathogens seen in coinfection, *S. pneumoniae* in particular, regularly colonizes the nasopharynx [1]. As the predominant co-pathogen in influenza coinfection, this mini review will focus on the proposed contributors to the pathogenesis of the synergistic coinfection of *S. pneumoniae* with influenza, as well as several therapeutic options being considered at this time.

## *2. Virus, bacterial and host factors contribute to the lethal synergism in Streptococcus pneumoniae superinfections.*

***2.1*** *Virus-induced epithelial injury.*

It has been shown that mice exposed to influenza have hyperinflammatory responses with increased bacterial burdens and decreased pulmonary clearance of *S. pneumoniae* following coinfection compared to controls [19]. Although the exact mechanisms behind the

lethal synergism seen with coinfection remain unclear, numerous possible pathways and their associated pathology have been identified to establish the connection. Researchers have discovered that a complex network of viral, bacterial, host and environmental factors all intertwine to create the lethal synergism seen with influenza and secondary bacterial infections. This section will break down and summarize much of that research to more fully elucidate this complex system.

**2.1a.** *Pulmonary Epithelial Barrier Damage*

Influenza infection cause extensive alveolar epithelial damage and surfactant disruption resulting in obstruction of small airways by sloughed cells, mucus and other debris [15, 20]. These pathologic changes help the invading bacteria to adhere and colonize in the respiratory tract. [21, 22] . The damage to the respiratory epithelium also leads to exposure of the underlying basement membrane and progenitor epithelial cells, resulting in an inability of the respiratory epithelium to repair itself and re-proliferate [23]. In addition, viral neuraminidase induces this exposure of bacterial adherence receptors and works in conjunction with bacterial neuraminidase to upregulate the viral infection and worsen this process [24]. As epithelial damage is worsened, a rise in lethality, likely due to bacteremia, is appreciated [23, 25]. Influenza has been shown to cause a long-lasting dysfunction of the alveolar-capillary barrier which can last for weeks after initial infection [26]. Exposure of the basement membrane and fibrin also increase bacterial adherence [4]. Further stimulation of angiopoietin-4 by influenza virus acts to worsen this barrier damage and promotes further inflammation and bacteremia [27]. Pandemic viral infections inflict high cytotoxicity on the alveolar epithelium, which could possibly cause increased bacterial superinfections and associated mortalities [2, 23]. In addition,

influenza infection also causes a decrease in mucociliary clearance and coordination, resulting in failure of removal of bacteria prior to the adherence to the damaged surfaces in the lung [15].

**2.1b.** *Receptor Exposure and Bacterial Adherence*

Sialylated mucins act as decoy receptors for the bacteria [1, 3, 4, 28]. The desialylation by influenza viral neuraminidase helps in bacterial adherence to epithelial cells. Damage of epithelial cells also expose glycans on their surface, thus enhancing pneumococcal adherence [28]. A variety of proteins are altered and displayed on epithelial cells following influenza virus infections, such as platelet activating factor receptor (PAFr), that promote bacterial adherence and disease [1, 29]. Despite this upregulation of PAFr, pneumococcal adhesion resulting in pneumonia and bacteremia is possible without PAFr, further highlighting the complexity of this disease [29]. Pneumococci also have a variety of virulence factors that allow adherence to these newly exposed receptors on damaged epithelium, laminin and fibrin, including pneumococcal surface protein A (PsaP) and pneumococcal serine-rich repeat protein (PsrP) [17]. PsaP is a lipoprotein pneumococcal antigen that aids in adherence to nasopharyngeal epithelial cells via E-cadherin, while PsrP is a lung-specific adherin [30].

**2.2.** *Influenza virus-related factors.*

The influenza virus is from the family *Orthomyxoviridae*, and there are four genera within this family currently recognized that are distinguishable based on their antigenic differences between nucleoproteins and matrix proteins: Influenza A, B, C, and D, the first two of which are most often associated with significant human disease. The influenza virus contains a segmented, single-stranded RNA genome which encodes for eight proteins: polymerase PB2, polymerase PB1, polymerase PA, hemagglutinin (HA), nucleoprotein, neuraminidase (NA), matrix proteins M1 and M2, and nonstructural proteins. Influenza A viruses are further divided

into subtypes based on their HA and NA serotypes. Hemagglutinin is responsible for viral recognition and binding to respiratory epithelial cells and subsequent entry, whereas neuraminidase, via the same sialic acid molecules, acts to aid in viral exit from the cell. As noted previously, both influenza virus and *S. pneumoniae* have neuraminidases which contribute to upregulating inflammation, infection and promoting colonization of bacteria in the lower respiratory tract [24]. Another viral protein, PB1-F2, has also been shown to enhance inflammation during coinfection through proapoptotic effects and mitochondrial dysregulation [31].

**2.3.** *S. pneumoniae* related factors.

*S. pneumoniae* produces several virulent factors that can potentially contribute to the lethal synergism in coinfections. Currently, there are over 90 serotypes of pneumococcal capsule recognized and these serotypes have various levels of pathogenicity. The serotypes with the highest rates of lethality include serotype 3, 6A/B, 9N, and 19F [17]. All these more lethal serotypes, as well as many others, also contain a critical virulence factor, pneumolysin. Pneumolysin can form pores in the membranes of cells to cause lysis and activate the innate response after recognition by toll-like receptors, in particular TLR4, and also trigger inflammation independent of TLR recognition [32-34]. Pneumococcal serine-rich repeat protein (PsrP) is an adhesion and another virulence factor which aids in bacterial binding to the alveolar epithelium and participates in the formation of biofilms and bacterial aggregation [35-37]. Bacterial pili, although not expressed in all strains, allow bacteria to bind to epithelial cells and survive in the lungs while promoting lung injury and inflammation through a TNF-dependent inflammatory response [35]. *S. pneumoniae* is also known to use molecular mimcry to degrade

platelet activating factor and disable neutrophils through a shared phosphorylcholine moiety between PAF and the bacterial cell wall [38].

**2.4.** *Host-related factors: The innate immune response*

Several studies have highlighted exaggerated immune responses in contributing to the synergism during bacterial co-infection. Among innate immune cells, high neutrophil influx has been linked with increased immunopathology in bacterial superinfections following influenza [19, 39]. Excessive, Mac-1 dependent [40], neutrophil accumulation that persists beyond 12 hours post bacterial infection results in a greater bacterial burden and worsened disease [41]. Neutrophils are short lived and terminally differentiated cells, primarily involved in phagocytic clearance of the bacteria. The ingested bacteria are destroyed through the generation of potent oxidants after activation of the NADPH oxidase complex (respiratory burst) or by lytic enzymes and antimicrobial peptides within the phagolysosome. After bacterial coinfection, neutrophil numbers become excessive within hours, but macrophages and dendritic cells do not share the same disproportionate increase [42]. Myeloperoxidase measurements do not increase at the same rate as the neutrophil quantity, suggesting that these rapidly recruited neutrophils will not have the same antibacterial function that the initial responders did [42]. Functional impairment of neutrophils is seen through several capacities.

Phagocytosis has been shown to be decreased in both neutrophils and macrophages following influenza infection [39, 42] and several pathways to this reduction have been evaluated including resistance to phagocytic granule components [43], and the downregulation of the MARCO receptor due to interferon production [4, 44, 45]. While some report that neutrophils and macrophages also have a marked decrease in reactive oxygen species following coinfection [45], others report that coinfection leads to increases in respiratory burst and

hydrogen peroxide production as well as increased neutrophil apoptosis, and decreased neutrophil survival [46]. TRAIL+ monocytes in coinfection are apoptosis inducing cells that cause significant lung damage as well [47]. Apoptosis of various cell types also appears to be affected by bacterial coinfection after influenza. Monocytes express a TNF-related apoptosis-inducing ligand (TRAIL) that can be blocked through CCR2 blockage and result in decreased bacterial load and protection if administered prior to coinfection [47]. *In vitro*, influenza virus has been shown to accelerate neutrophil apoptosis by enhancing Fas expression and activating caspase, decreasing neutrophil survival [46]. The significant neutrophil influx triggered by various viral and bacterial toxins such as PB1-F2 in a coinfection results in a cytokine storm and can lead to a severely damaging hyperinflammatory response which can be seen histopathologically as excessive neutrophilia, sloughing epithelium, hemorrhage, obstructed airways, pleuritic and large areas of lung consolidation [42]. Even the cellular response of natural killer cells to influenza infection is weakened, contributing to further risk of coinfection [48]. Innate cells can kill pathogens through oxidative burst, which creates toxic reactive oxygen species through NADPH oxidase complex or myeloperoxidase. Neutrophil killing of *S. pneumoniae*, however, does not appear to be dependent on NADPH –oxidase generation of reactive oxygen species, but does require neutrophil elastase and cathepsin G [49]. Gram positive bacteria such as *S. pneumoniae* can have a bacterial superoxide dismutase that can protect the pathogen from these toxic reactive oxygen species [43].

Neutrophils can potentially cause worsened inflammatory disease through the release of neutrophil extracellular traps (NETs). Brinkmann et al. was one of the first to describe the release of neutrophil extracellular traps, or NETs, as a form of microbial killing [50]. In response to inflammation, neutrophils are stimulated to release intracellular components through a process called NETosis. Over the last 15 years, NETOsis emerged as a programmed cell death

mechanism separate from apoptosis and necrosis. Morphologically, activated neutrophils involved in phagocytosis were shown to start the NETosis process by losing their nuclear lobulation as well as losing euchromatin and heterochromatin separation [51]. Next, membranes begin separating – first the nuclear membranes will separate and rearrange into vesicles and then the granular membranes also break down, resulting in a mixing of cytoplasmic, nuclear and granular components. Finally, the cell membrane disintegrates and the NETs are released [51, 52]. NETs not only bind gram-negative and gram-positive bacteria, but have been shown to bind fungi and viruses as well [50, 53, 54]. Through release of NETs, neutrophils are able to continue fighting infection even after their own cell death [see Figure 2.1].

We have previously shown that excessive neutrophils and NETs contribute to alveolar-capillary damage after influenza challenge in mice. NETs formation is dependent on redox enzyme activities [55]. NETs were first identified as a process of cell death that released DNA, histones and granular proteins such as elastase and myeloperoxidase to entrap and kill pathogens [50]. Since the initial identification of NETs, they have also been shown to be detrimental to the host – particularly through histones which induce endothelial and epithelial cell damage and worsened disease [56]. Further, using *Pneumococcal* superinfection following influenza, an extensive accumulation of NETs was recognized, especially in the damaged areas of the lungs, indicating their potential role in tissue injury. Moreover, NETs released during pneumococcal superinfection did not show any bactericidal or fungicidal activities. [57, 58]. Our recent studies have shown that NETs generation is dependent on the *Pneumococcal* capsule thickness and varies with the different serotype infections. The increase in thickness of the capsule results in enhanced tissue damage and lung pathology [18]. NETs have been identified in various inflammatory disease models other than pneumococcal pulmonary coinfection such as coinfection of otitis media and sepsis [59, 60]. Although the complete pathway for NETs

induction has yet to be discovered, *S. pneumoniae* has been shown to induce NETs through an enzyme called α-enolasae [61]. Paradoxically, a pneumococcal endonuclease, EndA, has been identified as an important virulence factor through its ability to degrade NETs and diminish their bactericidal response [62]. As with many other areas of the complex pathogenesis of coinfection, it appears that NETs too must be balanced between positive effects and those that are detrimental to the host.

### *2.4a. What is NETosis?*

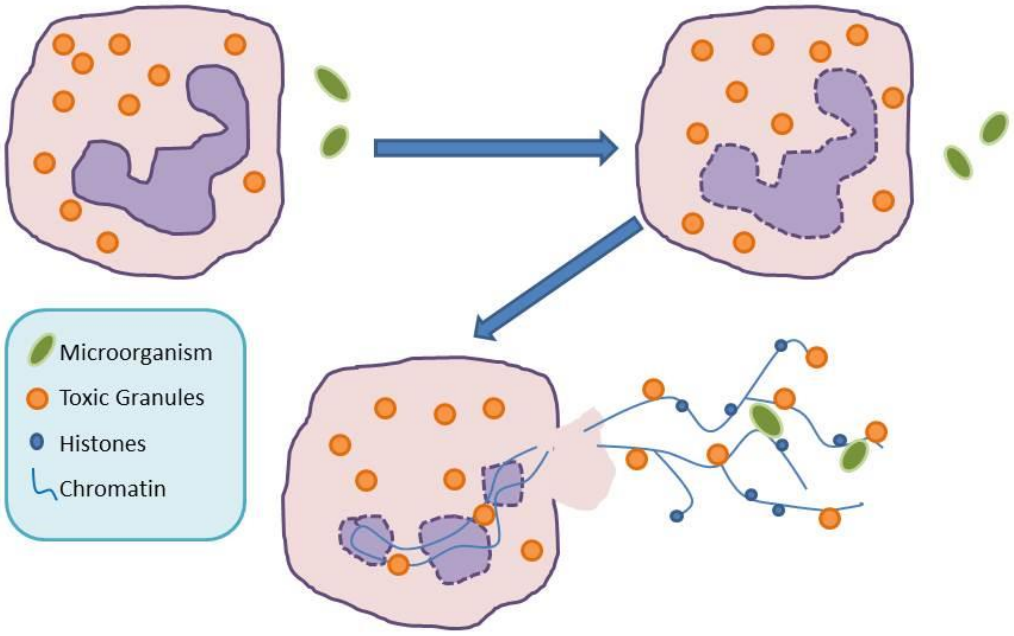


**Figure 2.1** *Neutrophil Extracellular Traps (NETs)*. This diagram summarizes the process of NETosis. Once neutrophils are activated and reactive oxygen species produced, chromatin and cellular membranes begin to break down so that NETs can be released. The release of this primarily nuclear material contains several key, toxic ingredients, including histones, neutrophil elastase, and myeloperoxidase which act to "trap" and kill pathogens in their sticky NETs.

The complete process of neutrophil activation leading to NETs formation and release is still being discovered. NETs release can be triggered by a variety of inflammatory mediators and proteins such as circulating histones, interleukin-8 (IL-8), bacterial enzymes (ie, α-enolase of *Streptococcus pneumoniae*), thick bacterial capsules, antibodies (possibly through the complement cascade), and viral PAMPs [18, 54, 58, 59, 61]. The most widely researched pathway of NETosis is NADPH oxidase 2 (NOX2) dependent where NOX2 generates reactive oxygen species (ROS) which are necessary for disintegration of the nuclear membrane during NETosis [51, 63]. A second mechanism has also been described that is NOX2 independent. This mechanism of NETosis relies on mitochondrial ROS and is triggered through rapid activation using calcium of a potassium channel, the SK3 channel [64, 65]. This novel mechanism was seen in response to *Staphylococcus aureus* infection and results in NETs release and entrapment without neutrophil lysis and death – it is rapid, oxidant independent, and aids in limiting bacterial dissemination [65]. It has also been suggested that NETosis is dependent on platelet-neutrophil interaction. In a model of sepsis, platelet TLR4 had to bind a ligand (such as lipopolysaccharide) to then bind neutrophils and trigger NETs formation in the hepatic sinusoids and pulmonary capillaries, where the small diameter of the vessels allowed the NETs to be more effective at trapping [66, 67]. Platelets are activated by a high bacterial loads with LPS concentrations 100 times greater than that which activates neutrophils – therefore, platelets likely play an even more critical role in high bacterial load situations where NETs are released as a final defense [63]. Once the neutrophils are activated and ROS produced, the chromatin and cellular membranes will break down so that the NETs can be released [52]. Chromatin decondensation requires histone hypercitrillunation of the arginine residues on H3 and H4 by peptidylarginine deiminase 4 (PAD4) [68-70]. PAD4 deficient mice cannot form NETs [71], and PAD4 inhibitors limit NETs formation as well [72]. In addition, it has been shown that both

neutrophil elastase and myeloperoxidase (MPO) regulate this process as well with elastase translocating to the nucleus to degrade histones in a synergistic fashion with MPO [73].

Released NETs contain DNA, nuclear proteins and neutrophil granules associated toxic proteins, which have been identified for their antibacterial and anti-fungal effects. However, NETs-mediated host tissue damage has been linked in several clinical and diseases conditions. Histone proteins are one of the major protein components in NETs. Histones are necessary for DNA condensation and help form the nucleosome structure by binding their positive charges to the negatively charged DNA – this results in the superhelical DNA being wound around four pairs of core histones to mold the structure of the chromatin [74]. Histones can also undergo post-translational modifications, such as methylation, which can regulate gene transcription and aid in the passage of epigenetic information through cell divisions as well [74]. Aside from their intracellular roles, the extracellular advantages and disadvantages of histones are crucial to understanding the effects of NETosis and will be described later. In addition to histones, NETs also release granular proteins such as neutrophil elastase and myeloperoxidase. These enzymes are not only effective microbial killers, but indiscriminately damage the host as well.

**Antimicrobial activities of NETs.**

Before discussing the deleterious effects of NETosis, it is important to recognize its role in microbial trapping and death. Scientists have known about the important role of the neutrophil as a first responder to microbial infection since the late 19$^{th}$ century [75]. Since then, scientists have discovered that circulating neutrophils are called to areas of injury or insult through cytokines and that these neutrophils are activated once they reach the site of infection. The activation results in phagocytosis of the microorganism where reactive oxygen species and antimicrobial peptides and enzymes can kill these infectious agents. This influx of neutrophils

has been shown to reduce progression to severe disease in many cases and is necessary to innate immunity [76]. Antimicrobial killing by neutrophils is not limited to phagocytosis. NETs also contain high numbers of antimicrobial molecules. During sepsis, LPS can bind platelet TLR4 receptors which in turn interact with and activate neutrophils to form NETs. These NETs are effective bacterial trappers within small diameter vessels such as pulmonary capillaries [66]. With seemingly effective bacterial killing performed by NETs, it's not surprising that bacteria have developed methods to evade killing. Many bacteria are trapped by NETs, but not actually killed. This trapping still allows the infection spread to be limited, but *S. pneumoniae* has been shown to evade NETs killing through expression of a DNase called endonuclease (EndA). This enzyme allows the bacteria not degrade the NET and escape [62, 77], and is required for full virulence of *S. pneumoniae* during pneumonia [62].

NETs capture and kill many microbes beyond bacteria. NETs have been shown to capture and kill both yeast and hyphal forms of *Candida albicans* [53]. In addition, viral-induced NETs also are important in the innate immune response to a variety of viruses, such as Influenza A Virus – interestingly, NETs induced by bacterial infection appear to be quite effective at trapping and neutralizing viruses, but those NETs induced by viral infections do not have the same effect on bacteria [54]. Not only do NETs trap virions, but they can directly neutralize them through defensins and MPO as well – virions removed from NETs have decreased ability to infect target cells [54].

The direct antimicrobial effects of histones within and outside of NETs have long been described and span various diverse microbes from bacteria and viruses to fungi and parasites as well. Methods of microbial killing are dependent on the type of histone and the pathogen. There are four core histones (H2A, H2B, H3, H4) and a linker histone (H1) that assist in nucleosome

formation. Although similar in structure, these five histones can further be divided into lysine-rich (H1, H2A, H2B) and arginine-rich (H3, H4) proteins [74, 78]. These different histones display different antimicrobial properties. The effects of arginine-rich histones have been compared with lysine-rich on bacterial outer membrane protease T (OmpT) gene-expressing *Escherichia coli* and found to have different modes of antimicrobial action with the lysine-rich penetrating the cellular membrane and the arginine-rich remaining on the cell surface to cause a blebbing similar to that of other antimicrobial peptides [78, 79]. Histones not only bind to form the core of the nucleosome within the cellular nucleus, but can convey antimicrobial properties outside of the nucleus. Within the cytosol, histones can bind lipid droplets and then disassociate to kill bacteria in a *Drosophila* and possibly a murine model [80]. More importantly, extracellular histones, such as those released with NETs, have antibacterial properties as well.

Besides antibacterial effects, NETs released-histones are also described for their antiviral effects. The arginine-rich histones (H3, H4) released in NETs have particularly potent ability to neutralize H3N2 and seasonal H1N1 influenza viral strains *in vitro*, although did not show any effect on the pandemic H1N1 strain [81]. The method of viral neutralization is still unclear, but the arginine-rich composition of these histones likely contributes to their innate immune effects. In addition to histones, NETs also release antimicrobial peptides and enzymes such as myeloperoxidase and elastase. Myeloperoxidase (MPO) converts hydrogen peroxidase to hypochlorous acid to defend the host against pathogens. Neutrophil elastase is also a proteinase that acts as an effective microbial killer.

**How is NETosis a detriment to the host during infection?**

Although NETosis may have shown positive effects in fighting infection, recent studies have emerged which indicate that these traps may play a larger role in facilitating disease than

fighting it. One of the biggest problems encountered with NETs release is their inability to identify friend versus foe when responding to infection. In models of sepsis, NETs have been shown to be significant players in the pathogenesis and severity of disease. Levels of NETs in the blood of septic patients correlates with organ dysfunction and disease severity, and, in an experimental setting, this damage is attenuated by degrading NETs with rhDNase in combination with antibiotic therapy [60]. In a dual infection murine model of pneumonia, NETs released during the primary influenza infection did not protect against secondary pneumococcal infection, but instead appeared to be associated with a synergistically worsened disease state as compared with influenza and bacterial infections alone [57]. Even within the middle ear, an antibody-induced NETs release was shown to create biofilms of pneumococcal bacteria secondary to influenza infection [59].

NETs are also identified in lung tissue and bronchoalveolar lavage fluid in a murine acute lung injury model and are present in higher numbers at areas of more severe damage [55, 56]. The sheer influx of neutrophils is shown to be associated with subsequent respiratory epithelial damage secondary to viral disease and others [82]. Specifically, NETs release is associated with a dose-dependent cytotoxicity to the alveolar epithelial cells. In addition, neutrophils and their release of NETs through platelet interaction have been shown to induce significant endothelial damage *in vitro* as well as hepatotoxicity [66].

Circulating histones including those associated with NETosis have been implicated in a variety of disease processes [56-58, 67, 74, 81, 83-89]. Not only are they known to damage cellular membranes due to their basic charge when unbound and outside the nucleus, but they also create a form of “sterile” inflammation through TLR2/4 activation of a variety of cell types eliciting a DAMP-like immunostimulatory effect [87]. In a study performed by Abrams et al.

assessing the role of circulating histones due to nonthoracic blunt trauma, high levels of histones were significantly associated with the incidence of subsequent acute lung injury and multiple organ failure [58]. More specifically, this lung injury was found to be mostly related to histone-induced endothelial damage and activation of coagulation. In addition, extracellular histones have been identified as important mediators in sepsis, directly related to significant endothelial damage, organ failure and death [88]. But how do these histones cause this damage? The charge differences between histones and DNA may contribute to more than just nucleosome structure – this charge difference allows extracellular histones bind to phospholipids in the cell membranes, and increase cellular permeability and a calcium influx which in turn triggers apoptosis leading to cell death [58]. Histone release with NETs, as well as myeloperoxidase release with NETs, have both been shown to result in dose-dependent alveolar epithelial cytotoxicity – if histones or myeloperoxidase are blocked, this cytotoxicity is diminished. Interestingly, the same effect is not seen with elastase inhibitors suggesting that this epithelial damage is more associated with histone and MPO release during NETosis [56]. Significant endothelial and epithelial damage is also evident secondary to histone cytotoxicity released during NETosis in severe glomerulonephritis [87]. Extracellular histones have been identified as cytotoxic toward endothelium in numerous studies, resulting in increased vascular permeability, hemorrhage, and thrombosis. The levels of histones also correlate with organ dysfunction and damage in a model of sepsis [88]. Perhaps most importantly for this project, histones have been shown to be crucial mediators of the damage caused in influenza pneumonia [83].

Microvascular and deep vein thrombosis further exacerbate disease associated with NETs release. Microvascular thrombosis has been hypothesized to occur due to platelet activation by extracellular histones. Thrombin formation is dose-dependently enhanced by

histones and dependent on histone-activation of platelets through platelet TLR2 and TLR4 [67]. This in turn can activate platelets resulting in excessive thrombi formation, especially in disease states such as sepsis [63]. It is also suggested that formation of microthrombi secondary to alterations in the microcirculation by NETs, can prevent necessary immune cells from reaching sites of infection [63]. NETs are also a key component of the scaffold of deep vein thrombi and PAD4 deficient mice (which cannot citrullinate histones prior to NETs release) have significantly lower incidences of thrombosis than wild type [70].

**In my particular model, why do I believe NETs to be more detrimental than helpful in ridding of the infection?**

Hirose, et al. looked at critically ill patients and evaluated levels of citrillunated H3 and NETs in their bloodstream to try and garner an idea of the role of NETs in the dissemination of inflammatory disease. During this study, they noted that the presence of bacteria within the tracheal aspirate at the time of intubation was a significant factor associated with the presence of NETs and Cit-H3, and then make a jump to conclude that NETs might play a pivotal role in innate defense [86]. Although the positive values of NETs in innate immunity are well-described, I tend to partially disagree with this assessment. Recent studies evaluating the detrimental effects of NETosis on the host during the innate immune response are becoming more numerous and show a significant link between NET release and tissue damage resulting in worsened disease severity. Although I have outlined many of these studies already, I will highlight a few again that relate closely to my model of dual infection and may help explain why I believe that NETs are an ideal potential target for therapy when planning combination therapies to treat dual infection pneumonia.

The infection model I used involves sublethal influenza infection administered intranasally to mice followed by a low dose of *Streptococcus pneumoniae* administered intranasally three day later. Although neither the influenza nor the bacterial infective doses are considered lethal on their own, this particular model has shown that the dual infection of these two results in a synergistically worsened and lethal disease course with the development of severe ARDS and bacteremia. Histopathology of the pulmonary tissue shows marked endothelial and epithelial damage resulting in vascular permeability that would most certainly aid in the dissemination of bacteria. In addition, markers of NETs (cit-H3/cit-H4) are clearly identified from samples taken from these infected mice. The severity of damage appears in conjunction with the neutrophil influx approximately three days after influenza infection and worsens drastically over the subsequent 72 hours.

In a recent study using an acid aspiration-induced model of ARDS, extracellular histones were shown to have an inflammatory role with significant stimulation of systemic inflammation and pulmonary collateral damage, while blockage of these histones alleviated these signs [89]. Although the model for ARDS we are using is different, our preliminary results support these findings with increased damage and inflammation being related to the presence of NETs and extracellular histones. Our preliminary findings are also consistent with those identified by Moorthy et al. (2013) – in this study NETs were not only shown to result in enhanced lung pathology, but were also shown to have limited to no bactericidal effects [57]. Significant damage to the alveolar-capillary barrier was identified in this model as well. In addition, preliminary studies have confirmed that administration of histones directly to a virally infected mouse worsen disease pathology contradicting claims that histones act as anti-viral defense. I look forward to further discovering the workings of dual infection pathogenesis and will be

interested to further assess the capabilities of blocking NETosis as a therapy when considering combination therapies to treat ARDS.

**2.5.** *Toll-like Receptors and their Contribution to Immunopathology and Interferon Signaling*

Toll-like receptors are an important part of the innate immune response and recognize conserved patterns in a variety of pathogens. Upon recognition, these receptors trigger a series of events resulting in activation of the innate immune response through production of various pro-inflammatory chemokines, cytokines, interferons and recruitment of those innate responders such as the neutrophils and macrophages [90]. In particular, these TLRs can recognize cellular wall components of gram-positive organisms, such as those in *S. pneumoniae* [91] as well as pneumolysin, which stimulates IL-6 and TNF-α after interacting with TLR4 [32]. Influenza virus-induced desensitization of lung epithelial cells to bacterial TLR ligands can last months after the initial viral infection, creating an environment for increased susceptibility to bacterial infection for a long time after clearing influenza [92]. Influenza induces expression of toll-like receptors, such as TLR3 which acts to recognize RNA and DNA of pathogens after phagocytosis, and this not only sensitizes cells to secondary infection with pneumococcal pneumonia, but also decreases bacterial clearance and increases type I interferons, which have been shown to negatively affect survival in a murine model [93, 94]. Upregulation of this TLR3 expression results in increased IL-12p70, which also plays a key role in coinfection [93]. In addition to impairment of phagocytosis, production of interferons after recognition of pathogens by TLRs plays a large role in pathogenesis of coinfection as well. Type I and II interferons are produced following recognition of viral nucleic acids by toll-like receptors (TLRs) [1]. The induction of type I interferon during a primary nonlethal influenza infection was shown to be sufficient to promote lethality with coinfection of *S. pneumoniae* [95]. IFN-1 targets

granulocytes in the bone marrow and prevents efficient recruitment to inflammatory sites [96]. Stimulation of type 1 interferons in coinfection also impairs macrophage recruitment due to decreased levels of CCL2, which promotes bacterial colonization [97]. In addition, mice deficient in type I interferon receptor signaling have improved survival and bacterial clearance [98]. With interferon signaling increase, an impaired production of the neutrophil attractants CXCL1 and CXCL2 was noted following coinfection. This may explain some of the impaired neutrophil response to the early phase of coinfection [98]. Pneumolysin, a cytolytic toxin *of S. pneumoniae,* induces substantial inflammation through activation of TLR4 [32]. TLR2 is also an important mediator of the damage associated with pneumococcal pneumonia [99]. As discussed, the innate immune response is necessary early in the disease course, but can result in worsened pathology if the response remains elevated for too long.

Induction of adaptive immune response is also a critical determinant on the outcome of the diseases in bacterial superinfections. One mechanism by which type I interferon release in response to influenza infection results in worsened bacterial superinfection is through the suppression of γδ T cell production of interleukin-17 (IL-17) [95]. γδ T cells in the lung act as specialized innate responders and normally produce the majority of IL-17 in response to a variety of viral and bacterial infections [95, 100, 101] which can suppress the effects of bacterial superinfection. If type I interferon signaling is upregulated and IL-17 production suppressed through decreased γδ T cell function, bacterial colonization in the lungs is increased causing in deteriorated pathology and disease [95]. Influenza has been shown to induce expression of indolamine 2,3-dioxygenase which alters the inflammatory response and promotes IL-10 susceptibility to *S. pneumoniae* [24, 102]. Pulmonary interferon-γ produced by T-cells can not only suppress phagocytosis, but also concurrently use this mechanism and others to inhibit bacterial clearance [44]. Coinfection has also been shown to result in a significant reduction in

the virus-specific CD8+ T-cell response within the sites of pulmonary inflammation [103]. B cells are also affected and lethal coinfection reduces the B cells' response to influenza [104, 105]. Identifying the pathways most involved in this synergism and filling in the gaps with the pathology of the disease will not only improve our general knowledge in all coinfections, but, more importantly help identify therapeutic targets to improve clinical outcome in those affected.

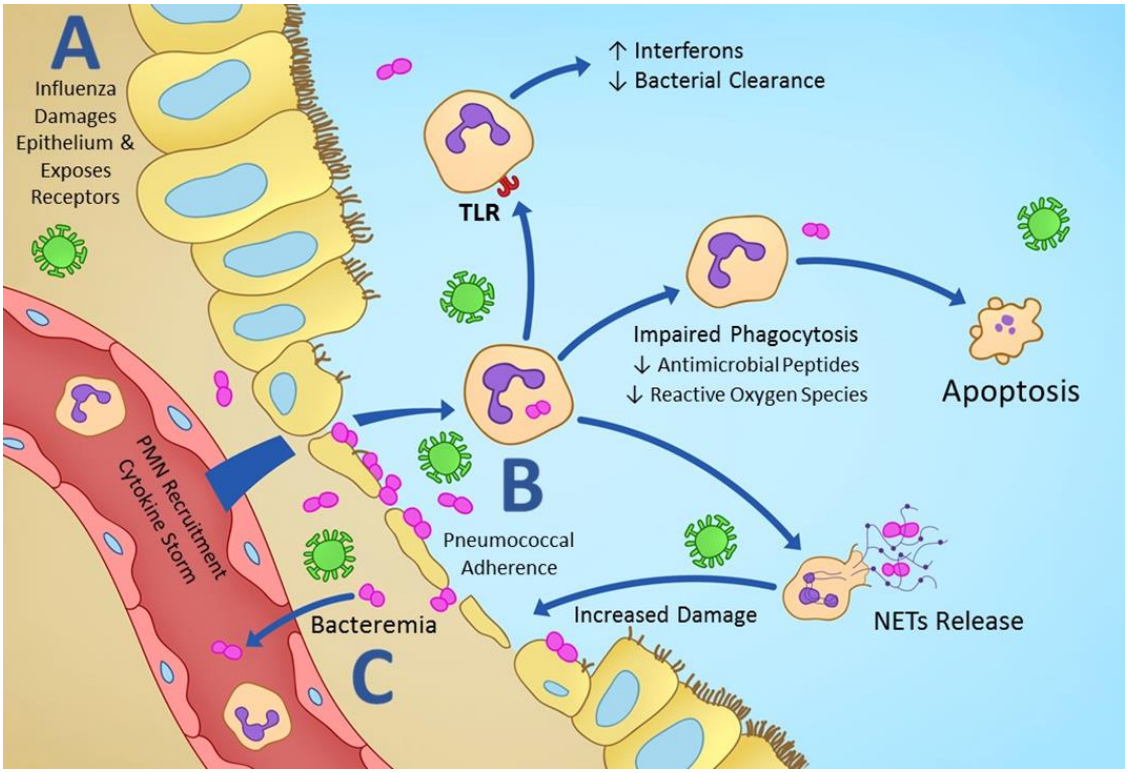


**Figure 2.2** ***Overview of the complexity of coinfection*.** The lethal synergism seen with secondary bacterial infections and influenza pneumonia is created by a network of viral, bacterial, host and environment factors. A few of these factors are summarized in the above figure. (A) The virus damages and exposes attachment sites for bacteria which migrate from the upper to lower respiratory tracts and adhere (B). This adherence and continued host, viral and bacterial factors damage the epithelial and endothelial pulmonary barriers, promoting bacteremia and worsened disease (C). In addition, functional changes and PMN interactions via TLRs with pathogen components alter innate and adaptive immune functions and continue to add to the lethal synergism.

## *3. Current Prospective Therapeutics for bacterial superinfections.*

Antivirals, antibiotics and supportive care have been the mainstay of treatment for influenza coinfections for quite some time. Many of the cases which end up hospitalized will result in ARDS which is often a precursor to sepsis. ARDS and sepsis are severe diseases with high rates of mortality. In addition, well documented resistance to both antiviral medications and antibiotics are being reported, making common options less effective than once believed. Another treatment difficulty is evident with pandemic outbreaks – pandemics primarily cause the most illness and death in developing countries where vaccines and antivirals are both too costly and have poor accessibility for those who most need it [11]. Due to these challenges, it is prudent to consider other treatment options that can both stand alone and act in combination with already available therapies to improve outcome in both seasonal and pandemic influenza outbreaks.

### **3.1.** *Antivirals, Antibiotics and Combination Therapies*

Due to the complex nature of coinfection, a wide variety of therapeutic options and combinations of therapy are being evaluated for efficacy in a dual infection model of influenza A virus with subsequent pneumococcal infection. Combination therapies suggest the best results at this time, with one element of the combination being anti-viral therapy. Anti-virals are a mainstay of treatment and many are looking for alternatives to oseltamivir and inhaled zanamivir due to increasing concern for resistance to this medication [106]. Peramivir is another neuraminidase inhibitor that reduced mortality in coinfected mice better than oseltamivir by inhibiting viral replication resulting in improved bacterial clearance and survival [107]. Although

oseltamivir has shown effectiveness to both viral and bacterial neuraminidase, peramivir only seems to inhibit viral neuraminidase, and must be administered intravenously [107, 108]. Another neuraminidase inhibiting compound, artocarpin, was shown to have a bactericidal effect in vitro, reducing pneumococcal viability by a factor of over 1000, and reduced biofilm formation [108]. Historically, amantadine and rimantadine have been used as antiviral therapy, but these medications are only affective toward influenza A, not B, and have significant (>99%) resistance recorded for several strains of Influenza A, including circulating H3N2 and the 2009 H1N1. For these obvious reasons, these medications are no longer recommended for use as antiviral therapy. There is increasing concern that similar resistance could develop with neuraminidase inhibitors, although levels of resistance this severe have yet to be documented.

A second component to combination therapy of coinfection is antibiotic therapy. Several classes of antibiotics have been evaluated. Although β-lactams were initially considered a mainstay of treatment for pneumococcal pneumonia, it has been shown well over the last decade that standalone therapies are no longer ideal and that combinations with macrolides and fluoroquinolones are more effective, especially in light of emerging antibiotic resistance [109-111]. Macrolides such as azithromycin and clarithromycin are bacteriostatic and work by binding the 50S ribosomal subunit, thereby inhibiting protein synthesis. In addition to their antimicrobial effects, macrolides also have an immunomodulatory effect, which poses an additional benefit in combatting superinfections. Azithromycin in particular has been shown to improve survival in a mouse model of influenza and pneumococcal dual infection with almost double the survival rate than ampicillin (92% versus 56%) as well as improved outcomes over clindamycin [112]. Combination ampicillin and azithromycin for treatment of pneumococcal pneumonia not only decreases lung inflammation, but also decreases pulmonary vascular permeability and increases bacterial clearance, limiting the chances of septicemia [113]. A lower

number of inflammatory cells and proinflammatory cytokines are seen with macrolide treatment than standalone β-lactams as well as less severe lung histopathology – as this antibiotic is bacteriostatic, the reduction in an otherwise exacerbated inflammatory response seen with β-lactam therapy may be due to lessening in bacterial lysis [99, 112]. Another study comparing the effects of moxifloxacin, a bactericidal drug, with azithromycin in a murine model of acute bacterial rhinosinusitis supports this as the azithromycin treatment resulted in rapid bacterial clearance and reduced inflammation compared with the relatively limited effect of moxifloxacin [114]. Further evaluation of the potential negative effects of azithromycin in human disease is still needed, but a 2015 study evaluating cardiotoxicity of azithromycin in community-acquired pneumonia (CAP) showed that the QT prolongation suggested to be an adverse effect of therapy was not associated with treatment, but instead with the disease of pneumonia, regardless of the therapy administered [115].

### **3.2.** *Anti-Inflammatories*

The use of corticosteroids in treatment of bacterial infections is always a hot topic and one heavily debated. On the one hand, some argue that the use of an immune inhibitor in combination with an antibiotic to reduce the bacterial burden can more effectively control the exaggerated inflammatory response seen in coinfection and that the use of steroids should improve survival rates. In a murine model, this seems to hold true – a susceptible murine model for the 2009 H1N1 pandemic showed that dexamethasone significantly improved survival rate and acute lung injury [116]. A reduction in the proinflammatory cytokine storm, and improved clinical outcomes was associated with combination treatment of dexamethasone and azithromycin in mice [42]. However, what is most concerning with corticosteroids was highlighted in a retrospective cohort study from 2011 in which the early use of glucocorticoids

was significantly linked with the development of more severe disease versus patients who did not receive the drug in pandemic H1N1 [117]. The in vivo benefits in human disease, particularly in a pandemic setting, are clearly still up for debate.

Toll-like receptor agonists and antagonists are a relatively new area showing promise as a potential combination therapeutic for pneumococcal coinfection. Special attention has been given to TLR2, which has been shown to mediate the extensive tissue damage, lung necrosis and mortality seen after bactericidal treatment of pneumococcal pneumonia in a murine coinfection model [99]. This mediation was independent of TLR4 or the pneumococcal virulence factor, pneumolysin. TLR2 also plays a role in transmission of disease, likely with a multitude of other factors – when a TLR2 agonist (Pam3Cys) was administered in a murine model of coinfection, contact transmission was diminished as well as inflammation and bacterial shedding [90]. A TLR2 agonist was again seen to reduce the severity of pneumococcal infection post-influenza in a murine model by decreasing bacterial loads and pro-inflammatory cytokines, subsequently leading to decreased vascular permeability and reduced bacteremia [118]. Macrophage-activating lipopeptide 2 (MALP-2) is a TLR2/6 agonist that, when administered prior to pneumococcal coinfection, increases proinflammatory cytokine and chemokine release and enhances neutrophil recruitment without creating excessive inflammation, so also reduces bacterial loads and improves survival [119]. Like TLR2 agonists, TLR5, or flagellin, agonists also act as immunostimulants. Given in combination with an antibiotic, flagellin will decrease bacterial load and boost antibiotic activity by stimulating CXCL1 to recruit neutrophils and reduce bacteremia [120]. TLR3 also participates in the immunostimulatory response when stimulated by pneumococcal RNA. TLR3 acts through TRIF to secrete IL-12. In a coinfection, influenza virus upregulates TLR3 in dendritic cells, which helps prime the cells for recognition of pneumococcal disease [93]. In another study, a TLR4 agonist, UT12, showed promise in

improving clinical outcome and disease in a murine coinfection model after hastening the macrophage recruitment response [121]. Modulating TLRs is an interesting approach to understanding the pathogenesis of coinfection and, with further evaluation, may provide some promising combination therapies to attempt. The timing of therapy and its clinical relevance should still be carefully considered, as this therapy is effective when administered after influenza infection, but prior to secondary infection.

The role of γδ T cells in interferon signaling and IL-17 production is also being explored as a therapeutic for bacterial superinfections. Since superinfected mice inhibit IL-17, resulting in worsened bacterial replication and disease, the administration of recombinant IL-17 in these mice has improved bacterial clearance indicating that induction of IL-17 remains a potential novel therapy [95]. In a recent study, recombinant IL-17F was administered just prior to *S. pneumoniae* infection in a murine model and the therapy resulted in decreased bacterial colonization in the lungs [122]. In general, modulation of IFN-I signaling, IL-17 production and the function of γδ T cells all remain intriguing areas of study for treatment of dual infections.

### **3.3.** *Chemokine receptor antagonists*

A rapidly developing area of therapeutic interest lies in the discovery of targeting chemokine receptors to modulate the hosts' immune response to infection and improve outcome. Chemokine receptor expression on the cell surface of human neutrophils has been shown to be altered by inflammation. Influenza infection triggers a swift and dramatic increase in inflammatory chemokines such as CCL2, CCL3, CCL5, and CXCL10 this are ligands for many of the receptors studied [123]. These phenotypic changes of the cell surface not only offer insight into the development and progression of ARDS from coinfection, but also potential therapeutic targets. Since a hallmark sign of influenza pneumonia coinfection includes uncontrolled

accumulation of neutrophils into the alveolar space, it follows that intervention to slow or block any step in neutrophil recruitment or migration should be explored as a potential therapeutic for this disease. In ARDS, a hallmark of severe influenza coinfection, there is one chemokine in particular that seems to play a pivotal role – IL-8 (CXCL8) which is seen in increased concentrations in pulmonary edema fluid from septic patients with ARDS [124] and is also found in lower concentrations in ARDS survivors as opposed to non-survivors and so can be used as a prognostic indicator [125]. Most chemokine receptors have multiple ligands and CXCR1 and CXCR2 are not exceptions. CXCL8 is one ligand that binds with both CXCR1 and CXCR2 in humans and is considered the most potent neutrophil chemoattractant in BAL fluid from ARDS patients [126].

CXCR1 and CXCR2 are both G protein coupled receptors and are expressed in several granulocytes including eosinophils, mast cells, T cells, and, most notably, neutrophils [127, 128]. In addition to granulocytes, CXCR2 is also found on pulmonary endothelial and bronchial epithelial cells, and the additional role of CXCR2 on these non-hematopoietic cells has been shown to be necessary for the marked increase in lung microvascular permeability seen in an LPS-induced model of ARDS [129]. In addition to IL-8 (CXCL8), CXCR2 has at least six other ligands including CXCL1, CXCL2, CXCL3, and CXCL6 [130]. These chemokines are called ELR+ chemokines (glutamic acid-leucine-arginine containing) and have been shown to mediate aberrant vascular remodeling in addition to inflammatory cell recruitment in both the exudative and fibroproliferative stages of alveoli damage in ARDS [131]. In addition to a role in ARDS, CXCR2 has been a hot topic of study for several years due to promising roles in numerous diseases ranging from cancer to arthritis to other more chronic pulmonary diseases [132-136].

As previously discussed, the challenge and limitations of using an animal model for ARDS include challenges with the chemokines, their receptors and the roles these play in the disease pathogenesis. One such difference is that CXCL8 does not exist in the rodent model, although homologues do exist as CXCL1 (KC) and CXCL2 (MIP-2). It is also unclear whether the mouse analog for CXCR1 is functional in the same way as human CXCR1 as it seems to be activated in different ways and does not seem to play the same central role in the pathogenesis of ARDS that it does in humans [137]. The application of studying CXCR1 in an animal model to evaluate human disease is still in question and needs further investigation.

CXCL8 is not the only chemokine that has been considered potentially important in the development and progression of influenza coinfection. Several chemokine receptors have been shown to be affected by inflammatory disease and further investigation may indicate a role as well. A study looking at chemokine receptor expression in patients with chronic obstructive pulmonary disorder (COPD) and rheumatoid arthritis found several significant alterations in neutrophil phenotype involving CCR1, CCR2, CCR3, CCR5, CXCR3, and CXCR4 in BAL fluid when compared to circulating neutrophils [138]. In addition to evaluating chemokine receptor expression, Hartl et al. also explored whether neutrophils would chemotax to a variety of CC and CXC ligands and found this to be the case [137]. These findings may have been inferred from chronic inflammatory disease, but do support that neutrophils with various receptors can respond to a variety of ligands, likely even in our model.

CCR1 appears to play a role in neutrophil recruitment in a variety of inflammatory models. Mice lacking CCR1 were found to have 35% fewer neutrophils than those with the receptor in a murine model of renal ischemia-perfusion injury, and blocking this receptor with BX471, a CCR1 antagonist, also suppressed neutrophil recruitment to the area of injury [139].

CCR1 antagonism with BX471 has further been shown to protect against subsequent lung injury in models of acute pancreatitis [140] and secondary lung and liver injury in a murine sepsis model [141]. CCR1 in addition to CCR2 and CCR5 antagonists have been evaluated in clinical trials for rheumatoid arthritis, but, unfortunately, have yet to show much success. In these trials, CCR2 and CCR5 are not critical for monocyte recruitment to the site of inflammation, but it has been pointed out that CCR1 blockade still has great potential in this area with continued, targeted research [142]. CCR5 shares about 74% identity with CCR2, and there are antagonists such as TAK-770 which will block both receptors [143]. In addition to CCR1, CCR2, and CCR5, another CC-receptor of interest is CCR3. This receptor has been primarily researched in models of asthma and is best known for its roles in mediating the recruitment of eosinophils. However, blockade of this receptor is still in question since a CCR3 antagonist, GW766944, does not significantly reduce eosinophils in the airways [144].The roles of CCR1, CCR2, and CCR3 have been further studied in a more acute, LPS-induced ALI model. Antagonism of these three receptors was shown to have a protective effect – when a CCR2b and CCR1 antagonist was used, decreases in fibrinolysis, vascular leakage and inflammatory gene expression were all noted. These findings were further supported in CCR1, CCR2, and CCR3 knockout mice which had less pulmonary edema, infiltration and overall disease as compared with controls with ALI [145]. Finally, CCL2 and CCL7 are also chemokines that may play an interesting part– in a study performed by Mercer et al, antibody neutralization of these ligands significantly reduced neutrophil accumulation in the BAL fluid in mice with LPS-induced lung injury [146].

Of the CXC-receptor antagonists, CXCR3 has also been further evaluated with its ligand CXCL10. CXCL10 is considered a non-ELR chemokine. In addition to CXCL10, CXCR3 also binds CXCL9 and CXCL11, but CXCL10 is most induced in infection [147]. These ligands are all induced by interferon-γ and are believed to promote Th1 responses [143]. CXCL10 is a primary

chemoattractant for both T cells and NK cells [148]. CXCR3 activation stimulates interferon responses which have been shown to contribute to severity in a ferret H5N1 model, where CXCL10 gene expression is markedly increased over H3N2 and control models [147]. A CXCR3 antagonist, AMG487, reduced disease severity through reducing viral leads, reducing pulmonary edema, and delaying lethality in this H5N1 model [147] and has also been shown to potently inhibit cellular recruitment [149]. Other CXCR3 antagonists of interest include SCH546738, which shows promise in autoimmune disease and transplant rejection [150], and VUF10085, a more specific CXCR3 antagonist of interest [143]. Ichikawa et al. evaluated both a viral and non-viral ARDS mouse model in mice deficient in CXCL10 and CXCR3 and found that mice lacking CXCL10 and CXCR3 had improved severity of disease and survival in both models [151]. CXCR3 inhibition is even being explored in breast cancer therapy as a metastasis suppressant [152] and has been shown to improve mitochondrial function and reduce apoptosis in liver disease [153]. One major challenge that is being addressed with CXCR3 antagonists is their inability to prove their efficacy by the time they reach Phase II clinical trials. The current approach to this problem is to embrace the complexity of these diseases and test broader spectrum antagonists, such as TAK-779, which target multiple receptors and may have greater efficacy *in vivo* [143]. Therefore, this receptor continues to be another intriguing potential target for therapeutic therapy in models of acute inflammation, such as influenza coinfection.

CXCL12 and its receptor, CXCR4, also appear to play a role in promoting chemotaxis of neutrophils as well as suppressing cell death. In a study looking at lipopolysaccharide (LPS)-induced lung injury, CXCL12 was shown to be a chemoattractant for cells expressing CXCR4 as well as a suppressant of neutrophil cell death and CXCR4 was found to be increased on the neutrophil cell surface after migrating from circulation into the inflamed lungs, possibly via an L-selectin mediated pathway [154]. Neutrophils leave trails rich in CXCL12 as they infiltrate and

migrate to sites of inflammation. These trails aid in migration of other cell types, such as T cells, as well [155]. AMD3100, a CXCR4 antagonist, has been shown to block these trails [155], but in another study, this same antagonist was shown to aid in the redistribution of neutrophils from primary immune organs to other sites without compromising the neutrophil tracking to these inflamed sites [156]. AMD3100 is well established as an FDA approved drug in cancer therapy and helps with mobilization of stem cells and mature leukocytes and has been used in nanotherapy to control lung cancer metastasis [156, 157].

Perhaps the most promising chemokine receptor blocking for the treatment of influenza pneumonia and secondary infections is with CXCR2. Blocking CXCR2 has been shown to inhibit release of neutrophils from the bone marrow as shown in a study evaluating neutrophils lacking CXCR2 which were retained in the bone marrow resulting in neutropenia similar to a human congenital disease called myelokathexis [158]. Of course, blocking CXCR2 to the degree of resultant neutropenia would be catastrophic in any acute inflammatory disease, but blocking 50% of the receptor can still have significant reduction in neutrophil recruitment to the alveoli while still being effective and not resulting in neutropenia [129]. Although CXCR2 antagonists seem to most affect release of neutrophils from the bone marrow, CXCR2 is present in neutrophils in every area – bone marrow, circulation, tethered at the endothelium, and within the tissues – so CXCR2 antagonism is likely to affect neutrophils at all locations [159].

Although there are a few selective CXCR2 antagonists that have been studied, finding an effective agent that blocks both CXCR1 and CXCR2 may be more appropriate since several CXC chemokines act on both receptors and both seem important. Several dual CXCR1/2 antagonists have been evaluated. One such antagonist is SCH527123, which has been shown to have a higher affinity for CXCR2 than CXCR1. In a study evaluating a rodent and nonhuman primate

model of pulmonary inflammation, this antagonist effectively reduced pulmonary neutrophilia and mucus hypersecretion which would be beneficial in combatting bacterial coinfection [160]. SCH527123 has also been shown to be potent *in vitro*, and inhibited human neutrophil chemotaxis as well as myeloperoxidase release in response to both CXCL1 and CXCL8 [161]. In another study performed in healthy humans exposed to an ozone challenge in order to induce neutrophil chemotaxis, SCH527123 effectively lowered neutrophil counts in sputum as well as decreased CXCL8 and myeloperoxidase in sputum as compared with glucocorticoid and placebo treatment [162].

Several other dual CXCR1/2 antagonists have also been evaluated [see Table 1]. Simvastatin initially appeared to be a promising therapeutic option when evaluated in a murine model of bacterial-induced ALI [163], but a more recent large study evaluating the agent in humans with ARDS showed no significant difference in outcome between those patients treated with Simvastatin versus those who received a placebo [164]. DF2156A, another dual antagonist, has been studied in radiation-induced lung disease in the murine model with reduction in lung fibrosis seen [165]. One more dual antagonist that has been studied is Reparixin. Reparixin is a little different in that it prefers CXCR1 antagonism to CXCR2 [166]. In a study evaluating the agent in a murine model of acid-induced ALI, the effect of Reparixin on vascular permeability and neutrophil recruitment into the lung vasculature, interstitium and alveoli was measured and shown to improve gas exchange and reduce neutrophil recruitment [167]. In general, Reparixin has mostly been studied in ischemia/reperfusion injury models and patients and further evaluation in a dual infection model is necessary to assess its efficacy.

| Therapeutic Agent | Action | Study Results in Lung Injury Models |
|---|---|---|
| DF2156A | CXCR1/2 antagonist | • Animal model – reduced pulmonary fibrosis in radiation-induced lung injury<br>• Human in vivo – No studies performed with ARDS |
| Reparixin | CXCR1/2 antagonist with selective preference for CXCR1 | • Animal model – improved gas exchange and decreased neutrophil chemotaxis in acid-induced murine ALI and reduced neutrophil influx in ischemia and reperfusion injuries |
| SB65933 | CXCR2 antagonist | • Human in vitro – Reduced neutrophil chemotaxis in isolated cells from COPD/cystic fibrosis patients<br>• Human in vivo – improved inflammatory biomarkers in cystic fibrosis; decreased neutrophil recruitment in healthy ozone-challenged and LPS-challenged lungs |
| SCH527123 | CXCR1/2 antagonist with selective preference for CXCR2 | • Animal model – Reduced pulmonary neutrophilia and mucus hypersectrion<br>• Human in vitro – inhibit neutrophil chemotaxis and myeloperoxidase release<br>• Human in vivo – decreased neutrophil counts and myeloperoxidase in sputum of ozone-challenged lungs |
| Simvastatin | CXCR1/2 antagonist | • Animal model – improved pulmonary edema and decreased neutrophil numbers in *Streptococcus*-induced murine ALI<br>• Human in vitro – primarily studied as treatment option for ischemia/reperfusion injury, anti-tumoral effects<br>• Human in vivo – No significant improvement in patients with ARDS |

**Table 1:** A summary of CXCR1/2 antagonists that have been tested in lung injury models.

### **3.4.** *Other Potential Therapeutics and Vaccination*

Multiple other therapies are being evaluated as well. Several agents to reduce vascular leakage have also been evaluated with varying effectiveness including Slit2N, vasculotide, atrial natriuretic peptide, S1P, activated protein C, and doxycycline [25, 168]. Mathieu, et al. has started evaluating the use of nanoparticles carrying a plant virus coat protein and ssRNA that trigger a strong innate immune response in the lung during a coinfection [169]. Antibodies to

angiopoitin-4 have been shown to reduce damage secondary to influenza since angiopoietin-4 causes barrier breakdown and furthers inflammation [27]. In a murine model, extracellular adenosine has alters the recruitment and bactericidal function of neutrophils which may improve outcome in coinfection [41].

Vaccinations are also a key area of research, especially when considering the effect these vaccinations may have in pandemic preparedness. Pneumococcal capsular polysaccharide conjugate vaccines have been shown to be very effective (100%) against otherwise lethal pneumococcal disease, but in coinfection, the results are not as promising with less than 40% survival with vaccination in a murine model [170]. The value of the current vaccine is evident already though, with the vaccine being 84-94% efficacious against the serotypes included and reducing the severity of disease and risk for hospitalization in those affected [4]. In the U.S. alone, we have seen a 39% reduction in clinical pneumonia in children since the vaccine has been introduced [171]. Imagine how effective the current vaccine will be once it's more available in developing countries.

Coinfection of *S. pneumoniae* with influenza promises to be a relevant disease for many years to come. Despite the many recent advances in our knowledge base regarding the disease, the complexity of pathogenesis implies that an effective "shotgun" approach to therapy is doubtful and a fine-tuned combination of antimicrobial agents with immunomodulators is likely to be more effective when treating the disease. Because of the expansive diversity in both influenza viral strains and pneumococcal disease and their ever-changing patterns of resistance and survival, therapy effective for one combination may not consistently work for all. This literature review touches on several approaches to consider in therapeutic design, but continued discovery will be needed to better prepare for the next pandemic.

My research project helps to fill some of these gaps. I hypothesize that chemokine receptors can be potential therapeutic target sites for combination therapy of severe dual infection pneumonia. As displayed in Figure 3.1, a variety of key factors contribute to the pathology seen in dual infection pneumonia, such as an exaggerated neutrophil influx, the release of neutrophil extracellular traps, and continued damage to the pulmonary epithelial-endothelial barrier caused primarily by host defenses to the pathogens. These factors contribute to the formation of acute respiratory distress syndrome and bacteremia, resulting in lethality seen in a murine model that mimics that seen in severe pandemics. Chemokine receptor antagonists can be used to control innate responses to infection and reduce damage to the host so that the coinfection may be better resolved or prevented entirely.

To test this hypothesis, we established a murine model of bacterial superinfection following influenza that mimics our proposed idea for pandemic influenza outbreaks and subsequent pneumococcal secondary infections. This model was established and the neutrophils' influx and NETs induction were analyzed. Next, based on the chemokine receptor expressions, we chose to target CXCR2 for therapeutic efficacy in the combination treatment together with antivirals and antibiotics. In addition, we also established a swine model for influenza pneumonia for further testing this combination therapy to explore the pathogenic role of neutrophils in an animal model closer to a human.

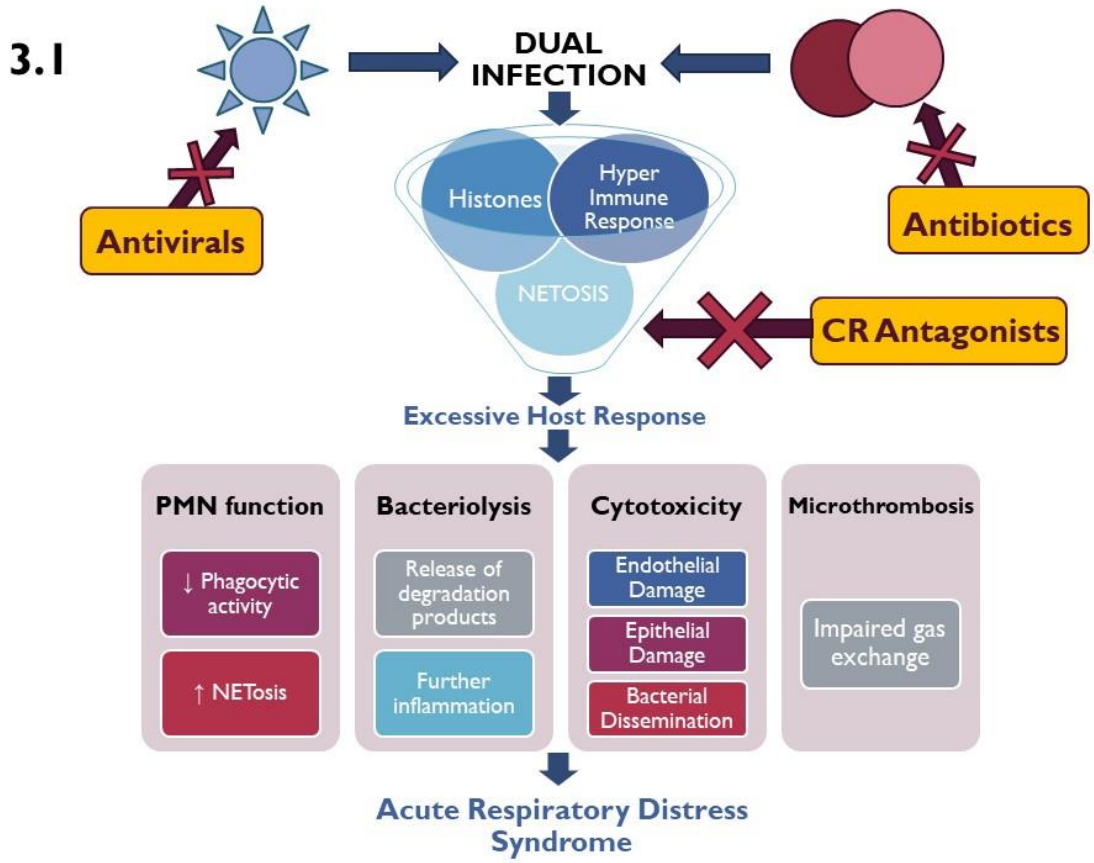


**Figure 3.1** ***Project overview***. Coinfection is a complex synergism resulting in increased morbidity and mortality. The lethal synergism of influenza and Streptococcus pneumoniae copathogens acts in conjunction with an excessive innate immune response to create acute respiratory distress syndrome through impaired neutrophil function, cytotoxicity, microthrombosis and additional damage from dead and dying bacteria. This project focuses on the neutrophil's response to infection and ways to target these responses in order to improve outcome. Our hypothesis is that if we target the innate immune response using chemokine receptor antagonists (CR Antagonists) in addition to targeting the pathogens involved with antiviral and antibiotic therapy, we can improve clinical outcome in a murine model of ARDS caused by influenza pneumonia with subsequent pneumococcal infection.

CHAPTER II

# ESTABLISHING AND CHARACTERIZING A MURINE MODEL FOR INFLUENZA PNEUMONIA WITH SUBSEQUENT PNEUMOCOCCAL PNEUMONIA

**Summary:** A murine model for pandemic H1N1 influenza outbreaks with secondary bacterial coinfection is proposed and characterized. Mice receiving 100 $TCID_{50}$ PR/8 H1N1 influenza A followed by 200 CFU *S. pneumoniae* 72 hours after initial viral infection have lethally synergistic disease with 100% mortality. Those mice receiving 200 CFU *S. pneumoniae* alone had minimal clinical disease. A significant and excessive neutrophil influx is noted on day 5 after viral infection (48 hours post bacterial infection). In addition, severe protein leakage, barrier breakdown, pulmonary pathology and bacteremia is evident at this same time. Neutrophil extracellular traps (NETs) are released in viral-alone and dual infected groups and byproducts of these NETs, histones, contribute to the pathology and barrier breakdown seen in this model. Dual infection animal models are complex and highly variable. We tested a variety of models to achieve a mode that best mimics a pandemic setting with a fairly severe pneumonia infection followed by a sublethal bacterial infection that together is lethally synergistic. The proposed murine model serves as a good base for further studies on the pathogenesis explaining the lethal synergism seen in influenza coinfection as well as for testing potential therapeutics.

**Background:** Influenza virus has long afflicted the human population and shaped the course of history over the last century. Since 1918, four major influenza pandemics have occurred with varying severity, but each pandemic has clearly illustrated the importance of better understanding the viral interactions with host and other organisms to be better prepared for future outbreaks. Arguably the deadliest outcome with influenza pneumonia is secondary bacterial infections. Coinfections are more frequent in pandemic outbreaks than in seasonal influenza and are linked to rates of higher mortality [6, 12]. Postmortem samples from victims of the 1918 H1N1 pandemic clearly show that secondary bacterial infections were present in over 95% of deaths, and it is believed that without these "pneumopathogens" most would have survived [6]. Throughout all pandemics, secondary bacterial infections continued to complicate the disease with *Streptococcus pneumoniae* being the most common pathogen identified [6, 11, 12]. About 41% of coinfections are due to *S. pneumoniae* during influenza pandemics and about 17% in seasonal outbreaks with *Staphylococcus* species as a close second [12].

As the scientific community becomes increasingly aware of the importance of coinfection with influenza pneumonia, we have also become increasingly aware of the complexity of coinfection. No single factor can be claimed solely responsible for the lethal synergism seen with coinfection, but instead a complex network of viral, bacterial, host and environmental factors contribute to the pathogenesis of the disease. Viral and bacterial neuraminidases work together to create more severe disease through exposure of bacterial adherence receptors and upregulation of the initial viral infection [24, 28]. Influenza virus has also been shown to desensitize sentinel lung cells to bacterial TLR ligands and these effects can last months after viral infection making coinfection more likely and severe [92]. Viral PB1-F2 enhances inflammation by promoting proapoptotic effects and disrupting mitochondria in coinfections [31]. Importantly, the influenza virus also induces destructive, long-lasting alveolar-

capillary barrier dysfunction [26, 27] and a loss of the ability to effectively repair this destruction [23].

Bacterial factors, in particular those of *S. pneumoniae*, are key contributors to pathogenicity in coinfection as well. Influenza has been shown to promote the migration of S. pneumoniae from the upper respiratory tract, where it can often live as a commensal bacteria, to the lower respiratory tract where it is considered pathogenic [21, 22]. Once in the lower respiratory tract, factors such as pneumococcal serine-rich repeat protein [35-37] and pili [35] allow the bacteria to better bind to the airway epithelium. As already stated, bacterial neuraminidases can upregulate influenza infections and promote epithelial binding through galectins [24, 28]. Virulence factors, most notably pneumolysin, also contribute significantly [32-34]. The complexity of coinfection is only compounded by the complexity of the bacterial pathogen itself – *S. pneumoniae* has over 90 recognized serotypes of capsule and a high rate of genetic variation [17].

The host's immune response is a significant contributor to pathology and clinical severity seen with influenza coinfections. Various innate responders are involved including monocytes, natural killer cells, dendritic cells, and neutrophils [47, 48, 57, 93]. An excessive neutrophil response beyond 12 hours post *S. pneumoniae* infection results in a greater bacterial burden [19, 39, 41] and significant host damage due to factors such as the release of neutrophil extracellular traps [55, 57]. Alterations in the function of innate responders can also contribute to coinfection lethality. In addition, interferon type 1 [44, 95-98] and interleukins such as IL-6 [32], IL-10 [24, 102], and IL-12 [93] contribute to the complexity of this disease. The adaptive immune response is also affected to promote coinfection – affecting not only virus-specific $CD8^+$ T cells [103], but γδ T cells [95] and B cells as well [104, 105].

What is clear from this brief summary is the need to better understand these pathogen and host interactions so that novel therapeutic options and pandemic planning can occur. As with any therapeutic development, a consistent and controlled animal model for the disease is needed to assess for therapeutic potential prior to future development of these drugs. Variation of dual infection in human disease outside of experimental conditions is so vast, that identifying a model that will work in all cases is near impossible. Many options have been considered in various animal models, including, but not limited to mice, ferrets and pigs. In addition to variety in animal type, the sequence and infectious doses need to be established to fit the needs of the researcher. Our goal is to identify and characterize a dual infection model the emulates a pandemic influenza outbreak resulting in lethal synergism and high rates of mortality. To do this, various models had to be tested and compared to ensure the appropriate choice for future experiments.

**Methods:**

*Pathogens*

Influenza A/Puerto Rico/8/34, H1N1 (PR/8) virus was obtained from the American Type Culture Collection (ATCC, VA). Viral titers were determined by tissue culture infectivity dose ($TCID_{50}$) assay via infection of Madin-Darcy canine kidney (MDCK) cells. *Streptococcus pneumoniae* (serotype 3) was also obtained from the ATCC. Bacterial growth curves were established prior to infection [Figure M.1]. All pathogens were stored at -80°C until use.

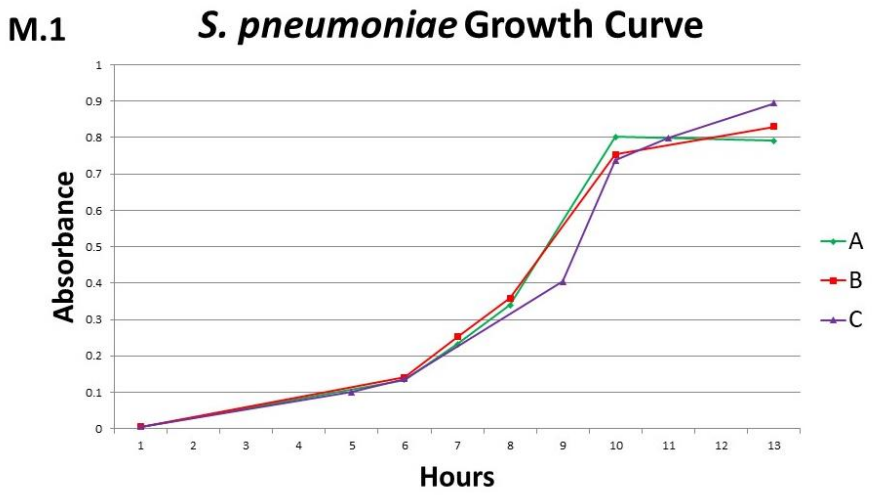


**Figure M.1**: ***Streptococcus pneumoniae growth conditions were optimized***. Absorbance was measured over a 12-hour period. Samples were plated at various dilutions at specific absorbance (0.150, 0.300, and 0.800 Abs). Bacterial growth concluded that 0.300 Abs results in 10^5 CFU/10 µL sample. The growth curve obtained was consistent among three independent experiments (A, B, and C).

*Animals*

Female Balb/c mice ranging from 6 to 10 weeks' old were purchased from Jackson Laboratories. Mice were group-housed in microisolator cages in a BSL-2 facility, and were provided with food and fresh water ad libitum. Mice were clinically scored based on a modified version of the "mouse clinical assessment scoring for sepsis" (M-CASS) [172] [Table M.2]. Infection was performed under a mixture of xylazine (0.1 mg/kg) and ketamine (7.5 mg/kg) anesthetic via intraperitoneal injection. Mice were infected intranasally (IN) with a sublethal dose of 1000-100 $TCID_{50}$ PR/8 (H1N1) influenza in a 50 µl volume or given an equal volume of sterile phosphate-buffered saline in controls. For dual infection studies, mice were administered either $10^4$, $5x10^3$, $10^3$, or 200 colony forming units (CFU) of *S. pneumoniae* IN in 50 µl volumes 72 hours after initial influenza infection, or administered PBS IN for controls. Mice were monitored closely for weight loss and clinical signs based on a modified "mouse clinical assessment score for sepsis" [172,

173]. All animal experiments were approved by the Institutional Animal Care and Use Committee (IACUC) of Oklahoma State University and were performed in strict accordance with their recommendations.

| CLINICAL SCORE | | | | |
|---|---|---|---|---|
| **CLINICAL CRITERIA** | **1** | **2** | **3** | **4** |
| **Fur Aspect** | Actively grooming | Dulling of hair coat | Rough hair coat | Piloerection |
| **Activity** | Normal | Reduced activity disturbed | No activity disturbed, reduced activity stimulated | Nil activity disturbed or stimulated |
| **Posture** | Normal | Slightly hunched, moving freely | Hunched with stiff movement/posture | Hunched with no movement stimulated |
| **Behavior** | Normal | Slow normal when disturbed | Abnormal disturbed, relocates only when stimulated | Abnormal when disturbed or stimulated; no relocation |
| **Chest Movements** | Normal | Mild dyspneic | Moderately dyspneic | Severely dyspneic with thoracic-abdominal respiration |
| **Chest Sounds** | No | Occasionally chirping | Frequently chirping | Wet chirping; increased when stimulated |
| **Eyelids** | Normally opened spontaneously | Normally opened disturbed | Near closed when stimulated and disturbed | Closed disturbed, near closed stimulated |
| **Body Weight Loss** | 0-5% | 5-15% | 15-25% | >25% |
| **Monitoring Frequency** | 12 hourly | 6 hourly during daytime | 4 hourly during daytime | Once any score of four, hourly until endpoint |

**Table M.2:** ***Murine Clinical Assessment of Septic Shock (MCASS) scoring was modified and used for murine studies***. Mice were observed in an unstimulated, stimulated and disturbed state for the following criteria and weighed daily. An overall score from 1 – 4 with 1 being healthy and 4 being most severe was assigned to each mouse. Any mouse receiving a score of 4 in any area was euthanized in these studies.

*Whole blood, bronchoalveolar lavage (BAL) fluid, and tissue collection*

For BAL fluid collection, the lungs were washed by intratracheal administration of 1.0 mL of sterile PBS in two 0.5 mL increments [55]. The recovery of BAL fluid was more than 85% for all animals. The BAL fluids were centrifuged at 200 xg for 10 minutes, and reconstituted in sterile PBS for cell counts and with 2% fetal bovine serum in PBS for flow cytometry analysis. BAL cells were concentrated using the CytoFuge 2 cytocentrifuge (StatSpin, Westwood, MA), and differential cell counts were performed using modified Giemsa staining. Whole blood was collected via terminal procedure of intra-cardiac collection. Blood and BAL cultures were performed at various dilutions after sterile collection. Cultures were performed on blood agar plates (Hardy Diagnostics) and incubated with $CO_2$ at 37° C. Bronchoalveolar lavage fluid and whole blood (intracardiac) were collected from 3 to 5 days' post influenza infection for many studies. Protein leakage was measured by the determination of the total BAL protein content using a DC Protein Assay Kit (Bio-Rad, CA).

*Histopathology*

Lungs from mice who did not have BAL collection were fixed with 4% formalin and collected for histopathology analysis after hematoxylin and eosin (H&E) staining. Mice were scored on a 1-4 scale (4 being most severe) for severity in the following areas by a blinded, board-certified anatomic veterinary pathologist: necrotizing bronchiolitis, bronchiolar infiltrates, alveolitis, interstitial inflammation, hemorrhage, edema, and microvascular thrombosis. Necrotizing

bronchiolitis was defined as damage to the airway epithelial cells, presence of necrotic bodies or the total denudation of the airway lining. Total histopathologic scores were evaluated as a sum of all individual scores.

*Western Blot Analysis of Pulmonary Damage and Extracellular Histones*

BAL fluids were analyzed for the release of epithelial damage marker, T1-α, and the endothelial damage marker, Claudin-5. In addition, samples were also tested for extracellular histone release, which are indicative of NETs formation, as described previously [55]. Antibodies against histone protein H2A and citrullinated H4 (Millipore, MA) were used. Due to the absence of effective loading controls for BAL, normalization of protein content was accomplished through BAL collection methodology. BAL was collected with 1.0 mL sterile PBS with consistent recovery of 80-85%. Densitometry analysis was performed on all Western blots using ImageJ software version 1.51 (NIH).

*Transwell System Histone Experiments*

Transwell systems were established using 24 well plates and 6.5mm diameter, 3µm pore sized inserts (Corning). Initially, conditions were tested and optimized using epithelial (A549) and human umbilical vein hybrid endothelial cells (Eahy926) cell lines in both monolayer and coculture techniques. Cells were initially cultured in T25 flasks with DMEM media including fetal bovine serum and penicillin/streptomycin. Cells were passaged once prior to culture on transwell membrane. In cocultures, Eahy926 cells were 2.0 x $10^5$ cells were seeded on the basolateral side of the membrane and allowed to adhere and grow before reverting the inserts and seeing 2.0 x $10^5$ A549 cells on the apical side. In monolayer cultures, only the apical side was

used. Epithelial resistance kinetics were established using an EVOM2 epithelial volt/ohm meter (World Precision Instruments).

Initial histone experiments used coculture and added 10µg/mL histones to the apical chamber for 1 hours at 37°C before removing and adding $10^6$ *S. pneumoniae*. Bacteria was then incubated with the cell culture for 6 hours and samples taken from the basolateral chamber for cultures at 30 minutes post inoculation, 2 hours, 4 hours, and 6 hours. Cultures were performed in multiple dilutions on blood agar plates. In addition, cells were stained with trypan blue at 6 hours to assess for viability. All samples were performed in duplicate. For subsequent experiments, A549 cells were cultured in monolayer. And various concentrations of histones (0, 10, 20, and 30 µg/mL) were incubated for 2 hours at 37°C before removal and addition of $10^6$ *S. pneumoniae* to the apical chamber. Samples from the basolateral chamber were removed every 2 hours for 12 hours starting at time 0 and cultured on blood agar plates. All samples were performed in duplicate and repeated for n=4.

*In vivo Histone Experiments*

Balb/c female mice were inoculated with either histones or PBS on day 0 ± $10^3$ *S. pneumoniae* or PBS 24 hours after histone inoculation. The following conditions were established: 100µg histones + bacteria; 50µg histones + bacteria; 100µg histones (-) bacteria, (-) histones + bacteria, (-) histones (-) bacteria. Each group contained 6 mice. An additional group with 3 mice was inoculated with 300µg histones (-) bacteria. BAL, blood and tissue samples were collected 48 hours after histone inoculation for cultures, cell counts, and histopathology. Mice were monitored closely and scored based on MCASS for the entire 48 hours.

*Statistical Analysis*

The data are expressed as the means ± SEM. Statistical analyses were performed using Student's unpaired t-test, paired t-test or analysis of variance (ANOVA) using GraphPad Prism 7 software. $p < 0.05$ was considered statistically significant.

**Results:**

***1. Influenza and pneumococcal coinfection results in significant weight loss, inflammation, bacteremia, and enhanced pulmonary pathology.*** The first murine model assessed was $10^3$ $TCID_{50}$ PR/8 H1N1 Influenza followed by $10^4$ CFU *S. pneumoniae* 72 hours after initial viral infection. Both influenza-only and dual-infected groups are severely affected in this model and these groups lost significantly more weight than bacterial-only infected and healthy controls starting after day 2 [Figure 1.1]. Bacterial-only infected mice lost over 2% body weight by day 5.

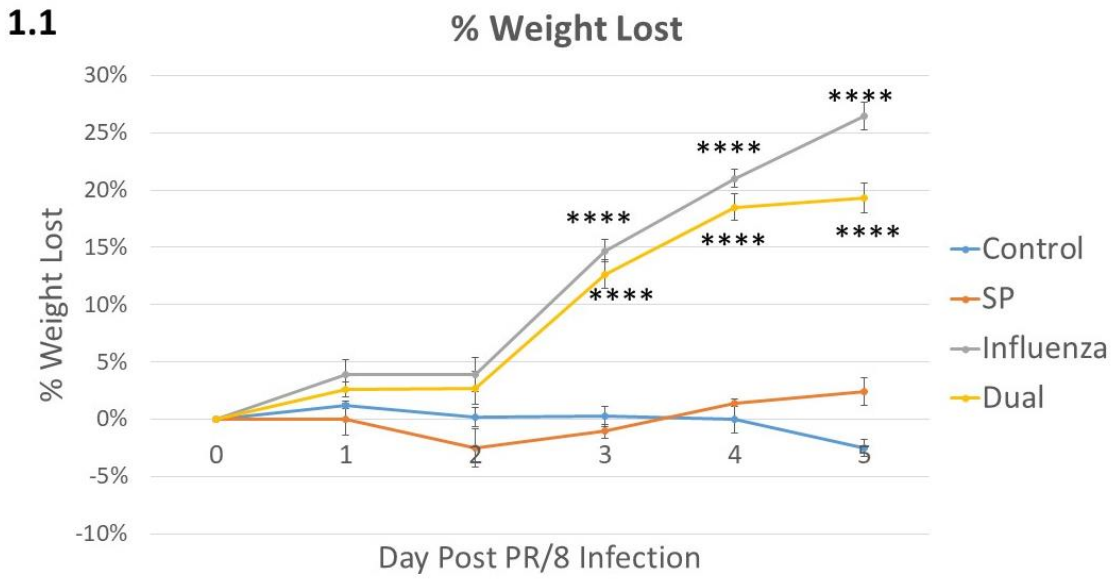


**Figure 1.1:** ***Mice with viral-alone and dual infection lose significant weight.*** Model tested: 1000 $TCID_{50}$ PR/8 H1N1 influenza ± $10^4$ CFU *S. pneumoniae* (Serotype 3). [**Control**: Mice receive only PBS; **Influenza**: mice receive 1000 $TCID_{50}$ PR/8 influenza; **SP**: mice receive 200 CFU *S. pneumoniae* on day 3; **Dual**: Dual infection model]. Bacterial infection was administered 72 hours after initial viral infection. Influenza-only and dual infected groups lost significantly more

weight than bacterial-only or healthy controls beginning at day 2. Bacterial-only lost an average of 2.3% body weight by day 5 (day 2 post infection), whereas healthy controls steadily gained weight. n=5 mice per group. Statistical comparison performed by one-way ANOVA. ****$p$<0.0001 (versus control).

In addition to weight loss, influenza-only and dual infected groups saw sharp clinical decline beginning at day 2. Although weight loss matched between these groups, the dual infected group had a more severe clinical decline and progressed to endpoint on day 5. This clinical decline seen in the dual-infected group may be explained by cultures performed on the BAL and blood on day 5 [Figure 1.2].

**1.2.**

**A.**

| GROUP | MOUSE | BLOOD CULTURE | BALF CULTURE |
|---|---|---|---|
| Control | 1 | No Growth | No Growth |
| | 2 | No Growth | No Growth |
| Influenza | 1 | No Growth | No Growth |
| | 2 | No Growth | No Growth |
| SP Only | 1 | No Growth | +++ |
| | 2 | No Growth | +++ |
| Dual | 1 | +++ | ++++ |
| | 2 | ++++ | ++++ |

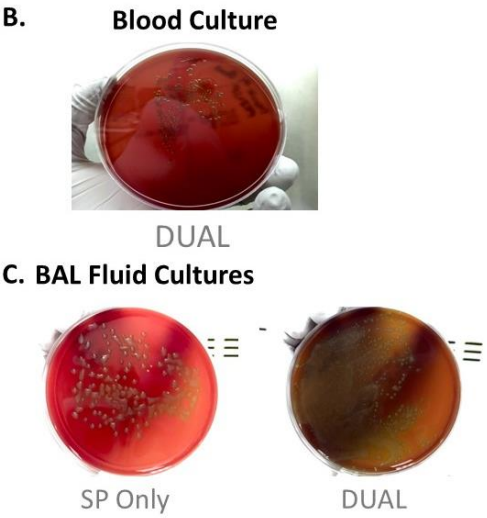


**Figure 1.2:** ***Dual infection results in bacteremia by day 5*****.** Balb/c mice were infected with 1000 $TCID_{50}$ PR/8 H1N1 influenza ± $10^4$ CFU *S. pneumoniae* 72 hours after viral infection. Cultures were performed from 10 µL BAL and blood from each sample. No growth was noted in control or influenza-only groups and no contamination seen. Dual infected mice grew *S. pneumoniae* from both blood and BAL samples, whereas bacterial-only infected mice only grew *S. pneumoniae* from BAL. Symbols for Table A (CFU per 10µL sample): 0<**+**<10. 10<**++**<100. 100<**+++**<1000. 1000<**++++.** n=2 shown in table.

Dual-infected mice had marked bacteremia evident on day 5. In contrast, no bacteremia was seen in bacterial-only infected groups. Bacterial cultures from BAL were also denser than

bacterial-only, indicating that viral infection enhances bacterial growth both within the lung and the bloodstream, likely through barrier breakdown. Protein leakage within the BAL supernatant was measured [Figure 1.3 A]. The more severely affected groups, viral-alone and dual, have significantly higher amounts of protein leakage as compared to bacterial-alone and healthy controls, indicating increased inflammation in these groups. BAL cell counts were also higher in these groups due to a large inflammatory cell influx. Dual-infected mice had significantly more inflammatory cells in their BAL than viral-alone [Figure 1.3 B].

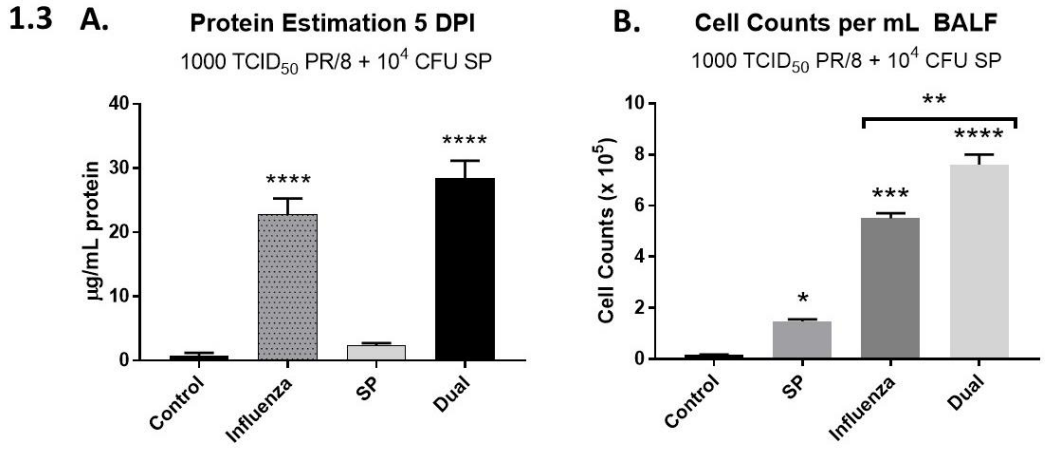


**Figure 1.3:** ***Viral-alone and dual infection results in marked vascular leakage and cellular infiltrations*****.** Balb/c mice were infected with 1000 $TCID_{50}$ PR/8 H1N1 influenza ± $10^4$ CFU *S. pneumoniae* 72 hours after initial infection. BAL was collected on day 5 and the supernatant used for protein estimation using a DC Protein Assay Kit. **A:** Infected mice in both the influenza-only and dual infection groups had significantly more protein than compared to healthy controls and bacterial only (SP) groups. There was no significant difference between influenza-only and dual-infected mice. **B:** Infected mice have significantly higher cell count numbers from BAL fluid collection. Dual infected mice are also significantly higher than influenza-only. Data are expressed as means ± SEM. n=4. Statistical comparisons performed via one-way ANOVA. **p*<0.05; ***p*<0.01; ****p*<0.001; *****p*<0.0001 (relative to bacterial-alone (SP) unless otherwise indicated).

Lung tissue was collected and formalin-fixed on day 5. Tissue sections were stained in hematoxylin and eosin for pathologic scoring, as performed by a blinded anatomic veterinary

pathologist. Mice were scored from 0 (healthy) to 4 (most severe) in 7 areas: necrotizing bronchiolitis, bronchiolar infiltrates, alveolitis, interstitial inflammation, hemorrhage, edema, and microvascular thrombosis. The sum of these scores for each mouse was calculated and used for overall comparisons between groups [Figure 1.4]. Mice receiving bacteria-alone had rare focal lesions with the majority of tissue mimicking that of healthy controls. Viral-alone infected mice were more severely affected with larger areas of pathology and more widespread disease. The most severely affected group was the dual-infected group with widespread pathology and large areas with complete loss of pulmonary architecture.

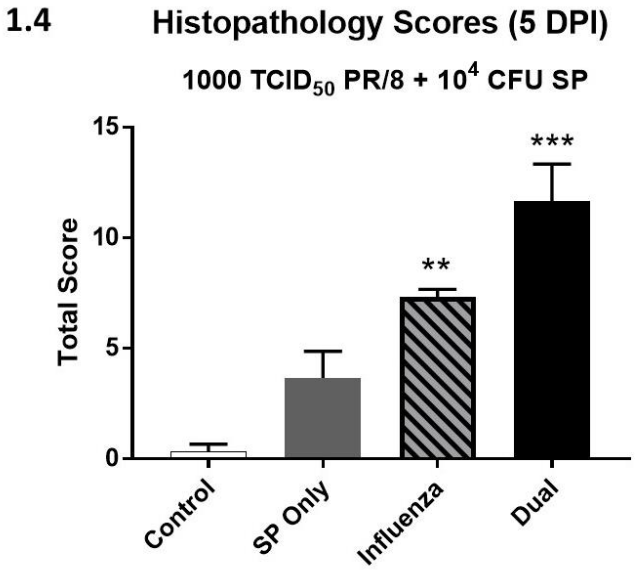


**Figure 1.4:** ***Pulmonary pathology is severely enhanced in dual infection on day 5***. Mice were scored from 0-4 in 7 areas: necrotizing bronchiolitis, bronchiolar infiltrates, alveolitis, interstitial inflammation, hemorrhage, edema, and microvascular thrombosis. After scoring, the sum of the scores for each mouse was calculated and used for overall comparisons. Severe pulmonary pathology was noted in influenza-only and dual infected groups as compared with healthy controls. Mice infected with only *S. pneumoniae* had few focal areas of moderate pathology, but were overall unaffected. Although no statistical difference was seen between influenza-only and dual infected mice, a trend toward enhanced pathology in dual infection was evident ($p$=0.0764). Data are expressed as means ± SEM. n=5 mice per group. Statistical comparisons made via one-way ANOVA. **$p$<0.01; ***$p$<0.001 (relative to controls).

***2. Lower infective doses of pathogens maintain clinical model.*** Three additional models were next assessed with lower infective doses of both virus and bacteria. First, the dose of influenza virus was reduced 10-fold to 100 $TCID_{50}$ while maintaining $10^4$ CFU *S. pneumoniae* (serotype 3) on day 3. Bacterial-alone infected mice lost an average of 7% body weight by day 5, while the more severely infected viral-alone and dual groups lost significantly more weight [Figure 2.1].

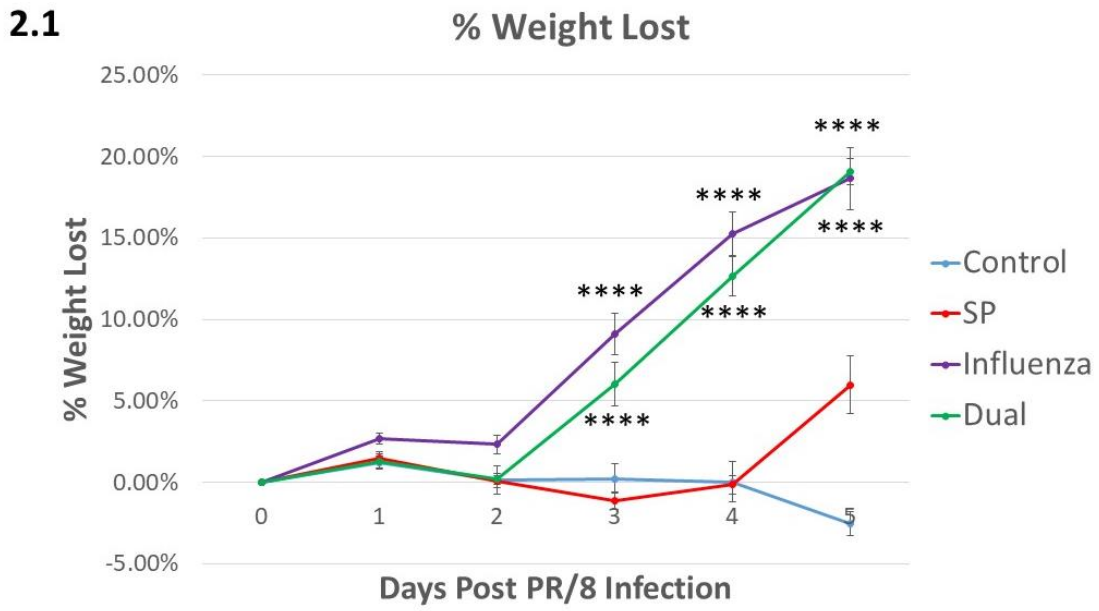


**Figure 2.1:** ***Viral-alone and dual infected mice continue to lose significant weight at decreased viral dosage.*** 100 $TCID_{50}$ PR/8 H1N1 influenza ± $10^4$ CFU *S. pneumoniae* (Serotype 3). Bacterial infection was administered 72 hours after initial viral infection. [**Control**: PBS only; **SP**: *S. pneumoniae* on day 3; **Influenza:** PR/8 influenza-only; **Dual**: dual infection]. Influenza-only and dual infected groups lost significantly more weight than bacterial only or healthy controls most apparent after day 3. Bacterial-only lost an average of 7% body weight by day 5 (day 2 post infection), whereas healthy controls steadily gained weight. n=5 mice per group. Weights compared via one-way ANOVA. ****$p$<0.0001 (relative to controls).

Bacterial cultures performed from BAL and blood samples on days 4-6 post viral infection mimicked that seen in the previous model. No growth was seen in viral-alone infected mice. Dual infected mice had significant growth of S. pneumoniae on all days in BAL with heavy bacterial burdens noted. In addition, bacteremia was evident in all dual samples on days 5 and

6, but not on day 4, indicating that barrier breakdown is occurring around this time. Interestingly, a single mouse had bacteremia on day 6 from the *S. pneumoniae*-alone infected group [Table 2.2].

**2.2**

| | BLOOD | | | BAL Fluid | | |
|---|---|---|---|---|---|---|
| **GROUPS** | **4 DPI** | **5 DPI** | **6 DPI** | **4 DPI** | **5 DPI** | **6 DPI** |
| **Influenza** | None | None | None | None | None | None |
| **SP** | None | None | + | ++++ | ++++ | ++++ |
| **Dual** | None | ++++ | ++++ | ++++ | ++++ | ++++ |

**Table 2.2:** ***Primary influenza infection enhances bacterial dissemination.*** Balb/c mice were infected with 100 $TCID_{50}$ PR/8 H1N1 influenza ± $10^4$ CFU *S. pneumoniae* 72 hours after viral infection. Cultures were performed from 10 µL BAL and blood from each sample. No growth was noted in influenza-only groups and no contamination seen. Dual infected mice grew *S. pneumoniae* from both blood and BAL samples, whereas bacterial-only infected mice grew *S. pneumoniae* from BAL and one sample grew *S. pneumoniae* 6 DPI from the blood. Symbols for Table A (CFU per 10µL sample): 0<**+**<100. 100<**++**<1000. 1000<**+++**<10,000. 10,000<**++++.** n=2 shown in table. Table shows average growth.

BAL was collected 4-6 days after viral infection (24-72 hours after bacterial infection) and used for cell counts and protein leakage estimation, both of which are indicative of inflammation. Viral-alone and dual infected groups had significantly more protein leakage as compared to healthy controls on days 5 and 6 [Figure 2.3 A]. On day 6, there is also a significant increase in protein leakage in the dual-infected group over viral-alone, indicated more severe damage to the lungs. Cell counts were also increased in dual infected mice on all three days [Figure 2.3 B].

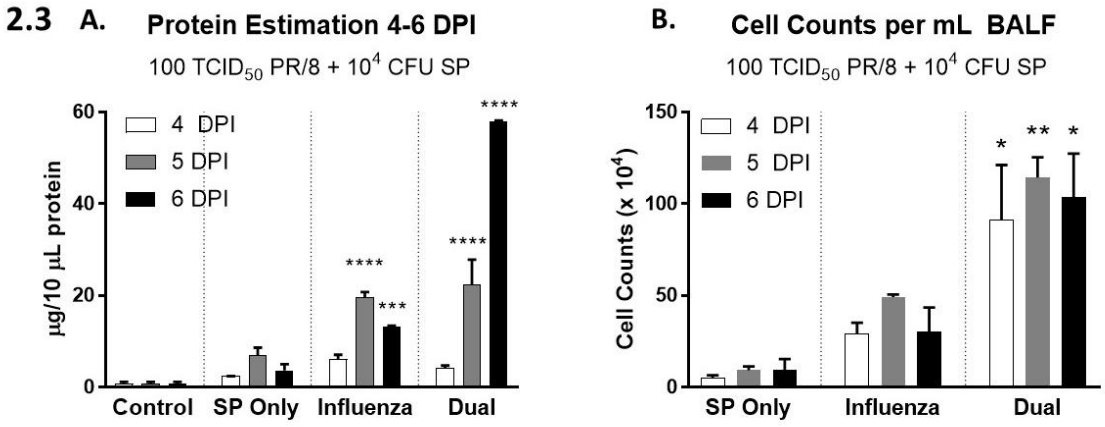


**Figure 2.3:** ***Infected mice exhibit significantly more inflammation***. In this model, balb/c mice were infected with 100 $TCID_{50}$ PR/8 H1N1 influenza ± $10^4$ CFU *S. pneumoniae* 72 hours after initial infection. BAL was collected on days 4-6 and the supernatant used for protein leakage estimation (DC Colorimetric Protein Assay Kit (Bio-Rad). **A:** Infected mice in both the influenza-only and dual infection groups had significantly more protein than compared to healthy controls and bacterial only groups on days 5 and 6 post influenza infection. In addition, there was a significant difference between influenza-only and dual-infected mice on day 6. **B:** Dual-infected mice have significantly higher cell count numbers from BAL fluid collection as compared with bacterial only groups. Dual infected mice are also significantly higher than influenza-only on day 6 ($p$<0.05). Data are expressed as means ± SEM. Statistical comparisons made via one-way ANOVA. n=4. ***$p$<0.001; ****$p$<0.0001 (relative to healthy controls in Fig. 2.3a; relative to SP in Fig. 2.3b).

Since this model resulted in a chance of bacteremia in bacterial-alone infected mice, the next two assessed models reduced the bacterial dose as well: 100 $TCID_{50}$ PR/8 H1N1 influenza followed by either $10^3$ or $5x10^3$ CFU *S. pneumoniae* 72 hours after viral infection. This model maintained the weight loss previously noted in influenza-alone and dual infected groups, but the bacterial-alone infected mice, which were administered $10^3$ CFU *S. pneumoniae*, gained weight over 5 days instead of losing weight [Figure 2.4].

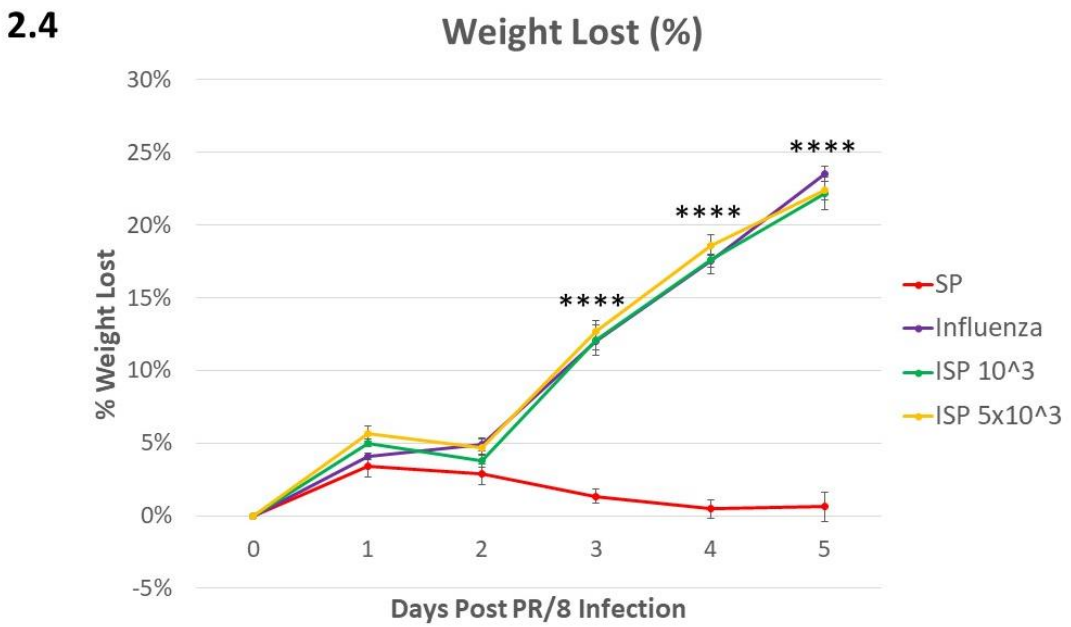


**Figure 2.4:** ***Influenza and Dual-Infected mice lose significant weight starting on day 3.*** Model: 100 $TCID_{50}$ PR/8 H1N1 influenza ± $10^3$ or $5x10^3$ CFU *S. pneumoniae* (Serotype 3). Bacterial infection was administered 72 hours after initial viral infection. Influenza-only and dual infected groups lost significantly more weight than bacterial beginning at day 2. Bacterial-only at this lower infective dose gained weight by day 5 (day 2 post infection). n=5 mice per group. Statistical comparisons made via one-way ANOVA. ****$p$<0.0001 relative to SP.

At this lower bacterial dosage, no mice from the bacterial-alone infected groups developed bacteremia and had a reduced bacterial burden within the lungs as well, based on BAL cultures [Figure 2.5]. Dual-infected mice mimicked that of previous groups with bacteremia developing on day 5 and significantly increased bacterial growth in BAL for both dual models.

**2.5**

| | BLOOD | | | BAL Fluid | | |
|---|---|---|---|---|---|---|
| **GROUPS** | **4 DPI** | **5 DPI** | **6 DPI** | **4 DPI** | **5 DPI** | **6 DPI** |
| **Influenza** | None | None | None | None | None | None |
| **SP $10^3$** | None | None | None | ++ | + | ++ |
| **Dual $10^3$** | None | ++++ | ++++ | ++++ | ++++ | ++++ |
| **Dual $5x10^3$** | None | ++++ | ++++ | ++++ | ++++ | ++++ |

**Table 2.5:** ***Dual infection results in bacteremia by day 5*****.** Balb/c mice were infected with 100 $TCID_{50}$ PR/8 H1N1 influenza ± $10^3$ or $5x10^3$ CFU *S. pneumoniae* 72 hours after viral infection. Cultures were performed from 10 µL BAL and blood from each sample. No growth was noted in influenza-only groups and no contamination seen. Dual infected mice grew *S. pneumoniae* from both blood and BAL samples, whereas bacterial-only infected mice only grew *S. pneumoniae* from BAL. Symbols for Table A (CFU per 10µL sample): 0<**+**<100. 100<**++**<1000. 1000<**+++**<10,000. 10,000<**++++.** n=3. Table shows average growth.

Cell counts performed from BAL collected on days 4-6 indicate a significant increase in inflammatory cell numbers in the dual infected samples, especially apparent on day 6 [Figure 2.6]. Overall, this latest murine model is similar to the previously tested models in severity for influenza-alone and dual infection groups with reduced disease in the bacterial-alone group.

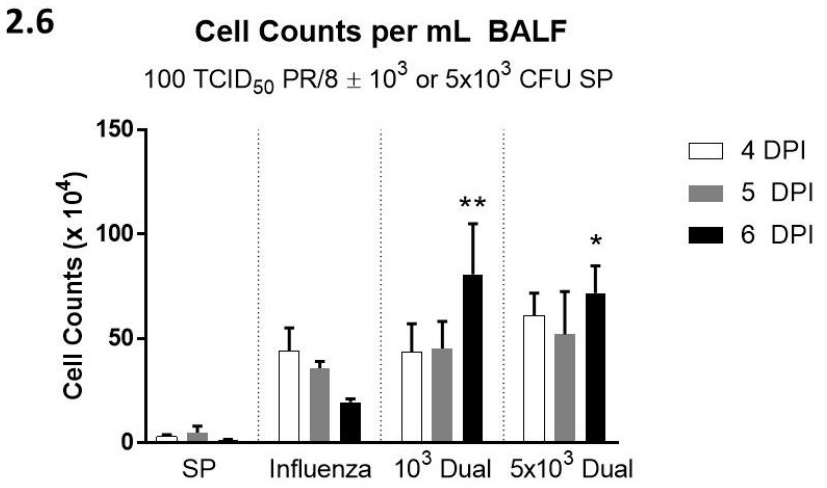


**Figure 2.6:** ***Inflammatory cell influx is most notable on day 6*****.** In this model, BAL fluid cell counts were significantly higher in influenza-only and dual-infected groups than that of bacterial-only infected mice. Data are expressed as means ± SEM. n=5 mice per group. Statistical comparison was performed via one-way ANOVA between same day samples. *$p$<0.05; **$p$<0.01 (relative to SP).

3. *Murine Models for dual infection result in significant pulmonary pathology and breakdown of the pulmonary epithelial and endothelial barriers.* Further analysis of histopathology supports the severe clinical decline and inflammatory response seen in these models. Pulmonary tissue was collected and formalin-fixed on days 4-6. Lungs were scored as previously described.

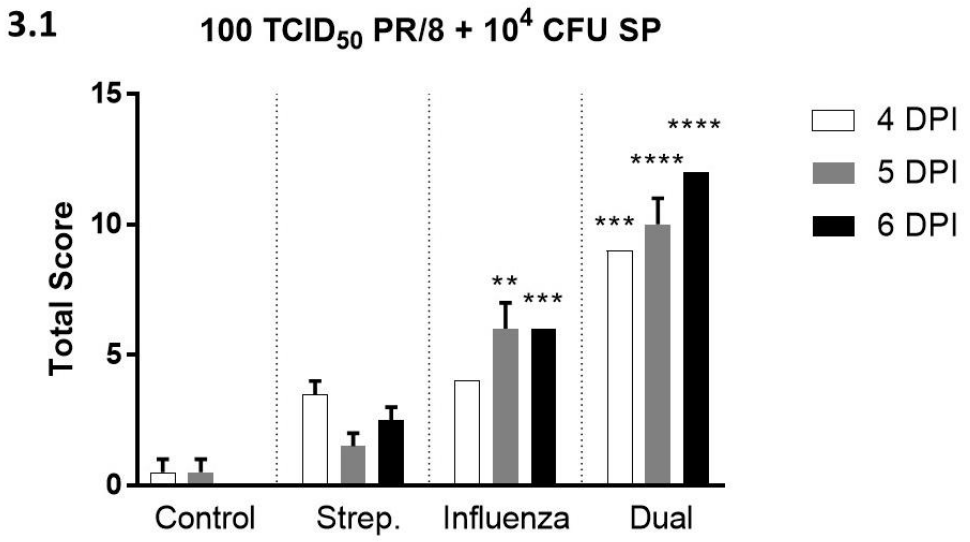


**Figure 3.1:** ***Dual infection results in severe pulmonary pathology***. Balb/c mice were infected with 100 $TCID_{50}$ PR/8 H1N1 influenza, then $10^4$ CFU *S. pneumoniae* 72 hours after initial infection. Bacterial only groups were administered $10^4$ CFU *S. pneumoniae*. Dual infected mice received significantly higher scores than control mice. Influenza-only infected mice received significantly higher scores than control mice on 5 and 6 DPI. In addition, the dual infected group was significantly worse than the influenza-only group on all days ($p$<0.05 on 4,5 DPI and $p$<0.01 6 DPI). Data are expressed as means ± SEM. Statistical comparison was performed via one-way ANOVA between same day samples. n=2 mice per group. ** $p$<0.01; *** $p$<0.001 (relative to healthy controls).

Histopathology scores for the group receiving 100 $TCID_{50}$ influenza ± $10^4$ CFU S. pneumoniae are more severe in viral-alone and dual-infected groups than healthy controls. The dual infected groups are also statistically more severe on all three days as compared with viral-alone, with more widespread pathology and extreme damage [Figure 3.1]. After reduction in bacterial dosage, these trends do not change much, with dual-infected groups remaining the most severe on all days [Figure 3.2].

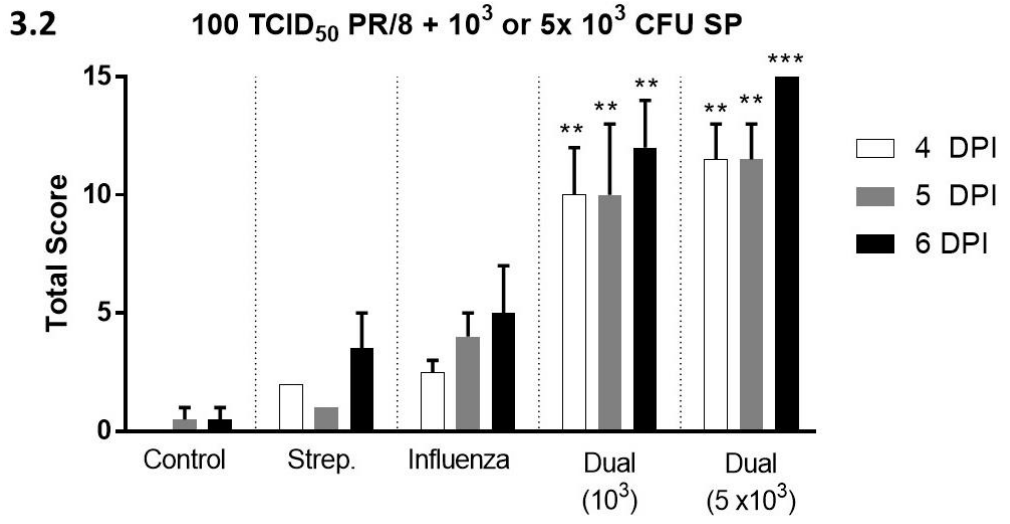


**Figure 3.2:** ***Dual infection continues to result in severe pulmonary pathology after lowering bacterial dose***. Balb/c mice were infected with 100 $TCID_{50}$ PR/8 H1N1 influenza, then either $10^3$ or 5 x $10^3$ CFU *S. pneumoniae* 72 hours after initial infection. Bacterial only groups were administered $10^3$ CFU *S. pneumoniae*. Both dual infection groups received significantly higher scores than control mice. In addition, the dual infected group receiving 5 x $10^3$ CFU bacteria was significantly worse than the influenza only group on all days ($p$<0.05). Data are expressed as means ± SEM. Statistical comparison was performed via one-way ANOVA between same day samples. n=2 mice per group. ** $p$<0.01; *** $p$<0.001 (relative to healthy controls).

As previously described, histopathology scores were based on 7 major pathologic lesions. Of these, no mice in the bacterial-infected groups had evidence of necrotizing bronchiolitis or microvascular thrombosis. These mice also had only mild disease with few foci affected and most tissue appearing like that of healthy controls. Dual-infected mice scored higher in all categories than viral-alone and had the most severe disease with widespread areas of necrosis, pyogranulomatous inflammation and subsequent breakdown of pulmonary architecture [Figure 3.3]. These severe, large areas of disease are clearly visualized in Figure 3.4 and can be compared with that of the other groups, showing less disease.

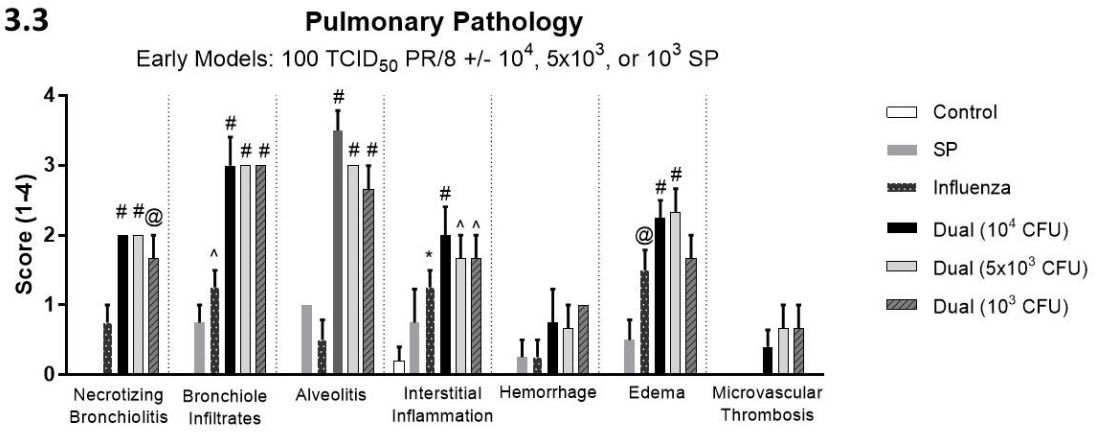


**Figure 3.3:** ***Dual infection results in significantly enhanced pathology in all infective models***. Lungs were collected and formalin-fixed on day 5. Fixed sections were scored from 0 (healthy) to 4 (severe) in the following areas: necrotizing bronchiolitis, bronchiole infiltrates, alveolitis, interstitial inflammation, hemorrhage, edema, and microvascular thrombosis. Bacterial-only infected mice had mild bronchiole infiltrates, alveolitis, interstitial inflammation, hemorrhage and edema at few focal locations. No necrotizing bronchiolitis or microvascular thrombosis were noted. Influenza-only and dual-infected mice had significantly more severe pathology. Data are expressed as means ± SEM. Statistical comparisons were made via one-way ANOVA. n=5 mice per group. *$p$<0.05; #$p$<0.01; @$p$<0.001; ^$p$<0.0001 (relative to healthy controls).

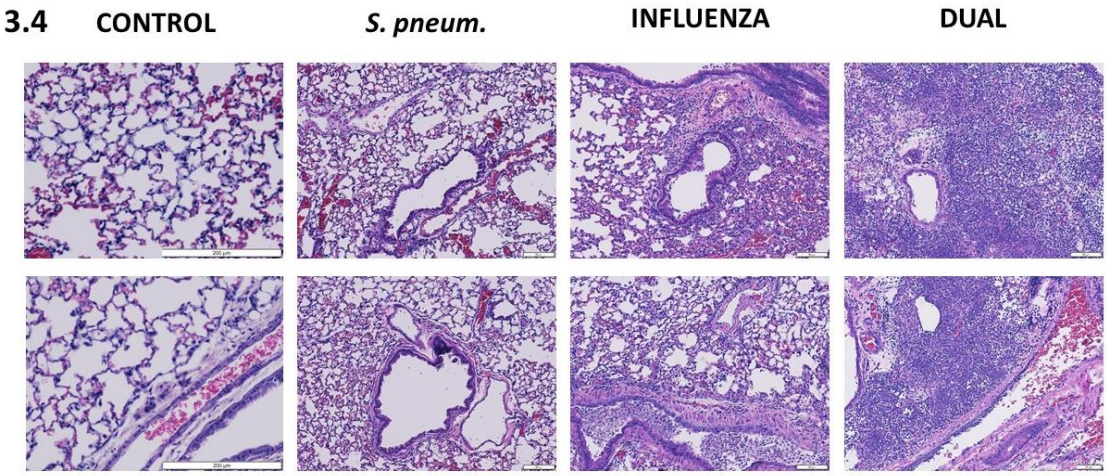


**Figure 3.4:** ***Severe pulmonary pathology and extensive damage is evident on hematoxylin and eosin stained tissue sections*.** This figure acts as a visual representation of Figure 3.3. In addition, the extensive nature of pulmonary pathology evident in dual infection is evident with

large areas of severe pyogranulomatous inflammation and destruction of the pulmonary epithelium and endothelium affecting large areas of pulmonary tissue.

The disease noted on histopathology is further confirmed by western blot analysis of Claudin-5 and T1α. Claudin-5 is normally found at the tight junction of the endothelium and so is considered a sign of endothelial damage when identified in high quantities in BAL supernatant. T1α is typically part of type I pneumocytes and so is used as a marker for epithelial barrier breakdown in the lungs. Evidence of endothelial breakdown is seen in all infected groups based on western blot analysis, but is quantifiably more severe in dual and viral-alone groups [Figure 3.5].

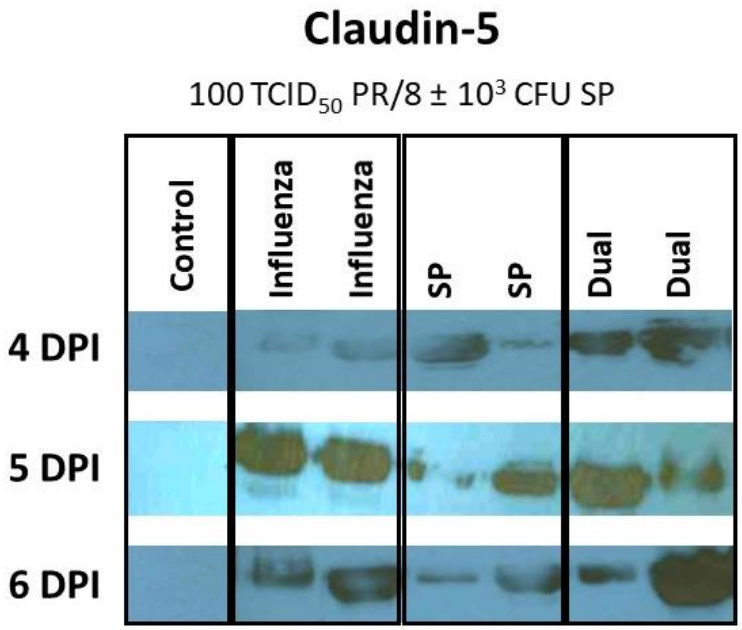


**Figure 3.5:** ***Dual infection results in significant pulmonary endothelial damage*****.** Claudin-5, a marker for endothelial barrier breakdown, was measured from BAL supernatant using western blot technique. Findings confirm significant protein within the BAL supernatant indicating endothelial barrier breakdown within the pulmonary tissue in all infected samples. Samples were normalized by BAL collection technique (see materials and methods).

Epithelial barrier breakdown was also noted in all influenza-alone and dual infected mice from day 4-6 [Figure 3.6]. Detectable presence of this marker in bacterial-alone infected mice was not consistently noted, indicating some variation in the effect of the bacteria alone to increase epithelial permeability.

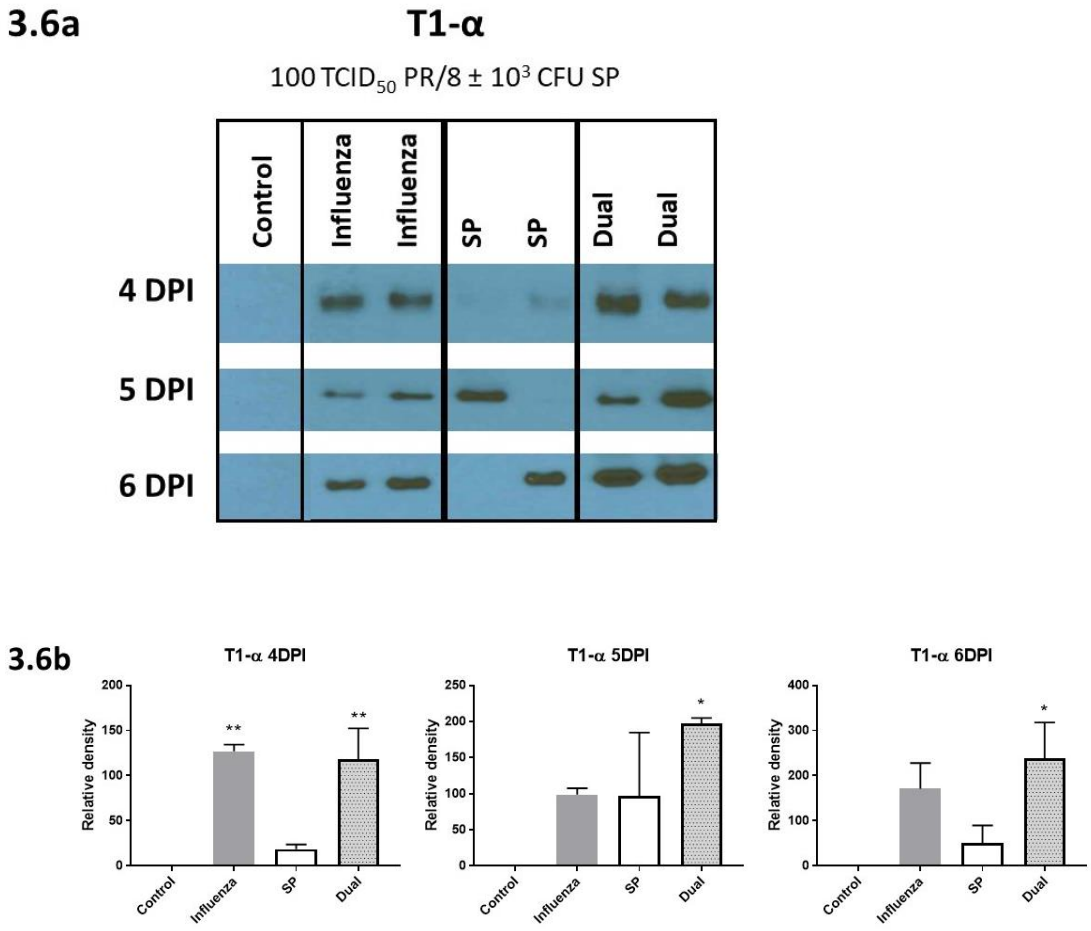


**Figure 3.6:** ***Dual infection results in significant pulmonary epithelial damage***. T1-α, a marker for alveolar epithelial breakdown, was measured from BAL supernatant using Western Blot technique. Epithelial breakdown is apparent in all infected samples, but most consistently in influenza-only and dual infected samples. Densitometry confirms that influenza-alone and dual infected mice have significantly more T1-α than bacterial-alone and healthy controls. Statistical comparisons made via one-way ANOVA. Data are expressed as means ± SEM. n=4. **p*<0.05; ***p*<0.01 (relative to heathy controls).

4. *Sublethal combination of influenza and S. pneumoniae results in a lethally synergistic murine model for influenza coinfection.* In order to assess the effects of a much lower dosage of *S. pneumoniae* in combination with a severe, but not lethal dose of influenza, 100 $TCID_{50}$ influenza was administered 3 days prior to administering 200 CFU of bacteria. Even at these low doses, viral-alone and dual infected mice lost significant weight between days 2-5, matching an increase in severity of clinical score. In addition, dual infected mice continued to be more severely affected than those with viral-alone infection [Figure 4.1].

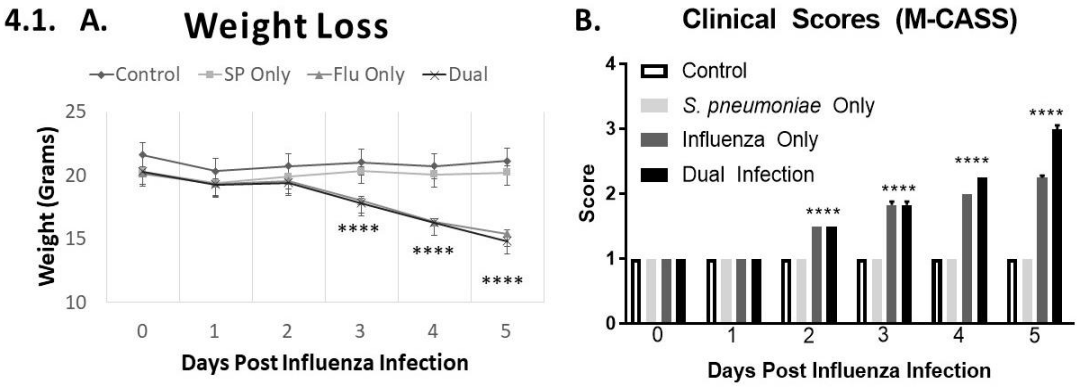


**Figure 4.1:** ***Dual-infected and influenza-alone infected mice have similar weight loss, but have differences noted in clinical decline***. Balb/c mice were infected with sublethal doses (100 $TCID_{50}$ intranasally) of influenza A/Puerto Rico/8/34 H1N1 virus or PBS followed by sublethal *S. pneumoniae* (200 CFU IN) or PBS three days after initial influenza infection. **A** and **B**: Infected mice lost significant weight and had significant increase in severity of clinical score starting on day 3 as compared with control and *S. pneumoniae*-only infected mice. In addition, significant differences ($p$<0.0001) in clinical score were noted between Influenza Only and Dual groups on days 4 and 5 post influenza infection. Data were expressed as means ± SEM. Statistical comparisons were made with one-way ANOVA and unpaired t-tests. n = 21 mice per group. **** p<0.0001.

An excessive neutrophil influx is also noted on day 5, with significantly more total inflammatory cells seen in both viral-alone and dual infected groups and a trend toward the most cells in dual infected mice [Figure 4.2 A]. Images from cytospins clearly show this difference with the predominant cell type being neutrophils [Figure 4.2 B]. Differentials performed from these

cytospins confirm that neutrophils are the predominant cell type in both viral-alone and dual infected groups, with a higher percentage of neutrophils noted in dual than viral-alone, which had more macrophages present as a percentage of the cell population [Figure 4.3].

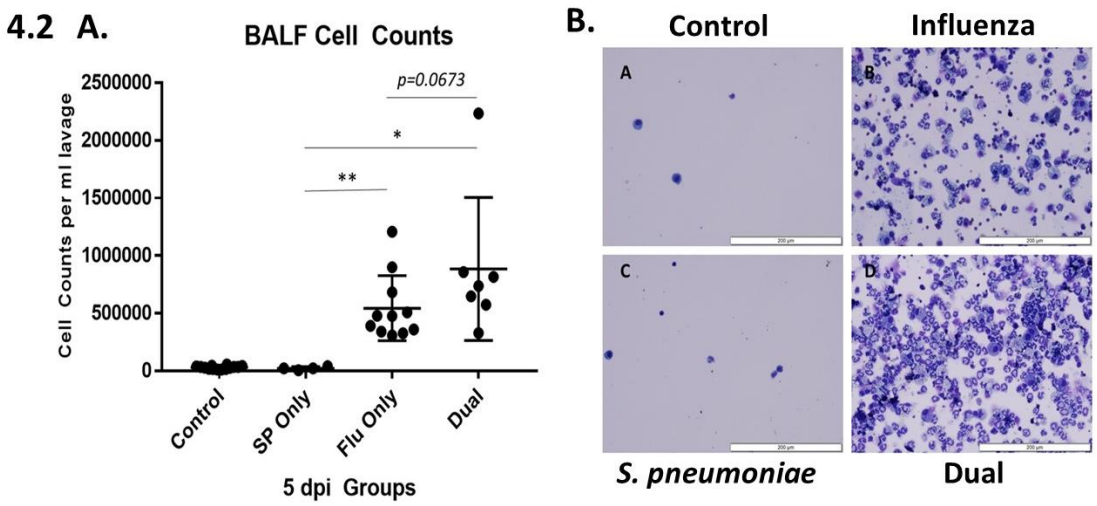


**Figures 4.2:** ***Excessive neutrophil influx seen in dual infection***. Balb/c mice were infected with sublethal doses (100 $TCID_{50}$ intranasally) of influenza A/Puerto Rico/8/34 H1N1 virus or PBS followed by sublethal *S. pneumoniae* (200 CFU IN) or PBS three days after initial influenza infection. **A** and **B**: Influenza-infected and dual-infected groups have significantly more cells in the BAL fluid than in *S. pneumoniae*-only infected groups as seen from cell counts performed via hemocytometer and cytospin data. A trend toward a significant increase in cell counts in dual infected mice compared with viral-only was also noted. Data were expressed as means ± SEM. Statistical comparisons were made via one-way ANOVA. n = 7-11 mice per group. * $p<0.05$; ** $p<0.01$ (relative to SP Only).

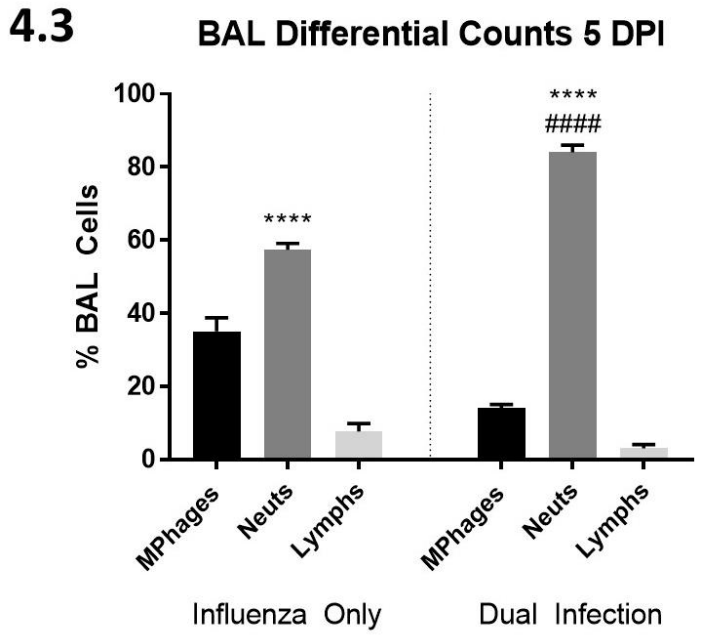


**Figure 4.3:** ***Neutrophils predominate inflammatory cell influx***. Balb/c mice were infected with sublethal doses (100 $TCID_{50}$ intranasally) of influenza A/Puerto Rico/8/34 H1N1 virus or PBS followed by sublethal *S. pneumoniae* (200 CFU IN) or PBS three days after initial influenza infection. Differentials performed on BAL fluid cells viewed after cytospin revealed majority neutrophils, especially noted in dual infections, with a significantly higher percentage of neutrophils in dual differentials compared with influenza alone. Data were expressed as means ± SEM. Comparisons made via paired t-test. n = 3 mice per group. **** $p<0.0001$ relative to lymphocytes. #### $p<0.0001$ (relative to macrophages).

Protein leakage as measured in BAL supernatant also supports the continued severity of the viral-alone and dual-infected models. Not only was more protein evident in these groups as compared with bacterial-alone and healthy groups, but these protein levels climbed from days 3 through 6 [Figure 4.4].

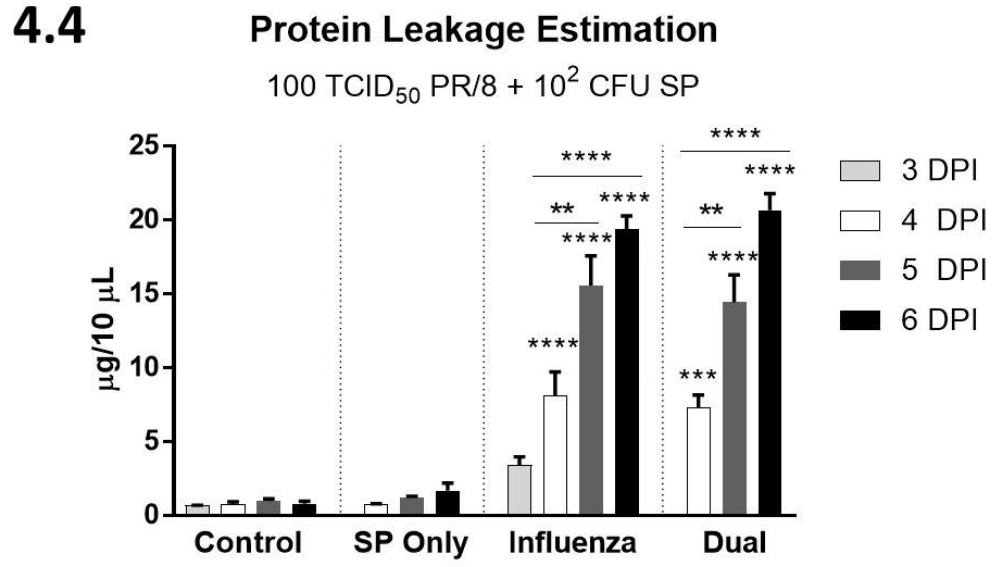


**Figure 4.4:** ***Protein leakage significantly increases between 3-6 DPI in both influenza-only and dual infected models***. In this model, balb/c mice were infected with 100 $TCID_{50}$ PR/8 H1N1 influenza ± $10^2$ CFU *S. pneumoniae* 72 hours after initial infection. BAL was collected on days 3-6 and the supernatant used for protein estimation. 4-6 DPI samples in both the influenza-only infected group and dual infected group were significantly higher than that of controls or bacterial-only infected mice. In addition, there is a significant increase in protein leakage in these same groups from 3-5 days after initial viral infection with maximum damage resulting in leakage appearing on days 5 and 6. Data are expressed as means ± SEM. Comparisons performed via one-way ANOVA. n=4-8 mice per group. ***p*<0.01; ****p*<0.001; *****p*<0.0001 (relative to healthy controls unless otherwise indicated).

Similar trends to previously assessed models are also evident when evaluating histopathology. Lungs were collected and formalin-fixed on days 3-6 to be sectioned and scored by an anatomic veterinary pathologist. These sections were scored in the same manner as described previously. Notable pulmonary edema, pyogranulomatous inflammation, hemorrhage and widespread disease are evident on dual-infected lungs [Figure 4.5]. When compared in each key area scored, results remain similar to previous models as well, with minimally affected pulmonary tissue from bacterial infection alone and markedly more severe disease seen in influenza and especially

dual-infected groups [Figure 4.6]. These findings are again further supported by evaluating Claudin-5 and T1α markers through Western Blot analysis (data not shown).

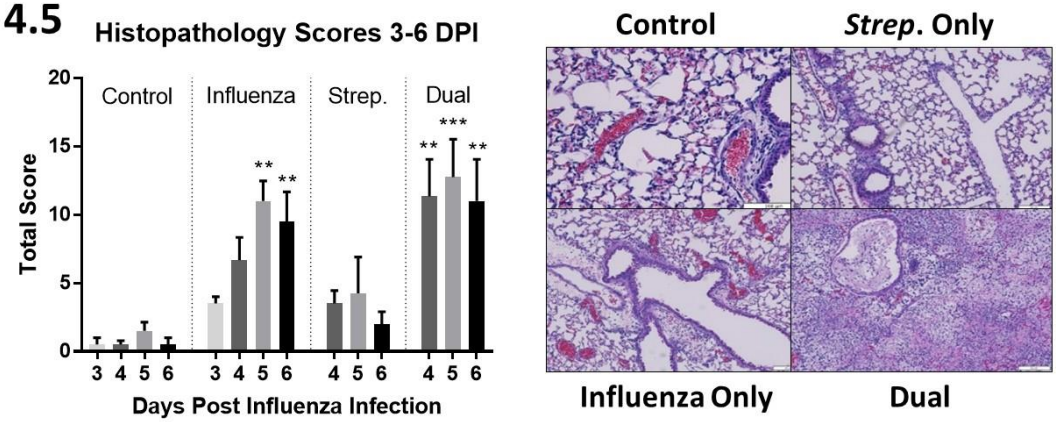


**Figure 4.5:** ***Dual infection results in severe pulmonary pathology.*** Lungs were collected and formalin-fixed for histopathology analysis between days 3-6 post influenza infection. Day 3 samples for *S. pneumoniae*-only and dual infections were not collected since bacterial inoculation was performed at that time. Figure presents sum of scoring. Paraffin-embedded lung tissues from 5 days post-challenge with infection or mock infection were stained with hematoxylin and eosin. Tissues affected through dual infection show most severe score with notable pulmonary edema, bronchiolitis, alveolitis, hemorrhage, microvascular thrombosis and interstitial disease. Infected samples were compared with controls. Data were expressed as means ± SEM. Comparisons evaluated via one-way ANOVA. n = 4 mice per group. * $p<0.05$; ** $p<0.01$; *** $p<0.001$.

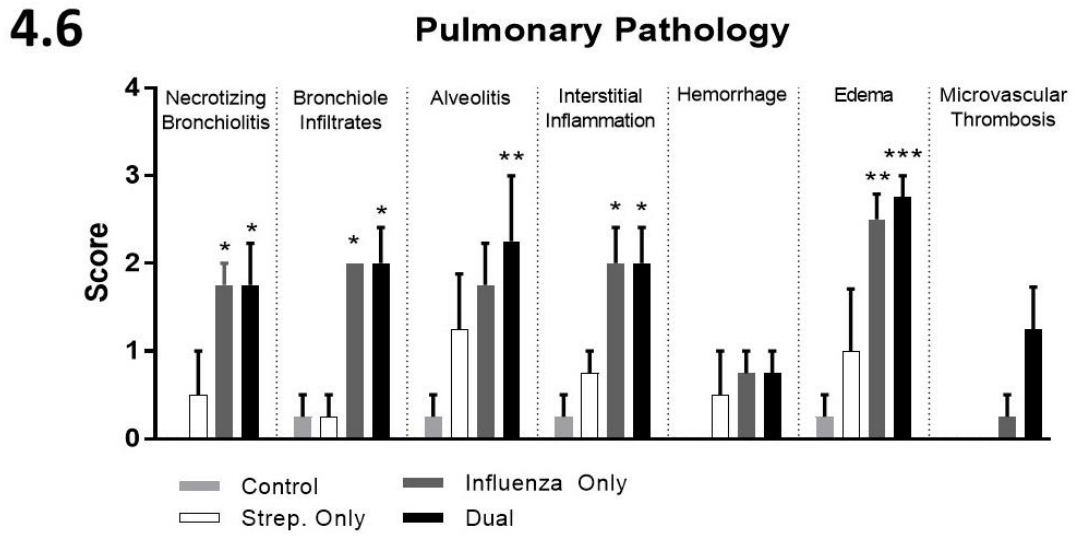


**Figure 4.6:** ***Dual infection results in significantly enhanced pulmonary pathology***. Individual areas scored include: necrotizing bronchiolitis, bronchiole infiltrates, alveolitis, interstitial inflammation, hemorrhage, edema, and microvascular thrombosis. Infected samples were compared with controls. Data were expressed as means ± SEM and compared via one-way ANOVA. n = 4 mice per group. * $p<0.05$; ** $p<0.01$; *** $p<0.001$.

5. *Lethally synergistic disease results in the release of neutrophil extracellular traps (NETs).* NETs have been reported as a significant cause of pulmonary pathology and worsened clinical disease in influenza pneumonia [55, 83]. To identify if NETs release is apparent in this murine model, extracellular histones were measured from BAL supernatant. Both H2A [Figure 5.1] and citrullinated H4 [Figure 5.2] are quantifiably present in viral-alone and dual infected mice in all models, with minimal detection in bacterial-alone groups. Citrullinated H4 is considered a more specific marker for NETosis as histones must undergo citrullination in order to be released through NETs.

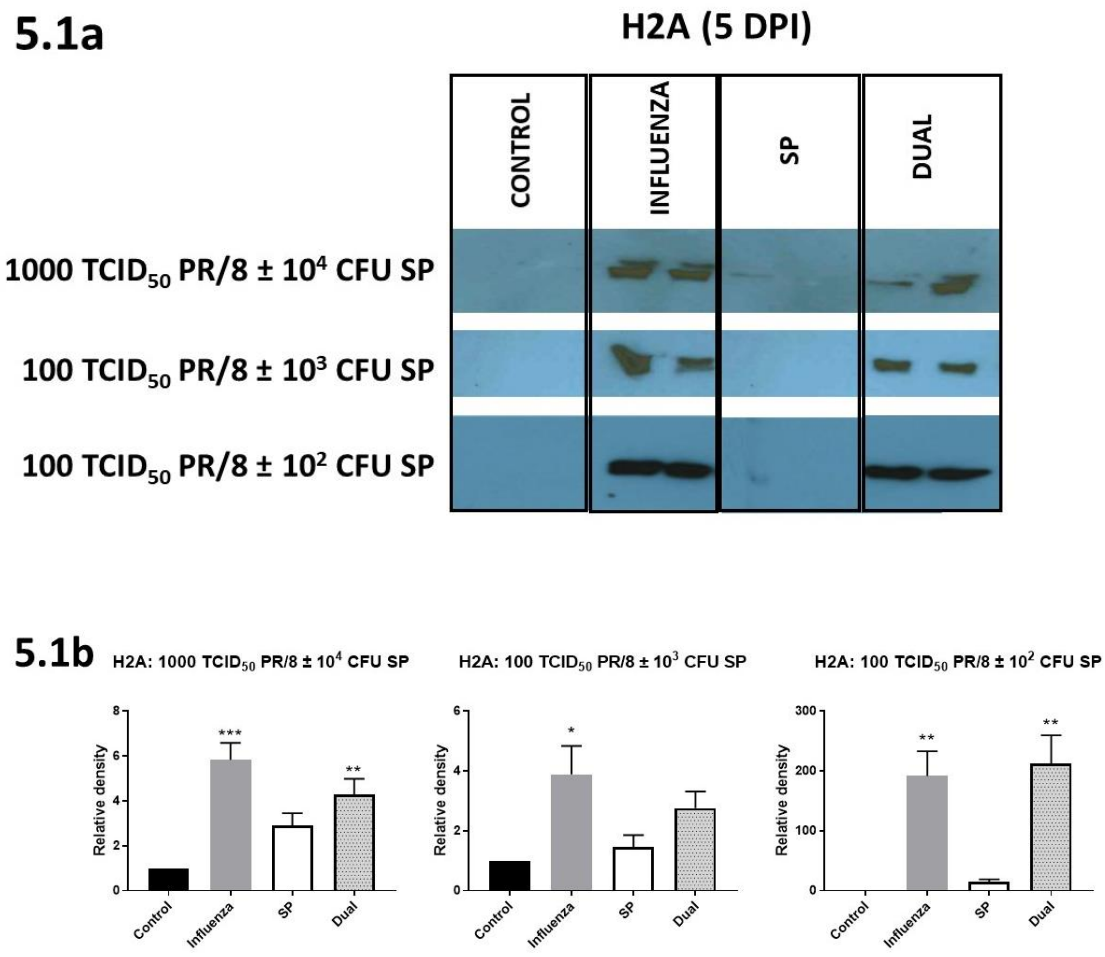


**Figure 5.1:** ***Accumulation of extracellular histones during influenza and dual infection.*** BAL supernatant was collected from all models on days 4-6. Figure shows sample of results on day 5 for three tested models. H2A, extracellular histone, is present in all viral-alone and dual infected samples. H2A is minimally present to absent in bacterial-alone samples and absent in healthy controls. Densitometry confirms the increased presence of extracellular histone, H2A, in the BAL. Data are expressed as means ± SEM and compared via one-way ANOVA. n=4. **p*<0.05; ***p*<0.01; ****p*<0.001 (relative to healthy controls).

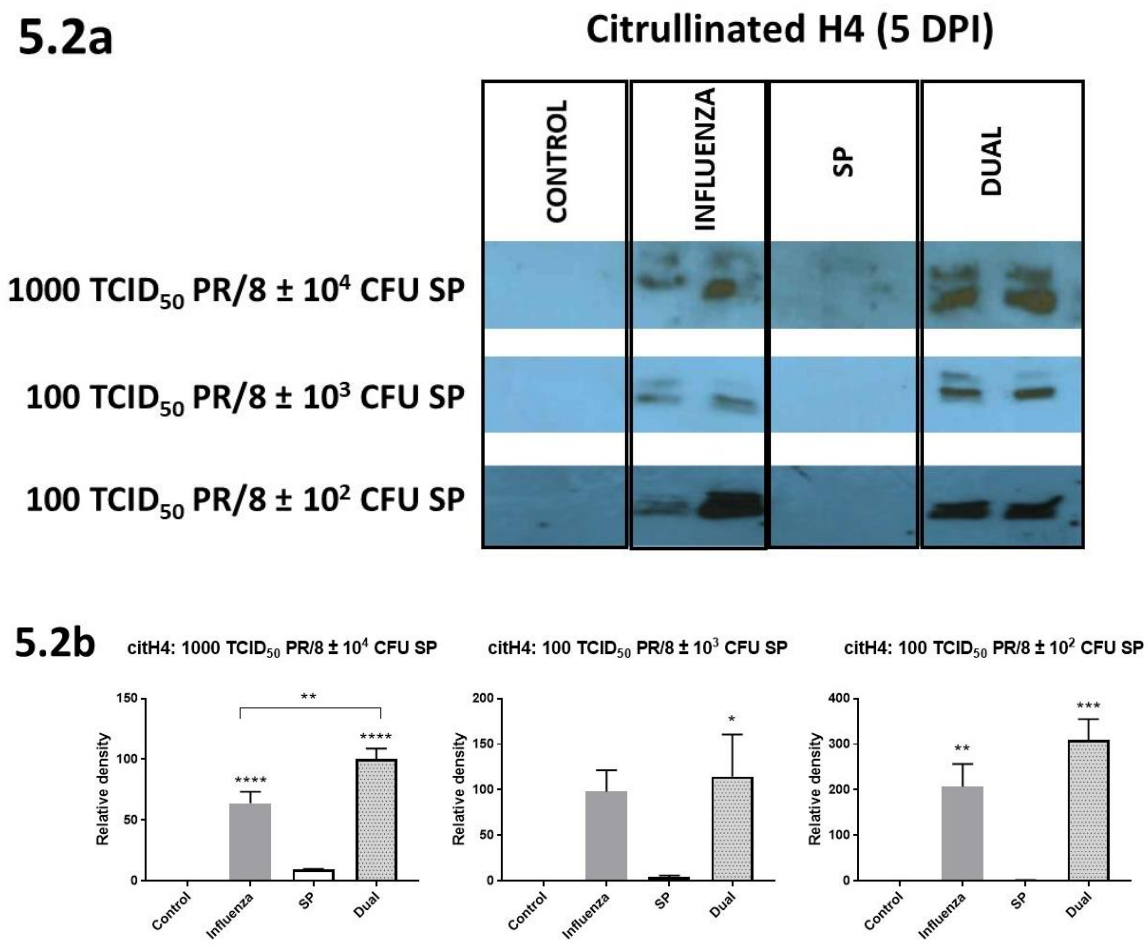


**Figure 5.2:** ***Neutrophil Extracellular Traps (NETs) are released in vivo during influenza-alone and dual infection.*** BAL supernatant was collected from all models on day 4-6 and western blot technique performed to assess presence of citrullinated H4 (citH4), an extracellular histone and by product of NETosis. Figure shows three results from day 5. CitH4 was present in all viral-alone and dual infection samples, while minimally present to absent in bacterial-alone groups. CitH4 is absent in healthy BAL. Data are expressed as means ± SEM and compared via one-way ANOVA. n=4. *$p$<0.05; **$p$<0.01; ***$p$<0.001 (relative to healthy controls unless otherwise indicated).

*Histones damage epithelial cells and increase bacterial translocation in vitro.* 10 µg/mL histones were added to half of the inserts on the apical chamber of a co-culture transwell with A549 cells (epithelial) on the apical side of the membrane and Eahy926 (endothelial) cells on the basolateral side of the membrane. Histones were incubated on these cells for 1 hour before removal and the addition of $10^6$ CFU *S. pneumoniae* to all apical chambers. Cultures from

basolateral chamber samples were performed over 6 hours by no growth was seen on any sample. However, after 6 hours, the cells were stained with trypan blue and a significant increase in the number of non-viable cells was noted in chambers treated with histones compared to those without (data not shown).

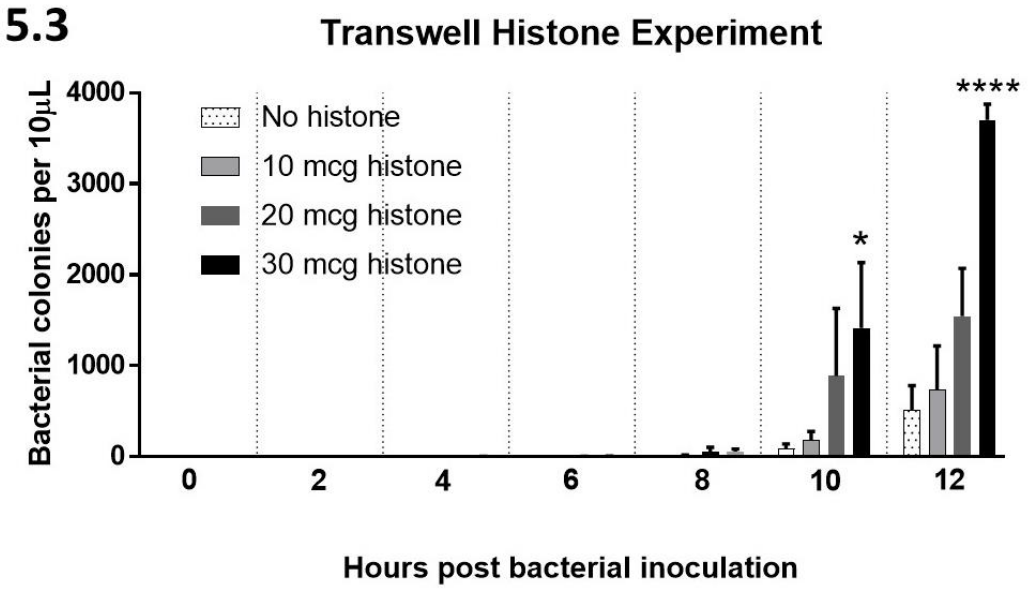


**Figure 5.3:** ***Histones directly contribute to epithelial barrier breakdown and bacterial dissemination*** An A549 epithelial cell monolayer was established on a transwell system and cells were exposed to varying levels of histones for one hour before incubation with S. pneumoniae. 10 µL samples were collected from the basolateral chamber and cultured over a 12-hour time period. High levels of histones resulted in significantly more bacteria translocating across the epithelial barrier, but was not significantly noted until after 10 hours. Data are expressed as means ± SEM and are compared via one-way ANOVA. n=2. *$p$<0.05; ****$p$<0.0001 (relative to no histone control).

Next, an A549 monolayer transwell system was established to test various concentrations of histones and their effects on translocation. The following conditions were tested: No histones, 10µg/mL histones, 20µg/mL histones, and 30µg/mL histones. After histone incubation, all wells were inoculated with $10^6$ CFU *S. pneumoniae* and allowed to grow for 12 hours. Samples were removed from the basolateral chamber every 2 hours for culture.

Statistical significance was only noted between groups starting at 10 hours post bacterial inoculation. The cells receiving 30µg/mL histones had significantly higher levels of bacterial translocation to the basolateral chamber than those receiving no or 10µg/mL histones at both 10 and 12 hours [Figure 5.3]. Although significance is only established late, a trend toward this is apparent from early on, as can be seen in Figure 5.4, which outlines the first 6 hours of incubation. Overall bacterial growth for all conditions exponentially increases after 8 hours, although it increases much more in the wells treated with the highest amounts of histone [Figure 5.4].

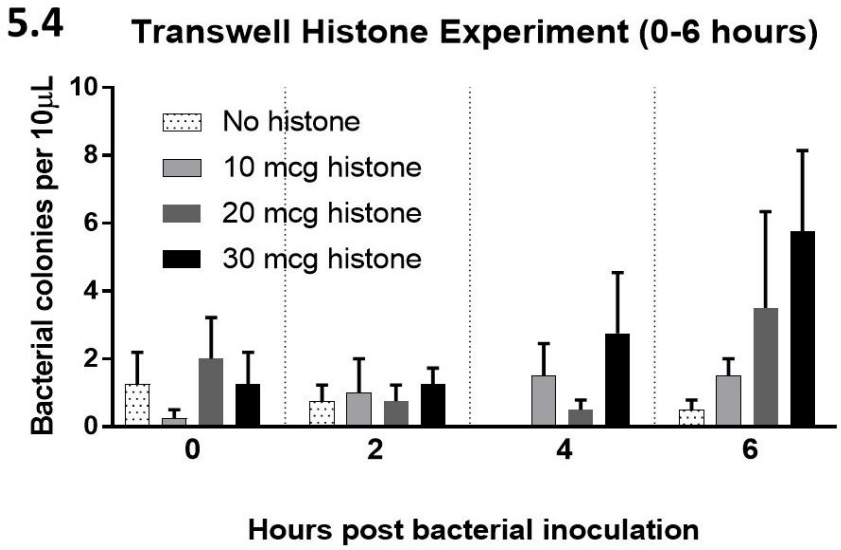


**Figure 5.4:** ***Histone effects on bacterial translocation***. Although sample size is insufficient for statistical significance, a trend can be seen toward increased histone concentrations and an increase in bacterial translocation and subsequent bacterial growth from the basolateral chamber. This figures helps to illustrate the first 6 hours after inoculation. Overall, bacterial growth in all groups exponentially increases after 8 hours, but wells receiving higher levels of histones result in statistically significant increases in bacterial translocation. Data are expressed as means ± SEM. n=2.

*Histone inoculation in vivo results in increased morbidity and bacterial growth.* Balb/c mice were inoculated with either 50 or 100 µg/mL histones IN ± $10^3$ CFU *S. pneumoniae* intranasally 24

hours after histone inoculation and monitored over 72 hours for clinical signs and weight loss. Mice were euthanized after 72 hours and samples collected for cell counts, culture and histopathology. In addition, a smaller group was inoculated with 300 µg/mL histones, but the mice receiving 300 µg/mL histones had to be euthanized within an hour of inoculation due to steep clinical decline, likely from histone toxicity.

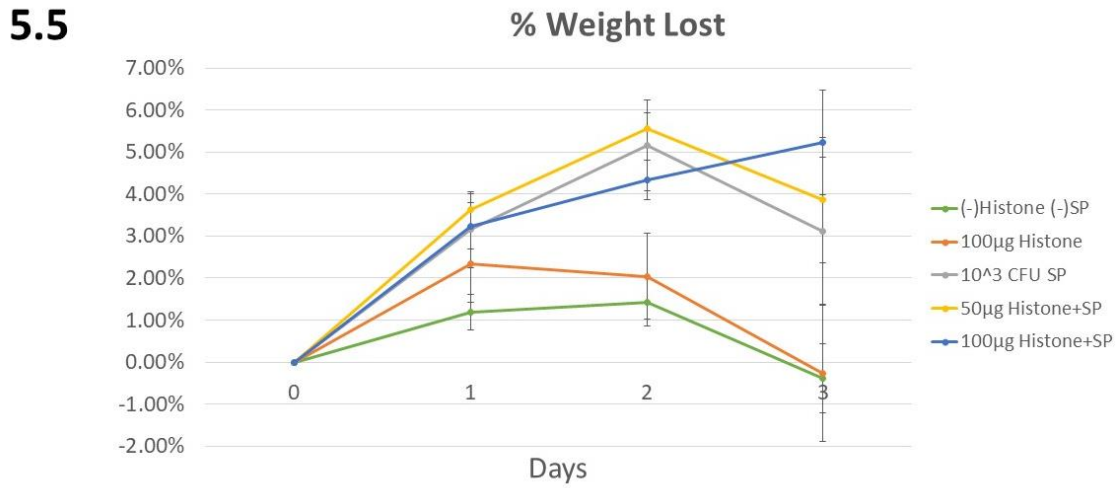


**Figure 5.5:** ***Histones in combination with pneumococcal infection result in more pronounced weight loss***. Balb/c mice were inoculated with either 50 or 100 µg/mL histones IN +/- $10^3$ CFU *S. pneumoniae* IN and monitored over 72 hours for clinical signs and weight loss. The mice receiving 300 µg/mL histones had to be euthanized within an hour of inoculation due to steep clinical decline. Percentage weight lost over 3 days: Groups receiving *S. pneumoniae* lost between 3-5% of their weight over three days with the greatest weight loss noted in groups receiving both bacteria and histone inoculation. Clinically, mild lethargy was noted in the 100µg histone groups on day 1, and in the 100µg histone + SP groups on days 1, 2, and 3 (data not shown). Data are expressed as mean ± SEM. n = 6 mice per group for all studies.

Groups receiving *S. pneumoniae* lost between 3-5% of their weight over three days with the greatest weight loss noted in groups receiving both bacteria and histone inoculation [Figure 5.5]. Clinically, mild lethargy was noted in the 100µg histone groups on day 1, and in the 100µg histone + SP groups on days 1, 2, and 3 (data not shown).

5.6

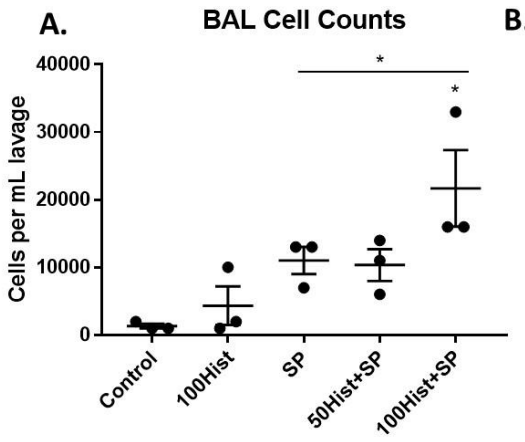


B.

| Culture Results (Average) | | |
|---|---|---|
| | Blood | BAL |
| (-)Histone (-)SP | No Growth | No Growth |
| 100µg Histone | No Growth | No Growth |
| $10^3$ CFU SP | No Growth | ++ |
| 50µg Histone+SP | + | +++ |
| 100µg Histone+SP | No Growth | ++ |

**Figure 5.6:** ***Histones enhance cellular influx and cause bacteremia in vivo***. Balb/c mice were inoculated with either 50 or 100 µg/mL histones IN +/- $10^3$ CFU *S. pneumoniae* IN and monitored over 72 hours for clinical signs and weight loss. Mice were euthanized after 72 hours and samples collected for cell counts, culture. **A:** BAL cell counts were significantly different between 100µgHist+SP and SP only and controls. No other significant differences were noted. **B:** Cultures were taken on day 3. Results reflected are CFU/20µL sample. +: <50 CFU; ++: 50<CFU<500; +++: 500<CFU<1000. n=3 Blood and BAL culture results indicated growth of SP in all BAL samples from mice inoculated with SP and in one blood sample, from a mouse within the 50 µg/mL histone+SP group. n=3. Data are expressed as mean ± SEM and compared via one-way ANOVA. n = 3 mice per group for all studies. * $p<0.05$ (compared with healthy controls unless otherwise indicated).

Blood and BAL cultures were performed on day 3. Blood and BAL culture results indicated bacterial growth in all BAL samples from mice inoculated with SP and in one blood sample, from a mouse within the 50 µg/mL histone+SP group [Figure 5.6 B]. BAL cell counts were significantly higher in the 100µgHist+SP group as compared with the bacterial only and mock infected mice [Figure 5.6 A]. Histopathology shows increased pulmonary hemorrhage, especially in the mice inoculated with 300 µg/mL histones who were euthanized shortly after inoculation due to severe clinical decline [Figure 5.7].

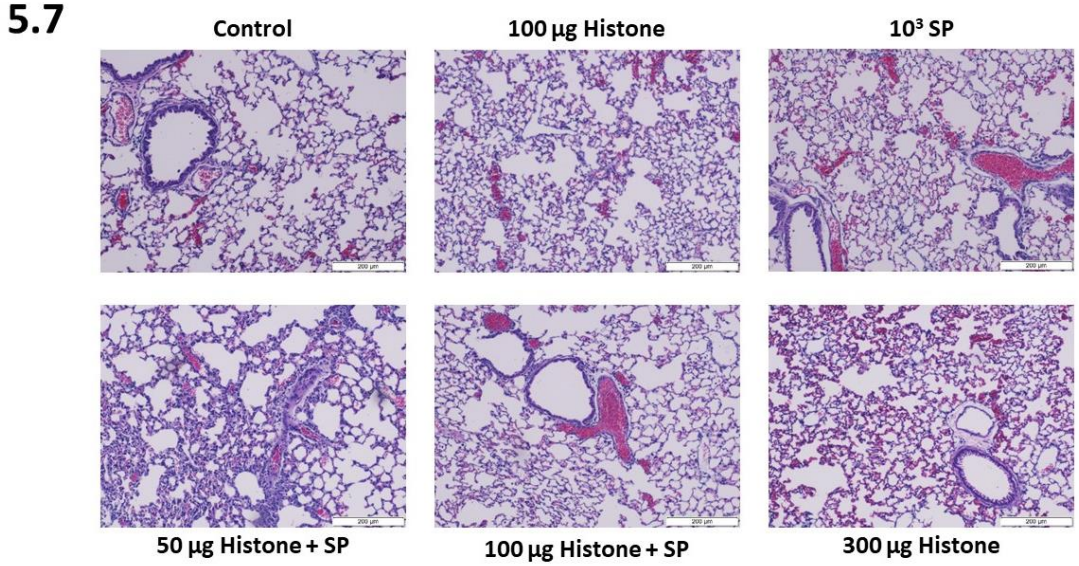


**Figure 5.7:** ***Histopathologic effects of histones in vivo include mild disease and hemorrhage***. Balb/c mice were inoculated with either 50 or 100 µg/mL histones IN +/- $10^3$ CFU *S. pneumoniae* IN. Mice were euthanized after 72 hours and samples collected for histopathology. The mice receiving 300 µg/mL histones were euthanized within an hour of inoculation due to steep clinical decline. Histopathology from mice show mild disease. Hemorrhage is most notable in the group receiving 300 µg histones. Mild alveolitis and bronchiolitis are also evident in those receiving histones. n = 3 mice per group for all studies.

**Discussion:**

Identifying animal models for influenza pneumonia with pneumococcal coinfection can be challenging due to the complexity of the disease. Variation of dual infection in human disease outside of experimental conditions is so vast, that identifying a model that will work in all cases is near impossible. My goal was to characterize and develop a murine model for dual infection pneumonia that resembles that seen in pandemic influenza outbreaks, where a severe H1N1 influenza strain is predominant and coinfection results in a lethally synergistic outcome with high rates of morbidity and increased mortality. A murine model that best mimics this process can be used to better understand the pathogenesis of the disease and develop therapeutics that

may work well in combination with antibiotics and antivirals to combat the high morbidity and improve clinical outcome.

Various models have been tested. Factors to be considered include host, pathogens, infective dosages, and timing of secondary infection. Various hosts have been utilized in assessing dual infection: in particular mice, rats, ferrets and pigs. Due to the availability, cost, and ability to repeat consistent experiments, murine models are the most commonly used. Ferret models also appear rather ideal, and a ferret model has shown the same synergism seen in mice, dependent on the pneumococcal strain [16], but availability and cost is a factor for many. PR/8 H1N1 influenza A was chosen due to its consistency in a mouse model to limit variation. A sublethal dosage better mimics a pandemic for a typical, healthy population, where an individual may develop moderate to even severe disease, but does not always succumb to the virus alone. *Streptococcus pneumoniae* is the most common secondary bacterial agent seen in dual infection influenza pneumonia with over 40% of coinfections culturing *S. pneumoniae* during pandemic outbreaks [6, 11, 12], and so was chosen for the bacterial pathogen. As an often opportunistic pathogen, *S. pneumoniae* can be subclinical and often cause mild disease, which is complicated in dual infection, creating a synergistic model. The models tested in this study indicate that even decreasing the infective dose of *S. pneumoniae* by almost 1000-fold, still resulted in severe, lethally synergistic disease with bacteremia. Bacteremia is a common sequelae for severe influenza coinfection – during the 1918 H1N1 pandemic, over 95% of lungs cultured bacteria and an alarming 70.3% of assessed victims were bacteremic [6]. In this chapter's proposed murine models, bacteremia is a consistent clinical finding from day 5 and 6 (48-72 hours after bacterial infection) and correlates with a breakdown in the pulmonary epithelial and endothelial barriers, as seen by T1α and Claudin-5 detection as well as histopathologic changes at that time. Drastic differences were not seen between the tested

models. Due to the chance of bacteremia in our bacterial-only infected group at higher bacterial doses and the severity of the disease, our model essentially reduced infective dose to the lowest amount that still causes lethal synergism, which not causing significant disease in bacterial-only infected mice.

Timing of infection must also be considered. Consideration must be made to which agent is administered first, bacterial or viral, and how many days apart are they administered? If bacteria is introduced into the lower airways first, there may be a protective effect and enhanced adaptive response to influenza virus initially, although the ability of the host to neutralize the virus one month after infection is reduced [105]. In addition, pandemic outbreaks involve viral introduction first, with secondary agents taking advantage of the viral-induced and immunopathologic damage to the host to enter the lower airways and cause increased disease. If viral and bacterial agents are administered simultaneously, the synergism normally seen in infection is not present to the same degree [29]. However, if the viral burden is allowed to clear and the bacteria introduced seven days after viral infection, this synergism is clearly evident with an enhanced inflammatory response and bacterial burden [19, 29]. Significant neutrophil accumulation and functional impairment is noted in mice receiving secondary bacterial infection 3 and 6 days after influenza infection as well [39]. The aim of our lab is to use this murine model to assess the therapeutic potential of neutrophils as a target for dual infection influenza pneumonia. Since the excessive inflammatory response is still present, our model allows for 3 days between administration of influenza and *S. pneumoniae*. Based on our results, clinical disease develops from influenza on day 2, at which point bacteria is introduced 24 hours later. An excessive neutrophil influx is apparent in both viral-alone and dual infected groups, most notable at day 5 and 6. At this same time, pulmonary pathology and protein leakage are severe

in these models and support that pulmonary epithelial and endothelial barrier breakdown at this time allows for the bacteremia introduced on day 5 in the dual infected mice.

There is also an increase in the release of neutrophil extracellular traps (NETs) in both influenza-only and dual infected BAL. We have previously shown that excessive neutrophils and NETs contribute to alveolar-capillary damage after influenza challenge in mice [174]. NETs formation is dependent on redox enzyme activities [55]. NETs were first identified as a process of cell death that released DNA, histones and granular proteins such as elastase and myeloperoxidase to entrap and kill pathogens [50]. Since the initial identification of NETs, they have also been shown to be detrimental to the host – particularly through histones which induce endothelial and epithelial cell damage and worsened disease [56]. Further, using *pneumococcal* superinfection following influenza, an extensive accumulation of NETs was recognized, especially in the damaged areas of the lungs, indicating their potential role in tissue injury. Moreover, NETs released during pneumococcal superinfection did not show any bactericidal or fungicidal activities. [57, 58]. A toxic byproduct of NETs, extracellular histones, are clearly present in those mice with more severe disease – the influenza-alone and dual-infected mice. Transwell studies further support that histones alone can lead to epithelial and endothelial barrier breakdown, increasing permeability into the bloodstream, allowing for bacteremia and subsequent sepsis. Histones administered in vivo also appear to cause more severe disease and allow for barrier breakdown and bacteremia. Our data supports that increased NETs release and the presence of histones correlate with worsened histopathologic changes and clinical outcome in our murine model for dual infection pneumonia.

In conclusion, the proposed murine model for influenza coinfection is a good representation of pandemic influenza outbreaks resulting in secondary infection that is lethally synergistic. Mice infected with 100 $TCID_{50}$ PR/8 H1N1 and 200 CFU S. pneumoniae 72 hours after

initial viral infection have an exaggerated innate response, with predominantly pyogranulomatous inflammation. Significant protein leakage, pulmonary pathology, and barrier breakdown is noted on days 5 and 6 after influenza infection (48 hours after bacterial infection) and correlates with bacteremia in all dual infected mice. This murine model will serve as a good animal model to further assess the pathogenesis of the barrier breakdown and development of bacteremia and sepsis, as well as provide a consistent model for the testing of potential therapeutics for pandemic influenza coinfection [Figure 6.1].

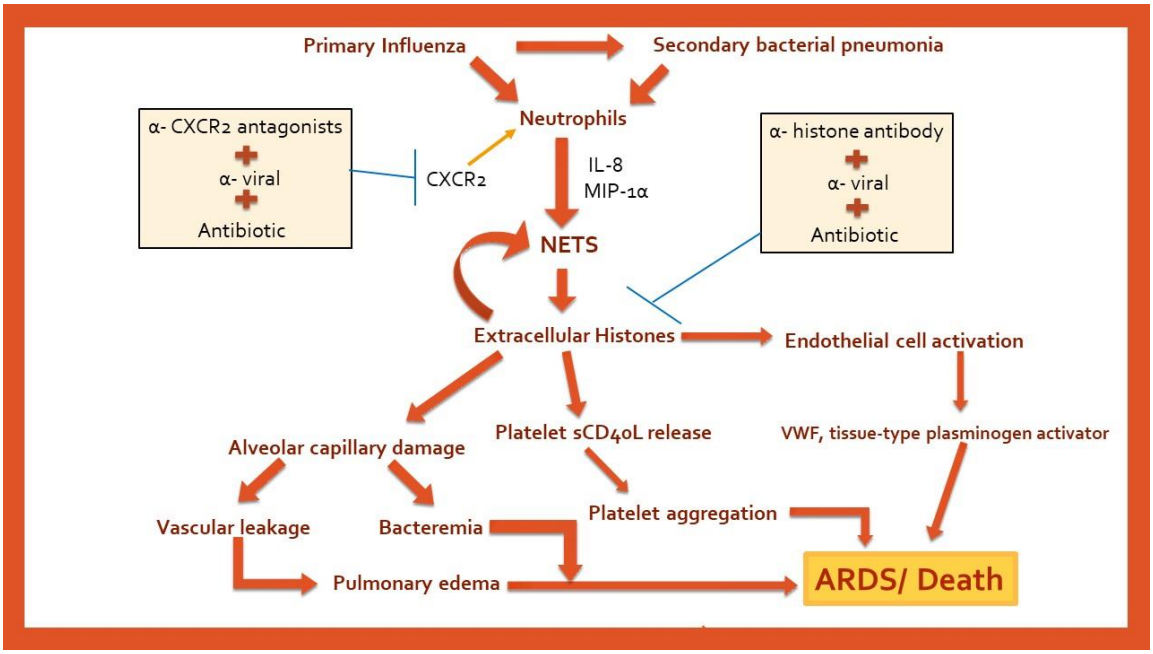


**Figure 6.1:** ***Various strategies to be considered for the development of potential therapeutic targets in influenza coinfection*****.** Upon development of the murine model, this schematic represents potential directions to consider for pathogenesis and therapeutic targets in severe dual infection pneumonia. This project focuses on targeting neutrophil influx in addition to bacterial and viral factors to improve clinical outcome.

# CHAPTER III

## ASSESSING NEUTROPHIL CHEMOKINE RECEPTOR EXPRESSION AND PHENOTYPE IN A MURINE MODEL OF DUAL INFECTION PNEUMONIA

**Summary:** It is well established that secondary bacterial infections complicate and promote lethality in cases of influenza pneumonia during pandemic outbreaks, and also in fatal cases of seasonal influenza infections. Current therapies rely on antibiotics and antivirals to work closely with supportive care measures to improve clinical outcome, but increasing evidence of antiviral resistance and continued severity associated with coinfection demand novel approaches to combination therapy be explored. The innate immune response to influenza pneumonia promotes coinfection and contributes significantly to pulmonary pathology and poor outcomes. We established a murine model for dual infection to evaluate the role of neutrophils in *S. pneumoniae* superinfection following influenza infection in mice. Previous studies in our lab has demonstrated pathogenic role of neutrophils in influenza pneumonia. Here, we characterized neutrophils for their phenotypic changes and functional responsiveness during primary influenza as well as secondary pneumococcal superinfection. Chemokine receptors are critical to neutrophil function and innate recruitment and are potential targets for the treatment of various diseases and clinical conditions. For characterization of neutrophils, we evaluated expression of chemokine receptors including CC (CCR1, CCR2, CCR3, CCR5) and CXC (CXCR1,

CXR2, CXCR3 and CXCR4) and integrin molecules (CD16, CD62L and CD11b) during primary influenza and secondary pneumococcal infection in circulating and lung-recruited neutrophils. Our results have demonstrated that CXCR2 is the most predominantly expressed and induced chemokine receptor in both circulating and lung-recruited neutrophils during primary influenza and also *S. pneumoniae* superinfection. We also found that neutrophils acquire a novel expression of chemokine receptors including CCR1, CCR2, CCR3, CCR5, CXCR1, CXCR3 and CXCR4 in lung-recruited neutrophils, but not in circulating neutrophils. CXCR2, which is highly expressed in both blood and bronchoalveolar lavage neutrophils, has diminished expression in pulmonary infiltrative neutrophils as compared with infected blood, but still is induced at the sites of inflammation in dual infection as compared with the less severe bacterial-only models. CC and other CXC chemokine receptors were minimally expressed (<10%) to absent in circulatory neutrophils, but acquire 30-40% expression on pulmonary neutrophils during severe infection. Expression of CD16 was decreased in both circulating as well as lung-recruited neutrophils, while CD62L showed significant decreased in circulating neutrophils. Interestingly, CD11b was increased in both circulating as well as lung-recruited neutrophils. Functionally, blocking receptors such as CCR5 and CXCR2 can alter reactive oxygen species and phagocytosis function, complicating their effects. Chemokine receptors offer an interesting target for novel combination therapy in influenza with secondary pneumococcal pneumonia, and this study ensures their availability and highlights their potential for this role in a murine model of this disease.

**A. Introduction**

Bacterial co-infection is a common and often lethal sequela of influenza pneumonia. Among seasonal influenza outbreaks, bacterial co-infections contribute to an estimated 65,000

deaths in the United States alone each year [2, 12]. The lethality seen with bacterial co-infection of influenza pneumonia is only compounded in pandemics, and has been well documented for all major pandemics of this previous century, starting with the 1918 "Spanish Flu" [1-4]. Preserved lung tissue sections and autopsy analysis from lethal cases of this outbreak suggest that 95% of these deaths can be attributed to co-infection [5, 6]. Of the bacterial co-infections seen in influenza pandemics over the last century, 41% have been attributed to *S. pneumoniae* – other major pathogens include *Staphylococcus spp*. (in particular *S. aureus*), *Haemophilus influenza*e, and other *Streptococcus spp*. [12].

Lethal pneumonia caused through coinfection often results in the development of acute respiratory distress syndrome (ARDS) and sepsis. Outside of anti-viral therapy and antibiotics, treatment of these complicating factors seen with dual infection pneumonia are largely supportive, and, unfortunately, many seemingly positive pharmacological agents (i.e., surfactant therapy, vasodilators, lisofylline, glucocorticoids) have no significant outcome on morbidity and mortality [175-180]. The need for more specific treatments is great, and neutrophils offer an intriguing prospect as a potential target for therapy. Unrestrained transmigration of neutrophils into areas of gas exchange in the lungs is a pathologic hallmark of influenza pneumonia and ARDS resulting in alveolar capillary damage, edema, parenchymal hemorrhage, pulmonary microvascular thrombosis, and hyperinflammatory cytokine responses. These changes are also documented in murine models of influenza pneumonia [55, 181, 182]. The excessive innate response to influenza virus leads to a series of virus-inflicted and host-mediated damages to the pulmonary epithelium and endothelium resulting in significant pathology and respiratory failure [3, 183, 184]. Acute lung damage seen in both influenza pneumonia and *S. pneumoniae* dual infections is well linked to excessive neutrophils and subsequent release of neutrophil extracellular traps (NETs) which are toxic to the host [18, 55,

57, 83, 185, 186]. The recruitment, extravasation, and activation of neutrophils are largely driven by chemokines and their receptors, justifying their value as potential therapeutic targets.

A seemingly uncontrolled influx of neutrophils during the innate immune response to acute lung injury has long been thought to be a major contributor to the development of Acute Respiratory Distress Syndrome (ARDS) seen in severe dual infection pneumonia and resulting morbidity and mortality. This transmigration of neutrophils into the interstitial and alveolar spaces is controlled in part by the interaction of chemokines released from the site of injury with their corresponding receptors. Chemokines function as chemotactic cytokines to control transmigration, recruitment, and activation of immune cells to specific areas within the body. Not only are they crucial in pathologic disease processes including the initial response to acute inflammation, they are also necessary for maintenance of homeostasis [187]. Neutrophils are rapid and powerful protectors in the innate immune response, but are thought to be limited in their chemokine receptor expression with comparison to other leukocytes [138]. Neutrophils also appear to have a different phenotype of receptors as opposed to other leukocytes, with predominant expression of the CXC receptor family as opposed to the CC ligands; although it has been more recently shown that the CCR family plays a role in chronic inflammatory conditions such as chronic respiratory disease and rheumatoid arthritis [138]. The approximately fifty endogenous chemokine ligands and their respective receptors can be classified in many ways. Expressed on all leukocytes, chemokine receptors are often divided into two groups – G-protein coupled receptors which can be activated by pertussis toxin (PTX)- sensitive $G_i$-type G proteins, and atypical chemokine receptors which are independent of G protein [187]. They can also be divided into either inflammatory or homeostatic chemokines depending on whether they are expressed in inflamed tissues to recruit leukocytes or maintain physiologic movement of leukocytes for immune reconnaissance [188].

**A.1 Integrin Receptor Expression and Functional Changes in Neutrophil Biology**.

Before focusing on chemokines and their receptors, attention must be given to integrin expression and phenotypic changes in neutrophil biology that occur during dual infection pneumonia and subsequent ARDS. Further understanding phenotypic changes in neutrophils may help to clarify why some individuals are more susceptible to secondary infections after influenza pneumonia and how neutrophil phenotypic heterogeneity contributes to disease pathology.

Various integrins and receptors have been used to characterize neutrophils via flow cytometry in addition to their forward and side scatter properties. Pillay, et al, described three morphologically distinct subsets of neutrophils that develop in response to chronic inflammation, two of which are not present in healthy controls [189]. In this study, the author used CD16 and CD62L to recognize these subsets, and defines the three groups as $CD16^{dim}/CD62L^{bright}$, $CD16^{bright}/CD62L^{dim}$, and $CD16^{bright}/CD62L^{bright}$. Phenotypically, the $CD16^{dim}/CD62L^{bright}$ neutrophils are immature cells that have recently been released from the bone marrow, also called “bands”. The $CD16^{bright}/CD62L^{dim}$ neutrophils are older and hypersegmented and the $CD16^{bright}/CD62L^{bright}$ neutrophil subset population is seen in both infected and healthy controls alike. CD16, also known as FcγRIII, is a cell surface molecule that is expressed on several cell types including neutrophils, macrophages and natural killer cells, and has been shown to have reduced expression in many inflammatory conditions such as vaginitis, trauma, bacterial infection and viral pneumonia [190-192]. It has also been suggested that the decreased CD16 expression seen with acute inflammation could be due to the influx on immature neutrophils which are $CD16^{dim}$ [189]. CD62L, also known as L-selectin, mediates neutrophil rolling and adhesion to the endothelial cells. This receptor is shed when stimulated

by pro-inflammatory cytokines such as TNF-α in acute inflammatory insults such as with trauma [191, 193] and uremia [194].

CD11b is another frequently assessed integrin in models of acute inflammation. CD11b is a β2-integrin adhesion molecule that is part of the Mac-1 heterodimer, and is a major player in neutrophil recruitment and adhesion [190, 191, 193]. In contrast to CD62L, most studies have shown that CD11b significantly increases in cases of acute inflammation, corresponding to increased neutrophil activation [190, 191, 193, 195]. To summarize, models of acute inflammation such as bacterial pneumonia (primary or secondary), viral pneumonia, trauma or burns all seem to shed CD62L and reduce CD16 expression while increasing expression of CD11b.

With increased activation during inflammatory conditions, the functional biology of these neutrophils is also drastically changed in an attempt to best combat the insult at hand. Apoptosis is downregulated during inflammation in order to prolong the neutrophil's survival and viability to fight the infection [138, 191, 192]. This downregulation is thought to be partially driven by both the intrinsic pathway – through stabilization of the mitochondrial membrane potential by increases in Mcl-1 and decreases in Bax protein, and the extrinsic pathways – increased Fas and reduced activation [191]. This decrease in rate of apoptosis is especially seen in infiltrated neutrophils, such as those in pulmonary alveoli, as opposed to those in peripheral circulation [195]. Pro-inflammatory activation of neutrophils also results in increased reactive oxygen species production [191, 193, 194], increased degranulation [194], increased release of neutrophil extracellular traps [191], and decreased phagocytosis [190, 191]. Many of these biological changes are acting in an effort to best fight the immediate insult, without regard to secondary damage to the host tissues and subsequent risk for secondary infections.

**A.2 Chemokines in dual infection pneumonia and subsequent ARDS**

Currently, treatment for ARDS is primarily supportive, and the need for more specific treatments is great. Several deceptively positive pharmacological agents have been evaluated in ALI (acute lung injury) and ARDS such as glucocorticoids, surfactants, nitric oxide and lysofylline, but several studies have now shown that these seemingly promising options do not have a significant effect on outcome and mortality [175]. Unrestrained transmigration of neutrophils into the areas of gas exchange in the lungs is a pathologic hallmark of the disease. The extravasation of these neutrophils is driven by chemokines and their receptors, justifying their value as potential therapeutic targets.

Chemokine receptor expression on the cell surface of human neutrophils has been shown to be altered by inflammation. These phenotypic changes of the cell surface not only offer insight into the development and progression of ARDS, but also potential therapeutic targets. Since a hallmark sign of ALI and ARDS includes uncontrolled accumulation of neutrophils into the alveolar space, it follows that intervention to slow or block any step in neutrophil recruitment or migration should be explored. In ARDS, there is one chemokine in particular that seems to play a pivotal role – interleukin-8 (IL-8/CXCL8) which is seen in increased concentrations in pulmonary edema fluid from septic patients with ARDS [124] and is also found in lower concentrations in ARDS survivors as opposed to non-survivors, making IL-8 a prognostic indicator [125]. CXCL8 is one ligand that binds with both CXCR1 and CXCR2 in humans and is considered the most potent neutrophil chemoattractant in BAL fluid from ARDS patients [126].

CXCR1 and CXCR2 are both G-protein coupled receptors and are expressed in several granulocytes including eosinophils, mast cells, T cells, and, most notably, neutrophils [127, 128].

In addition to granulocytes, CXCR2 is also found on pulmonary endothelial and bronchial epithelial cells, and the additional role of CXCR2 on these non-hematopoietic cells has been shown to be necessary for the marked increase in lung microvascular permeability seen in an LPS-induced model of ARDS [129]. In addition to IL-8 (CXCL8), CXCR2 has at least six other ligands including CXCL1, CXCL2, CXCL3, and CXCL6 [130]. These chemokines are called ELR+ chemokines (glutamic acid-leucine-arginine containing) and have been shown to mediate aberrant vascular remodeling in addition to inflammatory cell recruitment in both the exudative and fibroproliferative stages of alveoli damage in ARDS [131]. In addition to a role in ARDS, CXCR2 has been a hot topic of study for several years due to promising roles in numerous diseases ranging from cancer to arthritis to other more chronic pulmonary diseases [132-136].

CXCL8 is not the only chemokine that has been considered potentially important in the development and progression of ARDS. Several chemokine receptors have been shown to be affected by inflammatory disease, and further investigation may indicate a role in ARDS as well. A study looking at chemokine receptor expression in patients with chronic obstructive pulmonary disorder (COPD) and rheumatoid arthritis found several significant alterations in neutrophil phenotype involving CCR1, CCR2, CCR3, CCR5, CXCR3, and CXCR4 in BAL fluid when compared to circulating neutrophils [138]. In addition to evaluating chemokine receptor expression, Hartl et al. also explored whether neutrophils would chemotax to a variety of CC and CXC ligands and found this to be the case. These findings may have been inferred from chronic inflammatory disease, but do support that neutrophils with various receptors can respond to a variety of ligands, likely even in ARDS.

The roles of CCR1, CCR2, and CCR3 have been further studied in a more acute, LPS-induced ALI model. Antagonism of these three receptors was shown to have a protective effect

– when a CCR2b and CCR1 antagonist was used, decreases in fibrinolysis, vascular leakage and inflammatory gene expression were all noted. These findings were further supported in CCR1, CCR2, and CCR3 knockout mice which had less pulmonary edema, infiltration and overall disease as compared with controls with ALI [145]. CXCR3 has also been further evaluated for its role in ARDS with its ligand CXCL10. CXCL10 is considered a non-ELR chemokine. Ichikawa et al. evaluated both a viral and non-viral ARDS mouse model in mice deficient in CXCL10 and CXCR3 and found that mice lacking CXCL10 and CXCR3 had improved severity of disease and survival in both models [151]. Therefore, this receptor poses another intriguing potential target for therapeutics in ARDS. CXCL12 and its receptor, CXCR4, also appear to play a role in promoting chemotaxis of neutrophils as well as suppressing cell death. In a study looking at lipopolysaccharide (LPS)-induced lung injury, CXCL12 was shown to be a chemoattractant for cells expressing CXCR4 as well as a suppressant of neutrophil cell death and CXCR4 was found to be increased on the neutrophil cell surface after migrating from circulation into the inflamed lungs, possibly via an L-selectin mediated pathway [154]. CXCR4 has been further described as acting antagonistically with against CXCR2 – CXCR4 expression promotes neutrophil retention in the bone marrow, whereas CXCR2 expression drives release [158]. Finally, CCL2 and CCL7 are also chemokines that may play an interesting part in ARDS – in a study performed by Mercer et al, antibody neutralization of these ligands significantly reduced neutrophil accumulation in the BAL fluid in mice with LPS-induced lung injury [146].

Neutrophils are generally thought to be limited in their chemokine receptor expression with comparison to other leukocytes [138, 196, 197], but several recent studies have shown that neutrophils acquire a novel chemokine receptor expression under various conditions of inflammation and injury [138, 198, 199]. These various chemokine receptors have been shown to be significant contributors to many diseases such as cancer [132, 134], arthritis [133], acute

lung injury [145], and various chronic pulmonary diseases [135, 136]. Despite what is known about neutrophils and their role in the pathogenesis of dual infection influenza pneumonia, this study is the first to our knowledge to provide a more complete understanding of the novel chemokine receptor expression obtained on neutrophils after infiltration to the lung in dual infection influenza pneumonia.

A more thorough understanding of the neutrophils' phenotype after recruitment to the lung in acute dual infection influenza pneumonia is required to better evaluate the neutrophil for targets with clinical potential in human disease. To address this need, we established a murine model for dual infection influenza pneumonia and evaluated neutrophil numbers as well as chemokine receptor expression at various time points through the disease course. Using flow cytometry analysis, we evaluated expression of chemokine receptors between circulating neutrophils and those which have recruited into the lungs in primary influenza pneumonia and with subsequent bacterial coinfection. In addition, effects of these altered chemokine receptors on neutrophil functional responsiveness were evaluated by neutrophil phagocytic activities and respiratory burst (measured by reactive oxygen species generation) by activating these chemokine receptors with their corresponding ligands in the presence or absence of receptor antibodies or antagonists/inhibitors.

**B. Methods**

*Virus and Bacteria*

Influenza A/Puerto Rico/8/34, H1N1 (PR/8) virus was obtained from the American Type Culture Collection (ATCC, VA). Viral titers were determined by tissue culture infectivity dose ($TCID_{50}$) assay via infection of Madin-Darby canine kidney (MDCK) cells. *Streptococcus pneumoniae*

(serotype 3) was also obtained from the ATCC. Bacterial growth curves were established prior to infection. All pathogens were stored at -80°C until use.

*Animals*

Female Balb/c mice ranging from 6 to 10 weeks' old were purchased from Jackson Laboratories. Mice were group-housed in microisolator cages in a BSL-2 facility, and were provided with food and fresh water ad libitum. Mice were clinically scored based on a modified version of the "mouse clinical assessment scoring for sepsis" (M-CASS) [172]. Infection was performed under a mixture of xylazine (0.1 mg/kg) and ketamine (7.5 mg/kg) anesthetic via intraperitoneal injection. Mice were infected intranasally (IN) with a sublethal dose of 100 $TCID_{50}$ PR/8 (H1N1) influenza in a 50 µl volume or given an equal volume of sterile phosphate-buffered saline in controls. For dual infection studies, mice were administered 200 colony forming units (CFU) of *S. pneumoniae* IN in 50 µl volumes 72 hours after initial influenza infection, or administered PBS IN for controls. Mice were monitored closely for weight loss and clinical signs based on a modified "mouse clinical assessment score for sepsis" [172, 173]. All animal experiments were approved by the Institutional Animal Care and Use Committee (IACUC) of Oklahoma State University and were performed in strict accordance with their recommendations.

*Whole blood, bronchoalveolar lavage (BAL) fluid, and tissue collection*

For BAL fluid collection, the lungs were washed by intratracheal administration of 1.0 mL of sterile PBS in two 0.5 mL increments [55]. The recovery of BAL fluid was more than 85% for all animals. The BAL fluids were centrifuged at 200 xg for 10 minutes, and reconstituted in sterile PBS for cell counts and with 2% fetal bovine serum in PBS for flow cytometry analysis. BAL cells were concentrated using the CytoFuge 2 cytocentrifuge (StatSpin, Westwood, MA), and

differential cell counts were performed using modified Giemsa staining. Whole blood was collected via terminal procedure of intra-cardiac collection. Bronchoalveolar lavage fluid and whole blood (intracardiac) were collected from 3 to 5 days' post influenza infection for flow cytometry analysis and other studies. Lungs from mice who did not have BAL collection were fixed with 4% formalin and collected for histopathology analysis after hematoxylin and eosin (H&E) staining. Mice were scored on a 1-4 scale (4 being most severe) for severity in the following areas by a blinded, board-certified anatomic veterinary pathologist: necrotizing bronchiolitis, bronchiolar infiltrates, alveolitis, interstitial inflammation, hemorrhage, edema, and microvascular thrombosis. Total histopathologic scores were evaluated as a sum of all individual scores.

*Flow Cytometry*

The following antibodies were purchased from R&D (MN) Systems and used throughout the course of this study for chemokine receptor expression characterization of murine neutrophils: Mouse CCR1 Fluorescein isothiocyanate (FITC)-conjugated antibody, mouse CCR2 phycoerythrin (PE)-conjugated antibody, mouse CCR3 PE-conjugated antibody, mouse CCR5 FITC-conjugated antibody, mouse CXCR1/IL-8 RA PE-conjugated antibody, mouse CXCR2/IL-8 RB PE-conjugated antibody, mouse CXCR3 PE-conjugated antibody, and mouse CXCR4 fluorescein-conjugated antibody. These antibodies were selected due to their previously reviewed relevance in chronic inflammatory conditions and potential for therapeutic targeting [138]. Additional antibodies used in this study include mouse Ly6G (1A8) Peridinin Chlorophyll Protein Complex (PerCP)-conjugated antibody (Biolegend, CA), mouse Fc gamma RIII (CD16) FITC-conjugated antibody (R&D, MN), mouse L-selectin (CD62L) PE-conjugated antibody (R&D, MN), mouse integrin alpha M/CD11b FITC-conjugated antibody (R&D, MN). In all flow cytometry studies, control BAL fluid

was not compared due to a lack of pulmonary neutrophils in naïve Balb/c mice. The collected whole blood and BAL fluid were aliquoted into 200 µl volumes for antibody staining. 2.0 ml of 1x PharmLyse Buffer was used for red blood cell lysis and allowed to lyse for 15 minutes at room temperature. Samples were allowed to stain for 30 minutes, covered, at room temperature on a shaker. All samples were then centrifuged and washed with chilled PBS (with 2% FBS) 1-3 times before performing flow cytometry. Flow cytometry was performed on the BD FACSCalibur flow cytometer and analyzed with the corresponding CellPro software. Neutrophils were gated as Ly6G-1A8$^{+}$SSC$^{med\text{-}hi}$. CD11b analysis was performed comparing mean fluorescence intensity between samples.

*PMN Functional Assays*

A 2'-7'-Dichlorodihydrofluorecein diacetate (DCFH-DA) flow cytometric assay (Invitrogen, CA) was used to assess reactive oxygen species production (ROS) in neutrophils from BAL fluid. In brief, BAL cells, with no added stimulation after collection, were treated with DCFH-DA and Ly6G-1A8 (Per-CP) antibody for 30 minutes at room temperature. The cells were then immediately analyzed using flow cytometry, and mean fluorescence intensity (X-Mean) compared between samples. In order to assess ROS function for CCR1, CCR3, CCR5, CXCR2, CXCR3, and CXCR4, a DCFH-DA (abcam, UK) flow cytometric assay was again used. BAL and blood were collected 3 days' post influenza infection (1000 $TCID_{50}$ PR/8) from 6 mice. Two mice were pooled for each sample. Neutrophils were isolated using the MACS neutrophil isolation kit (Miltenyi Biotec, Germany) as per protocol. Neutrophils were then divided between tubes with $10^5$ cells/100 µL volume per sample. 1 µg BX 471 (CCR1 Antagonist; Cayman Chemicals, MI), SB328437 (CCR3 Antagonist; Sigma, MN), CCR5 (Novus, CO), CXCR2 (Cell Applications, CA), CXCR3 (Bio X Cell, NH) blocking antibodies, and AMD3100 (CXCR4 Antagonist (R&D, MN) were

added in half the samples and incubated for 30 minutes at 37° C before adding 10 ng of the appropriate ligand (CCL3, CCL11, CCL4 (R&D, MN), IL-8, CXCL11, and CXCL12 (R&D, MN)) to all samples. 20 μM DCFH-DA was then added to each sample and the samples were incubated at 37°C for 30 minutes before analysis via flow cytometry. Flow cytometry was performed on the BD FACS Aria. Results were compared via mean fluorescence intensity (MFI) using X-means. Data was graphed as relative function of the blocked samples to unblocked (x:1).

For phagocytosis assays, BAL and blood were collected 3 days' post influenza infection (1000 $TCID_{50}$ PR/8) and neutrophils isolated, divided and treated with or without the appropriate CCR1, CCR3, CCR5, CXCR2, CXCR3, and CXCR4 blockers and ligands as per ROS assay. 1 μg BX 471 (CCR1 Antagonist; Cayman Chemicals, MI), SB328437 (CCR3 Antagonist; Sigma, MN), CCR5 (Novus, CO), CXCR2 (Cell Applications, CA), CXCR3 (Bio X Cell, NH) blocking antibodies, and AMD3100 (CXCR4 Antagonist (R&D, MN) were added in half the samples and incubated for 30 minutes at 37° C before adding 10 ng of the appropriate ligand (CCL3, CCL11, CCL4 (R&D, MN), IL-8, CXCL11, and CXCL12 (R&D, MN)) to all samples. pHrodo™ Red *E. coli* BioParticles (ThermoFisher, MA) were added to each sample (1 mg/mL), and cells were allowed to incubate at 37°C for 1.5 hours. Cells were then stained with Ly6G-1A8 antibody for 30 minutes at room temperature and washed twice to remove excess bacteria before flow cytometry. Flow cytometry was performed on the BD FACS Aria. Unstained, single-stained and no cell controls were used for data analysis. Results were compared via MFI. Data was graphed as relative function of the blocked samples to the unblocked (x:1).

*Statistical Analysis*

The data are expressed as the means ± SEM. Statistical analyses were performed using Student's unpaired t-test, paired t-test or analysis of variance (ANOVA) using GraphPad Prism 7 software. $p < 0.05$ was considered statistically significant.

**C. Results**

***C.1. Dual infection results in excessive neutrophil influx and extensive pulmonary damage.*** Our murine model for dual infection pneumonia is highlighted by the development of bacteremia (confirmed by culture) approximately 48-60 hours after administration of *S. pneumoniae* with 100% lethality before day 7 post influenza infection. Clinically, the mice receiving the dual infection have severe weight loss [Fig. 1.1] and rapid clinical decline from the time of bacterial superinfection on day 3 [Fig. 1.2]. *S. pneumoniae* alone infected mice did not lose significant weight. The weight loss seen in the dual infection groups mimic that in the influenza-only infected groups with a matched decline beginning at three days' post infection [Fig. 1.1]. Although the decline in clinical scores is similar start at day 2 post infection with influenza-only and dual-infected mice, the clinical scores for mice with dual infection pneumonia is more severe by the endpoint, day 6, than in viral infection only [Fig. 1.2]. The sharp decline in clinical scores in the dual-infected mice correlates with the onset of bacteremia and the development of severe ARDS.

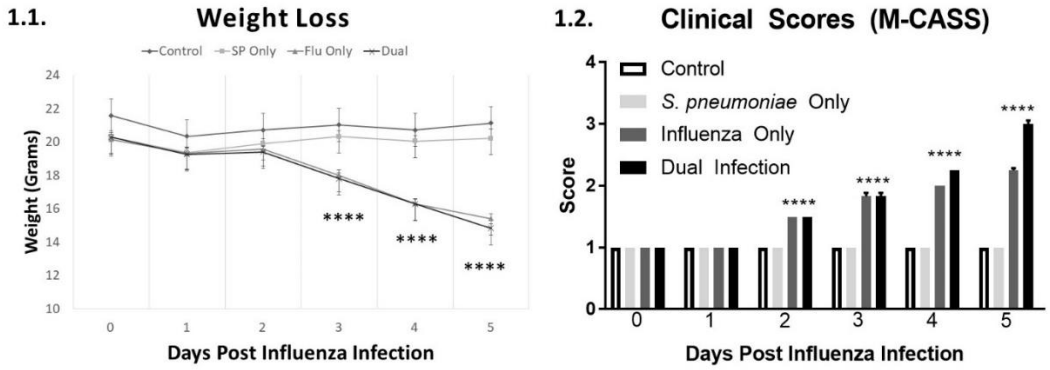


**Figure 1.1 and 1.2 (see also Fig. 4.1 in Ch. 2):** ***Dual infected mice lose considerable weight and have most severe clinical score by day 5***. Balb/c mice were infected with sublethal doses (100 $TCID_{50}$ intranasally) of influenza A/Puerto Rico/8/34 H1N1 virus or PBS followed by sublethal *S. pneumoniae* (200 CFU IN) or PBS three days after initial influenza infection. **1.1** and **1.2**: Infected mice lost significant weight and had significant increase in severity of clinical score starting on day 3 as compared with control and *S. pneumoniae*-only infected mice. Significant differences ($p$<0.0001) were also noted between influenza only and dual infected clinical scores on days 4 and 5. Data were expressed as means ± SEM and compared via one-way ANOVA. n = 21 mice per group. **** p<0.0001 (relative to healthy controls).

BAL fluid cell counts performed on days 3-5 post influenza infection show an increase in total cell numbers through day 5 of the dual-infected group with cell counts about 1.5 times higher in dual infected BAL as compared with influenza-only groups [Fig. 1.3, 1.4].

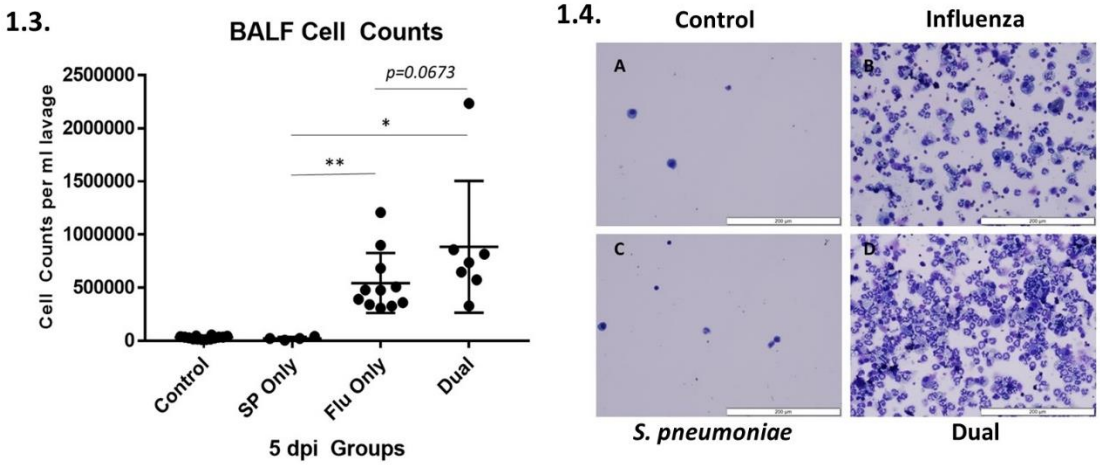

**Figures 1.3 and 1.4 (See also Fig. 4.2 in Ch. 2): *Significant inflammatory cell influx noted in both dual and influenza only infected mice***. Balb/c mice were infected with sublethal doses (100 $TCID_{50}$ intranasally) of influenza A/Puerto Rico/8/34 H1N1 virus or PBS followed by sublethal *S. pneumoniae* (200 CFU IN) or PBS three days after initial influenza infection. **1.3** and **1.4**: Influenza-infected and dual-infected groups have significantly more cells in the BAL fluid than in *S. pneumoniae*-only infected groups as seen from cell counts performed via hemocytometer and cytospin data. A trend toward a significant increase in cell counts in dual infected mice compared with viral-only was also noted. Data were expressed as means ± SEM and compared via unpaired t-tests. n = 7-11 mice per group. * $p<0.05$; ** $p<0.01$ (relative to SP Only).

BAL differentials consistently indicate that the majority of these cells are neutrophils in both the influenza-only and dual infected groups, however there is a significantly greater percentage of neutrophils in the dual-infected mice than in the influenza-only infected mice [Fig. 1.5].

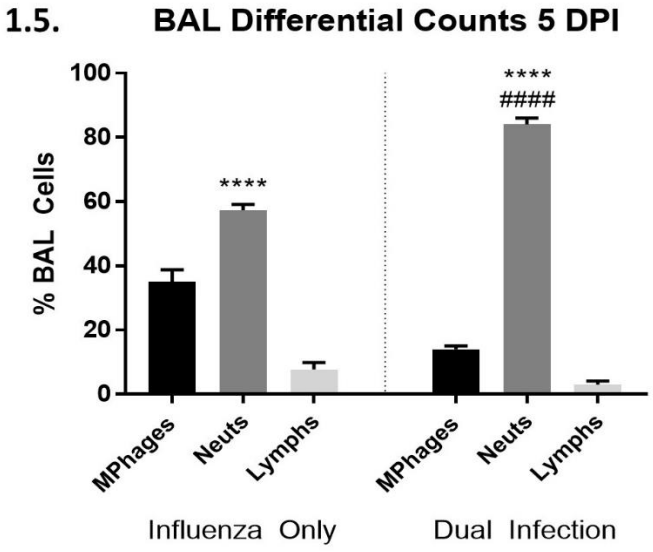


**Figure 1.5 (see also Fig. 4.3 in Ch. 2): *Inflammatory cell influx is marked by neutrophilia***. Balb/c mice were infected with sublethal doses (100 $TCID_{50}$ intranasally) of influenza A/Puerto Rico/8/34 H1N1 virus or PBS followed by sublethal *S. pneumoniae* (200 CFU IN) or PBS three days after initial influenza infection. Differentials performed on BAL fluid cells viewed after cytospin revealed majority neutrophils, especially noted in dual infections, with a significantly higher percentage of neutrophils in dual differentials compared with influenza alone. Data were expressed as means ± SEM and compared via unpaired t-test. n = 3 mice per group. **** $p<0.0001$ relative to lymphocytes and #### $p<0.0001$ relative to macrophages.

***C.2. Histopathology analyses.*** The clinical decline seen in our murine model can further be explained by examining histopathology. The following pulmonary pathologies were scored on a 1-4 scale with 4 being most severe: necrotizing bronchiolitis, bronchiolar infiltrates, alveolitis, interstitial inflammation, hemorrhage, edema, and microvascular thrombosis. Total score (sum of individuals) was most severe in viral-only and dual-infected mice with only mild pathology noted in bacterial-only infected mice [Fig. 2.1].

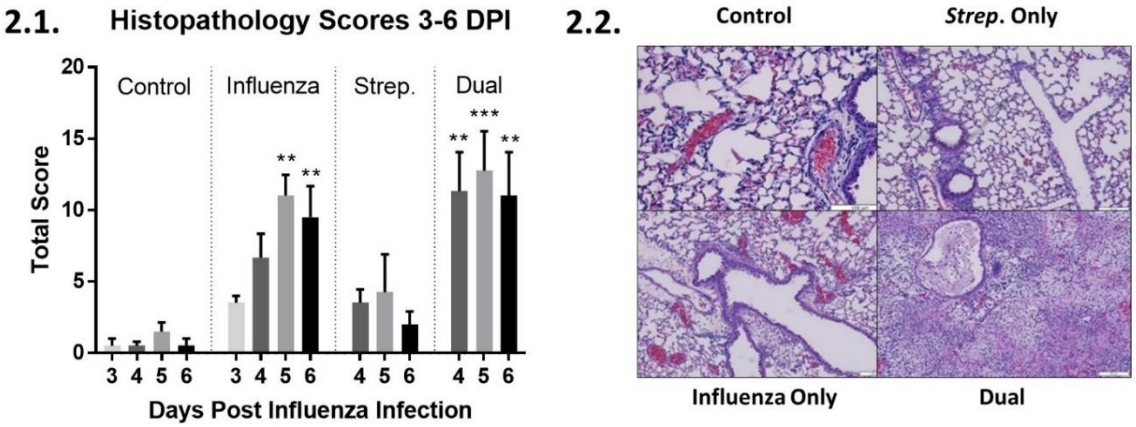


**Figures 2.1 and 2.2 (See also Fig. 4.5 in Ch. 2):** ***Dual infection results in severe pulmonary pathology and extensive damage.*** **2.1**: Lungs were collected and formalin-fixed for histopathology analysis between days 3-6 post influenza infection. Day 3 samples for *S. pneumoniae*-only and dual infections were not collected since bacterial inoculation was performed at that time. Figure presents sum of scoring. **2.2:** Paraffin-embedded lung tissues from 5 days post-challenge with infection or mock infection were stained with hematoxylin and eosin. Tissues affected through dual infection show most severe score with notable pulmonary edema, bronchiolitis, alveolitis, hemorrhage, microvacular thrombosis and interstitial disease. Infected samples were compared with controls. Data were expressed as means ± SEM and compared via one-way ANOVA. n = 4 mice per group. * $p<0.05$; ** $p<0.01$; *** $p<0.001$ (relative to healthy controls).

Mice infected with influenza-only and dual infection develop marked pulmonary edema, interstitial inflammation, necrotizing bronchiolitis, alveolitis, and hemorrhage, with dual infected lungs more severely and diffusely affected than that of influenza-only infected pulmonary tissue

[Fig. 2.2, 2.3]. This damage as well as a heavy influx of neutrophils is evident when viewing the tissue from fixed specimens. In addition, large areas of pulmonary tissue are severely affected in our dual-infected model with little recognizable pulmonary architecture [Fig. 2.2]. Microvascular thrombosis was only recognized in influenza-only and dual-infected mice [Fig. 2.3]. No pathology was noted in the heart, liver, kidney, spleen, esophagus, small intestine, pancreas, or brain in any sample (data not included) in our model.

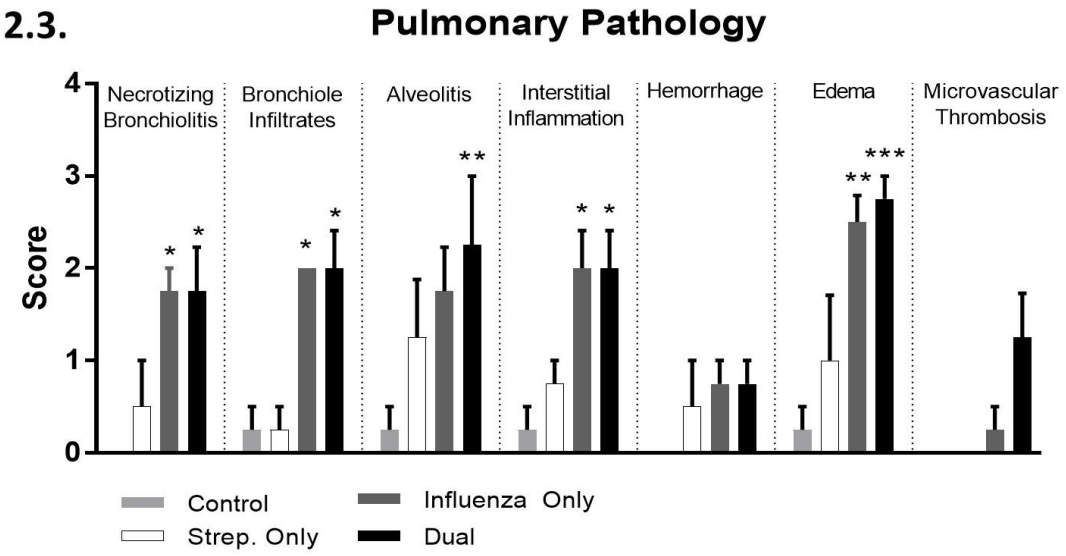


**Figure 2.3 (See also Fig. 4.6 in Ch. 2):** ***Dual and Influenza Only infected mice have significant pulmonary pathology and microvascular thrombosis*****.** Individual areas scored include: necrotizing bronchiolitis, bronchiole infiltrates, alveolitis, interstitial inflammation, hemorrhage, edema, and microvascular thrombosis. Infected samples were compared with controls. Data were expressed as means ± SEM and compared via one-way ANOVA. n = 4 mice per group. * $p<0.05$; ** $p<0.01$; *** $p<0.001$ (relative to healthy controls).

***C.3. Lung-Infiltrated neutrophils acquire a novel chemokine receptor expression in a murine dual infection model*****.** We gated circulatory and infiltrated pulmonary neutrophils based on their FSC/SSC characteristics and expression of Ly6G-1A8. This approach was able to differentiate neutrophils ($FSC^{med}SSC^{med\text{-}hi}Ly6G\text{-}1A8^{+}$) from other leukocytes present in the samples [Fig 3.1].

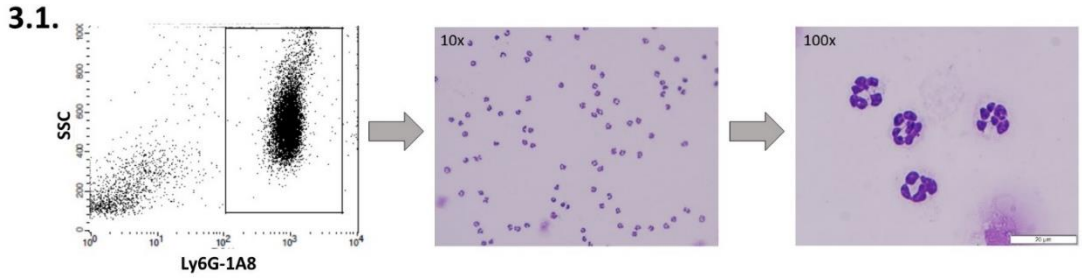


**Figure 3.1:** ***Selection of neutrophils using flow cytometry*****.** $FSC^{med}SSC^{med\text{-}hi}Ly6G\text{-}1A8^{+}$ cells are over 99% neutrophils as confirmed through cell sorting using the FACSAria flow cytometer.

We selected a wide variety of chemokine receptors to assess through flow cytometry (CCR1-3, CCR5, CXCR1-4) from day 3 through day 5 after influenza infection, based in part by their clinical potential and previous interest in other models [138]. In dual infection samples, *S. pneumoniae* was administered on day 3, hence the lack of variance between influenza-only and dual infection groups on day 3. Our results indicate that neutrophils acquire a novel chemokine receptor expression upon infiltration into the lungs after infection with both influenza and influenza with subsequent pneumococcal pneumonia.

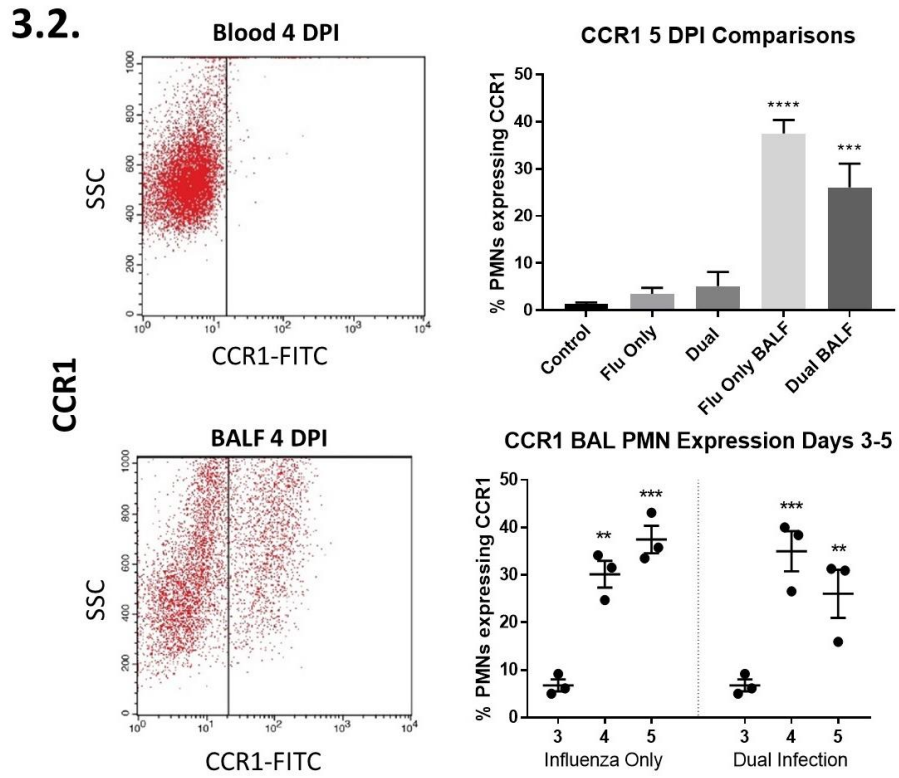


**Figure 3.2:** ***CCR1-Receptor Expression is induced in infiltrative pulmonary neutrophils*.** Blood and bronchoalveolar lavage (BAL) fluid were collected from influenza-only, dual, and mock-infected mice on days 3-5 post initial infection. Sample were analyzed via flow cytometry and % expression on neutrophils compared between groups. Neutrophils were gated as Ly6G-1A8$^{+}$ cells for subsequent analysis. Column 1 shows dot plots for blood and BAL fluid neutrophil flow analysis, respectively, from 4 days' post influenza infection. Column 2 shows comparisons in % of neutrophils expressing the indicated receptor in blood and BAL fluid samples from 5 days' post influenza infection and demonstrates the overall trend in % expression of receptor on neutrophils in all samples from days 3 through 5 post influenza infection. **3.2**: CCR1 is induced in infiltrative pulmonary neutrophils (compared to control blood), most notably on days 4-5 (compared to day 3), but no differences are noted between influenza-only and dual-infected groups. Data are expressed as mean ± SEM and comparisons were made via one-way ANOVA and unpaired t-tests. n = 3 mice per group for all studies. * $p$<0.05; ** $p$<0.01; *** $p$<0.001; **** $p$<0.0001

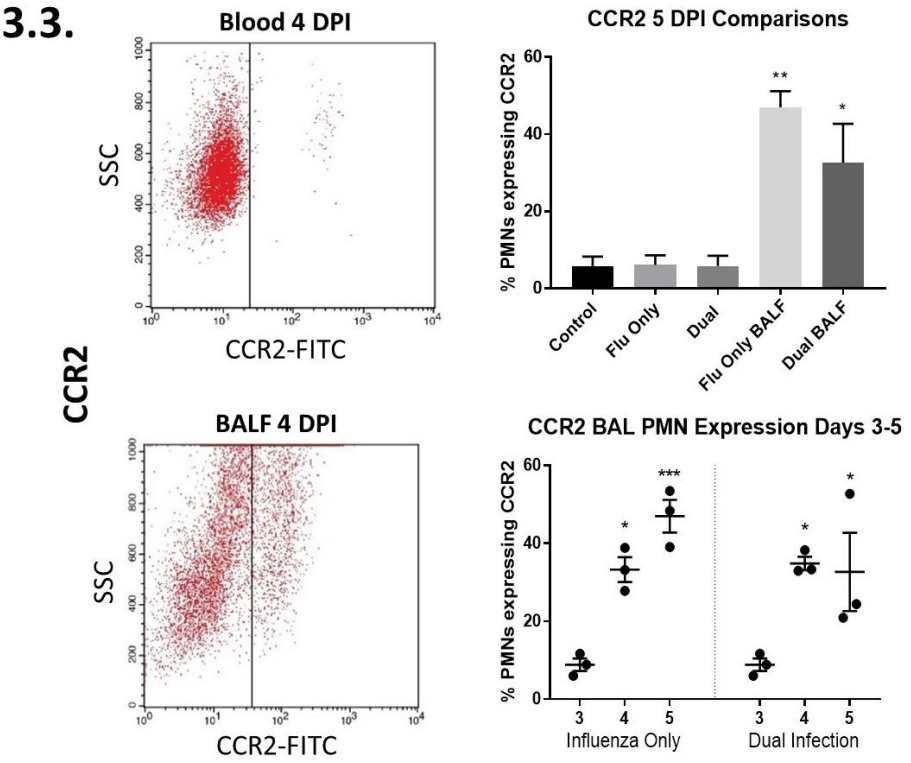


**Figure 3.3:** ***CCR2-Receptor Expression is induced in infiltrative pulmonary neutrophils.*** CCR2 is induced in infiltrative pulmonary neutrophils (compared to control blood), most notably on days 4-5 (compared to day 3), but no differences are noted between influenza-only and dual-infected groups. Data are expressed as mean ± SEM and were compared via one-way ANOVA and t-tests. n = 3 mice per group for all studies. * $p<0.05$; ** $p<0.01$; *** $p<0.001$; **** $p<0.0001$

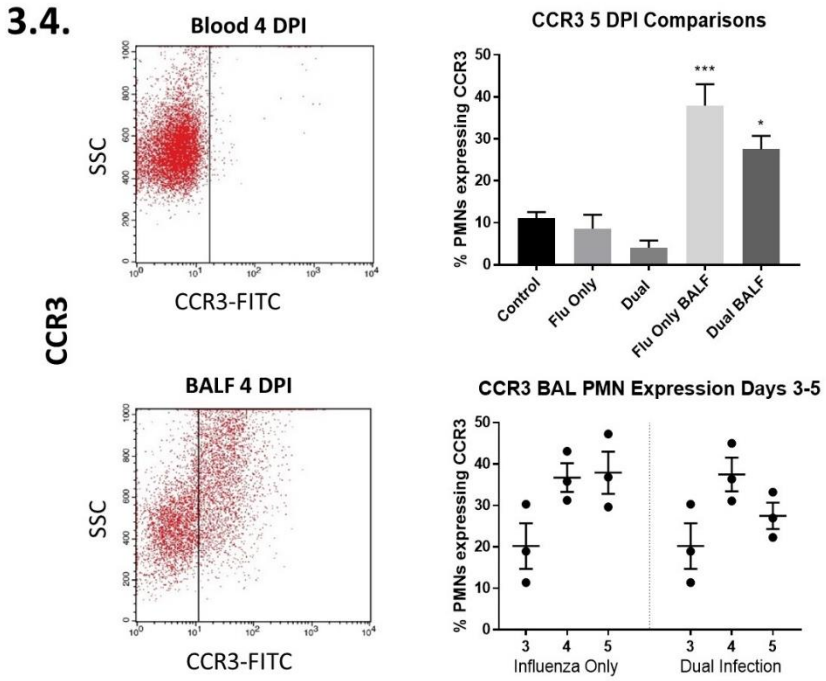


**Figure 3.4:** ***CCR3-Receptor Expression is induced in infiltrative pulmonary neutrophils.*** CCR3 is induced in infiltrative pulmonary neutrophils (compared with control blood), with no significant changes in BAL neutrophils from days 3-5, and no significant differences between influenza-only and dual-infected groups. Data are expressed as mean ± SEM and comparisons made via one-way ANOVA and t-tests. n = 3 mice per group for all studies. * $p<0.05$; ** $p<0.01$; *** $p<0.001$; **** $p<0.0001$.

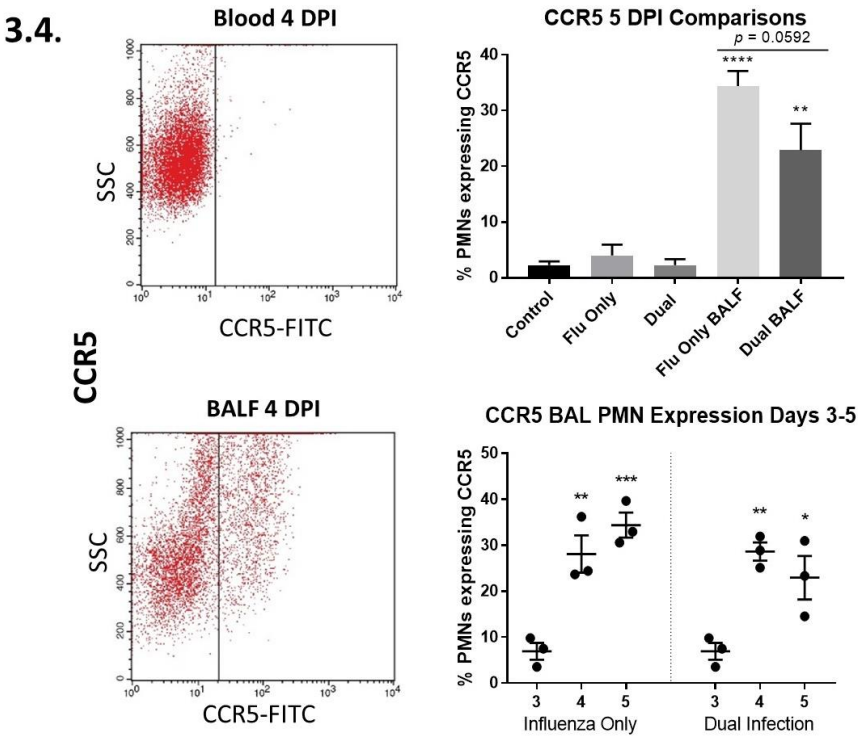


**Figure 3.5:** ***CCR5-Receptor Expression is induced in infiltrative pulmonary neutrophils.*** CCR5 is induced in infiltrative pulmonary neutrophils (compared to healthy blood), most notably on days 4-5 (compared to day 3), and a trend toward differences exists between influenza-only and dual-infected groups. Data are expressed as mean ± SEM and comparisons made via one-way ANOVA and t-tests. n = 3 mice per group for all studies. * $p<0.05$; ** $p<0.01$; *** $p<0.001$; **** $p<0.0001$

Aside from CXCR2, chemokine receptor expression was minimal to absent in control, influenza-only, or dual-infected blood samples [Figures 3, 4] with fewer than 10% of circulating neutrophils expressing these receptors. In comparison with circulatory neutrophils, our results show that infiltrated neutrophils in BAL fluid have a significant increase in chemokine receptor expression for all receptors analyzed other than CXCR2 [Figures 3, 4] with most resulting in about 30-40% expression on pulmonary neutrophils. The acquisition of this novel receptor expression is most notable on days 4 and 5 post influenza infection with significant increases in expression seen in CCR1, CCR2, CCR5, CXCR1, CXCR3, and CXCR4 by day 4 as compared with day

3 [Figures 3, 4]. CCR5 expression appears to be higher in dual-infected pulmonary neutrophils than in viral-only infected pulmonary neutrophils ($p$=0.0592) [Fig. 3.5], and a significant difference seen between viral and dual-infected pulmonary neutrophils with CXCR4 [Fig. 3.9].

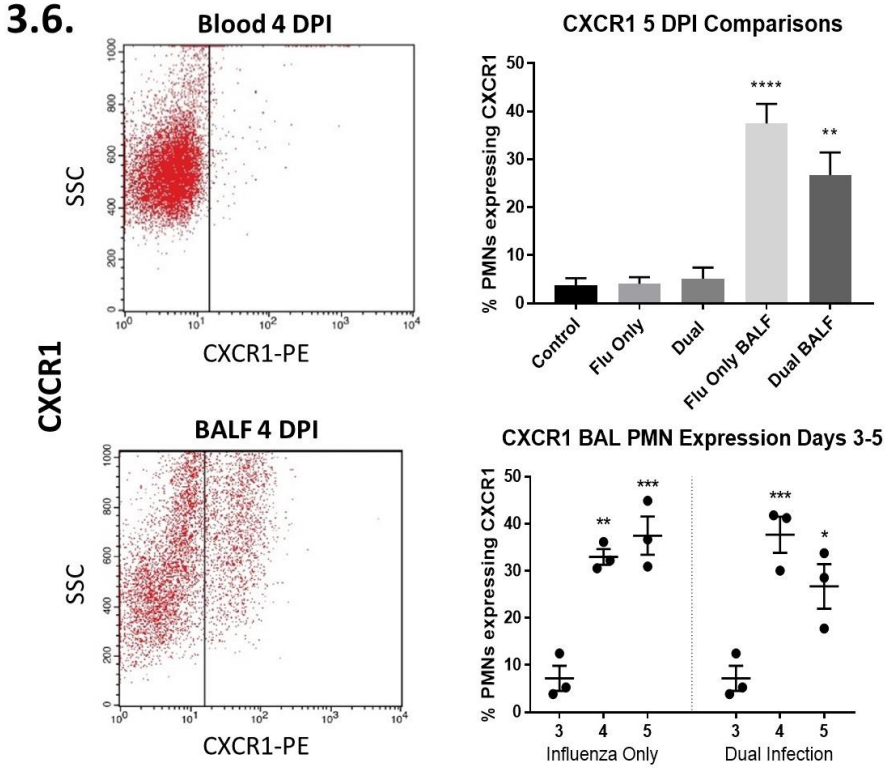


**Figure 3.6:** ***CXCR1-Receptor Expression is induced in infiltrative pulmonary neutrophils*****.** Blood and bronchoalveolar lavage (BAL) fluid were collected from influenza-only, dual, and mock-infected mice on days 3-5 post initial infection. Sample were analyzed via flow cytometry and % expression on neutrophils compared between groups. Neutrophils were gated as Ly6G-1A8$^{+}$ cells for subsequent analysis. Column 1 shows dot plots for blood and BAL fluid neutrophil flow analysis, respectively, from 4 days post influenza infection. Column 2 shows comparisons in % of neutrophils expressing the indicated receptor in blood and BAL fluid samples from 5 days post influenza infection and demonstrates the overall trend in % expression of receptor on neutrophils in all samples from days 3 through 5 post influenza infection. CXCR1 is induced in infiltrative pulmonary neutrophils (compared to control blood), most notably on days 4-5 (compared to day 3), but no differences are noted between influenza-only and dual-infected groups. Data are expressed as mean ± SEM and comparisons were made via one-way ANOVA and t-tests. n = 3 mice per group for all studies. * $p$<0.05; ** $p$<0.01; *** $p$<0.001; **** $p$<0.0001.

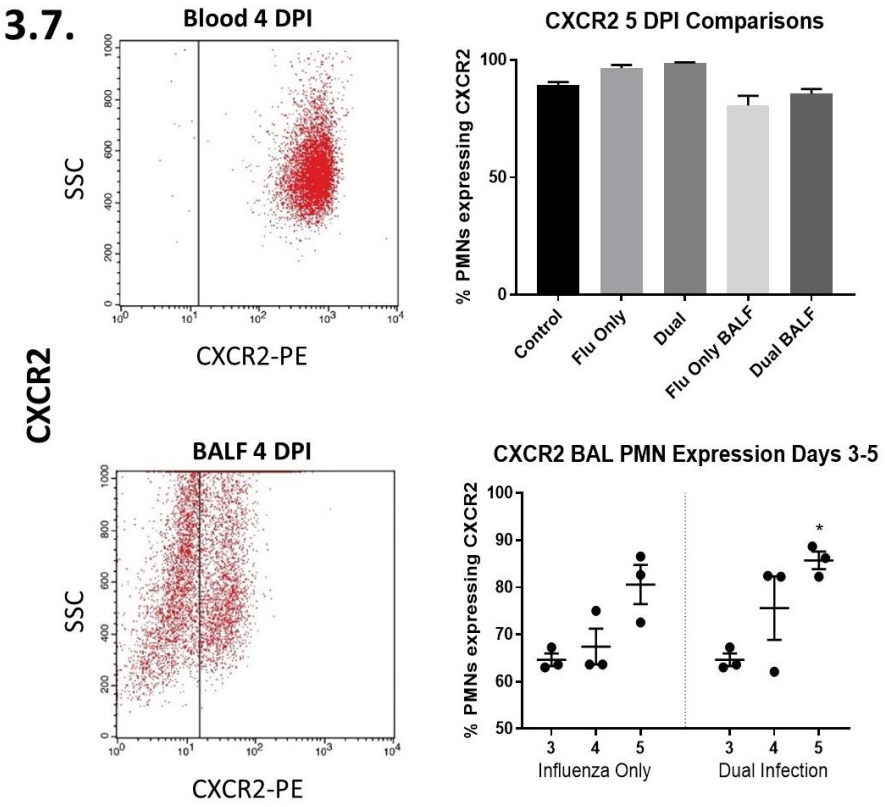


**Figure 3.7:** ***CXCR2-Receptor Expression is induced in infiltrative pulmonary neutrophils*****.** CXCR2 is reduced in infiltrative pulmonary neutrophils as compared with blood, but induced within the BAL between days 3-5 post infection, but no differences in % expression are noted between influenza-only and dual-infected groups on 5 DPI. Data are expressed as mean ± SEM and comparisons made via one-way ANOVA and t-tests. n = 3 mice per group for all studies. * $p<0.05$; ** $p<0.01$; *** $p<0.001$; **** $p<0.0001$.

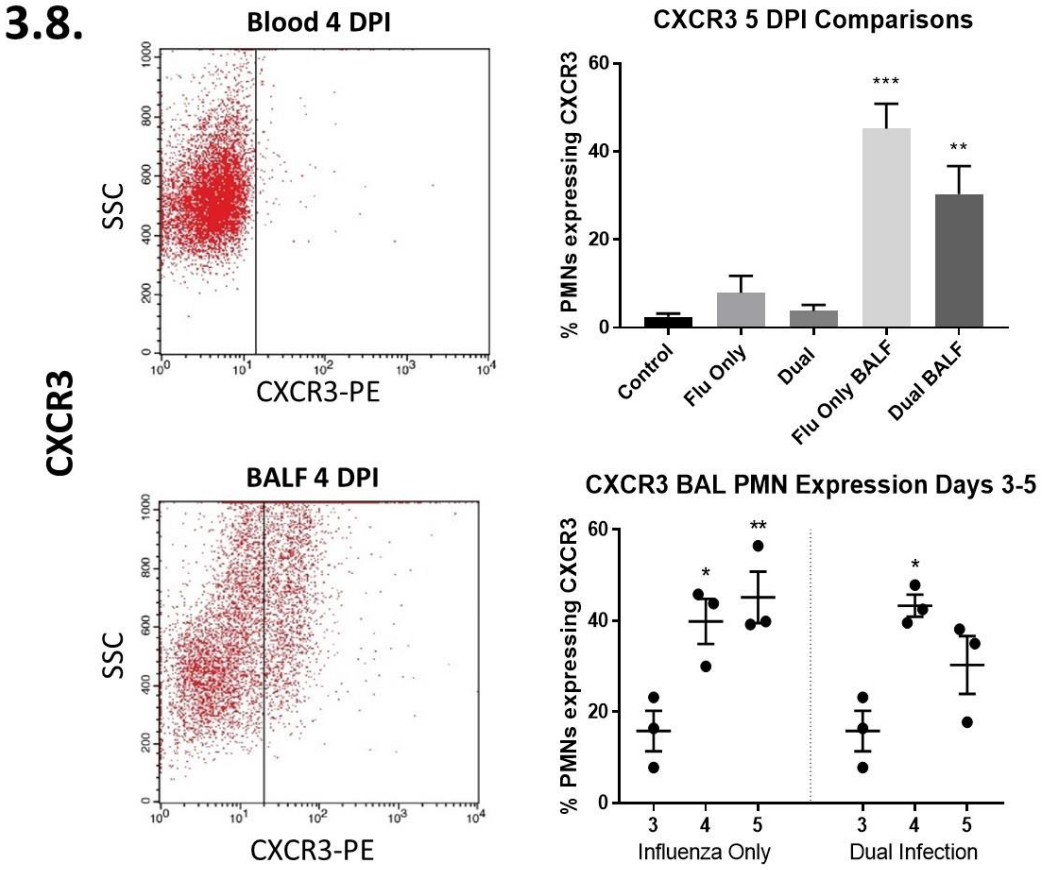


**Figure 3.8:** ***CXCR3-Receptor Expression is induced in infiltrative pulmonary neutrophils*****.** CXCR3 is induced in infiltrative pulmonary neutrophils (compared with control blood), most notably on days 4-5, but no differences are noted between influenza-only and dual-infected groups. Data are expressed as mean ± SEM and comparisons made via one-way ANOVA and t-tests. n = 3 mice per group for all studies. * $p<0.05$; ** $p<0.01$; *** $p<0.001$; **** $p<0.0001$.

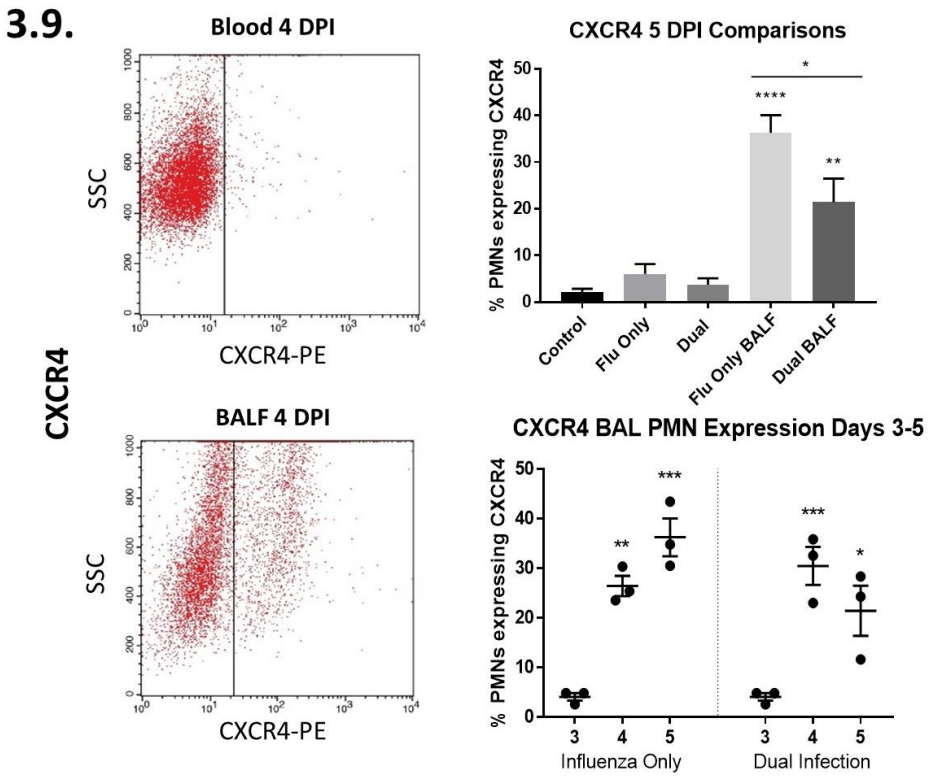


**Figure 3.9:** ***CXCR4-Receptor Expression is induced in infiltrative pulmonary neutrophils*.** CXCR4 is induced in infiltrative pulmonary neutrophils (compared with control blood), most notably on days 4-5, and a significant difference exists between influenza-only and dual-infected BAL groups on day 5 post influenza infection. Data are expressed as mean ± SEM and comparisons made via one-way ANOVA and t-tests. n = 3 mice per group for all studies. * $p$<0.05; ** $p$<0.01; *** $p$<0.001; **** $p$<0.0001.

These overall trends can be further visualized through Figure 3.10, 3.11, and 3.12 which show significant differences in pulmonary infiltrated neutrophils versus those in circulation from day 3 through 5 post initial influenza infection. Although this induction is apparent from 3 days after influenza infection, it significantly increases after the third day and is maximally expressed on days 4 and 5 post initial influenza infection. Figure 5 also clearly shows that CXCR2 is highly expressed in both blood and BAL neutrophils under healthy conditions, and this chemokine receptor is the only one tested that has reduced expression upon infiltration into the infected lung.

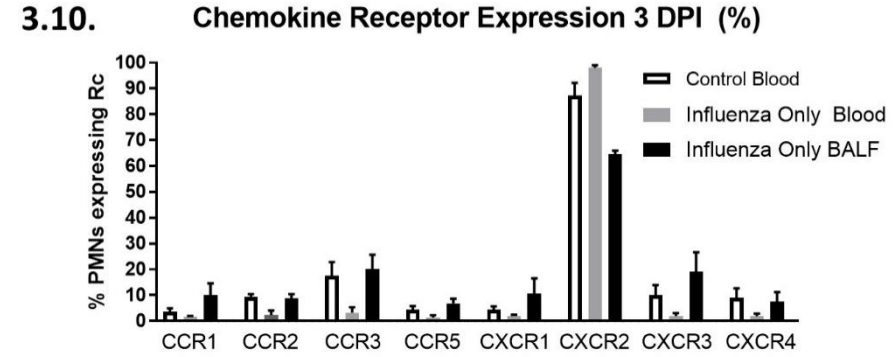


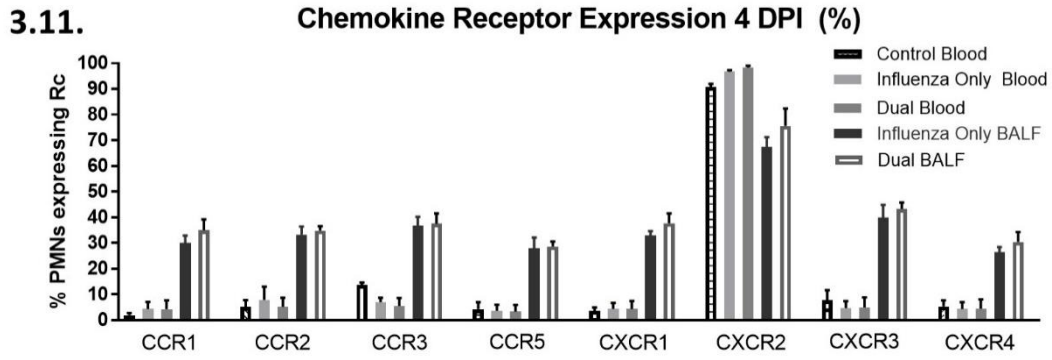


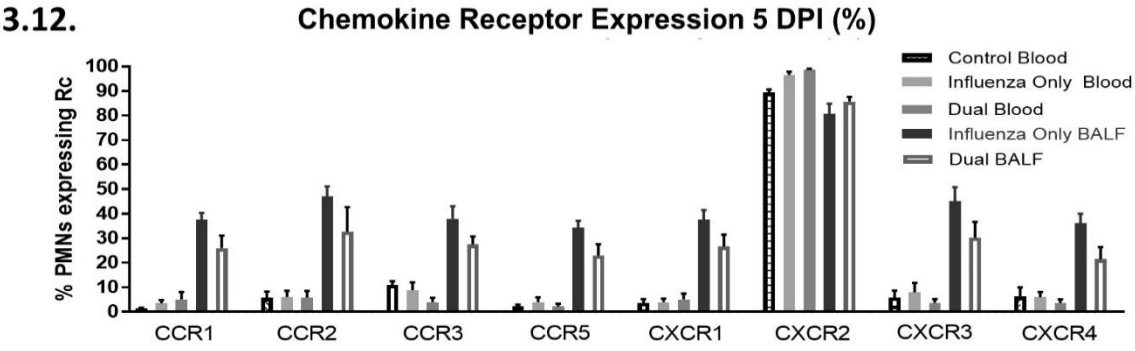


**Figures 3.10-3.12:** ***Novel chemokine receptor expression apparent in influenza-only and dually infected PMNs – CXCR2 is especially highly expressed on infected neutrophils.*** Overall view of chemokine receptor expression comparing % expression with numbers of neutrophils expressing each receptor. Blood and bronchoalveolar lavage (BAL) fluid were collected from influenza-only, dual, and mock-infected mice on days 3-5 post initial infection. Samples were analyzed via flow cytometry and % expression on neutrophils compared between groups. Neutrophils were gated as Ly6G-1A8$^{+}$ cells for all analysis. Since *S. pneumoniae* was administered on day 3, there is no difference between influenza-only and dual-infected groups on day 3. CXCR2 expression is

reduced on infiltrative pulmonary neutrophils, but remains high in all samples. Remaining receptors are minimally expressed in blood and significantly induced in infected BAL neutrophils. No significant differences are noted between influenza-only and dual-infected groups when comparing % neutrophils expressing receptor. Data are expressed as mean ± SEM. n = 3 mice per group for all studies. Statistical comparisons shown on previous figures.

***C.4. CXCR2 expression is induced in dual-infected mice.*** In contrast to other chemokine receptors analyzed in our study, our results indicate that CXCR2 is highly expressed in all circulating neutrophils with about 90% of neutrophils in healthy blood expressing CXCR2 and 97-100% of neutrophils expressing CXCR2 in infected blood samples. Upon infiltration into areas of pulmonary inflammation, these neutrophils lose some CXCR2 expression, but the receptor remains highly expressed with over 75% of infiltrated pulmonary neutrophils expressing CXCR2 [Fig. 3.7]. Despite the overall decrease in expression of CXCR2 upon pulmonary infiltration compared with circulatory neutrophils, expression is still induced in our dual infection model by day 5 as compared with day 3 [Figure 3.7]. This contrast between CXCR2 and other receptors analyzed can be especially visualized in Figure 3.10-3.12.

**4.1.**

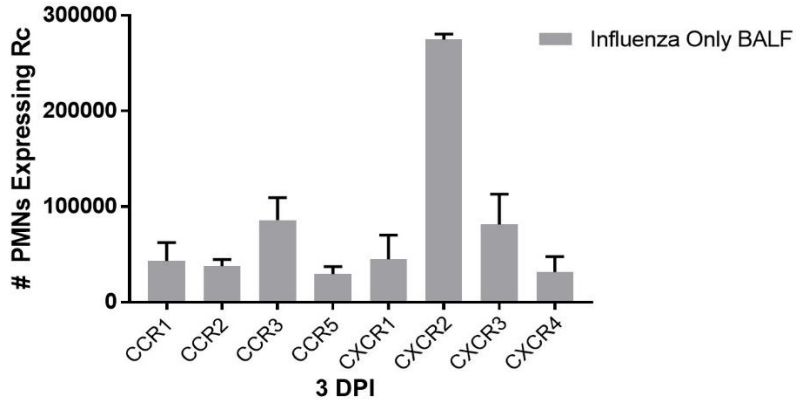
300000
200000
100000
0
# PMNs Expressing Rc
Influenza Only BALF
CCR1
CCR2
CCR3
CCR5
CXCR1
CXCR2
CXCR3
CXCR4
3 DPI

**4.2.**

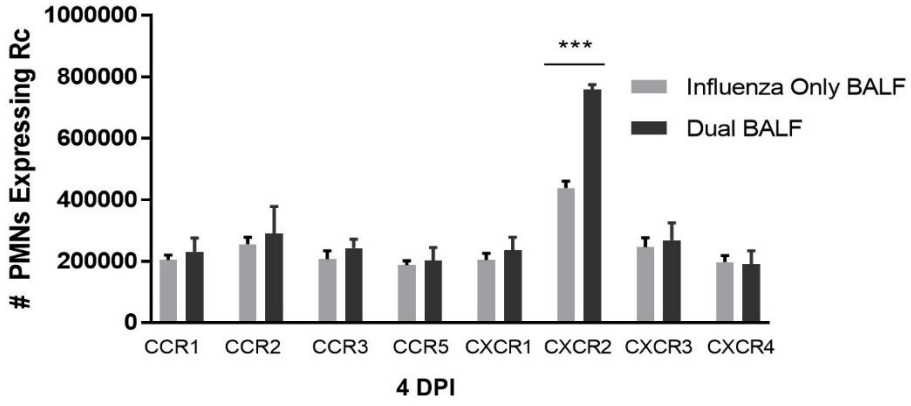
1000000
800000
600000
400000
200000
0
# PMNs Expressing Rc
***
Influenza Only BALF
Dual BALF
CCR1
CCR2
CCR3
CCR5
CXCR1
CXCR2
CXCR3
CXCR4
4 DPI

**4.3.**

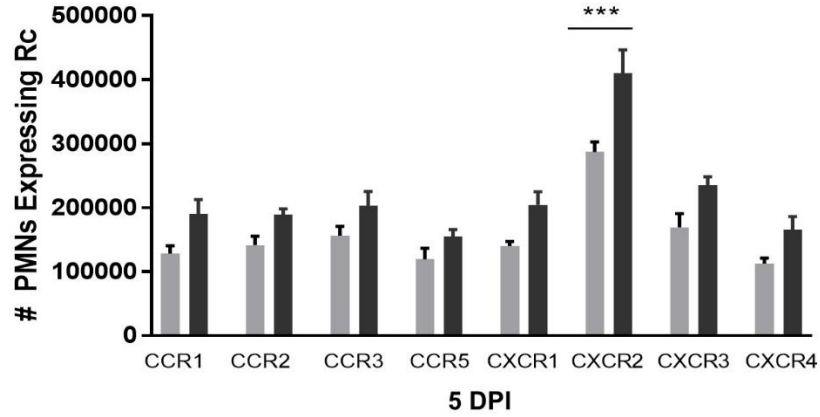
500000
400000
300000
200000
100000
0
# PMNs Expressing Rc
***
CCR1
CCR2
CCR3
CCR5
CXCR1
CXCR2
CXCR3
CXCR4
5 DPI

**Figures 4.1-4.3:** ***CXCR2 is induced in dual infection pneumonia.*** % neutrophils expressing a specified receptor was converted to quantity based on cell counts from BAL samples. After conversion, an overview is given comparing all receptors from 3-5 days after influenza infection. 3 DPI is shown in **4.1**. As clearly shown in % graphs, CXCR2 is significantly higher expressed than other chemokine receptors evaluated in this study. No dual comparison is provided since bacterial infection is administered on day 3 in our model. **4.2 and 4.3**: A significant difference is seen in the numbers of pulmonary neutrophils expressing CXCR2 between influenza-only and dual-infected groups on days 4 and 5 post initial infection. Data are expressed as mean ± SEM and comparisons made via one-way ANOVA. n = 3 mice per group for all studies. *** $p<0.001$.

Since the BAL fluid cell counts are about 1.5 times higher in our dual infection model than they are in the influenza-only model, we used differences in BAL cell counts to convert these percentages to reflect numbers of neutrophils expressing each receptor type. After conversion from percentage to quantity, we clearly show a significant difference between the numbers of neutrophils expressing CXCR2 in our dual-infected versus our influenza-only infected models on day 5 post influenza infection [Figure 4].

***C.5. Reduced CD16 and CD62L integrin expression in severely infected models.*** Various integrins present on neutrophils have been evaluated for their roles and prognostic potential in inflammatory models of disease. Two frequently assessed integrins are CD16 (Fc Gamma RIII) and CD62L (L-selectin). These integrins have been previously shown to be shed or expression decreased in several models including trauma, bacterial infection and viral pneumonia [190-192].

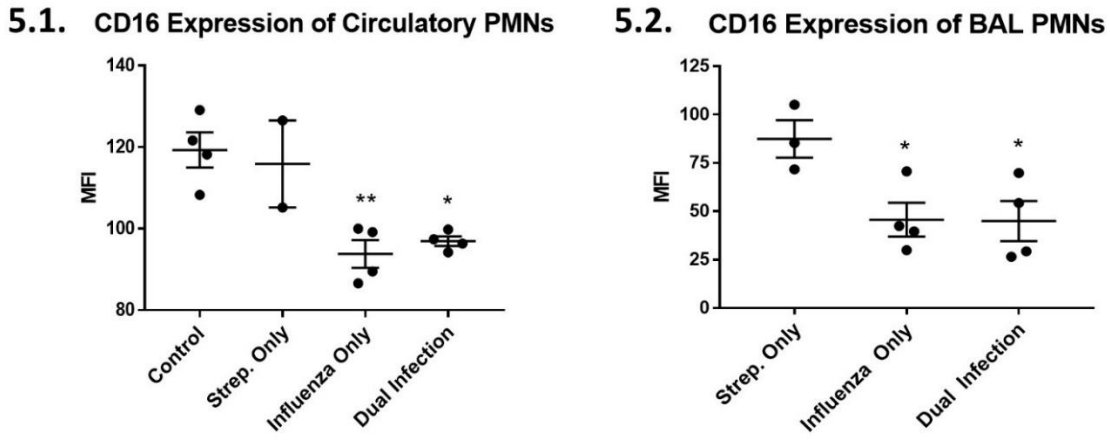


**Figures 5.1 and 5.2:** ***CD16 expression is reduced in more severe influenza-only and influenza coinfection.*** Blood and BAL were collected from mice 4 days' post influenza infection for comparison. *S. pneumoniae*-only infected BAL is used as a model with minimal to no clinical disease for comparison. CD16 expression is significantly reduced in more severely affected models (influenza-only and dual-infected) as compared with *S. pneumoniae*-only and control samples in both circulatory **[5.1]** and pulmonary infiltrated PMNs **[5.2]**. Data are expressed as mean ± SEM and comparisons made via one-way ANOVA. n = 3-4 mice per group for all studies. * $p<0.05$; ** $p<0.01$ (relative to control blood or SP Only BAL).

Integrin expression was evaluated 3-5 days' post initial infection and results are shown from 4 days' post infection. Pulmonary infiltrative neutrophils from influenza and dual-infected mice have significantly reduced expression of CD16 when compared with bacterial-only infected mice [Fig. 5.1]. A significant difference was not seen in CD62L from the same samples [Fig. 5.3]. We show a significant reduction in both CD16 and CD62L expression in viral and dual-infected blood as compared with the less severe *S. pneumoniae*-only infected mice and healthy controls [Fig. 5.2, 5.4].

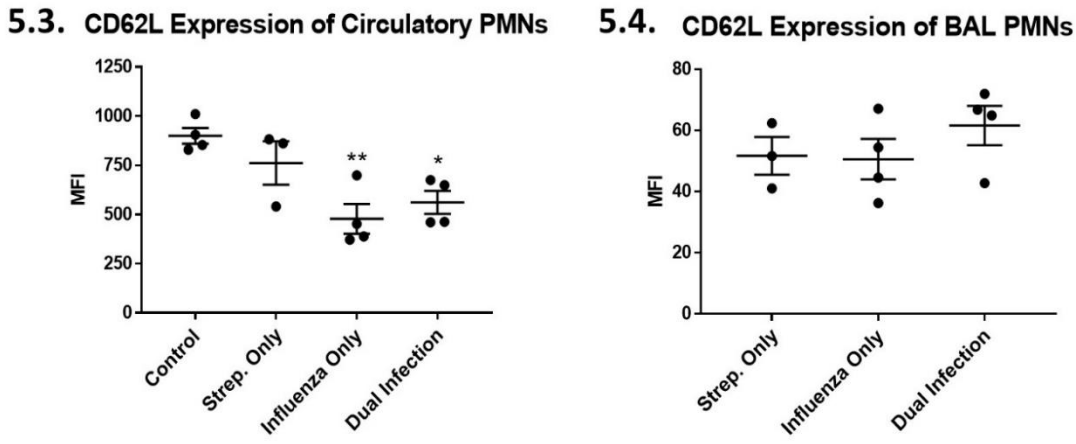


**Figures 5.3 and 5.4:** ***CD62L expression is reduced in circulatory PMNs in more severe disease.*** Blood and BAL were collected from mice 4 days' post influenza infection for comparison. *S. pneumoniae*-only infected BAL is used as a model with minimal to no clinical disease for comparison. CD62L expression is significantly reduced in more severely affected (influenza-only and dual-infected) blood samples as compared with control **[5.3]**, but no significant differences are noted in infiltrated pulmonary neutrophils between models **[5.4]**. Data are expressed as mean ± SEM. n = 3-4 mice per group for all studies. * $p<0.05$; ** $p<0.01$ (relative to control blood).

**C.6.** ***Increases in CD11b Expression as a result of acute inflammation****.* CD11b is part of the Mac-1 heterodimer that plays an active role in neutrophil recruitment and adhesion [200]. CD11b is also known as a potential prognostic indicator and marker for acute inflammation due to its role in neutrophil activation [201, 202]. CD11b was measured in control and infected blood samples as well as infected BAL fluid samples. There was no significant difference noted between control and infected blood [Fig. 6.1]. In addition, no difference was noted between CD11b expression of infiltrative pulmonary neutrophils in viral-infection alone and coinfection models. Although no significant differences were seen within blood and BAL samples, a significant increase in expression of CD11b was noted in infiltrative neutrophils from BAL collection over neutrophils in circulation [Fig. 6.1].

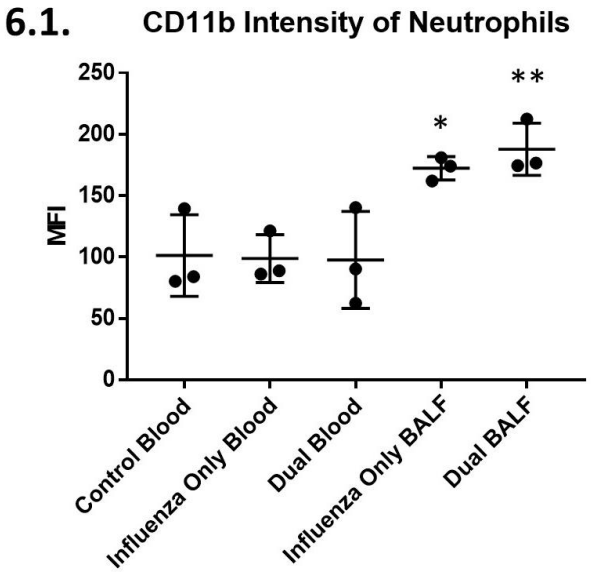


**Figure 6.1:** ***CD11b expression is enhanced in more severe disease.*** Blood and BAL were collected from mice 4 days' post influenza infection for comparison. *S. pneumoniae*-only infected BAL is used as a model with minimal to no clinical disease for comparison. CD11b is significantly increase in influenza and dual-infected BAL as compared with all blood samples. Data are expressed as mean ± SEM and comparisons made via one-way ANOVA. n = 3-4 mice per group for all studies. * $p<0.05$; ** $p<0.01$ (relative to control blood).

**C.7.** ***Effects of induced chemokine receptors on neutrophil functional responsiveness.*** In order to further assess chemokine receptor function in dual infection pneumonia, we selected six receptors (CCR1, CCR3, CCR5, CXCR2, CXCR3 and CXCR4) to perform functional studies based on their presence in BAL collected neutrophils and previously reported therapeutic potential in other models of inflammatory and chronic disease. CCR2 was not included due to its primary role and expression on macrophages. CXCR1 was not included due to differences in mouse versus human CXCR1 receptors and ligands. Functional properties evaluated include reactive oxygen species production and phagocytosis capacity.

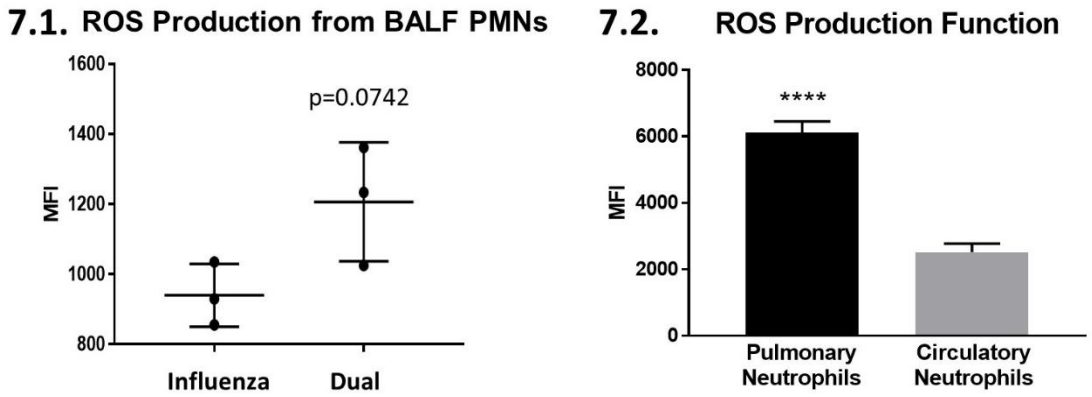


**Figures 7.1 and 7.2:** ***Blocking specific chemokine receptors affects functional potential of the neutrophil.*** Infected BAL and blood were collected from mice. Reactive oxygen species (ROS) production was assessed using DCFH-DA ROS flow cytometric assays and phagocytosis was measured using pHrodo *E. coli* BioParticles and flow cytometry. **7.1:** A trend (*p*=0.0742) toward increased ROS production in dual-infected pulmonary infiltrative neutrophils is seen as compared with influenza-only infected PMNs. **7.2:** In an influenza infected model, there was a significant difference noted in ROS production between circulatory and pulmonary PMNs, with significantly more ROS production within the infected BAL PMNs. Data are expressed as mean ± SEM and comparisons made via paired t-test. n = 3 mice per group for 7.1 and n=9 mice per group for 7.2. Two mice were pooled per sample. ****p<0.0001 relative to circulatory neutrophils.

**C.7a.** ***Reactive oxygen species (ROS) production assay.*** ROS effect of chemokine receptor expressions on ROS generation was first evaluated between influenza-only and dual-infected mice and was measured using a DCFHda flow cytometric assay on recently collected BAL neutrophils. Significant production was measured in all infected samples with a trend toward greater ROS production in dual infected BAL neutrophils over influenza-only infected samples, but no significant difference was noted between the groups [Figure 7.1]. Since the chemokine receptor expressions were showing similar pattern between influenza and dual-infected mice, we chose to evaluate the effects of these chemokine receptors expression on ROS generation. An influenza-only infected mouse model was then used for further ROS production studies as

expression of all chemokine receptors were comparable between primary influenza and *S. pneumoniae* superinfection. Blood and BAL were collected from infected mice 3 days after viral infection and neutrophils were isolated. Neutrophils collected from the infected BAL had significantly higher ROS production than those in the blood [Fig. 7.2].

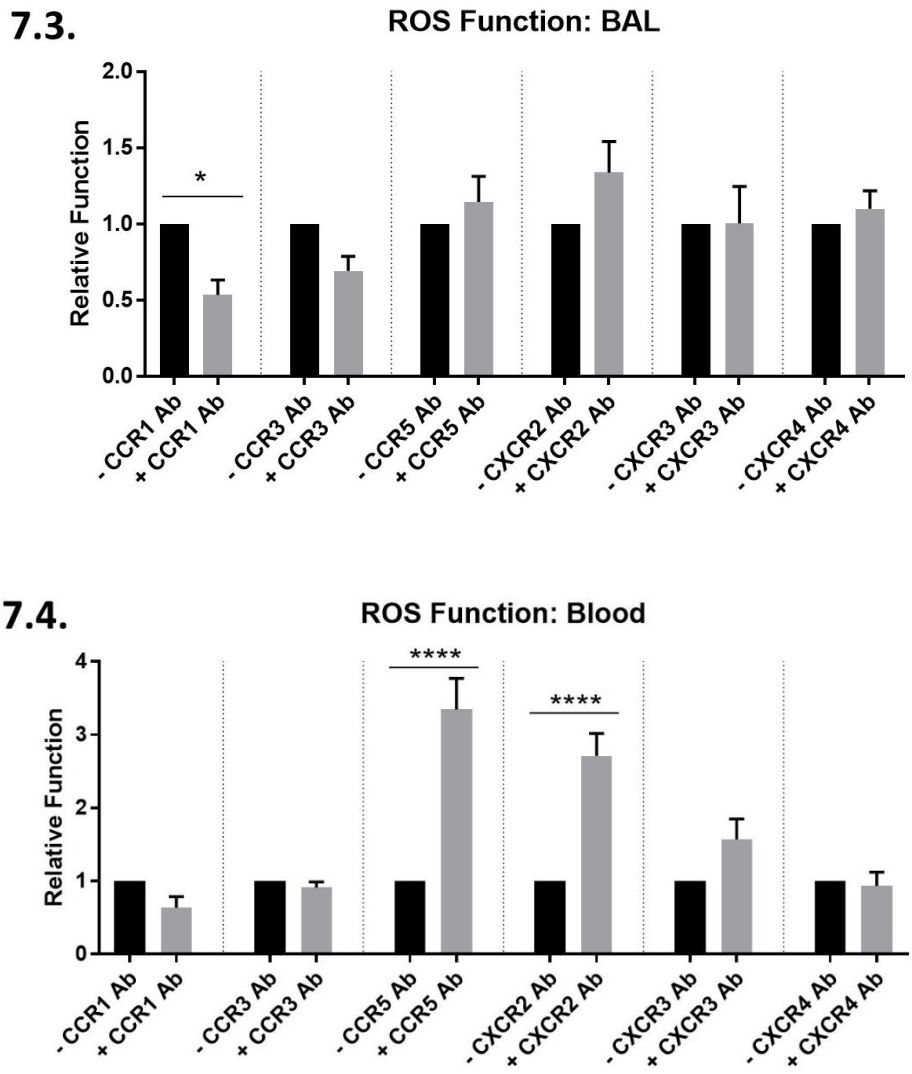


**Figures 7.3 and 7.4:** ***Blocking specific chemokine receptors affects functional potential of the neutrophil.*** Infected BAL and blood were collected from mice. Reactive oxygen species (ROS) production was assessed using DCFH-DA ROS flow cytometric assays and phagocytosis was measured using pHrodo *E. coli* BioParticles and flow cytometry. Data was compared as relative function of neutrophils with receptor blocked as compared with no blocking (x:1) **7.3:** Blocking CCR1 significantly reduced ROS function for neutrophils within the BAL. Blocking CCR3, CCR5,

CXCR2, CXCR3, and CXCR4 had no significant effect. **7.4:** For circulating neutrophils, blocking CCR5 and CXCR2 significantly enhanced production. Blocking CCR1, CCR3, CXCR3, or CXCR4 had no significant effect on ROS production. Data are expressed as mean ± SEM and comparisons made via paired t-test. n = 3 mice per group for all studies. *$p$<0.05; **** $p$<0.0001. Two mice were pooled per sample.

Isolated neutrophils were also incubated in the presence or absence of CCR1, CCR3, CCR5, CXCR2, CXCR3 and CXCR4 blocking antibodies to assess changes in function. Our results indicate that blocking CCR1 significantly reduces ROS function in lung-infiltrated neutrophils [Figure 7.3]. In contrast, blocking CCR5 and CXCR2 in the circulating neutrophils significantly enhanced ROS production [Figure 7.4]. No other significant differences were noted in blocking the remaining receptors.

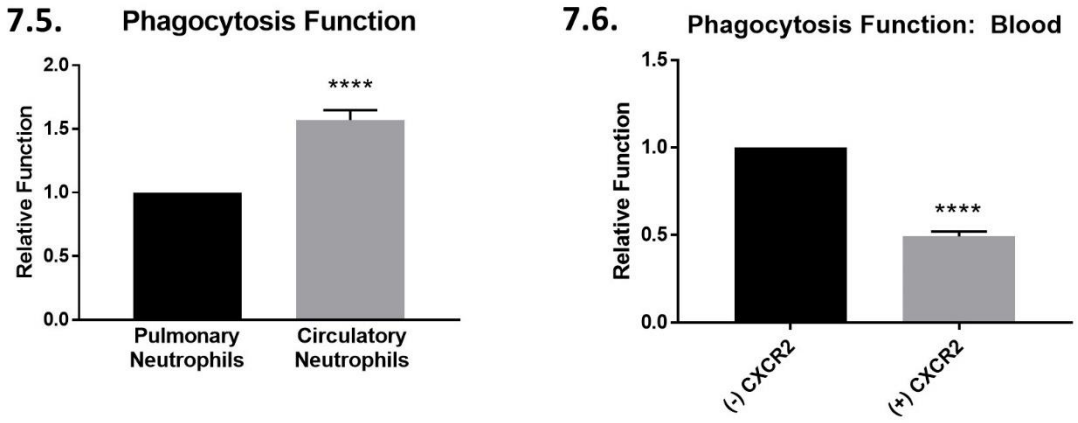


**Figures 7.5 and 7.6:** ***Blocking specific chemokine receptors affects functional potential of the neutrophil.*** Infected BAL and blood were collected from mice. Phagocytosis was measured using pHrodo *E. coli* BioParticles and flow cytometry. Data was compared as relative function of neutrophils with receptor blocked as compared with no blocking (x:1). **7.5:** Pulmonary neutrophils had reduced phagocytic capacity when compared with those in circulation. **7.6:** Blocking CXCR2 reduced phagocytic capacity of circulatory neutrophils in a viral-infection model. Data are expressed as mean ± SEM and comparisons made via paired t-test. n = 3 mice per group for all studies. **** p<0.0001. Two mice were pooled per sample.

**C.7b.** ***Phagocytic activity.*** We measured phagocytosis capacity using pHrodo™ *E.coli* BioParticles on isolated neutrophils from viral-infected mice under a variety of conditions. Phagocytosis function is significantly reduced in neutrophils collected from infected BAL as compared with those from infected blood [Fig. 7.5]. Isolated neutrophils from blood were also incubated in the presence or absence of CXCR2 blocking antibodies. Blocking CXCR2 significantly reduced phagocytosis function in the blood [Fig. 7.6]. Isolated neutrophils from infected BAL were also incubated with CCR1, CCR3, CCR5, CXCR2, CXCR3, and CXCR4 blocking antibodies in the presence of their appropriate ligand to assess for receptor roles in phagocytic functions. Interestingly, blocking CCR5 and CXCR2 significantly reduces phagocytosis capacity of the pulmonary infiltrative neutrophil, while no significant effect was seen when blocking the remaining receptors [Fig. 7.7].

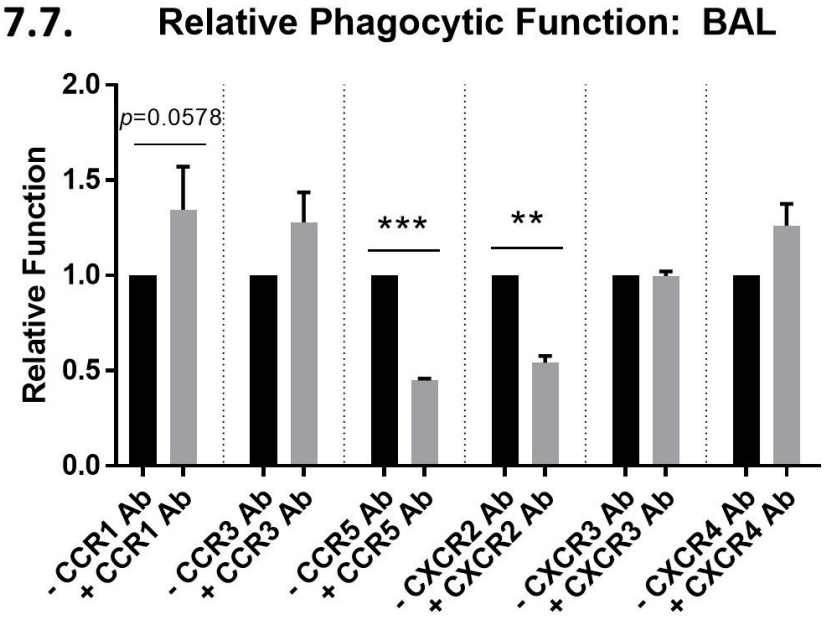


**Figure 7.7:** ***Blocking CCR5 and CXCR2 significantly reduce phagocytic capacity of pulmonary infiltrated neutrophils.*** Infected BAL and blood were collected from mice. Phagocytosis was measured using pHrodo *E. coli* BioParticles and flow cytometry. Data was compared as relative function of neutrophils with receptor blocked as compared with no blocking (x:1). Blocking CCR5 and CXCR2 reduced phagocytic capacity of pulmonary infiltrative neutrophils in a viral-infection

model while no change was noted with blocking CXCR3. In addition, a reduction in phagocytic capacity was also seen when blocking CXCR2 in circulatory neutrophils which also have high levels of this receptor. Circulatory neutrophils without blocking were also performed to further compare blood to BAL neutrophils in other groups. Data are expressed as mean ± SEM and comparisons made via paired t-test. n = 3 mice per group for all studies. *** $p<0.001$; **** $p<0.0001$. Two mice were pooled per sample.

## Discussion

One of the primary goals of this study is to characterize the changes seen in chemokine receptor expression, and identify the availability key receptors that may act as important targets with therapeutic potential. As seen in our results, the influenza-only infected and dual infected mice lose significant weight and show rapid and severe progression of clinical scores between days 3 and 5. Those mice given only *S. pneumoniae* showed mild weight loss without any obvious clinical signs and recovered shortly after infection. The viral-infected mice that are administered the subsequent pneumococcal infection decline rapidly and become bacteremic within 48-60 hours after bacterial administration, reaching their endpoint by day 6. Histopathology of pulmonary tissue from these infected mice showed pathologic lesions of ARDS with severe pulmonary damage, alveolitis and endothelial necrosis. Widespread disruption of alveolar epithelial-endothelial barrier was more prominently seen in dual-infected mice and this could cause exposure of basement membrane. The exposure could facilitate bacterial adherence and dissemination into deeper lungs. In support of this, we found increased bacterial load, dissemination into deeper lungs and bacteremia within 48 hours after *S. pneumoniae* superinfection, while mice infected with bacteria-alone clear the bacteria within 24 hours. This model will serve as a good representation for pathogenic progression and severity that can be seen with pandemic influenza outbreaks wherein bacterial superinfections are involved. Due to complexity of the coinfections that can occur in nature, we had tested various coinfection

models as described in Chapter 2 and based on our analysis, we chose sublethal influenza followed by sublethal *S. pneumoniae* to explore the role of neutrophils.

Previous studies from our laboratory and other investigators have demonstrated pathogenic role of neutrophils in bacterial superinfection following influenza [18]. Although neutrophils are essential in bacterial clearance, accumulated evidences indicate pathogenic contribution of excessive neutrophils recruited during bacterial superinfection. Interestingly, chronic inflammatory disease conditions have shown altered neutrophil phenotypic signature, which potentially influence their functional responsiveness [138]. It is not known whether neutrophils display any change in phenotypic changes or functional responsiveness during acute influenza pneumonia or bacterial superinfections. Hence, this study aimed to fill this critical void by characterizing neutrophils during primary influenza and *S. pneumoniae* superinfection for their phenotypic signature by evaluating chemokine receptors (CRs) expressions and their functional responsiveness. We evaluated CC and CXC CRs and integrins in circulating as well as in lung-recruited neutrophils. Because healthy Balb/c lab mice contain extremely low numbers of neutrophils in their lung alveolar air spaces, it is difficult to draw comparisons using control mice to the healthy uninfected human population. Hence, we compared bacterial-only infected mice, which display minimum neutrophil influx without clinical signs. Our results clearly demonstrate a large influx of neutrophils in dual-infected mice and also influenza-alone infected mice compared to bacteria-only infected group that is most drastic at 5 dpi. This can be clearly seen both in our flow results and in cell counts. This neutrophil influx was found to be more prominent in dual infected samples with overall BAL fluid cell counts being over 1.5 times higher in dual infected samples at 5 dpi than in influenza-only infected samples.

Our data has shown that CXCR2 is a most predominant chemokine receptor expressed in circulating neutrophils. Neutrophils were positively identified by Ly6G positive expression and the total percent of CXCR2 positive cells were significantly increased in circulation in both primary influenza and secondary *S. pneumoniae* superinfection. Interestingly, all CC chemokine receptors were minimally expressed in circulating neutrophils in controls as well as infected mice. These findings suggest that CXCR2 is most critical chemokine receptor involved in neutrophil recruitment in response to these infections. In support of this, our recent findings demonstrated significant increase in CXCR2 ligand, mouse KC, levels in blood and BAL samples from influenza infected mice [83, 203].

On the other hand, CXCR2 has a slight decrease in percentage of neutrophils expressing in the BAL compared with peripheral blood. This finding is supported by previous studies evaluating receptor expression in chronic inflammation [204]. CXCR2 has been shown to be suppressed by TNF-α previously with a suggestion that this allows for a modulation in the IL-8 response so that neutrophils can be retained in the vascular space and also have enhanced production of reactive oxygen species [205]. CXCR2 is highly expressed in infected blood with almost all neutrophils present having the receptor. Despite this relative downregulation, CXCR2 is the majorly expressed chemokine receptor found in lung-recruited neutrophils. Targeting CXCR2 has been shown to ameliorate lung injury in sublethal infected-infected mice [206]. Our recent study demonstrated that a combination of a CXCR2 antagonist together with antiviral agent confers high protection against lethal-influenza challenge in mice [83] thus suggesting a potential pathogenic role of CXCR2 induction during influenza. Another critical finding from our studies is that influenza and *S. pneumoniae* superinfection, triggers induction of CC chemokine receptors (CCR1, CCR2, CCR3, CCR4 and CCR5) in lung-recruited neutrophils. Expression of these

CC chemokine receptors were minimally expressed in circulating neutrophils from control as well as infected mice.

Antagonism of CCR1, CCR2, and CCR3 receptors was shown to have a protective effect – when a CCR2b and CCR1 antagonist was used, decreases in fibrinolysis, vascular leakage and inflammatory gene expression were all noted. These findings were further supported in CCR1, CCR2, and CCR3 knockout mice which had less pulmonary edema, infiltration and overall disease as compared with controls with ALI [145]. CCR1 antagonism also has shown promise in limiting pulmonary injury resulting from acute pancreatitis [140] and sepsis [141] as well as in a renal ischemia model [139].

In addition, we also found increased CXCR3 and CXCR4 expressions in the lung-recruited neutrophils. CXCR3 has also been further evaluated for its role in ARDS with its ligand CXCL10. Ichikawa et al. evaluated both a viral and non-viral ARDS mouse model in mice deficient in CXCL10 and CXCR3 and found that mice lacking CXCL10 and CXCR3 had improved severity of disease and survival in both models [151]. Antagonism of CXCR3 has also been shown to reduce disease severity in an H5N1-infected ferret model [147]. Therefore, this receptor poses another intriguing potential target for therapeutics in coinfections. CXCL12 and its receptor, CXCR4, also appear to play a role in promoting chemotaxis of neutrophils as well as suppressing cell death. In a study looking at lipopolysaccharide (LPS)-induced lung injury, CXCL12 was shown to be a chemoattractant for cells expressing CXCR4 as well as a suppressant of neutrophil cell death and CXCR4 was found to be increased on the neutrophil cell surface after migrating from circulation into the inflamed lungs, possibly via an L-selectin mediated pathway [154]. CXCR4 has been further described as acting antagonistically with against CXCR2 – CXCR4 expression promotes neutrophil retention in the bone marrow, whereas CXCR2 expression drives release [158].

Finally, CCL2 (ligand for CCR1/2) and CCL7 (ligand for CCR1-3, 5) are also chemokines that may play an interesting part in ARDS – in a study performed by Mercer et al, antibody neutralization of these ligands significantly reduced neutrophil accumulation in the BAL fluid in mice with LPS-induced lung injury [146]. Although the full potential of these receptors as therapeutic targets in pneumonia must still be explored, this study shows availability of each of these receptors in dual infection pneumonia and recommends further studies to elucidate their potential.

Various integrins have been used to characterize neutrophils in addition to their forward and side scatter properties. We found that the expression of integrins, including CD16 and CD62L, decreased in circulating neutrophils isolated from both primary influenza and *S. pneumoniae* superinfection compared to the *S. pneumoniae* alone infected animal group. CD16 expression was reduced on both circulating and lung-recruited neutrophils. Expression of CD62 was decreased in both circulating as well as in pulmonary infiltrative neutrophils. CD16, also known as FcγRIII, is a cell surface molecule that is expressed on several cell types including neutrophils, macrophages and natural killer cells, and has been shown to have reduced expression in many inflammatory conditions such as vaginitis, trauma, bacterial infection and viral pneumonia [190-192]. It has also been suggested that the decreased CD16 expression seen with acute inflammation could be due to the influx on immature neutrophils which are $CD16^{dim}$ [189]. CD62L, also known as L-selectin, mediates neutrophil rolling and adhesion to the endothelial cells. This receptor is shed when stimulated by pro-inflammatory cytokines such as TNF-α in acute inflammatory insults such as with trauma [191, 193] and uremia [194]. CD11b is a frequently assessed integrin in models of acute inflammation and is a β2-integrin adhesion molecule that is part of the Mac-1 heterodimer, and is a major player in neutrophil recruitment and adhesion [190, 191, 193]. In contrast to CD62L, most studies have shown that CD11b significantly increases in cases of acute inflammation, corresponding to increased neutrophil

activation [190, 191, 193, 195]. Models of acute inflammation such as bacterial pneumonia (primary or secondary), viral pneumonia, trauma or burns all seem to shed CD62L and reduce CD16 expression while increasing expression of CD11b. Our results indicate that there is a significant increase in CD11b expression on infiltrative pulmonary neutrophils over those neutrophils identified in circulation, as seen by comparing mean fluorescence intensity between the two groups. Not only does this imply a heightened level of neutrophil activation from the neutrophils within the lavage, but CD11b also presents itself as an interesting target with high availability to block neutrophil recruitment and activation. CD11b has been shown to be a necessary component for successful diapedesis of neutrophils from the pulmonary microvasculature to the alveoli spaces in a LPS-induced model of acute pulmonary inflammation [200]. In addition, blocking CD11b has been shown to have significant effect in controlling the early inflammatory response by reducing neutrophil numbers in both the BAL fluid and lung tissue in an LPS-induced model of pulmonary inflammation [207]. Therefore, CD11b blockade may present an interesting and novel approach to treating dual infection pneumonia and improving clinical outcome for ARDS.

Reactive oxygen species have long been shown to be important contributors to the endothelial damage seen in models of ARDS, sepsis and pneumonia. These ROS are released by neutrophils after being sequestered and activated in the pulmonary vasculature and are key substances in modulating pulmonary endothelial damage [208]. Production of reactive oxygen species from neutrophils collected in infected BAL fluid is significant, as expected, and our results also suggest a trend toward increased ROS production in dual-infected BAL versus that infected with influenza alone. Our results also concluded that ROS production was significantly enhanced with neutrophils from within the BAL versus those in circulation. Since the effect of ROS on the endothelium has been well-established, it would be logical to believe that these

toxic products are contributing to the severe histopathologic changes seen in the lungs of dual-infected mice and potentially to bacterial dissemination as well. Further, to determine the role of induced chemokine receptors on ROS generation, we incubated neutrophils isolated from influenza infected mice with receptor specific ligands in the presence or absence of antagonists or antibodies to the receptors. Our data show that blocking CCR1 in the lung-infiltrated neutrophils results in a reduction in ROS production. In addition, blocking CCR1 in the circulating neutrophils also trends to a decrease in ROS production. In contrast to CCR1, our data show that blockade of CCR5 and CXCR2 results in enhanced ROS production from circulating neutrophils. CCR3, CXCR3 and CXCR4 blockage had no effect on ROS production in either infected blood or BAL neutrophils. Due to the excessive neutrophil-mediated damage already noted [55, 83, 186], this should be taken into consideration when designing therapeutics. Our studies indicate a different result with phagocytosis capacity. Pulmonary infiltrative neutrophils have significantly reduced phagocytic ability as compared with those in circulation and blockade of CCR5 and CXCR2 in BAL and CXCR2 in blood further weakened the phagocytic ability of the cell. Reduced neutrophil function can contribute to the likelihood of severe co-infections and should also be considered when evaluating potential for antagonists in clinical disease.

There are several challenges and limitations of using an animal model for ARDS including the host-specific differences in chemokines, their receptors and the roles these play in the disease pathogenesis. One such difference is that CXCL8 does not exist in the rodent model, although homologues do exist as CXCL1 (KC) and CXCL2 (MIP-2). It is also unclear whether the mouse analog for CXCR1 is functional in the same way as human CXCR1 as it seems to be activated in different ways and does not seem to play the same central role in the pathogenesis of ARDS that it does in humans [137]. The application of studying CXCR1 in an animal model to evaluate human disease is still in question and needs further investigation. In addition to

challenges common to animal models, this study is merely a partial characterization of the neutrophil during dual infection. Chemokine receptors, integrins, and functional studies were selected based on clinical therapeutic potential and previous studies. In particular, a more complete analysis of the functional impact of each receptor should be evaluated in this model. CCR1, CCR3, CCR5, CXCR2, CXCR3, and CXCR4 were chosen for initial analysis due to a variety of reasons. CXCR2 is highly expressed during infection and is a readily available target being analyzed in a variety of models. CXCR3 and CCR5 were also consistently induced after infiltration to sites of pulmonary infection and also show therapeutic potential in other models of disease that make these readily available antagonists to be tested in future trials. CCR2 is primarily involved in macrophage function and so was excluded. CXCR1 was also excluded due to limited functional role in murine models due to homology concerns with human CXCR1. Work should continue to gain a more complete picture of the neutrophil during dual infection.

In conclusion, our study revealed several novel findings. Firstly, we found that neutrophils acquire new phenotypic characteristics after they recruit into the lungs during acute influenza infection and also *S. pneumoniae* superinfection. Expression of CC chemokine receptors (CCR1, CCR2, CCR3, and CCR5) and CXC chemokine receptors (CXCR3, and CXCR4) were induced in lung-recruited neutrophils in primary influenza and *S. pneumoniae* superinfection compared to *S. pneumoniae* alone infected animal groups. Secondly, CXCR2 is the most predominant chemokine receptor expressed in both circulating as well as lung-recruited neutrophils compared to S. pneumoniae infected animals. Thirdly, these findings also demonstrate significant decrease in integrins expression on neutrophils during infection. Our findings also demonstrate that induced chemokine receptors including CCR5 and CXCR2 significantly influence neutrophil functional responsiveness including phagocytic activities and respiratory burst. Our recent studies have demonstrated that stimulation of CXCR2 with IL-8

significantly induce NETs, which can potentially contribute to the acute lung injury. Overall, identifying induction of novel chemokine receptor expressions on neutrophils helps in not only understanding their pathogenic role in influenza as well as *S. pneumoniae* superinfection but also opens a new avenue to develop novel therapeutic strategies in alleviating lung pathogenesis during primary influenza as well as *S. pneumoniae* superinfection.

CHAPTER IV

# THE THERAPEUTIC POTENTIAL OF SCH527123, A CXCR1/2 ANTAGONIST, IN A MURINE MODEL OF DUAL INFECTION PNEUMONIA

## A. Introduction

Our work to identify availability and functional properties of chemokine receptors achieves relevance through their clinical application in the dual infection model. As previously outlined, influenza coinfection is complex, and a lethally synergistic response is clear when bacterial, viral and host influences are all considered. The immune system's response to infection is well documented to further aggravate injury and breakdown epithelial and endothelial barrier integrity within the pulmonary tissue, resulting in increased chances of bacteremia and worsened disease. Due to the complexity of coinfections, a simple targeted monotherapy is insufficient to treat such cases [109]. In addition, resistance to antivirals and antibiotics further insists on a combined approach to treatment. Combinations of antibiotics, and effective antiviral, and therapies that target the immune response are considered more optimal approach to treating these infections.

Antibiotic therapy is a mainstay for treatment of any pneumococcal pneumonia, whether community acquired, healthcare-associated, or seen as secondary to viral infection. Three main classes of antibiotics have been more thoroughly considered in treatment of these infections:

β-lactams, macrolides, and fluoroquinolones. β-lactams – such as penicillin, cephalosporins and ampicillin – are broad spectrum and widely used drugs that inhibit cell wall synthesis in the bacteria by preventing the final cross-linking in the peptidoglycan layer. The result is a bacteriocidal effect. Historically, this class is the most commonly used for pneumococcal pneumonia, but a shift in the last couple of decades is pushing for other classes in combination or instead of β-lactams. Studies have shown significant resistance to penicillin in pneumococcal strains – one study revealed that in the United States, 34% of pneumococcal strains are penicillin non-susceptible with over 18% fully resistant [209]. In addition to resistance profiles, β-lactams such as ampicillin are not as effective as other classes either. In another model of secondary bacterial infection to influenza pneumonia, ampicillin only resulted in 56% survival, while azithromycin was at 92% survival with improved inflammation and less severe histopathology [112].

Macrolides (such as azithromycin, clarithromycin, and erythromycin) act by reversibly binding to the 50S subunit in ribosomes and therefore, preventing bacterial protein synthesis. The effects are bacteriostatic. Macrolides have been shown to not affect granule mobilization, but inhibit $O_2^-$ generation from neutrophils selectively, which may contribute to their effects [210]. One approach considered is to use macrolides in combination with β-lactams for treatment in influenza coinfections and other forms of pneumococcal pneumonia. An ampicillin/azithromycin treatment effectively reduced inflammation, improved bacterial clearance, decreased inflammatory cytokines such as TNF-α, IFN-γ and IL-6, reduced damaging myeloperoxidase, improved permeability, and decreased overall inflammatory cell recruitment in pneumococcal pneumonia [113]. Combination therapy of amoxicillin and clarithromycin in community-acquired pneumonia is more effective than either monotherapy [211]. In addition, the dosing regimen may also be influential to clinical outcome – pulsatile therapy, such as giving

an antibiotic every two hours for the first 6 hours of each day, results in improved outcome as compared with more standard dosing regimens such as every 12 hours [211]. Using mutant prevention concentration as a novel approach to evaluate drug-bacterial interactions for resistance, several studies have more thoroughly detailed resistance patterns between macrolides [212]. Interestingly, azithromycin is shown to be more likely to develop resistance than other macrolides, in particular clarithromycin [212-214]. Concerns regarding adverse effects of macrolides, in particular azithromycin are also to be considered. Some suggest that the cardiotoxicity seen with azithromycin usage in healthcare-associated pneumonia outweighs the benefits of the drug, making azithromycin usage contraindicated in this particular form of pneumonia [215].

Fluoroquinolones (most ending in –floxacin) are bacteriocidal drugs which prevent bacterial DNA from unwinding and replicating. Flouroquinolone resistance has also been shown to be on the rise, as opposed to most other classes which are starting to decline [209]. There is also some question as to the effectiveness of fluoroquinolones as compared with macrolides. In a murine bacterial rhinosinusitis model, moxifloxacin had a limited effect while azithromycin rapidly cleared the bacteria and reduced inflammation [114]. However, it is unclear if these differences would be apparent in a human host. Fluoroquinolones may become especially essential to treatment of otherwise resistant pneumococcal pneumonia. A combination therapy including levofloxacin and ceftriaxone shows promise in such cases by downregulating inflammation, improving clearance of the bacteria, and, additionally, downregulating expression of two key pneumococcal virulence factors – pneumolysin and autolysin [111]. Outside of these classes of antibiotics, there are several other therapeutics targeting bacterial virulence factors. For example, artocarpin, a bacterial neuraminidase inhibitor, shows promise in future therapies

by providing bactericidal effects without harming pulmonary epithelial cells in pneumococcal pneumonia [108].

Antivirals are a mainstay of treatment for any influenza pneumonia. Oseltamivir is the primary antiviral used at this current time to combat influenza outbreaks. Oseltamivir an oral antiviral that is a neuraminidase inhibitor acting on both influenzas A and B, the primary causes of seasonal influenza outbreaks. Although most agree that oseltamivir improves clinical outcome, the evidence is controversial. A fairly recent, and controversial, report indicated that oseltamivir did not reduce hospitalizations or severe complications associated with influenza, but these findings and the benefits of oseltamivir continue to be debated today [216]. Combination of antivirals with antibiotics are especially important during influenza pandemics and in high risk individuals. A study performed in human volunteers with confirmed influenza A and no comorbid pneumonia showed that combination therapy of oseltamivir and azithromycin resulted in earlier resolution of clinical disease [217]. Many are looking for alternatives to oseltamivir and inhaled zanamivir due to increasing concern for resistance to this medication [106]. Peramivir is another neuraminidase inhibitor that reduced mortality in coinfected mice better than oseltamivir by inhibiting viral replication resulting in improved bacterial clearance and survival [107]. Although oseltamivir has shown effectiveness to both viral and bacterial neuraminidase, peramivir only seems to inhibit viral neuraminidase, and must be administered intravenously [107, 108]. Historically, amantadine and rimantadine have been used as antiviral therapy, but these medications are only effective toward influenza A, not B, and have significant (>99%) resistance recorded for several strains of Influenza A, including circulating H3N2 and the 2009 H1N1. For these obvious reasons, these medications are no longer recommended for use as antiviral therapy. There is increasing concern that similar resistance could develop with neuraminidase inhibitors, although levels of resistance this severe have yet to be documented.

The importance of controlling both the bacterial infections and host responses to those infection is clear. In a dual infection model, a clear link can be seen between severe pulmonary neutrophilia with resultant immunopathology and poor clinical outcome [42]. If neutrophils are depleted, the immunopathology is improved, but clinical outcome remains unchanged; on the other hand, if only azithromycin is used to treat the infection, we see improved outcome and bacterial clearance, but no improvement in immunopathology [42]. These findings support a combined approach. CXCR2 antagonists are currently showing the most promise in treatment of both chronic and acute inflammatory diseases, especially disease such as Chronic Obstructive Pulmonary Disorder (COPD) [218-221]. Under healthy, basal conditions, less than 2% of the neutrophil pool is in circulation at any one time [222]. CXCR2 activation releases mature neutrophils from the bone marrow as an innate response to inflammation, which is counteracted by CXCL12 activation of CXCR4, which retains neutrophils in the bone marrow [158]. There are several potent CXCR1/2 and CXCR2 selective antagonists on the market or in trials at this time. AZD5069, a selective CXCR2 antagonist, shows good potential as a drug in COPD models and human trials [220, 223, 224]. MK-7123 is another currently being tested in models of COPD [218]. Another well studied antagonist is Sch527123, a dual CXCR1/2 antagonist. The full name is 2-hydroxy-N,N-dimethyl-3- [[2-[[1(R)-(5-methyl-2-furanyl)propyl]amino]-3,4-dioxo-1-cyclobuten-1-yl] amino] benzamide [225]. First characterized in 2006 [225], this therapeutic has been shown to have good oral availability and acts as an allosteric antagonist binding both receptors, but having a preference for CXCR2 [161]. These pharmacological properties have also been thoroughly evaluated in a murine, rat and non-human primate model [160]. Sch527123 binds with high affinity in mice ($K_d$ = 0.20 nM) and is a potent antagonist of CXCR2-mediated chemotaxis ($IC_{50}$ ~ 3-6 nM) [160]. When evaluated in COPD, Sch527123 effectively decreased neutrophil chemotaxis, while dexamethasone did not

[221]. In addition, Sch527123 has been shown to block pulmonary neutrophilia in an LPS-induced murine model for pneumonia with an $ED_{50}$ of 1.2 mg/kg [160]. There may be some benefit to using a CXCR1/2 antagonist. Although CXCR1 and CXCR2 may appear functionally redundant in their effects, this really isn't true. Very different outcomes are derived from their activation and CXCR1 has a wider range of antimicrobial effects than CXCR2 activation [226]. As a dual CXCR1/2 antagonist, Sch527123 more effectively reduces neutrophil migration and activation than the selective CXCR2 antagonist, SB265610 [227].

After establishing an influenza coinfection model with significant neutrophil influx and resultant immunopathology and identifying availability of chemokine receptor targets, we selected a combination therapy including oseltamivir, clarithromycin and Sch527123 to test in this model. I hypothesized that a CXCR2 antagonist would reduce neutrophil recruitment to the lungs, and when used in combination with antiviral and antibiotic therapy, reduce immunopathology and improve clinical outcome.

**B. Materials and Methods:**

*Pathogens*

Influenza A/Puerto Rico/8/34, H1N1 (PR/8) virus was obtained from the American Type Culture Collection (ATCC, VA). Viral titers were determined by tissue culture infectivity dose ($TCID_{50}$) assay via infection of Madin-Darcy canine kidney (MDCK) cells. *Streptococcus pneumoniae* (serotype 3) was also obtained from the ATCC. Bacterial growth curves were established prior to infection. All pathogens were stored at -80°C until use.

*Animals and Murine Model*

Female Balb/c mice (6-8 weeks old) were purchased from the Jackson Laboratories. Mice were group-housed in microisolator cages in a BSL-2 facility, and were provided with food and fresh water ad libitum. Mice were clinically scored based on a modified version of the "mouse clinical assessment scoring for sepsis" (M-CASS) [172]. Infection was performed under a mixture of xylazine (0.1 mg/kg) and ketamine (7.5 mg/kg) anesthetic via intraperitoneal injection. Mice were infected intranasally (IN) with a sublethal dose of 100 $TCID_{50}$ PR/8 (H1N1) influenza in a 50 µl volume or given an equal volume of sterile phosphate-buffered saline in controls. For dual infection studies, mice were administered 200 colony forming units (CFU) of *S. pneumoniae* IN in 50 µl volumes 72 hours after initial influenza infection, or administered PBS IN for controls. Mice were monitored closely for weight loss and clinical signs based on a modified "mouse clinical assessment score for sepsis" [see supplemental figure 1] [172, 173]. All animal experiments were approved by the Institutional Animal Care and Use Committee (IACUC) of Oklahoma State University and were performed in strict accordance with their recommendations.

*Therapeutic Model*

Mice were treated with combinations of the following three drugs: oseltamivir phosphate, clarithromycin, and SCH527123. Oseltamivir 75 mg phosphate capsules (Alvogen) were stored at room temperature. Before use, the capsules were emptied and powder weighed for the appropriate amount. 75 mg of drug were present in 160 mg of total weight powder. The powder was then redistributed in phosphate-buffered saline to the appropriate volume. Clarithromycin 500 mg tablets (Citron Pharma L) were crushed with mortar and pestle and coating removed. The powder was also measured (500 mg drug per 780 mg total powder

weight) for the appropriate dosages and redistributed in PBS to be delivered in set volumes of 100 µL per mouse. SCH5271213 was dissolved in dimethyl sulfoxide (DMSO) at 50 mg/500 µL and stored at -20°C. Before use, the appropriate volume of SCH527123 was dissolved in 0.4% methyl cellulose to be administered. All drugs were administered via gastric lavage.

For survival studies, mice were infected intranasally (IN) with a sublethal dose of 100 $TCID_{50}$ PR/8 (H1N1) influenza in a 50 µl volume and then were administered 200 colony forming units (CFU) of *S. pneumoniae* IN in 50 µl volumes 72 hours after initial influenza infection. All combinations of therapeutics were tested. Depending on the particular experiment, oseltamivir phosphate was administered at 10-20 mg/kg every 24 hours for 3 doses starting on day 3 post influenza infection. Clarithromycin was administered at either 40, 50 or 100 mg/kg every 24 hours for 3-7 doses beginning on day 3 post influenza infection. SCH527123 was administered at 3 mg/kg every 24 hours for 3 doses beginning on day 3 post initial infection. All mice were monitored for weight loss and clinical score as per our approved guidelines.

*Whole blood, bronchoalveolar lavage (BAL) fluid, and tissue collection*

For BAL fluid collection, the lungs were washed by intratracheal administration of 1.0 mL of sterile PBS in two 0.5 mL increments [55]. The recovery of BAL fluid was more than 85% for all animals. The BAL fluids were centrifuged at 200 xg for 10 minutes, and reconstituted in sterile PBS for cell counts and with 2% fetal bovine serum in PBS for flow cytometry analysis. BAL cells were concentrated using the CytoFuge 2 cytocentrifuge (StatSpin, Westwood, MA), and differential cell counts were performed using modified Giemsa staining. Whole blood was collected via terminal procedure of intra-cardiac collection. Bronchoalveolar lavage fluid and whole blood (intracardiac) were collected from 3 to 5 days' post influenza infection for flow cytometry analysis and other studies. Lungs from mice who did not have BAL collection were

fixed with 4% formalin and collected for histopathology analysis after hematoxylin and eosin (H&E) staining. Mice were scored on a 1-4 scale (4 being most severe) for severity in the following areas by a blinded, board-certified anatomic veterinary pathologist: necrotizing bronchiolitis, bronchiolar infiltrates, alveolitis, interstitial inflammation, hemorrhage, edema, and microvascular thrombosis. Total histopathologic scores were evaluated as a sum of all individual scores. BAL and blood cultures were also performed on blood agar plates, incubated overnight at 37° C.

*Flow Cytometry*

The following antibodies were purchased from R&D Systems and used throughout the course of this study for chemokine receptor expression characterization of murine neutrophils: mouse CCR2 PE-conjugated antibody, mouse CXCR2/IL-8 RB PE-conjugated antibody, mouse CXCR3 PE-conjugated antibody, and mouse CXCR4 fluorescein-conjugated antibody. These antibodies were selected based on availability and due to their previously reviewed relevance in chronic inflammatory conditions and potential for therapeutic targeting [138]. Additional antibodies used in this study include mouse Ly6G (1A8) PerCP-conjugated antibody (Biolegend). In all flow cytometry studies, control BAL fluid was not compared due to a lack of pulmonary neutrophils in naïve Balb/c mice. The collected whole blood and BAL fluid were aliquoted into 200 µl volumes for antibody staining. 2.0 ml of 1x PharmLyse Buffer was used for red blood cell lysis and allowed to lyse for 15 minutes at room temperature. Samples were allowed to stain for 30 minutes, covered, at room temperature on a shaker. All samples were then centrifuged and washed with chilled PBS (with 2% FBS) 1-3 times before performing flow cytometry. Flow cytometry was performed on the BD FACSCalibur flow cytometer and analyzed with the corresponding CellPro software. Neutrophils were gated as Ly6G-1A8$^{+}$SSC$^{med\text{-}hi}$.

*Statistical Analysis*

The data are expressed as the means ± SEM. Statistical analyses were performed using Student's unpaired t-test, paired t-test or analysis of variance (ANOVA) using GraphPad Prism 7 software. Survival studies were analyzed using GraphPad Prism 7 as well and statistical analyses performed using Mantel-Cox and Gehan-Breslow-Wilcoxon tests. $p < 0.05$ was considered statistically significant.

**C. Results**

**C.1. *Sch527123, a CXCR1/2 antagonist, effectively reduces neutrophil influx in dual infection pneumonia*.** Before assessing the effect of Sch527123 in a murine survival model, I first had to establish that the drug would effectively reduce the inflammatory neutrophil influx to the lungs during infection. Balb/c mice were infected with either 100 $TCID_{50}$ PR/8 H1N1 influenza only or in combination with 200 CFU *S. pneumoniae* (day 3) and BAL cell counts compared on day 5 post influenza infection [Figure 1.1].

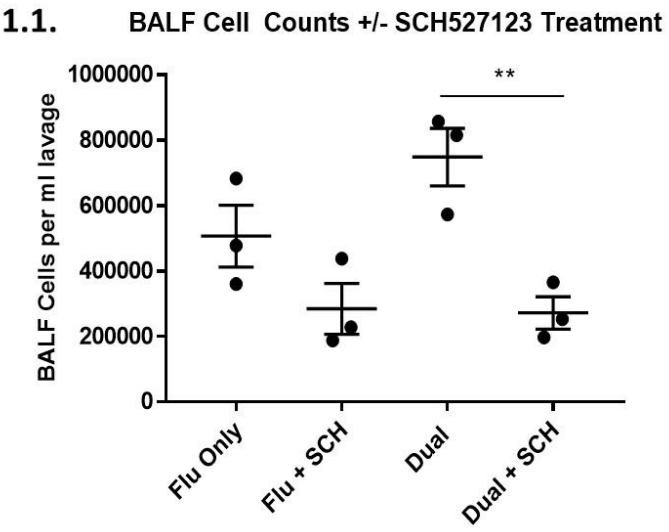


**Figure 1.1:** ***A CXCR2 antagonist, Sch527123, significantly reduces inflammatory neutrophil influx in dual infection pneumonia***. 8 week old Balb/c mice were infected with either 100 $TCID_{50}$ PR/8 H1N1 influenza only or in combination with 200 CFU *S. pneumoniae* (day 3 post infection). Sch527123 was administered at 3 mg/kg every 24 hours via gastric lavage 3-5 days post influenza infection. Sch527123 effectively reduces neutrophil influx in either infection model, but is most notable in dual infection. Data are expressed as means ± SEM and comparisons made via unpaired t-test. n=5 mice per group. ** $p<0.01$.

These cell counts were then more thoroughly compared over a 3-day period from 4 through 6 days after influenza infection using both the influenza-only and dual infection models. Although Sch527123 appears to effectively reduce neutrophil influx regardless of day or model, this impact is most notable in the murine dual infection model on day 5 [Figure 1.2]. Day 5 after influenza infection (48 hours post bacterial infection) has the highest cell count numbers of the days measured as well as the most significant reduction in this population via Sch527123.

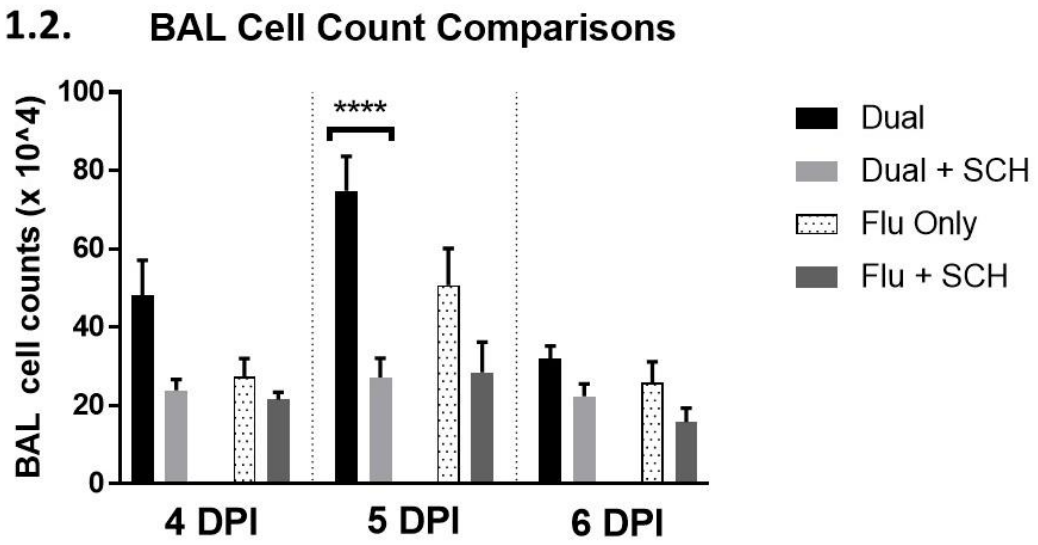


**Figure 1.2:** ***Sch527123 significantly reduces inflammatory cell influx with peaking effects 5 day after influenza infection.*** Balb/c mice were infected with either 100 $TCID_{50}$ influenza PR/8 or 100 $TCID_{50}$ influenza PR/8 + 200 CFU *Strep. pneumoniae* (Dual) and then either treated with 3 mg/kg Sch527123 every 24 hours for 3 days beginning on day 3 or with water for mock treatment. Cell counts were highest in untreated groups on day 5 [dual $p$=<0.05; flu $p$=0.0683]. Sch527123 significantly reduced cell influx in dual infected mice on day 5 post influenza infection. All data expressed as means ± SEM and comparisons made via unpaired t-test. n=3 mice per group. **** $p$<0.0001.

**C.2.** ***CXCR2 expression on infiltrated PMNs is reduced in dual infection pneumonia***. In addition to an overall reduction in the numbers of cells infiltrating the lungs during infection, there is also an apparent reduction in CXCR2 expression on these cells when treated with the CXCR2 antagonist, Sch527123 [Figure 2.1]. This change in expression is not evident in circulatory neutrophils in the dual infection model. Although this study was limited in sample size, flow cytometry was used to assess the expression of CXCR2 with and without Sch527123 treatment in both influenza-only and dual infection models. Analysis was performed from day 3-6 post infection. In addition to CXCR2, a handful of other chemokine receptors were tested to see if

there was any obvious effect of the treatment on the expression in receptors other than CXCR2. The other receptors tested were CCR2, CXCR3, and CXCR4. No changes were noted in these other receptors regardless of treatment or model (data not shown).

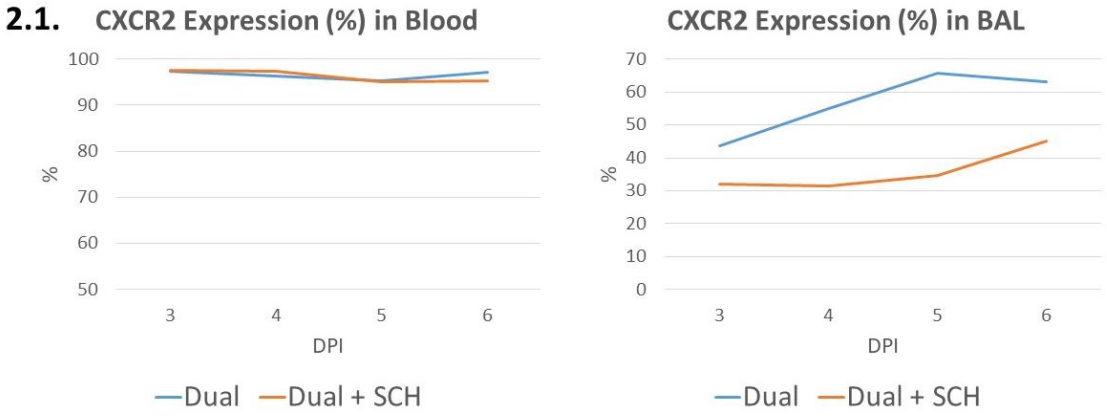


**Figure 2.1:** ***CXCR2 Expression is suppressed in infiltrated neutrophils with Sch527123 Treatment.*** CXCR2 expression was measured on PMNs (Ly6G-1A8$^{+}$) via flow cytometry 3-6 days post influenza infection. Although the sample size is too small for statistical significance, it is apparent that treatment Sch527123, a CXCR2 antagonist, reduces expression of CXCR2 on neutrophils infiltrating the lung in dual infection, while not affecting circulatory neutrophil expression. No differences were noted in either the BAL or circulatory samples for other receptors tested – CCR2, CXCR3, and CXCR4. n=1.

**C.3.** ***Sch527123 significantly delays lethality when used in combination with oseltamivir and clarithromycin.*** In order to assess the clinical potential of Sch527123 in influenza coinfection, the established murine dual infection model was used as outlined in Figure 3.1.

3.1.

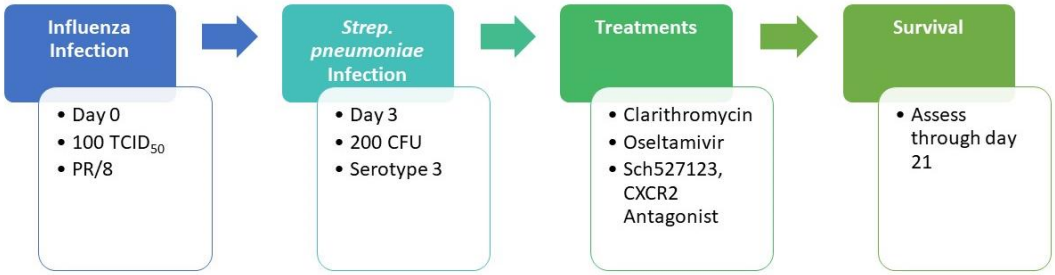


**Figure 3.1:** ***An outline of the survival study plan*****.** PR/8 H1N1 influenza was administered at 100 $TCID_{50}$ intranasally on day 0. 200 CFU *S. pneumoniae*, a sublethal infectious dose, was then administered 72 hours later. Various combinations of therapy including oseltamivir, clarithromycin, and Sch527123 were used. Survival studies were not carried out beyond 21 days after influenza infection.

3.2.

| Group Number | Oseltamivir | Clarithromycin | Sch527123 |
|---|---|---|---|
| **Group 1** | 10 mg/kg q 24 hrs for 3 doses; starting 12 hrs post *Strep.* | 100 mg/kg q 24 hrs for 3 doses; starting 12 hrs post *Strep.* | 3 mg/kg q 24 hrs for 3 doses; starting 12 hrs post *Strep.* |
| **Group 2** | 20 mg/kg q 24 hrs for 3 doses; starting 12 hrs ***prior*** to *Strep.* | 50 mg/kg q 24 hrs for 7 doses; starting 12 hrs post *Strep.* | 3 mg/kg q 24 hrs for 3 doses; starting 12 hrs ***prior*** to *Strep.* |
| **Group 3** | 20 mg/kg q 24 hrs for 3 doses; starting 12 hrs post *Strep.* | 50 mg/kg q 24 hrs for 7 doses; starting 12 hrs post *Strep.* | 3 mg/kg q 24 hrs for 3 doses; starting 12 hrs post *Strep.* |

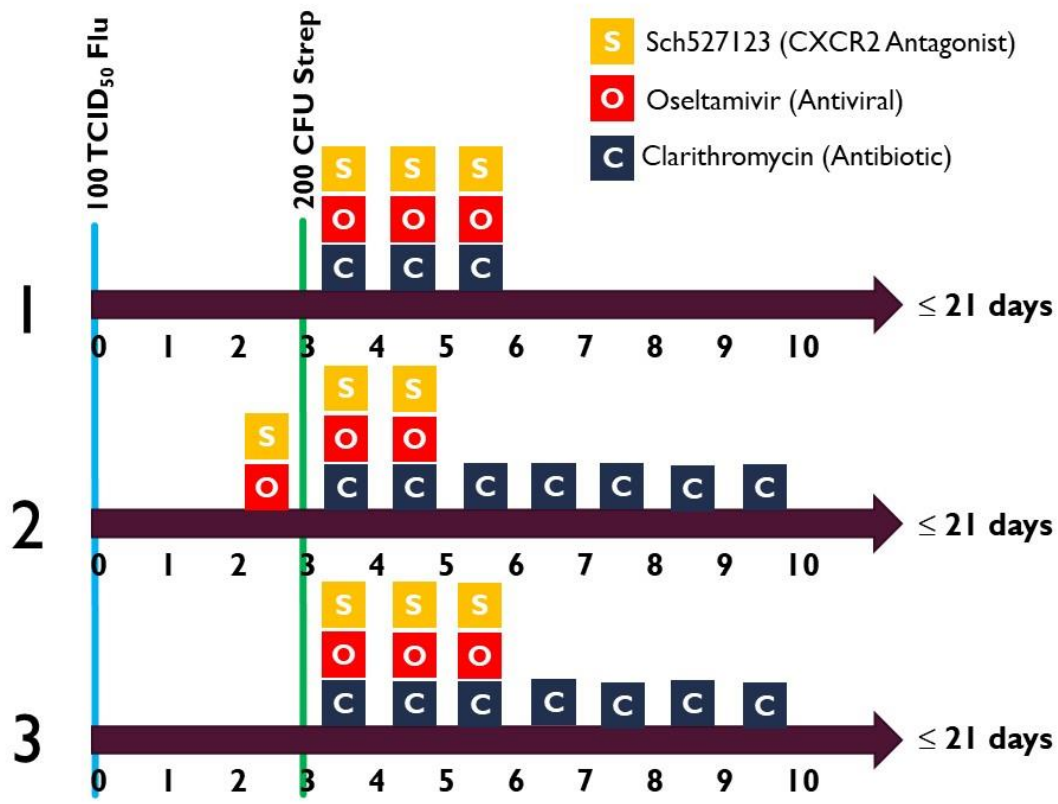


**Figure 3.2:** ***Treatment outline for each survival study***. This figure outlines the treatment protocols used for each survival study group in both table and schematic formats. Variations in dosage, frequency and timing were all employed to assess differences in treatment.

Combinations of therapy tested are outlined in Figure 3.2. For initial comparison, we will look at group 1 – this treatment model did not start any treatment until 12 hours after bacterial infection. All medications were administered via gastric lavage every 24 hours. For group 1, 3 doses of each medication were administered – 10 mg/kg oseltamivir, 100 mg/kg clarithromycin, and 3 mg/kg Sch527123 respectively. In group 1, four combinations of therapy were tested: no treatment, clarithromycin (antibiotic) only, Clarithromycin + Sch527123, and Clarithromycin + oseltamivir + Sch527123.

3.3.

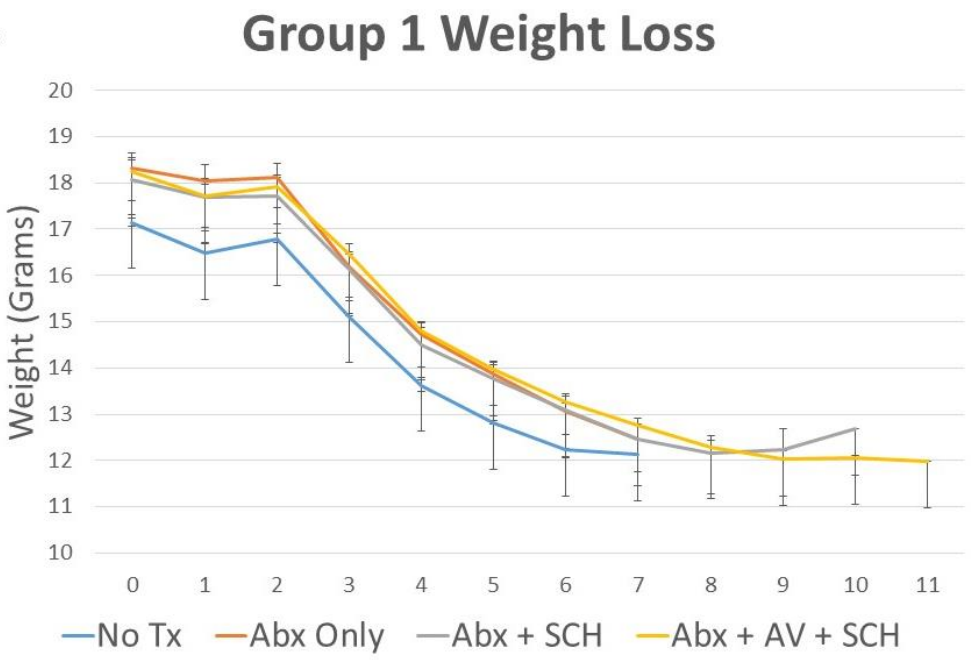


**Figure 3.3:** Group 1 did not have any significant differences in weight loss between the four tested groups. Data displayed as means ± SEM and comparisons made via one-way ANOVA each day. n=5 mice per group.

As can be seen in Figure 3.3, no significant differences in weight loss between groups is noted. However, when clinical score is assessed using the modified murine scoring system for assessment of septic shock (MCASS), the combination therapy does show statistically significant improvement in clinical score when comparing groups seven days after initial influenza infection [Figure 3.4]. The outline for this scoring system is available in Chapter 2. In general, clinical features such as lethargy, hair coat, respiratory distress, posture and behavior are closely observed in both a stimulated and unstimulated state. Mice are assigned a score from 1 through 4 with 1 being healthy and 4 being severely affected and requiring euthanasia.

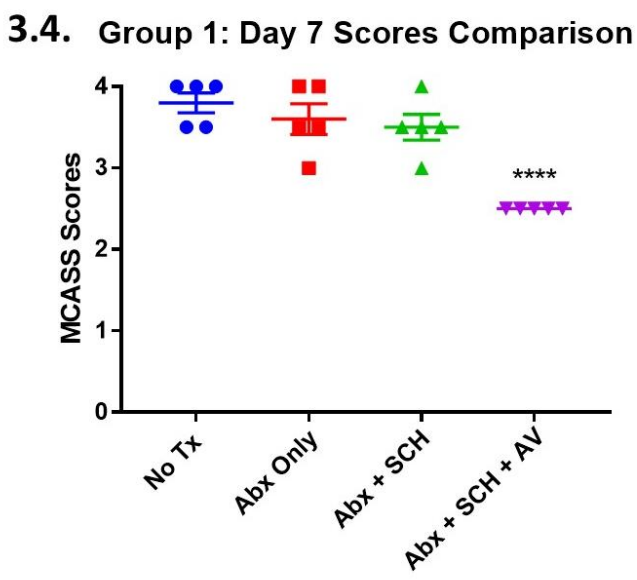


**Figure 3.4:** ***Combination therapy slows clinical decline of dual infection influenza pneumonia in a murine model*****.** Balb/c mice were infected with influenza and *S. pneumoniae* as per the dual infection protocol. No significant clinical improvement can be seen with antibiotic only or antibiotic + Sch527123 therapy, but those mice treated with a combination of all three therapies – antibiotic, antiviral, and the CXCR2 antagonist – have a slower clinical progression and a significantly improve clinical score on day 7 post influenza infection. Data expressed as means ± SEM and comparisons made via one-way ANOVA. n=5 mice per group. **** $p<0.0001$ (relative to no treatment group).

As expected upon comparing clinical progression of the treatment groups, a delay in lethality is also noted in the combination therapy group [See Figure 3.5]. No difference in survival was seen between the group receiving no treatment and that receiving clarithromycin only with 100% fatality by day 7. The group receiving clarithromycin in combination with Sch527123 had 80% lethality by day 8 and 100% by day 10. In contrast, the group receiving all three medications survived the longest with 100% still surviving through day 9. Between days 9 and 11 all mice in the final group reached their endpoint, which correlated with completion of their medication and subsequent clinical decline. Overall, the groups receiving antibiotic and SCH527123 had

significantly improved lethality over that with no treatment. Combination therapy resulted in significant delay in lethality over all other groups.

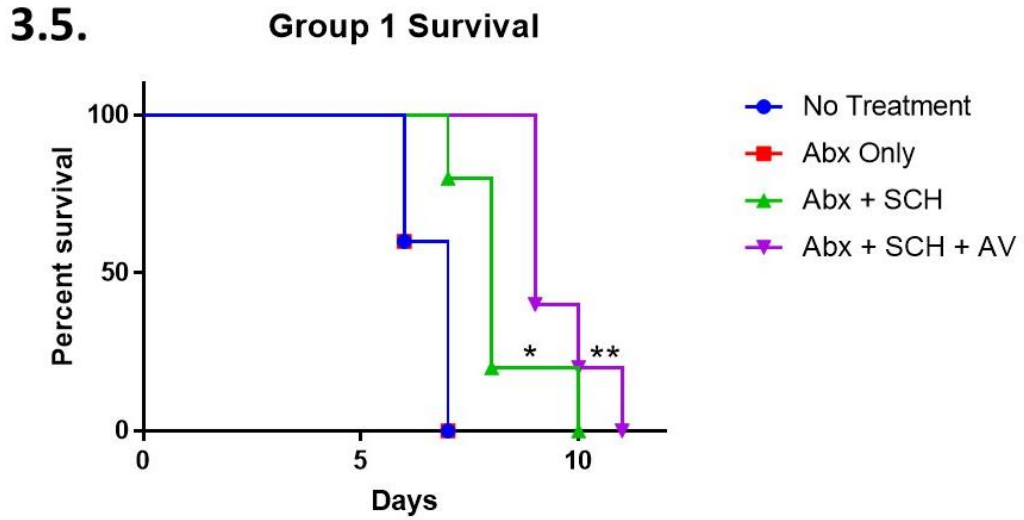


**Figure 3.5:** ***Combination therapy results in delayed lethality in a murine model of dual infection pneumonia*.** Mice were infected with PR/8 H1N1 influenza and *S. pneumoniae* as previously described. Treatments were administered as outlined in Table 3.2. No differences were seen in survival between the untreated group and that treated with clarithromycin alone. Clarithromycin in combination with Sch527123 delayed lethality slightly with only 20% survival on day 8 and 100% lethality by day 10, but was significantly improved survival over mice receiving no treatment. Combination therapy with all three – clarithromycin, oseltamivir, and Sch527123 – resulted in 100% survival through day 9 and was significantly improved over all other groups. Rapid clinical decline occurred between days 9-11 with 100% lethality by day 11. Overall, this combination was a statistically significant improvement over the other treatment models and the untreated group. n=5 mice per group. *$p$<0.05; **$p$<0.01 (relative to no treatment group.

**C.5*. Modulation of treatment groups can result in survival in our murine dual infection model*.**

After thorough evaluation of the previously described treatment model, an addition two protocols were outlined to be assessed. See figure 3.2 for treatment outlines for groups 2 and 3. Based on the previous steep decline of the combination therapy group between 9-11 days

resulting in 100% lethality, a model was proposed that allowed for 7 doses of antibiotic to be administered instead of just 3. This more closely mimics a typical antibiotic course in human disease. In addition, groups were compared starting antiviral and Sch527123 treatments at the start of more evident clinical disease (about 12 hours prior to bacterial infection), or only after the secondary infection was established.


**Figure 4.1:** ***Surviving mice begin to recover weight after day 9****.* No significant differences were noted between groups regarding weight lost during infection. Group 2 included treatment groups which were administered antiviral and Sch527123 prior to bacterial infection – this group had more overall weight recovery between days 7-10, whereas Group 3, with fewer surviving, did not see weight recovery until after day 12. Abx: 50 mg/kg Clarithromycin, AV: 20 mg/kg oseltamivir; SCH: 3 mg/kg Sch527123. n=5 mice per group.

Although weight loss was similar between all groups in the first week of infection, Figure 4.1 shows that of those mice surviving beyond 7-10 days, a steady increase in weight gain can be seen as early as day 7-9 in some groups, with most surviving mice fully recovering their weight lost by day 21. In general, this steady improvement in weight gain is more evident about 2-3 days earlier in those mice surviving group 2 compared with those in Group 3, which did not receive any medication prior to bacterial infection. This further highlights the importance of early intervention when there is a risk for coinfection.

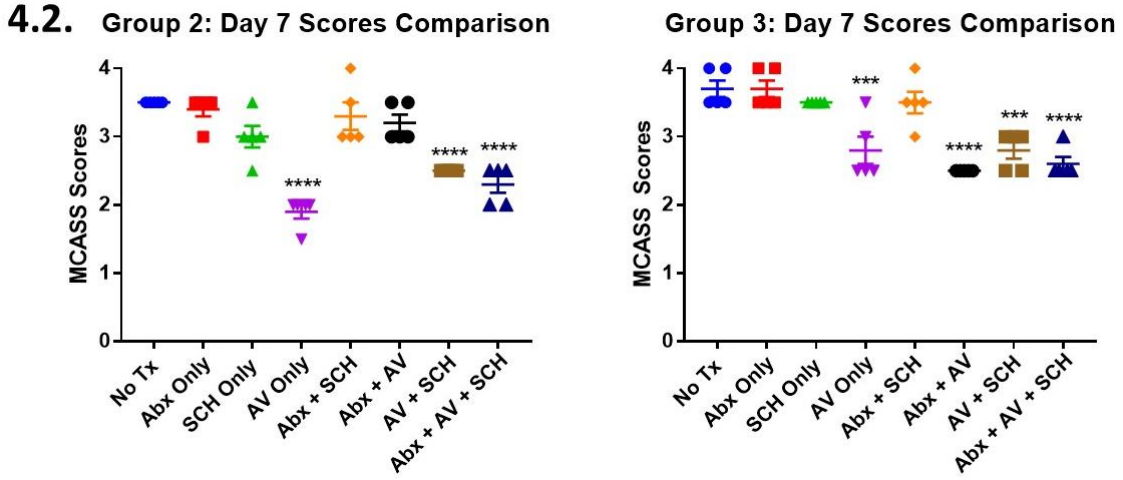


**Figure 4.2:** ***Effective combination therapy requires antiviral administration***. The above figure illustrates clinical scores comparisons on day 7 post influenza infection. Significant improvement in clinical scores is only noted in those groups receiving antiviral therapy, regardless of group. Treatment groups receiving the antiviral oseltamivir 12 hours prior to bacterial infection had the least severe clinical decline based on MCASS scoring through the first week. Of those treatment groups in Group 3, groups receiving both antibiotic and antiviral out-performed others. Full combination therapy with all three agents had significantly improved clinical scores ($p<0.001$) compared with no treatment and monotherapy, other than antiviral only. Abx: 50 mg/kg clarithromycin; AV: 20 mg/kg oseltamivir; SCH: 3 mg/kg Sch527123. Data expressed as means ± SEM. N=5 mice per group. ***$p<0.001$; ****$p<0.0001$ (relative to no treatment group).

A closer look at clinical scoring through MCASS also illustrates significant differences between treatment groups that help to explain this recovery. Figure 4.2 compares clinical scores on day 7 after infection, which is the time point where most mice either commit to their endpoint or start to show signs of clinical recovery, even if their weight loss persists for a few more days. Early intervention with antiviral therapy plays a large role in improved clinical score at day 7 as seen by viewing results from Group 2. In group 3, treatment groups receiving antibiotic and antiviral therapy did best. Combination therapy with all three medications was significantly improved as compared with no treatment and most monotherapy in both groups. These differences in

clinical scores also help to explain differences in survival seen between treatment groups. Group 2 had to most overall survival [Figure 4.3].

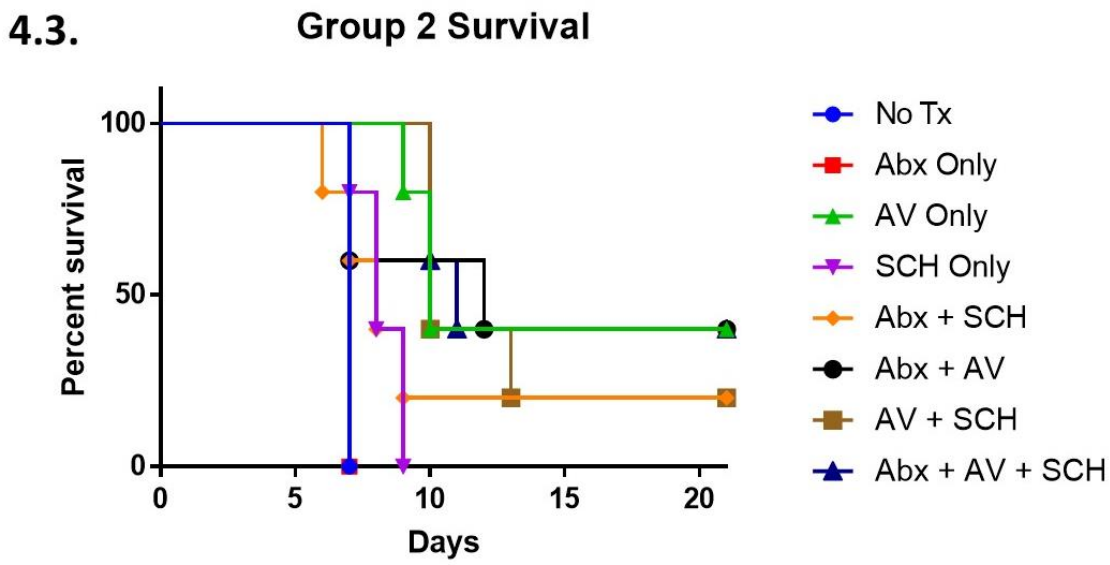


**Figure 4.3:** ***Early intervention key to survival***. Treatment groups performing best were those receiving early intervention with antiviral therapy. Combination (**), AV+SCH (**), Abx+AV (*), and AV monotherapy all performed significantly better than the untreated mice. There was no statistical improvement between untreated mice and Abx+SCH or SCH/Abx monotherapies. Combination therapy also outperformed monotherapy except for antiviral monotherapy. Antiviral monotherapy was the exception with 40% overall survival and 80% of mice surviving through day 10. 40% overall survival was also seen in Abx+AV and Abx+AV+SCH groups. Most mice survived through day 10-11 in the Abx+AV+SCH group as compared to Abx+AV where a decline was noted at day 7. 20% survival was seen in dual therapy groups – Abx+SCH and AV+SCH. No statistical significance is seen between dual and combination therapy groups. n=5 mice per group. *$p$<0.05; **$p$<0.01 (listed in text – relative to no treatment group).

The antibiotic only group matched the group receiving no treatment in survival with 100% lethality by day 7. Only mild improvement was noted in Sch527123 monotherapy, with 100% lethality on day 9. The only monotherapy that performed well was the oseltamivir only group, with 80% still alive through day 10 and 40% surviving through day 21. As a part of group 2, these mice received antiviral therapy at the start of significant clinical signs, which was 12 hours prior to bacterial infection. In addition to the antiviral monotherapy group, 40% overall survival was

also seen in the antibiotic + oseltamivir and antibiotic + oseltamivir + Sch527123 groups. Sch527123 improved combination therapy group outcome over Abx+AV – although their ultimate survival matched, the remaining mice survived through days 10/11 whereas a decline was noted in the group not receiving Sch527123 treatment on day 7. 20% survival was noted in the antibiotic + Sch527123 and oseltamivir + Sch527123 groups as well. Overall, combination therapy with 2 or 3 therapeutic agents outperformed monotherapy and early intervention appears to be significant in improving clinical outcome.

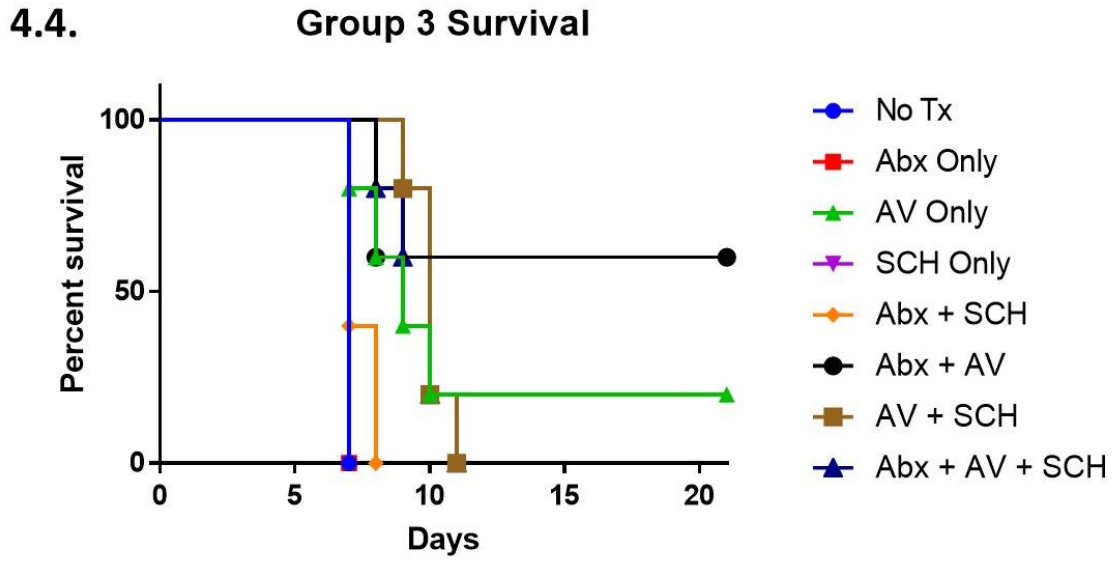


**Figure 4.4: *Sch527123 therapy less effective when administered after bacterial infection*.** Overall, fewer mice survived from the Group 3 study than Group 2. 60% survival is noted in the Abx+AV dual therapy group and 20% in the antiviral monotherapy group. Most mice declined and reached end point at earlier time points compared with Group 2 as well. Several groups performed significantly better than the untreated mice: antiviral monotherapy (*), Abx+AV (**), AV+SCH (**), and combination therapy (**). Combination therapy also performed significantly better than Abx or SCH monotherapy (**) and Abx+SCH dual therapy (**). Abx: 50 mg/kg clarithromycin; AV: 20 mg/kg oseltamivir; SCH: 3 mg/kg Sch527123. n=5 mice per group. *$p$<0.05; **$p$<0.01 (listed in text – relative to no treatment group).

Group 3 focused on initiating therapy only after bacterial infection, with all medications starting 12 hours after the administration of *S. pneumoniae*. Severe clinical decline is seen about 24

hours prior to this time, so it is not surprising that survival was not as prominent in these treatment groups as it was in Group 2. Only two groups saw any survival – antiviral monotherapy and antibiotic/antiviral dual therapy. A remarkable 60% survived in the antibiotic/antiviral dual therapy group. The 40% which did not survive were euthanized quickly by day 8. Overall, most groups saw significant declines in survival around day 8. Antiviral/SCH dual therapy fared better with 80% survival through days 10 and 11. However, without antibiotic therapy, none of this group survived to 21 days. Combination therapy with all three medications also saw a delay in lethality with mice surviving through day 10, even though none survived to day 21. Another interesting comparison comes from looking at the Sch527123 monotherapy treatment groups between Group 2, where it was administered 12 hours prior to bacterial infection, and group 3, 12 hours after bacterial infection. In Group 3, all the mice reached endpoint on day 7, but these mice survived an extra 1-2 days when therapy was initiated earlier. Finally, combination therapy was compared between groups 1, 2 and 3 in Figure 4.5. Although combination therapy effectively delayed lethality as compared with most monotherapy groups, only mice with early intervention antiviral and Sch527123 therapy survived through day 21.

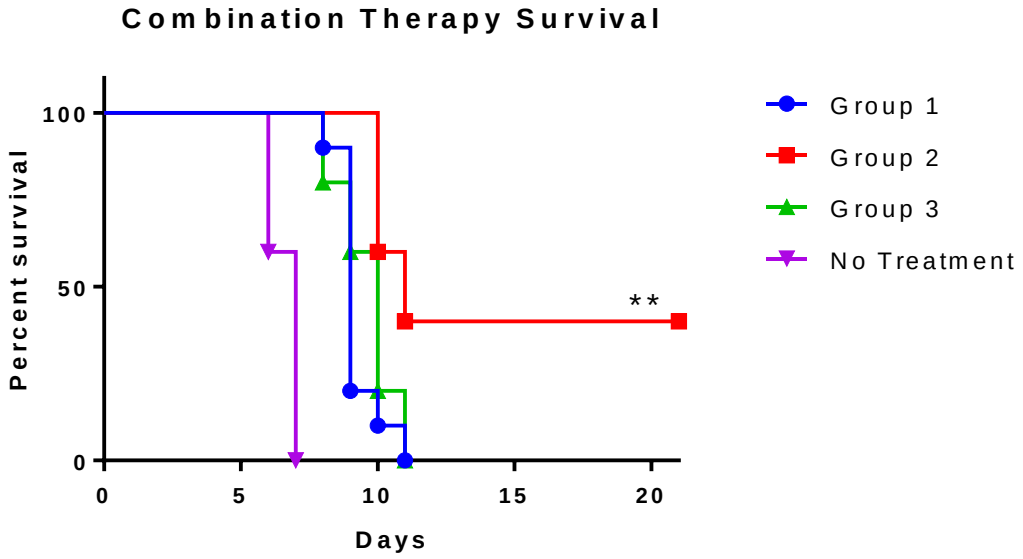


**Figure 4.5:** ***Early intervention is key in successful combination therapy***. Mice receiving combination therapy (clarithromycin, oseltamivir and Sch527123) had significantly delayed lethality over most monotherapy groups and those not receiving treatment. Survival (40%) is only noted in mice receiving combination therapy with early intervention of antiviral and Sch527123 treatments, starting at the onset of severe clinical decline, approximately 12 hours prior to bacterial administration. Refer to Table 3.2 for group descriptions. n=5 mice per treatment group. ***p*<0.01 (relative survival to both groups 1 and 3).

**C.5.** ***Combination therapy reduces pulmonary pathology and clinical disease by day 5.*** In order to more thoroughly investigate why combination therapy is effective in delaying lethality in mice infected with dual infection pneumonia, an experiment was performed comparing no treatment, antibiotic-only, SCH527123-only and combination therapy (antiviral, antibiotic and SCH527123) on day 5 after influenza infection. Therapeutics were administered based on the Group 2 model, with antiviral and SCH527123 treatment beginning 12 hours prior to bacterial infection and antibiotic therapy starting 12 hours after bacterial infection. Our results indicate that combination therapy significantly reduces weight loss on day 4 and 5 when compared with

untreated groups. Antibiotic therapy also had significant reduction in weight loss compared with the group receiving no treatments [Figure 5.1].

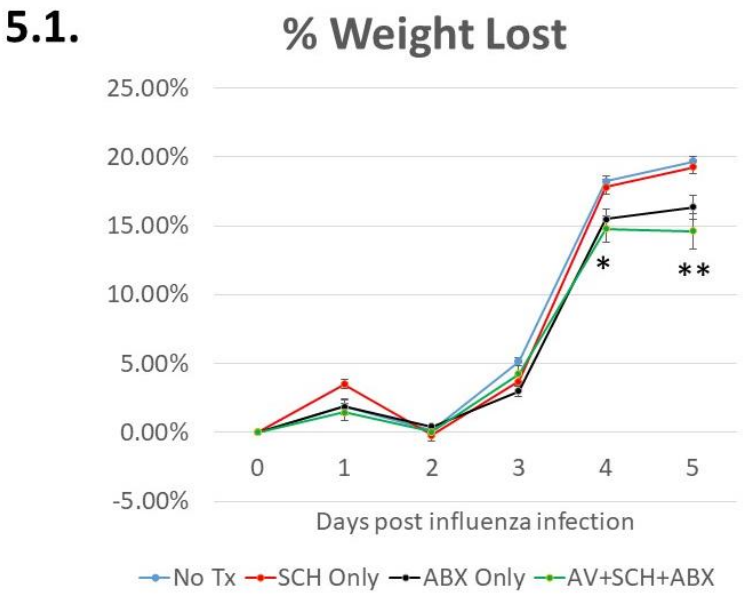


**Figure 5.1:** ***Mice treated with combination therapy lose less weight*.** Balb/c mice were infected with 100 $TCID_{50}$ PR/8 H1N1 followed by 200 CFU *S. pneumoniae* 72 hours after viral infection. SCH527123 was administered at 3 mg/kg every 24 hours beginning 12 hours prior to bacterial infection. Oseltamivir was administered at 20 mg/kg beginning 12 hours prior to bacterial infection. Clarithromycin was administered at 50 mg/kg beginning 12 hours after bacterial infection. Mice treated with antibiotic alone and combination therapy did not lose as much weight as the untreated mice on day 5 ($p<0.01$ for combination and $p<0.05$ for antibiotic monotherapy). Combination therapy also lost less weight than the SCH527123 treated group on day 5 ($p<0.05$). These same groups were also statistically different on day 4 ($p<0.05$). Data are expressed as means ± SEM. n=6 mice per group per day. $^{**}p<0.01$; $^{*}p<0.05$ (relative to no treatment group).

Clinically, improvement was also seen with combination therapy. M-CASS scores over the 5-day period were used to compare groups. By day 5, mice treated with monotherapy have significantly lower clinical scores than untreated mice and combination therapy is significantly improved over all other groups. No differences were noted between antibiotic-alone and SCH-alone treated mice [Figure 5.2].

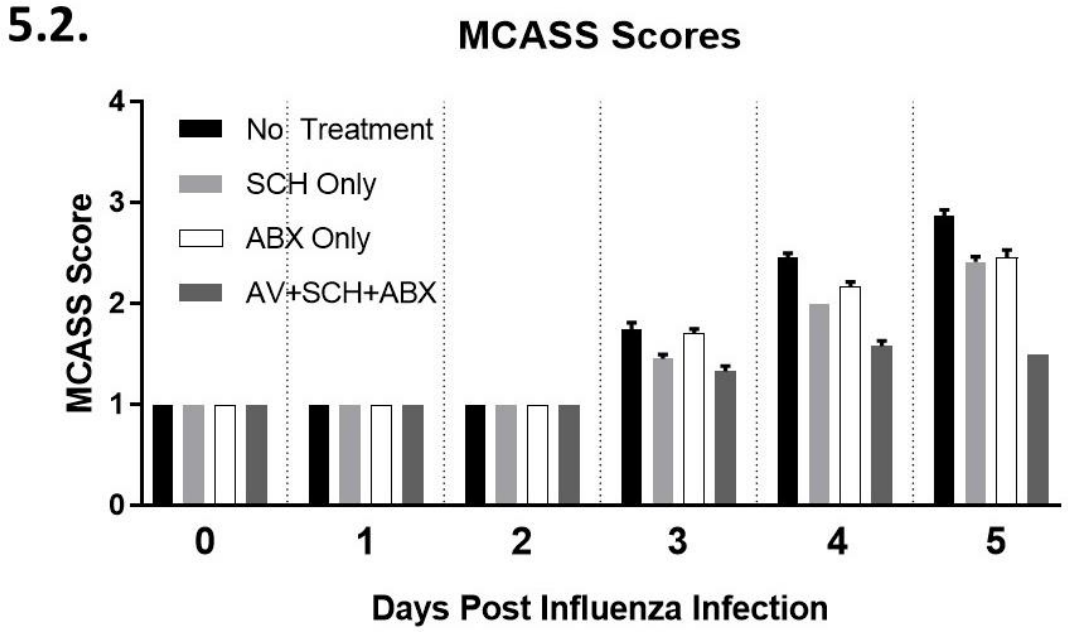


**Figure 5.2:** ***Combination therapy reduces clinical severity more than monotherapy***. Dual-infected mice were monitored over 5 days for clinical severity and scored based on the MCASS System (1 (healthy) to 4 (severe)). Beginning at day 3, there is statistical significance in differences between all groups ($p<0.0001$) other than SCH Only and combination therapy on day 3 and the two monotherapies on day 4. Clinically, mice were statistically improved with monotherapy over no treatment and combination therapy of all three agents was better than any other group. Data are expressed as means ± SEM and comparisons made via one-way ANOVA. n=6 mice per group.

Bronchoalveolar lavage was collected from 3 mice in each group on day 5 and cell counts were performed [Figure 5.3]. Mice receiving no treatment had significantly higher inflammatory cell influx compared with all other groups. Treatment with SCH527123 alone reduced the inflammatory cell influx by about 50%. Combination therapy had the greatest effect with the lowest number of inflammatory cells in the BAL on day 5. These findings can be further visualized with the provided images from cytospins of those BAL samples.

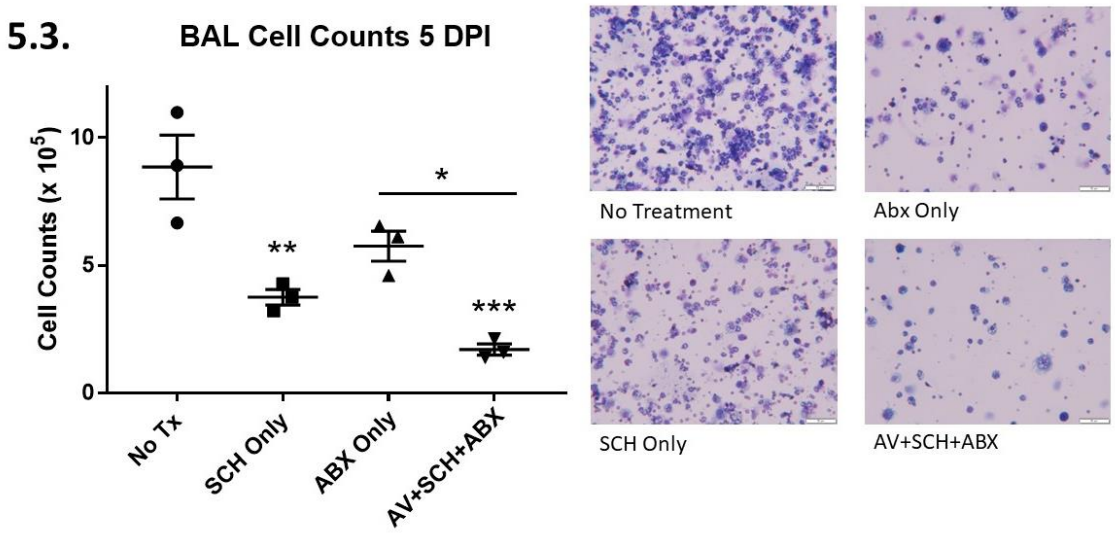


**Figure 5.3:** ***SCH527123 effectively reduces neutrophil influx in both monotherapy and with combination therapy***. BAL was collected from dual-infected mice 5 days after influenza infection (48 hours post bacterial infection) and cell counts were performed. Mice receiving no treatment had the most excessive inflammatory cell response. Treatment with SCH527123 reduced this response by over 50%. Combination therapy with all three treatments had the lowest cell counts on day 5. Cytospins were stained and pictures provided. Data are expressed as means ± SEM. n=3 mice per group. ***$p$<0.001; **$p$<0.01; *$p$<0.05 (relative to no treatment group).

Finally, histopathology was scored and compared between groups on day 5. Three mice in each group were euthanized and lungs collected and fixed in formalin for comparison. Lungs were scored from 0-4 (4 being most severe) based on 7 focus areas: necrotizing bronchiolitis, bronchiolar infiltrates, alveolitis, interstitial inflammation, hemorrhage, edema, and microvascular thrombosis. A sum of scores is provided for comparison in Figure 5.4. Combination therapy has significantly reduced pulmonary pathology on day 5 compared with untreated and antibiotic-alone infected mice. This reduction in severity as compared with other groups is clearly evident when viewing the lung tissue in the provided images.

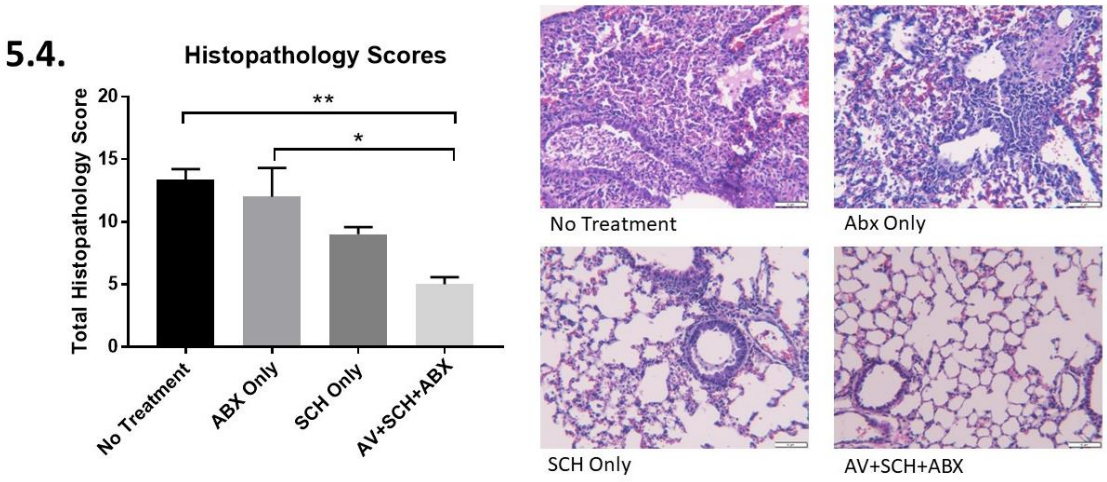


**Figure 5.4:** ***Combination therapy reduces pulmonary pathology on day 5****.* Mice were euthanized on day 5 after influenza infection (48 hours after bacterial infection). Lungs were collected and formalin-fixed for histopathology scoring and comparison. Lung pathology was scored from 0-4 (4 being most severe) in these areas: necrotizing bronchiolitis, bronchiolar infiltrates, alveolitis, interstitial inflammation, hemorrhage, edema and microvascular thrombosis. These individual scores were summated and used from comparisons. On day 5, combination therapy resulted in significantly improved scores compared with both untreated and antibiotic monotherapy. Sample images from hematoxylin and eosin stained slides used for scoring are provided. Data are expressed as means ± SEM and comparisons made via one-way ANOVA. n=3 mice per group. *$p$<0.05; **$p$<0.01.

**D. Discussion**

These research findings support that Sch527123 is an effective CXCR2 antagonist in murine models of influenza coinfection with a significant reduction in neutrophil influx seen by day 5 after influenza infection (48 hours after bacterial infection). In addition to controlling the hyperinflammatory innate response to infection, Sch527123 appears to reduce CXCR2 expression on these infiltrated neutrophils within the lungs.

Overall, a delay in lethality is noted with this use of combination, triple agent therapy. These results are promising despite lack of significant survival. Our murine model used for these

studies is very severe with 100% lethality seen in all dual infected mice between days 6-7 after influenza infection. With combination therapy, most mice survive through day 10-11, regardless of when the therapy is initiated. In our dual infection murine model, the untreated mice decline rapidly. Without supportive care and fluid therapy, all mice lose significant weight within the first week, even those in treated groups. This makes it difficult to have mice recover before reaching their endpoint for the study. However, this makes survival in this model all the more impressive and supports that delays in lethality are also clinically relevant.

Not surprisingly, Sch527123 monotherapy is ineffective at improving survival and clinical outcome in this model. With the complexity of influenza coinfection, it is relatively well established that monotherapy is unlikely to improve outcome in most severe cases of coinfection, especially during a pandemic outbreak. Interestingly, even though we do not see survival with any Sch527123 monotherapy treatment group, we do see a delay in lethality when started early (12 hours prior to bacterial infection) as opposed to after bacterial infection. Our results also support the need for early antiviral intervention. These are both key findings in our influenza coinfection research which provide evidence for the importance of early intervention with combination therapy by healthcare professionals, and the need for patients who think they may have influenza to see a healthcare provider as soon as possible. In our experiment comparing SCH527123 monotherapy, antibiotic monotherapy and combination therapy with untreated mice, we can see that even by day 5 there are marked differences between groups. Combination therapy effectively reduces pulmonary pathology and inflammatory cell influx. Both antiviral therapy and Sch527123 therapy lost some effectiveness when administered later. The mice in these studies saw a significant clinical decline due to their influenza infection between days 2 and 3. Therapy should really be administered at the start of moderate clinical signs, before a patient is hospitalized.

This research opens up several avenues for continued work in the area of combination therapy in influenza coinfection. One question yet to be answered asks how effective is Sch527123 if given over various time points? And is there a point at which it could be considered detrimental? When reviewing results from treatment groups receiving early intervention of Sch527123, the greatest effect on clinical outcome is noted in those groups receiving this drug near the start of severe clinical signs and before a secondary bacterial infection has occurred. In contrast, we can shift our focus to Group 3 which did not receive any medication prior to bacterial infection, regardless of treatment group. In this group we see 60% survival in those mice treated with dual therapy antibiotic and antiviral (no Sch527123), but by merely adding Sch527123 to this group to make it a triple combination therapy, we see 100% lethality. Does this mean that antagonizing CXCR2 and inhibiting neutrophil influx after bacterial infection is present can lead to poorer outcomes in influenza coinfection? We can't draw that conclusion at this time, but continued studies in other animal models with various protocols should be continued to fully understand the nature of this antagonism before suggesting it be used in human disease.

In conclusion, chemokine receptors continue to be an intriguing target for combination therapy in influenza coinfection. As the effectiveness of antiviral therapy and antibiotics alone is continually questioned due to resistance and variation in potency, identifying further therapies that can be used in combination with these two will be critical to improving clinical outcome moving forward. Influenza coinfection is complex and identifying an effective animal model difficult. In addition, antagonists may target multiple receptors, which has the potential to have an even greater effect, but may prove to be quite complicated in fully understanding how these therapies work. Although significant progress has been made in studying the potential for chemokine receptor antagonists is models of chronic inflammation, immune-mediated disease,

and cancer, this progress has not been as detailed in acute inflammatory conditions, in particular influenza coinfections. Results from this study support exciting findings that these antagonists may offer some hope to improving clinical outcome in severe cases, especially during pandemic influenza outbreaks when mortality is higher and treatments often prove ineffective.

# CHAPTER V

# INFLUENZA PNEUMONIA IN A SWINE MODEL RESULTS IN A HYPERINFLAMMATORY INNATE REPSONSE AND THE RELEASE OF NEUTROPHIL EXTRACELLULAR TRAPS

## A. Introduction

The sharing of influenza viruses between pigs and humans has been apparent since at least 1918 [228, 229]. Even though the role of the pig in human influenza pandemics has long been speculated, it has been more widely recognized and researched over the last 25 years, especially due to the "swine flu" pandemic in 2009 [229]. Pigs are natural hosts for influenza A viruses, and pose an increased risk of transmission to humans with direct contact, as well as through aerosolized droplets and fomites. Transmission may occur from any swine source, but reports have detailed that increased risk to humans is present whenever pigs and humans come in close contact [230], such as in show pigs [231] and pigs as companion animals [232]. In addition, feral swine serve as a reservoir for swine influenza since they are often in close contact with wild birds and water fowl. In the US, it is estimated that about 5% of feral pigs carry antibodies to influenza A – these antibodies are mostly to swine influenza, but avian influenza is also present in substantial amounts [233]. Surveillance methods will be key to pandemic planning in the future [228], but are difficult due to variation in serological data collected and

a lack of standardization [234]. RT-PCR methods have been developed and protocols are now available for more standardized diagnostics [235].

Pigs are animals of interest primarily due to their capability to serve as mixing vessels for various strains of influenza viruses to reassert and potentially cause more significant human disease. A recent review looked at over 1400 cases of swine and avian influenza in naturally-infected humans and found that the avian-influenza infections were primarily H5N1, but other H5, H6, H7, H9 and H10 were all reported as well [230]. Of the highly pathogenic H5N1 human cases (HPAI), the World Health Organization reported that 59% of those infected died, and death spanned 15 countries. This high mortality associated with avian viruses emphasized the threat of reassortment in pigs to make an even more pathogenic virus which can more readily infect humans. Of the swine viruses, H1 and H3 predominate [230]. A primary consideration includes the availability of sialic acid receptors to bind the virus and create disease. The human respiratory tract has predominantly α-2,6 receptors on the ciliated cells of the upper respiratory tract, but a mixture of α-2,6 and α-2,3 as the tract progresses to the non-ciliated respiratory epithelium [236]. Human influenza viruses include α-2,6 galactose viruses which prefer to bind to α-2,6 sialic acid receptors [237]. Avian influenza viruses prefer α-2,3 receptors [238]. Pigs are infected by both α-2,3 and α-2,6 SA-galactose viruses and have both receptor types present in the respiratory epithelium, somewhat similar to human [239]. Transmission is much more complex than just receptor availability and many factors are still being researched to better understand this transmission.

Since pigs can naturally be infected with both avian and human influenza A viruses, they serve as high risk vessels for viral reassortment. The segmented viral genome facilitates simple exchange of genetic material if a pig is co-infected with two different influenzas, referred to as

antigenic shift if hemagglutinin is involved in this reassortment of genetic material [230]. Humans have little to no pre-existing immunity to viruses undergoing antigenic shift. The influenza virus may also undergo a series of mutations during replication, often amino acid substitutions. If hemagglutinin is directly affected by these mutations, the virus can undergo antigenic drift, which also exposes an otherwise naïve population to a virus with novel surface antigens [230]. Pigs have been used more recently in experimental models to try to recreate this antigenic shift or drift with varying levels of success. It has proven difficult for pigs to experimentally create the pandemic virus from 2009 through introducing triple reassortment virus and Eurasian swine influenza virus, supporting that this particular pandemic was a relatively rare event involving many complex and yet unknown factors [240]. More recently, a pig model has been successfully used to reassert H3N2 swine influenza with H1N1 avian/duck influenza [241]. In another study more closely evaluating the evolutionary dynamics of influenza virus in pigs, serial passages of virus effectively created a reassorted virus with enhanced pathogenicity [242].

These shifts in viral subtypes can occur over longer periods of time between pandemics and season to season. During the 1918 “Spanish flu” pandemic, the predominant strain was H1N1, but a shift to H2N2 was seen around the time of the “Asian Flu” pandemic in 1957 and then another shift to H3N2 for the “Hong Kong” pandemic in 1968. Since the “swine Flu” pandemic in 2009-2010, seasonal influenza outbreaks have been predominantly the pandemic 2009 strain of H1N1, which stems from the North American triple reassortment and Eurasian avian-like swine influenza viruses, as opposed to the previous H1N1 strains. H3N2 has replaced H2N2, which is now circulating in birds and pigs, but not humans. Climate and time of year also contributes to viral outbreaks and should be considered when planning for pandemics [243].

Various animal models have been considered for further studying influenza virus vaccines, treatment, and the pathogenesis behind the disease. Mouse models are the most widely used due to their availability and affordability, but several downsides are present to using mice to model this disease. First, mice require adapted viruses to see the same clinical disease anticipated in humans [244]. They also lack the influenza virus receptors found in humans [245] and don't shed the virus, so transmission studies are not possible [246]. Ferrets are better models because they work well for transmission studies [247] and don't need adaptation [244], but come at a much higher cost with limited availability and fewer available reagents [244]. Guinea pigs are a smaller, more manageable size and so have reduced cost, but also have few available reagents [244] and diminished clinical signs [248].

In contrast to many of the setbacks with other animal models, pigs are excellent models for influenza infection studies. Anatomically, their respiratory tract is very similar to the human anatomy [249] and has similar distribution of influenza A virus receptors [250]. The virus replicates easily in both the upper and lower respiratory tracts [251], and, as a natural host, can be infected with the same subtypes endemic in both species [250]. Swine influenza has a high morbidity and low mortality and results in a high fever and nasal discharge in most models – the clinical disease and pathogenesis are also similar to that of human disease [250, 251]. Pigs also make a great model for human immune parameters and response to infection since the H1N1 virus induces a similar acute inflammatory immune response [251, 252]. In the last few years, the entire swine genome has been sequenced as well [253] and been found to be similar in size and complexity to the human genome. Several coinfection models have been evaluated in pigs [254-257]. In coinfection models with *Bordetella bronchiseptica* [255, 256], pigs have similar synergism to that noted in human disease and increased viral replication, enhanced bacterial colonization, production of proinflammatory cytokines, and exacerbated pulmonary pathology

are all seen in coinfection. This synergism is also evident in a coinfection model of swine influenza with *Actinobacillus pleuropneumoniae* [257]. Identifying and characterizing a swine model allows for many opportunities for studies related to viral pathogenesis, coinfection, therapeutics, and vaccine development [258]. This chapter outlines a swine model for influenza pneumonia that shows great potential for further studies assessing therapeutics and potential coinfection models of disease.

**B. Materials and Methods:**

*Pathogen*

Influenza A/swine/Iowa/15/30 (H1N1) virus was obtained from the American Type Culture Collection (ATCC, VA). Viral titers were determined by tissue culture infectivity dose ($TCID_{50}$) assay via infection of Madin-Darby canine kidney (MDCK) cells. Virus was stored at -80°C until use.

*Animals*

Piglets ranging from 10 to 12 weeks' old were purchased from controlled farms and housed in large cages in a BSL-2 facility. Fresh food and water were provided ad libitum. Piglets were clinically evaluated each day for weight loss, nasal or ocular discharge, resting respiratory rates, lethargy and rectal temperatures. Infection was performed under a mixture of xylazine (2 mg/kg) and ketamine (10 mg/kg) administered via intramuscular injection. Piglets were infected intranasally with a sublethal dose of $1 \times 10^6$ $TCID_{50}$ Influenza A/swine/Iowa/15/30 (H1N1) delivered in two 0.5 mL increments. All animal experiments were approved by the Institutional

Animal Care and Use Committee (IACUC) of Oklahoma State University and were performed in strict accordance with their recommendations.

*Whole blood, bronchoalveolar lavage (BAL) fluid, and tissue collection*

Sample collection occurred on days 3 or 6 after influenza infection. Piglets were anesthestized with a xylazine (2 mg/kg) and ketamine (33 mg/kg) combination administered intramuscularly. Euthanasia was performed with 1 mL/10lbs pentobarbital administration via intravenous injection. For BAL fluid collection, the left lung was washed by intratracheal administration of 20 mL of sterile PBS in two 10 mL increments. The recovery of BAL fluid was more than 85% for all animals. The BAL fluids were centrifuged at 200 xg for 10 minutes, and reconstituted in sterile PBS for cell counts. BAL cells were concentrated using the CytoFuge 2 cytocentrifuge (StatSpin, Westwood, MA), and differential cell counts were performed using modified Giemsa staining. Bronchoalveolar lavage fluid was collected on days 3 and 5 for infected piglets and at day 0 for healthy controls.

*Immunohistochemistry*

Immunohistochemistry analysis was performed on formalin-fixed pulmonary tissue sections for the detection of neutrophils and viral particles in the lungs using anti-CXCR2 and anti-PR/8 antibodies respectively.

*Histopathology*

The right lung was fixed with 4% formalin and collected for histopathology analysis after hematoxylin and eosin (H&E) staining. Mice were scored on a 1-4 scale (4 being most severe) for severity in the following areas: necrotizing bronchiolitis, bronchiolar infiltrates, alveolitis, interstitial inflammation, hemorrhage, edema, and microvascular thrombosis. Necrotizing

bronchiolitis was defined as damage to the airway epithelial cells, presence of necrotic bodies or the total denudation of the airway lining. Total histopathologic scores were evaluated as a sum of all individual scores.

**C. Results:**

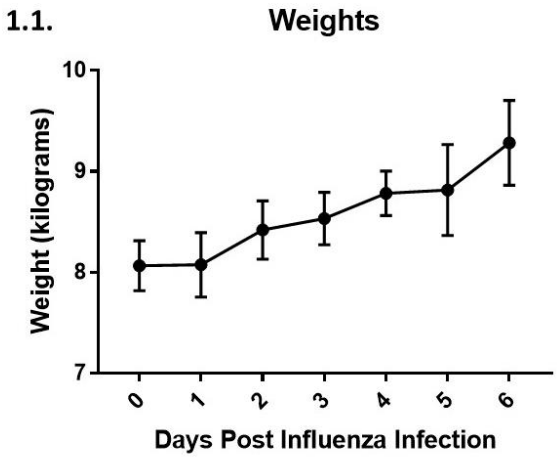


**Figure 1.1:** ***Infected piglets do not lose weight.*** Piglets were infected with Influenza A/swine/Iowa/15/30 (H1N1) at 1 x $10^6$ $TCID_{50}$ per piglet. Pigs were monitored daily for weight, rectal temperature, resting respiratory rate and clinical signs. Weights were unaffected by infection with an overall slight increase in piglet weight over 6 days. Other clinical signs included mild ocular and mild to moderate nasal discharge, first noted at 2 DPI and sustaining through 6 DPI. Data are expressed as mean ± SEM. n = 6 pigs per group for all studies.

*1. Infected piglets have mild clinical disease in our model.* Before assessing treatment efficacy in piglets infected with H1N1 influenza, a model for the clinical disease course was established. Our lab infected piglets with 1 x $10^6$ $TCID_{50}$ Influenza A/swine/Iowa/15/30 (H1N1) intranasally and compared weight loss, clinical signs, cell counts and gross and histopathology with mock-

infected piglets. Infected piglets did not lose any weight and continued to eat and drink through the course of infection [Fig. 1.1].

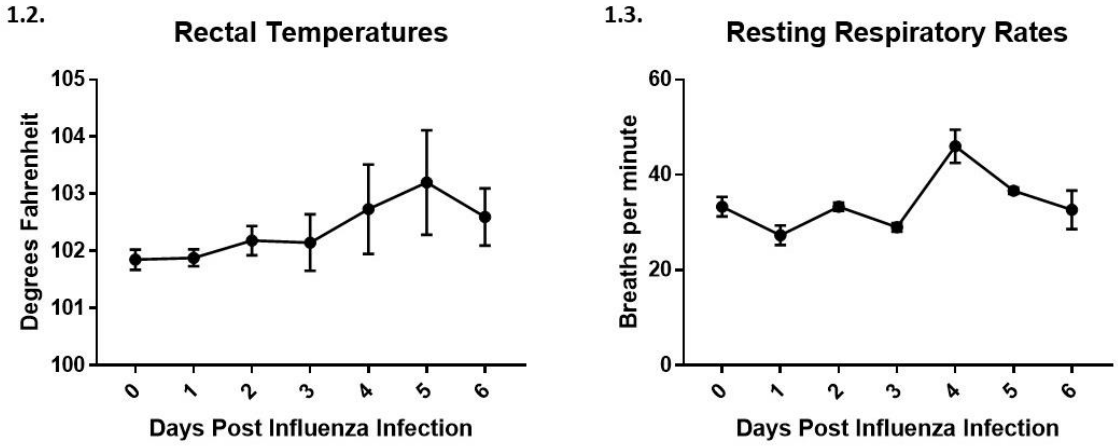


**Figures 1.2 and 1.3:** ***Clinical signs in infected piglets peak on days 4 and 5 post infection.*** Piglets were infected with Influenza A/swine/Iowa/15/30 (H1N1) at 1 x $10^6$ $TCID_{50}$ per piglet. Pigs were monitored daily for weight, rectal temperature, resting respiratory rate and clinical signs. **1.2:** Rectal temperature peaked at day 5 with an average temperature of 103.2°F (Normal: 101.5-102.5°F). **1.3:** Resting respiratory rate peaked on day 4. Other clinical signs included mild ocular and mild to moderate nasal discharge, first noted at 2 DPI and sustaining through 6 DPI. Data are expressed as mean ± SEM. n = 6 pigs per group for all studies.

Rectal temperatures peaked at day 5 with an average rectal temperature of 103.2°F (normal 101.5-102.5°F) [Fig. 1.2]. Resting respiratory rates peaked at day 4 post influenza infection [Fig. 1.3]. Mild to moderate nasal discharge was noted in all infected piglets beginning at day 2 and two infected piglets had mild ocular discharge. The pigs remained active and only mild lethargy was noted starting at day 3 post infection.

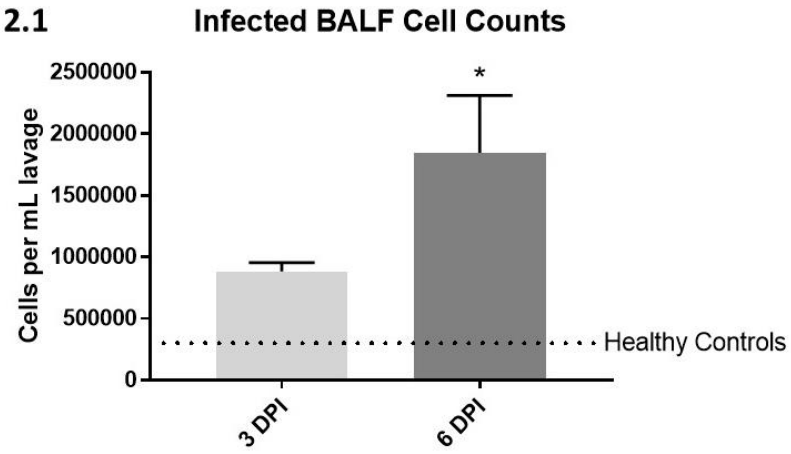


**Figure 2.1:** ***Inflammatory cellular influx is noted in infected pigs***. BAL was collected in control pigs as well as on days 3 and 6 post influenza infection. Data from control pigs was unreliable due to some secondary infections present in the piglets at the time of sample collection. Therefore, an established average for cell counts in healthy pigs is provided as a comparison. An increase in BAL fluid cell counts is noted highest at day 6, and is significantly higher that day 3 Both day 3 and day 6 cell counts are significantly higher than typical healthy pigs. Data are expressed as mean ± SEM. n = 6 pigs per group for infected studies and n=2 for control. *$p$<0.05 relative to healthy controls.

*2. Infected piglets have hyperresponsive neutrophil recruitment to the lungs*. As noted in our murine model, infected piglets continue to an excessive innate response despite a mild clinical disease course. Cell counts from bronchoalveolar lavage samples collected at 3 and 6 days after influenza infection are higher than healthy controls with an exaggerated response noted by day 6 [Fig. 2.1]. In addition, the populations within these BAL cells shift over the course of infection – macrophages predominate at day 3, but by day 6, significant neutrophil recruitment is noted with neutrophils being the predominant cell type [Fig. 2.2]. These populations can be better visualized with the images provided in Figure 2.3.

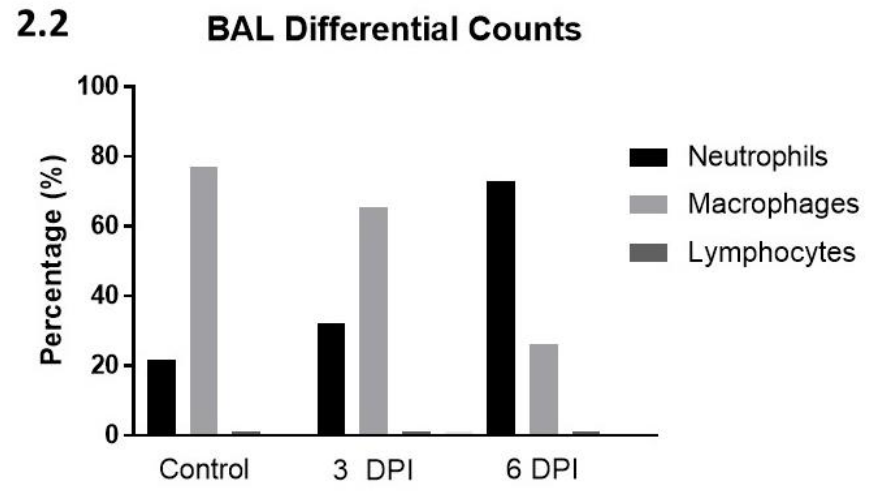


**Figure 2.2:** ***Differential counts shift from predominantly macrophages to neutrophil by day 6.*** BAL was collected on day 3 and day 6 post influenza infection. Cytospins were prepped and differential counts performed manually. Alveolar macrophages predominate in control pigs as well as those 3 days post infection, but a clear shift to marked neutrophilia is seen by day 6. Other cells noted in minimal numbers include lymphocytes and eosinophils.

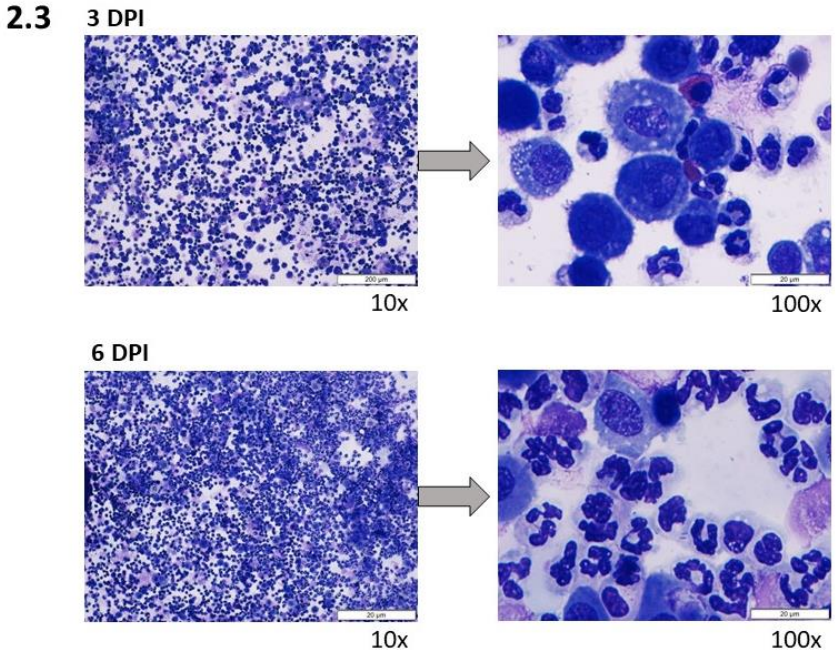

**Figure 2.3:** ***Neutrophils predominate on day 6 post influenza infection.*** BAL was collected from pigs 3 and 6 days after influenza infection. Cells were spun down for cytospin and stained with Diff Quick for differential counts and imaging. Stained cytospin samples provide a visual for the differential counts. On day 3, macrophages predominate with neutrophils as the second most populous cell type. On day 6, a marked shift to neutrophilia can clearly be seen in BAL cells with macrophages as the second most populous cell type. Eosinophils and lymphocytes were also present in small numbers.

Immunohistochemistry was performed to further visualize the extent of neutrophil influx and to assess for viral spread with influenza infection. Fixed lungs were sectioned, prepped and stained with anti-CXCR2 antibodies to assess for pulmonary infiltrated neutrophils. CXCR2 is a chemokine receptor predominantly expressed on neutrophils. A marked increase in neutrophil influx is seen on day 6 after influenza infection as compared with healthy controls [Figure 2.4].

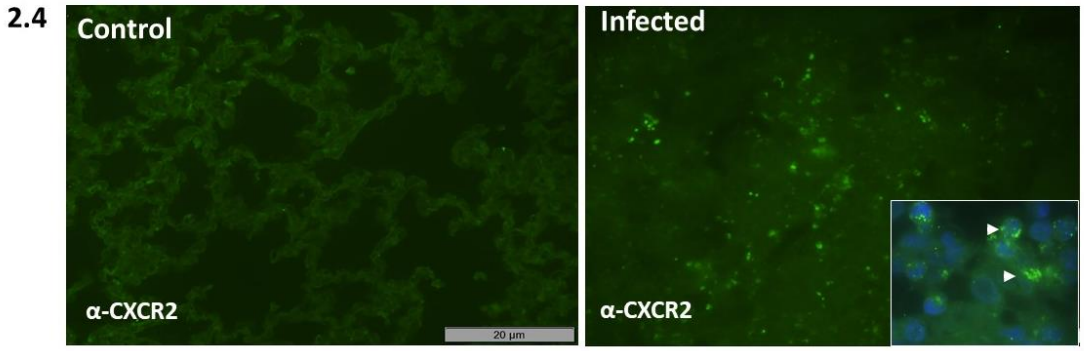


**Figure 2.4:** ***Neutrophil influx noted in viral-infected lung***. Lungs were collected at 6 DPI and fixed for immunohistochemistry. Anti-CXCR2 were used to assess pulmonary-infiltrated PMNs. A marked increase in neutrophil influx is noted in infected lung samples [arrowheads indicate CXCR2 staining on pulmonary-infiltrated neutrophils].

In addition to the extensive influx of neutrophils seen with influenza infection, the virus also has a widespread effect on the lung. Additional immunohistochemistry was performed on day 6

infected lungs sections using anti-PR/8 H1N1 antibodies which bind to the virus for visualization. As seen in Figure 2.5, infected lungs are diffusely infected with viral particles.

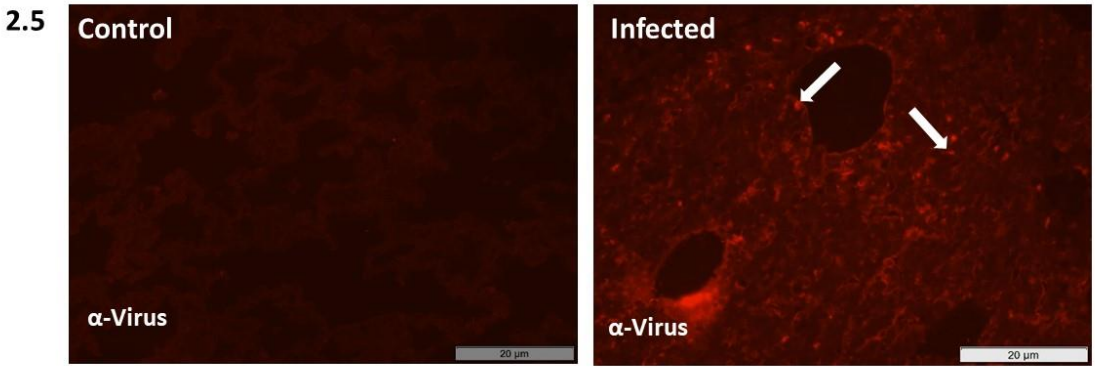


**Figure 2.5:** ***Diffuse viral load present in influenza-infected pig lungs***. Lungs were collected at 6 DPI and fixed for immunohistochemistry. Anti-PR/8 antibodies were used to assess for viral particles within the lung section. Infected lung samples are diffusely infected with Influenza H1N1 particles as can be seen by extensive red fluorescence in infected tissue. Viral particles were detected in both the bronchioles and alveoli, as marked by the white arrows.

3. *Influenza infection causes multifocal pulmonary disease and extensive release of neutrophil extracellular traps*. Lungs were grossly evaluated at the time of collection (day 3 and day 6) and compared with healthy control. On gross examination, infected lungs have expanses of dark red, multifocal pathology affecting all lung lobes, with some lung lobes being more severely affected than others [Figure 3.1 and 3.2]. The remaining pulmonary tissue appeared normal on examination.

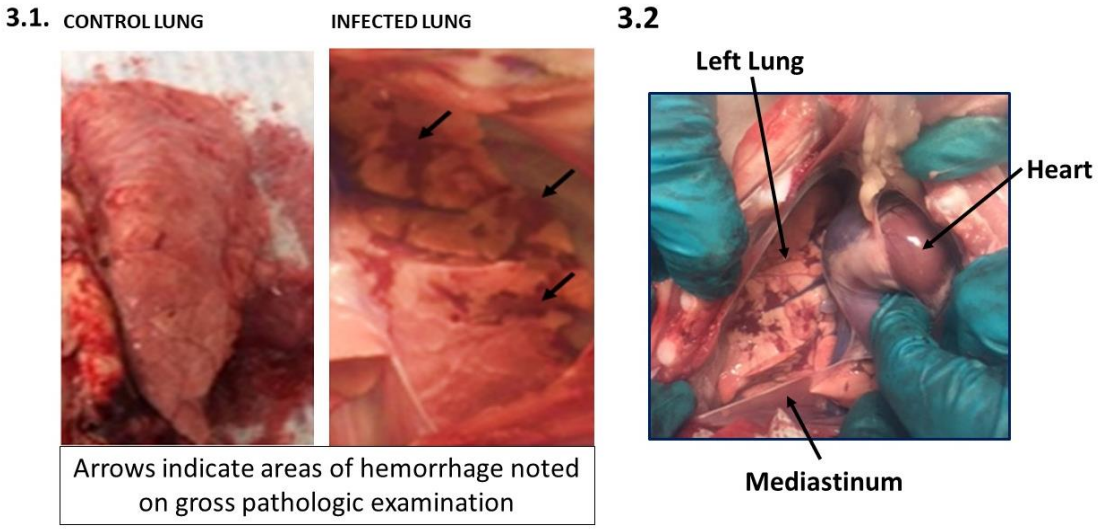


**Figure 3.1 and 3.2:** ***Influenza infection results in focal areas of hemorrhage on gross pathology examination***. Lungs were evaluated in all pigs at the time of sample collection. **3.1:** Control lungs appeared healthy on gross examination, whereas those of infected pigs had expanses of dark red, multifocal disease affecting all lung lobes, with some more severely affected than others. The remaining pulmonary tissue was normal on gross examination. **3.2**: Another view is provided for gross examination. Heart and mediastinum are labeled for reference. Within this left lung there are multifocal, dark red, well outlined regions affecting the entire lung. Remaining tissue unaffected by lesions appears normal on gross examination. Lungs were removed and formalin-fixed for further histopathologic analysis.

Formalin-fixed lungs were sectioned and prepped on slides before being stained with hematoxylin and eosin for histopathology scoring. Lungs were scored from 0 (healthy) to 4 (severe) in the following areas: necrotizing bronchiolitis, bronchiolar infiltrates, alveolitis, interstitial inflammation, hemorrhage, pulmonary edema, and microvascular thrombosis. A sum of each set of scores was calculated and used to compare overall pulmonary pathology between groups [Figure 3.3]. Severe alveolitis and necrotizing bronchitis with massive neutrophil influx in alveolar air spaces and bronchioles were prominently seen in 6 dpi infected lungs compared to 3 dpi infected piglets. Alveolar epithelium showed disintegration and collapsed alveolar architecture within the damaged areas of the lungs. Although statistical significance was not

established for every area scored due to the small sample size, infected pigs showed increased pathology in every key area compared with controls [Figure 3.4].

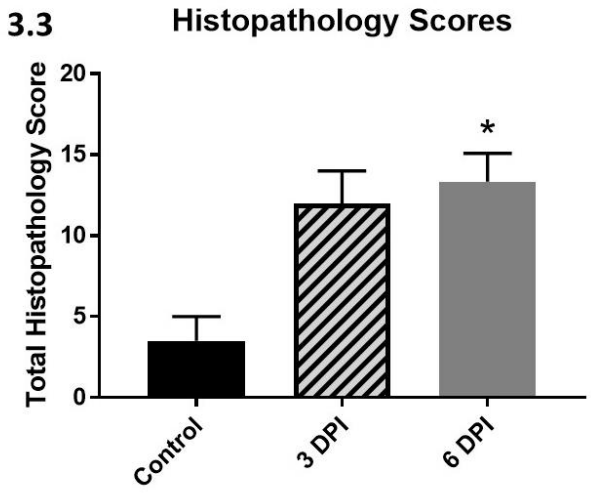


**Figure 3.3:** ***Infected pigs have enhanced pulmonary pathology and disease***. Lungs were collected and formalin-fixed to be sectioned and stained with hematoxylin and eosin for histopathology. Samples were scored from 0 (healthy) to 4 (severe) in seven areas: necrotizing bronchiolitis, bronchiolar infiltrates, alveolitis, interstitial inflammation, hemorrhage, edema, and microvascular thrombosis. A sum of these scores is used in this figure for overview. Infected piglets scored significantly higher on day 6 as compared with controls. Data are expressed as means ± SEM and compared via one-way ANOVA. n=2-3 pigs per group. *$p$<0.05 (relative to healthy control).

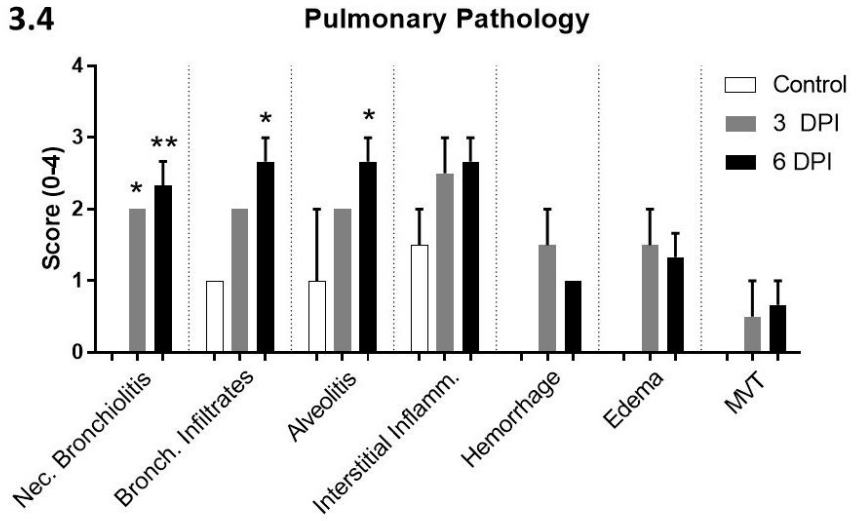


**Figure 3.4:** ***Infected pigs have enhanced pulmonary pathology***. Formalin-fixed lungs were sectioned and stained for histopathology. Scores were given in seven areas: necrotizing bronchiolitis, bronchiolar infiltrates, alveolitis, interstitial inflammation, hemorrhage, edema, and microvascular thrombosis. Pigs on both 3 and 6 days after influenza infection scored significantly higher than controls for necrotizing bronchiolitis. Infected pigs also scored higher than controls in bronchiolar infiltrates and alveolitis on day 6. Although statistical significance is not noted in other groups due to the limited samples size, it appears that infected pigs have notably worse pathology in all areas scored. Data are expressed as means ± SEM and comparisons made via one-way ANOVA. n=2-3 pigs per group. *$p$<0.05; **$p$<0.01 (relative to controls).

Histopathology sections were also examined for the release of neutrophil extracellular traps (NETs). NETs were especially prevalent in areas of severe pyogranulomatous inflammation and disease in infected lung sections [Figure 3.4]. The areas with significant NETs release were mostly areas with complete disruption of the pulmonary architecture and severe alveolitis. Healthy controls did not have the same abundance of NETs, nor did the less severely affected areas of infected lungs.

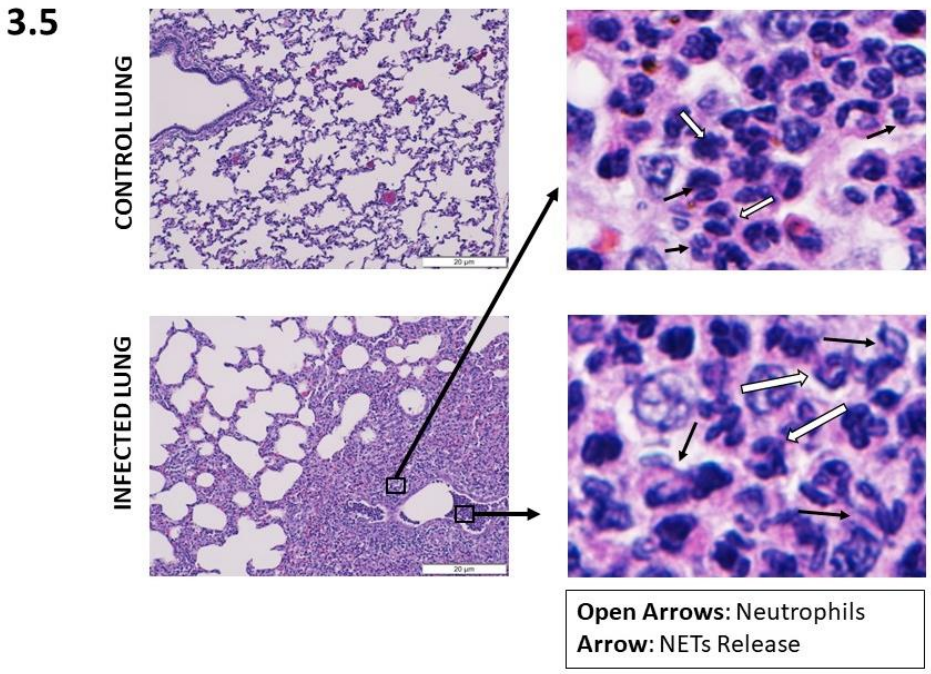


**Figure 3.4:** ***Neutrophil extracellular trap (NET) release abundant in areas of severe pyogranulomatous inflammation***. Infected lungs have large areas of moderate to severe pyogranulomatous inflammation. These areas are extensive and disrupt the pulmonary architecture. Upon closer examination of these more severely affected areas, neutrophils can be seen releasing neutrophil extracellular traps, NETs, through cellular membrane breakdown and the release of nuclear contents (appears as dark purple extruding from neutrophils). Control lungs retain normal architecture with no notable NETs release.

**D. Discussion:**

Establishing a swine model for influenza virus offers such potential for future studies. But before this experimental model can be put to use, we must ensure that it accurately reflects the clinical disease and inflammatory response required to best mimic human disease appropriate to the study. Our goal was to identify a swine model for influenza that resulted in moderate clinical disease and an excessive innate immune response to infection, of which neutrophilia predominated. Results indicate that piglets infected with 1 x $10^6$ $TCID_{50}$ Influenza A/swine/Iowa/15/30 (H1N1) intranasally developed clinical signs from days 2-6, with fever and

nasal discharge predominating as generally noted in swine influenza. Signs were mild to moderate and seemed to peak on day 4. Piglets did not lose weight over the 6-day time frame. This clinical disease is a great base for an experimental model to test therapeutics over a limited period of 6 days since the disease appeared to peak at day 4-5.

In addition to clinical disease, infected piglets saw a sharp increase in cell counts responding to pulmonary infection. Although neutrophilia predominates throughout clinical infection in mice, pigs initially have a majority macrophage population within the bronchoalveolar lavage, which shifts to a marked, predominant neutrophilia by day 6. Areas of severe pulmonary pathology were marked by heavy neutrophil influx through large areas of expansive pyogranulomatous inflammation. Areas of heavy neutrophil influx also resulted in increased viral particles in those regions and the release of neutrophil extracellular traps, which are known to cause worsened disease in influenza pneumonia [55, 83]. Due to these findings, this swine model offers a consistent and effective model for influenza to test various novel combination therapies targeting the innate immune response and subsequent damage to the host. This project was aimed to test the therapeutic efficacy of SCH527123, a CXCR2 antagonist, which has been tested in murine models on combination with antiviral agent, oseltamivir. Due to constraints on availability of the space the project has been temporarily stalled. The present study demonstrates that influenza infection in piglets show widespread alveolar damage accompanied by massive neutrophil-influx and NETs accumulation in swine-influenza infected piglets. Small airways show occlusions with neutrophils and NETs and a strong CXCR2-staining. These findings confirm the results obtained in a murine-model and demonstrate pathogenic role of neutrophils and NETs in influenza infection in piglets.

# CHAPTER VI

## PROJECT SUMMARY

Influenza virus has long afflicted the human population and shaped the course of history over the last century. Arguably the deadliest outcome with influenza pneumonia is secondary bacterial infections. Throughout all pandemics, secondary bacterial infections complicate the disease with *Streptococcus pneumoniae* being the most common pathogen identified.

As the scientific community becomes increasingly aware of the importance of coinfection with influenza pneumonia, we have also become increasingly aware of the complexity of coinfection. No single factor can be claimed solely responsible for the lethal synergism seen with coinfection, but instead a complex network of viral, bacterial, host and environmental factors contribute to the pathogenesis of the disease. The host's immune response is a significant contributor to pathology and clinical severity seen with influenza coinfections. An excessive neutrophil response beyond 12 hours post *S. pneumoniae* infection results in a greater bacterial burden and significant host damage due to factors such as the release of neutrophil extracellular traps. Chemokine receptors are critical to neutrophil function and innate recruitment and are potential targets for the treatment of various diseases and clinical conditions. The importance of controlling both the bacterial infections and host responses to those infection is clear. In a dual infection model, a clear link can be seen between

severe pulmonary neutrophilia with resultant immunopathology and poor clinical outcome.

Various animal models have been considered for further studying influenza virus vaccines, treatment, and the pathogenesis behind the disease. Mouse models are the most widely used due to their availability and affordability, but several downsides are present to using mice to model this disease. In contrast to many of the setbacks with other animal models, pigs are excellent models for influenza infection studies, and should be considered for future studies.

What is clear from this brief summary is the need to better understand these pathogen and host interactions so that novel therapeutic options and pandemic planning can occur. Our goal was to identify and characterize a dual infection model the emulates a pandemic influenza outbreak resulting in lethal synergism and high rates of mortality. Upon characterization of the model, the availability of chemokine receptors as therapeutic targets in disease was assessed in order to best control the excessive innate response seen in dual infection. Finally, identifying and characterizing a swine model allows for many opportunities for studies related to viral pathogenesis, coinfection, therapeutics, and vaccine development.

We first worked to characterize a murine model for influenza pneumonia with subsequent pneumococcal infection that mimicked a pandemic outbreak. Several models were tested and each evaluated for excessive innate response, pulmonary pathology and clinical effect. In addition, histones were evaluated for their role in the pathogenesis of the disease. Next, we characterized neutrophils for their phenotypic changes and functional responsiveness during primary influenza as well as secondary pneumococcal superinfection. For characterization of neutrophils, we evaluated expression of chemokine receptors including CC (CCR1, CCR2, CCR3, CCR5) and CXC (CXCR1, CXR2, CXCR3 and CXCR4) and integrin molecules (CD16, CD62L and CD11b) during primary influenza and secondary pneumococcal infection in

circulating and lung-recruited neutrophils. Effects of chemokine receptors on functional changes – reactive oxygen species production and phagocytosis – were also evaluated.

After establishing an influenza coinfection model with significant neutrophil influx and resultant immunopathology and identifying availability of chemokine receptor targets, we selected a combination therapy including oseltamivir, clarithromycin and Sch527123 to test in this model. We hypothesized that a CXCR2 antagonist would reduce neutrophil recruitment to the lungs, and when used in combination with antiviral and antibiotic therapy, reduce immunopathology and improve clinical outcome. Finally, a swine model for influenza pneumonia was characterized in order to assess innate immune response to infection and the potential of this model for future therapeutic studies.

The proposed murine model for influenza coinfection is a good representation of pandemic influenza outbreaks resulting in secondary infection that is lethally synergistic. Mice infected with 100 $TCID_{50}$ PR/8 H1N1 and 200 CFU *S. pneumoniae* 72 hours after initial viral infection have an exaggerated innate response, with predominantly pyogranulomatous inflammation. Significant protein leakage, pulmonary pathology, and barrier breakdown is noted on days 5 and 6 after influenza infection (48 hours after bacterial infection) and correlates with bacteremia in all dual infected mice. This murine model will serve as a good animal model to further assess the pathogenesis of the barrier breakdown and development of bacteremia and sepsis, as well as provide a consistent model for the testing of potential therapeutics for pandemic influenza coinfection.

In the next aim, we found that neutrophils acquire new phenotypic characteristics after they recruit into the lungs during acute influenza infection and also *S. pneumoniae* superinfection. Expression of CC chemokine receptors (CCR1, CCR2, CCR3, and CCR5) and CXC

chemokine receptors (CXCR3, and CXCR4) were induced in lung-recruited neutrophils in primary influenza and *S. pneumoniae* superinfection compared to *S. pneumoniae* alone infected animal groups. Secondly, CXCR2 is the most predominant chemokine receptor expressed in both circulating as well as lung-recruited neutrophils compared to *S. pneumoniae* infected animals. Thirdly, these findings also demonstrate significant decrease in integrins expression on neutrophils during infection. Finally, our findings also demonstrate that induced chemokine receptors including CCR5 and CXCR2 significantly influence neutrophil functional responsiveness including phagocytic activities and respiratory burst.

Overall, identifying induction of novel chemokine receptor expressions on neutrophils helps in not only understanding their pathogenic role in influenza as well as *S. pneumoniae* superinfection but also opens a new avenue to develop novel therapeutic strategies in alleviating lung pathogenesis during primary influenza as well as *S. pneumoniae* superinfection. Sch527123 monotherapy is ineffective at improving survival and clinical outcome in this model. Interestingly, even though we do not see survival with any Sch527123 monotherapy treatment group, we do see a delay in lethality when started early (12 hours prior to bacterial infection) as opposed to after bacterial infection. Our results also support the need for early antiviral intervention. These are both key findings in our influenza coinfection research which provide evidence for the importance of early intervention with combination therapy by healthcare professionals, and the need for patients who think they may have influenza to see a healthcare provider as soon as possible. Results from this study support exciting findings that these antagonists may offer some hope to improving clinical outcome in severe cases, especially during pandemic influenza outbreaks when mortality is higher and treatments often prove ineffective.

With the final aim, our goal was to identify a swine model for influenza that resulted in moderate clinical disease and an excessive innate immune response to infection, of which neutrophilia predominated. Results indicate that piglets infected with 1 x $10^6$ $TCID_{50}$ Influenza A/swine/Iowa/15/30 (H1N1) intranasally developed clinical signs from days 2-6, with fever and nasal discharge predominating as generally noted in swine influenza. The present study demonstrates that influenza infection in piglets show widespread alveolar damage accompanied by massive neutrophil-influx and NETs accumulation in swine-influenza infected piglets. Small airways shown occlusions with neutrophils and NETs and a strong CXCR2-staining. These findings confirm the results obtained in a murine-model and demonstrate pathogenic role of neutrophils and NETs in influenza infection in piglets.

# REFERENCES


1. McCullers, J.A., *The co-pathogenesis of influenza viruses with bacteria in the lung.* Nat Rev Microbiol, 2014. **12**(4): p. 252-62.
2. Chertow, D.S. and M.J. Memoli, *Bacterial coinfection in influenza: a grand rounds review.* Jama, 2013. **309**(3): p. 275-82.
3. Kash, J.C. and J.K. Taubenberger, *The role of viral, host, and secondary bacterial factors in influenza pathogenesis.* Am J Pathol, 2015. **185**(6): p. 1528-36.
4. Madhi, S.A., B. Schoub, and K.P. Klugman, *Interaction between influenza virus and Streptococcus pneumoniae in severe pneumonia.* Expert Rev Respir Med, 2008. **2**(5): p. 663-72.
5. Rynda-Apple, A., K.M. Robinson, and J.F. Alcorn, *Influenza and Bacterial Superinfection: Illuminating the Immunologic Mechanisms of Disease.* Infect Immun, 2015. **83**(10): p. 3764-70.
6. Morens, D.M., J.K. Taubenberger, and A.S. Fauci, *Predominant role of bacterial pneumonia as a cause of death in pandemic influenza: implications for pandemic influenza preparedness.* J Infect Dis, 2008. **198**(7): p. 962-70.
7. Walters, K.A., et al., *1918 pandemic influenza virus and Streptococcus pneumoniae co-infection results in activation of coagulation and widespread pulmonary thrombosis in mice and humans.* J Pathol, 2016. **238**(1): p. 85-97.
8. Viboud, C., et al., *Global Mortality Impact of the 1957-1959 Influenza Pandemic.* J Infect Dis, 2016. **213**(5): p. 738-45.
9. Ortiz, J.R., et al., *Pandemic influenza in Africa, lessons learned from 1968: a systematic review of the literature.* Influenza Other Respir Viruses, 2012. **6**(1): p. 11-24.
10. McCullers, J.A., *Planning for an influenza pandemic: thinking beyond the virus.* J Infect Dis, 2008. **198**(7): p. 945-7.
11. Gupta, R.K., R. George, and J.S. Nguyen-Van-Tam, *Bacterial pneumonia and pandemic influenza planning.* Emerg Infect Dis, 2008. **14**(8): p. 1187-92.
12. Wang, X.Y., et al., *Influenza and bacterial pathogen coinfections in the 20th century.* Interdiscip Perspect Infect Dis, 2011. **2011**: p. 146376.
13. Herzog, H., H. Staub, and R. Richterich, *Gas-analytical studies in severe pneumonia; observations during the 1957 influenza epidemic.* Lancet, 1959. **1**(7073): p. 593-7.
14. Simonsen, L., *The global impact of influenza on morbidity and mortality.* Vaccine, 1999. **17 Suppl 1**: p. S3-10.

15. McCullers, J.A., *Insights into the interaction between influenza virus and pneumococcus.* Clin Microbiol Rev, 2006. **19**(3): p. 571-82.
16. McCullers, J.A., et al., *Influenza enhances susceptibility to natural acquisition of and disease due to Streptococcus pneumoniae in ferrets.* J Infect Dis, 2010. **202**(8): p. 1287-95.
17. Dockrell, D.H., M.K. Whyte, and T.J. Mitchell, *Pneumococcal pneumonia: mechanisms of infection and resolution.* Chest, 2012. **142**(2): p. 482-91.
18. Anandi Narayana Moorthy, P.R., Jiao Huipeng, Shi Wang, Kong Bing Tan, Liang Qin, Hiroshi Watanabe, Yongliang Zhang, Teluguakula Narasaraju and Vincent Tak Kwong Chow, *Capsules of virulent pneumococcal serotypes enhance formation of neutrophil extracellular traps during in vivo pathogenesis of pneumonia [Accepted].* Oncotarget, 2016.
19. LeVine, A.M., V. Koeningsknecht, and J.M. Stark, *Decreased pulmonary clearance of S. pneumoniae following influenza A infection in mice.* J Virol Methods, 2001. **94**(1-2): p. 173-86.
20. Loosli, C.G., et al., *The destruction of type 2 pneumocytes by airborne influenza PR8-A virus; its effect on surfactant and lecithin content of the pneumonic lesions of mice.* Chest, 1975. **67**(2 Suppl): p. 7s-14s.
21. Takase, H., et al., *Facilitated expansion of pneumococcal colonization from the nose to the lower respiratory tract in mice preinfected with influenza virus.* Microbiol Immunol, 1999. **43**(9): p. 905-7.
22. Lee, K.H., A. Gordon, and B. Foxman, *The role of respiratory viruses in the etiology of bacterial pneumonia: an ecological perspective.* Evol Med Public Health, 2016.
23. Kash, J.C., et al., *Lethal synergism of 2009 pandemic H1N1 influenza virus and Streptococcus pneumoniae coinfection is associated with loss of murine lung repair responses.* MBio, 2011. **2**(5).
24. van der Sluijs, K.F., et al., *Influenza-induced expression of indoleamine 2,3-dioxygenase enhances interleukin-10 production and bacterial outgrowth during secondary pneumococcal pneumonia.* J Infect Dis, 2006. **193**(2): p. 214-22.
25. Florescu, D.F. and A.C. Kalil, *The complex link between influenza and severe sepsis.* Virulence, 2014. **5**(1): p. 137-42.
26. Gotts, J.E., J. Abbott, and M.A. Matthay, *Influenza causes prolonged disruption of the alveolar-capillary barrier in mice unresponsive to mesenchymal stem cell therapy.* Am J Physiol Lung Cell Mol Physiol, 2014. **307**(5): p. L395-406.
27. Li, L., et al., *Angiopoietin-like 4 Increases Pulmonary Tissue Leakiness and Damage during Influenza Pneumonia.* Cell Rep, 2015.
28. Nita-Lazar, M., et al., *Desialylation of airway epithelial cells during influenza virus infection enhances pneumococcal adhesion via galectin binding.* Mol Immunol, 2015. **65**(1): p. 1-16.
29. McCullers, J.A. and J.E. Rehg, *Lethal synergism between influenza virus and Streptococcus pneumoniae: characterization of a mouse model and the role of platelet-activating factor receptor.* J Infect Dis, 2002. **186**(3): p. 341-50.
30. Feldman, C. and R. Anderson, *Review: current and new generation pneumococcal vaccines.* J Infect, 2014. **69**(4): p. 309-25.
31. McAuley, J.L., et al., *Expression of the 1918 influenza A virus PB1-F2 enhances the pathogenesis of viral and secondary bacterial pneumonia.* Cell Host Microbe, 2007. **2**(4): p. 240-9.

32. Malley, R., et al., *Recognition of pneumolysin by Toll-like receptor 4 confers resistance to pneumococcal infection.* Proc Natl Acad Sci U S A, 2003. **100**(4): p. 1966-71.
33. McNeela, E.A., et al., *Pneumolysin activates the NLRP3 inflammasome and promotes proinflammatory cytokines independently of TLR4.* PLoS Pathog, 2010. **6**(11): p. e1001191.
34. Sabroe, I., et al., *Toll-like receptors in health and disease: complex questions remain.* J Immunol, 2003. **171**(4): p. 1630-5.
35. Sanchez, C.J., et al., *The pneumococcal serine-rich repeat protein is an intra-species bacterial adhesin that promotes bacterial aggregation in vivo and in biofilms.* PLoS Pathog, 2010. **6**(8): p. e1001044.
36. Kadioglu, A., et al., *The role of Streptococcus pneumoniae virulence factors in host respiratory colonization and disease.* Nat Rev Microbiol, 2008. **6**(4): p. 288-301.
37. Preston, J.A. and D.H. Dockrell, *Virulence factors in pneumococcal respiratory pathogenesis.* Future Microbiol, 2008. **3**(2): p. 205-21.
38. Hergott, C.B., et al., *Bacterial exploitation of phosphorylcholine mimicry suppresses inflammation to promote airway infection.* J Clin Invest, 2015. **125**(10): p. 3878-90.
39. McNamee, L.A. and A.G. Harmsen, *Both influenza-induced neutrophil dysfunction and neutrophil-independent mechanisms contribute to increased susceptibility to a secondary Streptococcus pneumoniae infection.* Infect Immun, 2006. **74**(12): p. 6707-21.
40. Kadioglu, A., et al., *The integrins Mac-1 and alpha4beta1 perform crucial roles in neutrophil and T cell recruitment to lungs during Streptococcus pneumoniae infection.* J Immunol, 2011. **186**(10): p. 5907-15.
41. Bou Ghanem, E.N., et al., *Extracellular Adenosine Protects against Streptococcus pneumoniae Lung Infection by Regulating Pulmonary Neutrophil Recruitment.* PLoS Pathog, 2015. **11**(8): p. e1005126.
42. Damjanovic, D., et al., *Marked improvement of severe lung immunopathology by influenza-associated pneumococcal superinfection requires the control of both bacterial replication and host immune responses.* Am J Pathol, 2013. **183**(3): p. 868-80.
43. Okumura, C.Y. and V. Nizet, *Subterfuge and sabotage: evasion of host innate defenses by invasive gram-positive bacterial pathogens.* Annu Rev Microbiol, 2014. **68**: p. 439-58.
44. Sun, K. and D.W. Metzger, *Inhibition of pulmonary antibacterial defense by interferon-gamma during recovery from influenza infection.* Nat Med, 2008. **14**(5): p. 558-64.
45. Robinson, K.M., J.K. Kolls, and J.F. Alcorn, *The immunology of influenza virus-associated bacterial pneumonia.* Curr Opin Immunol, 2015. **34**: p. 59-67.
46. Engelich, G., M. White, and K.L. Hartshorn, *Neutrophil survival is markedly reduced by incubation with influenza virus and Streptococcus pneumoniae: role of respiratory burst.* J Leukoc Biol, 2001. **69**(1): p. 50-6.
47. Ellis, G.T., et al., *TRAIL+ monocytes and monocyte-related cells cause lung damage and thereby increase susceptibility to influenza-Streptococcus pneumoniae coinfection.* EMBO Rep, 2015. **16**(9): p. 1203-18.
48. Small, C.L., et al., *Influenza infection leads to increased susceptibility to subsequent bacterial superinfection by impairing NK cell responses in the lung.* J Immunol, 2010. **184**(4): p. 2048-56.
49. Marriott, H.M., et al., *Reactive oxygen species regulate neutrophil recruitment and survival in pneumococcal pneumonia.* Am J Respir Crit Care Med, 2008. **177**(8): p. 887-95.
50. Brinkmann, V., et al., *Neutrophil extracellular traps kill bacteria.* Science, 2004. **303**(5663): p. 1532-5.

51. Fuchs, T.A., et al., *Novel cell death program leads to neutrophil extracellular traps.* J Cell Biol, 2007. **176**(2): p. 231-41.
52. Ermert, D., et al., *Mouse neutrophil extracellular traps in microbial infections.* J Innate Immun, 2009. **1**(3): p. 181-93.
53. Urban, C.F., et al., *Neutrophil extracellular traps capture and kill Candida albicans yeast and hyphal forms.* Cell Microbiol, 2006. **8**(4): p. 668-76.
54. Jenne, C.N. and P. Kubes, *Virus-induced NETs--critical component of host defense or pathogenic mediator?* PLoS Pathog, 2015. **11**(1): p. e1004546.
55. Narasaraju, T., et al., *Excessive neutrophils and neutrophil extracellular traps contribute to acute lung injury of influenza pneumonitis.* Am J Pathol, 2011. **179**(1): p. 199-210.
56. Saffarzadeh, M., et al., *Neutrophil extracellular traps directly induce epithelial and endothelial cell death: a predominant role of histones.* PLoS One, 2012. **7**(2): p. e32366.
57. Narayana Moorthy, A., et al., *In vivo and in vitro studies on the roles of neutrophil extracellular traps during secondary pneumococcal pneumonia after primary pulmonary influenza infection.* Front Immunol, 2013. **4**: p. 56.
58. Abrams, S.T., et al., *Circulating histones are mediators of trauma-associated lung injury.* Am J Respir Crit Care Med, 2013. **187**(2): p. 160-9.
59. Short, K.R., et al., *Antibodies mediate formation of neutrophil extracellular traps in the middle ear and facilitate secondary pneumococcal otitis media.* Infect Immun, 2014. **82**(1): p. 364-70.
60. Czaikoski, P.G., et al., *Neutrophil Extracellular Traps Induce Organ Damage during Experimental and Clinical Sepsis.* PLoS One, 2016. **11**(2): p. e0148142.
61. Mori, Y., et al., *alpha-Enolase of Streptococcus pneumoniae induces formation of neutrophil extracellular traps.* J Biol Chem, 2012. **287**(13): p. 10472-81.
62. Zhu, L., et al., *Competence-independent activity of pneumococcal EndA [corrected] mediates degradation of extracellular dna and nets and is important for virulence.* PLoS One, 2013. **8**(7): p. e70363.
63. Hamzeh-Cognasse, H., et al., *Platelets and infections - complex interactions with bacteria.* Front Immunol, 2015. **6**: p. 82.
64. Douda, D.N., et al., *SK3 channel and mitochondrial ROS mediate NADPH oxidase-independent NETosis induced by calcium influx.* Proc Natl Acad Sci U S A, 2015. **112**(9): p. 2817-22.
65. Pilsczek, F.H., et al., *A novel mechanism of rapid nuclear neutrophil extracellular trap formation in response to Staphylococcus aureus.* J Immunol, 2010. **185**(12): p. 7413-25.
66. Clark, S.R., et al., *Platelet TLR4 activates neutrophil extracellular traps to ensnare bacteria in septic blood.* Nat Med, 2007. **13**(4): p. 463-9.
67. Semeraro, F., et al., *Extracellular histones promote thrombin generation through platelet-dependent mechanisms: involvement of platelet TLR2 and TLR4.* Blood, 2011. **118**(7): p. 1952-61.
68. Li, P., et al., *PAD4 is essential for antibacterial innate immunity mediated by neutrophil extracellular traps.* J Exp Med, 2010. **207**(9): p. 1853-62.
69. Wang, Y., et al., *Histone hypercitrullination mediates chromatin decondensation and neutrophil extracellular trap formation.* J Cell Biol, 2009. **184**(2): p. 205-13.
70. Martinod, K., et al., *Neutrophil histone modification by peptidylarginine deiminase 4 is critical for deep vein thrombosis in mice.* Proc Natl Acad Sci U S A, 2013. **110**(21): p. 8674-9.
71. Hemmers, S., et al., *PAD4-mediated neutrophil extracellular trap formation is not required for immunity against influenza infection.* PLoS One, 2011. **6**(7): p. e22043.

72. Lewis, H.D., et al., *Inhibition of PAD4 activity is sufficient to disrupt mouse and human NET formation.* Nat Chem Biol, 2015. **11**(3): p. 189-91.
73. Papayannopoulos, V., et al., *Neutrophil elastase and myeloperoxidase regulate the formation of neutrophil extracellular traps.* J Cell Biol, 2010. **191**(3): p. 677-91.
74. Hoeksema, M., et al., *Histones as mediators of host defense, inflammation and thrombosis.* Future Microbiol, 2016.
75. Kanthack, A.A. and W.B. Hardy, *The Morphology and Distribution of the Wandering Cells of Mammalia.* J Physiol, 1894. **17**(1-2): p. 80.1-119.
76. Tate, M.D., et al., *Neutrophils ameliorate lung injury and the development of severe disease during influenza infection.* J Immunol, 2009. **183**(11): p. 7441-50.
77. Beiter, K., et al., *An endonuclease allows Streptococcus pneumoniae to escape from neutrophil extracellular traps.* Curr Biol, 2006. **16**(4): p. 401-7.
78. Tagai, C., et al., *Antimicrobial properties of arginine- and lysine-rich histones and involvement of bacterial outer membrane protease T in their differential mode of actions.* Peptides, 2011. **32**(10): p. 2003-9.
79. Park, C.B., et al., *Structure-activity analysis of buforin II, a histone H2A-derived antimicrobial peptide: the proline hinge is responsible for the cell-penetrating ability of buforin II.* Proc Natl Acad Sci U S A, 2000. **97**(15): p. 8245-50.
80. Anand, P., et al., *A novel role for lipid droplets in the organismal antibacterial response.* Elife, 2012. **1**: p. e00003.
81. Hoeksema, M., et al., *Arginine-rich histones have strong antiviral activity for influenza A viruses.* Innate Immun, 2015. **21**(7): p. 736-45.
82. Wang, S.Z. and K.D. Forsyth, *The interaction of neutrophils with respiratory epithelial cells in viral infection.* Respirology, 2000. **5**(1): p. 1-10.
83. Ashar, H.K., et al., *The Role of Extracellular Histones in Influenza Virus Pathogenesis.* Am J Pathol, 2018. **188**(1): p. 135-148.
84. Allam, R., et al., *Extracellular histones in tissue injury and inflammation.* J Mol Med (Berl), 2014. **92**(5): p. 465-72.
85. Gould, T.J., Z. Lysov, and P.C. Liaw, *Extracellular DNA and histones: double-edged swords in immunothrombosis.* J Thromb Haemost, 2015. **13 Suppl 1**: p. S82-91.
86. Hirose, T., et al., *Presence of neutrophil extracellular traps and citrullinated histone H3 in the bloodstream of critically ill patients.* PLoS One, 2014. **9**(11): p. e111755.
87. Kumar, S.V., et al., *Neutrophil Extracellular Trap-Related Extracellular Histones Cause Vascular Necrosis in Severe GN.* J Am Soc Nephrol, 2015. **26**(10): p. 2399-413.
88. Xu, J., et al., *Extracellular histones are major mediators of death in sepsis.* Nat Med, 2009. **15**(11): p. 1318-21.
89. Zhang, Y., et al., *Extracellular histones play an inflammatory role in acid aspiration-induced acute respiratory distress syndrome.* Anesthesiology, 2015. **122**(1): p. 127-39.
90. Richard, A.L., et al., *TLR2 signaling decreases transmission of Streptococcus pneumoniae by limiting bacterial shedding in an infant mouse Influenza A co-infection model.* PLoS Pathog, 2014. **10**(8): p. e1004339.
91. Yoshimura, A., et al., *Cutting edge: recognition of Gram-positive bacterial cell wall components by the innate immune system occurs via Toll-like receptor 2.* J Immunol, 1999. **163**(1): p. 1-5.
92. Didierlaurent, A., et al., *Sustained desensitization to bacterial Toll-like receptor ligands after resolution of respiratory influenza infection.* J Exp Med, 2008. **205**(2): p. 323-9.

93. Spelmink, L., et al., *Toll-Like Receptor 3/TRIF-Dependent IL-12p70 Secretion Mediated by Streptococcus pneumoniae RNA and Its Priming by Influenza A Virus Coinfection in Human Dendritic Cells.* MBio, 2016. **7**(2).
94. Tian, X., et al., *Poly I:C enhances susceptibility to secondary pulmonary infections by gram-positive bacteria.* PLoS One, 2012. **7**(9): p. e41879.
95. Li, W., B. Moltedo, and T.M. Moran, *Type I interferon induction during influenza virus infection increases susceptibility to secondary Streptococcus pneumoniae infection by negative regulation of gammadelta T cells.* J Virol, 2012. **86**(22): p. 12304-12.
96. Navarini, A.A., et al., *Increased susceptibility to bacterial superinfection as a consequence of innate antiviral responses.* Proc Natl Acad Sci U S A, 2006. **103**(42): p. 15535-9.
97. Nakamura, S., K.M. Davis, and J.N. Weiser, *Synergistic stimulation of type I interferons during influenza virus coinfection promotes Streptococcus pneumoniae colonization in mice.* J Clin Invest, 2011. **121**(9): p. 3657-65.
98. Shahangian, A., et al., *Type I IFNs mediate development of postinfluenza bacterial pneumonia in mice.* J Clin Invest, 2009. **119**(7): p. 1910-20.
99. Karlstrom, A., et al., *Toll-like receptor 2 mediates fatal immunopathology in mice during treatment of secondary pneumococcal pneumonia following influenza.* J Infect Dis, 2011. **204**(9): p. 1358-66.
100. O'Brien, R.L., et al., *gammadelta T-cell receptors: functional correlations.* Immunol Rev, 2007. **215**: p. 77-88.
101. Negishi, H., et al., *Cross-interference of RLR and TLR signaling pathways modulates antibacterial T cell responses.* Nat Immunol, 2012. **13**(7): p. 659-66.
102. van der Sluijs, K.F., et al., *IL-10 is an important mediator of the enhanced susceptibility to pneumococcal pneumonia after influenza infection.* J Immunol, 2004. **172**(12): p. 7603-9.
103. Blevins, L.K., et al., *Coinfection with Streptococcus pneumoniae negatively modulates the size and composition of the ongoing influenza-specific CD8(+) T cell response.* J Immunol, 2014. **193**(10): p. 5076-87.
104. Wu, Y., et al., *Lethal coinfection of influenza virus and Streptococcus pneumoniae lowers antibody response to influenza virus in lung and reduces numbers of germinal center B cells, T follicular helper cells, and plasma cells in mediastinal lymph Node.* J Virol, 2015. **89**(4): p. 2013-23.
105. Wolf, A.I., et al., *Coinfection with Streptococcus pneumoniae modulates the B cell response to influenza virus.* J Virol, 2014. **88**(20): p. 11995-2005.
106. Dixit, R., et al., *Emergence of oseltamivir resistance: control and management of influenza before, during and after the pandemic.* Infect Disord Drug Targets, 2013. **13**(1): p. 34-45.
107. Onishi, M., et al., *Intravenous peramivir inhibits viral replication, and leads to bacterial clearance and prevention of mortality during murine bacterial co-infection caused by influenza A(H1N1)pdm09 virus and Streptococcus pneumoniae.* Antiviral Res, 2015. **117**: p. 52-9.
108. Walther, E., et al., *Antipneumococcal activity of neuraminidase inhibiting artocarpin.* Int J Med Microbiol, 2015. **305**(3): p. 289-97.
109. Waterer, G.W., G.W. Somes, and R.G. Wunderink, *Monotherapy may be suboptimal for severe bacteremic pneumococcal pneumonia.* Arch Intern Med, 2001. **161**(15): p. 1837-42.
110. Watkins, R.R. and T.L. Lemonovich, *Diagnosis and management of community-acquired pneumonia in adults.* Am Fam Physician, 2011. **83**(11): p. 1299-306.

111. Majhi, A., et al., *Levofloxacin-ceftriaxone combination attenuates lung inflammation in a mouse model of bacteremic pneumonia caused by multidrug-resistant Streptococcus pneumoniae via inhibition of cytolytic activities of pneumolysin and autolysin.* Antimicrob Agents Chemother, 2014. **58**(9): p. 5164-80.
112. Karlstrom, A., et al., *Treatment with protein synthesis inhibitors improves outcomes of secondary bacterial pneumonia after influenza.* J Infect Dis, 2009. **199**(3): p. 311-9.
113. Majhi, A., et al., *Combination therapy with ampicillin and azithromycin in an experimental pneumococcal pneumonia is bactericidal and effective in down regulating inflammation in mice.* J Inflamm (Lond), 2014. **11**(1): p. 5.
114. Luxameechanporn, T., et al., *The effect of treatment with moxifloxacin or azithromycin on acute bacterial rhinosinusitis in mice.* Int J Infect Dis, 2006. **10**(5): p. 401-6.
115. Goldstein, L.H., et al., *Azithromycin is not associated with QT prolongation in hospitalized patients with community-acquired pneumonia.* Pharmacoepidemiol Drug Saf, 2015. **24**(10): p. 1042-8.
116. Li, C., et al., *Corticosteroid treatment ameliorates acute lung injury induced by 2009 swine origin influenza A (H1N1) virus in mice.* PLoS One, 2012. **7**(8): p. e44110.
117. Han, K., et al., *Early use of glucocorticoids was a risk factor for critical disease and death from pH1N1 infection.* Clin Infect Dis, 2011. **53**(4): p. 326-33.
118. Mifsud, E.J., et al., *Reducing the impact of influenza-associated secondary pneumococcal infections.* Immunol Cell Biol, 2016. **94**(1): p. 101-8.
119. Reppe, K., et al., *Pulmonary immunostimulation with MALP-2 in influenza virus-infected mice increases survival after pneumococcal superinfection.* Infect Immun, 2015. **83**(12): p. 4617-29.
120. Porte, R., et al., *A Toll-Like Receptor 5 Agonist Improves the Efficacy of Antibiotics in Treatment of Primary and Influenza Virus-Associated Pneumococcal Mouse Infections.* Antimicrob Agents Chemother, 2015. **59**(10): p. 6064-72.
121. Tanaka, A., et al., *Toll-like receptor 4 agonistic antibody promotes innate immunity against severe pneumonia induced by coinfection with influenza virus and Streptococcus pneumoniae.* Clin Vaccine Immunol, 2013. **20**(7): p. 977-85.
122. Chen, L., et al., *Effects of recombinant IL-17F intranasal inoculation against Streptococcus pneumoniae infection in a murine model.* Biotechnol Appl Biochem, 2015. **62**(3): p. 393-400.
123. Damjanovic, D., et al., *Immunopathology in influenza virus infection: uncoupling the friend from foe.* Clin Immunol, 2012. **144**(1): p. 57-69.
124. Miller, E.J., A.B. Cohen, and M.A. Matthay, *Increased interleukin-8 concentrations in the pulmonary edema fluid of patients with acute respiratory distress syndrome from sepsis.* Crit Care Med, 1996. **24**(9): p. 1448-54.
125. Baughman, R.P., et al., *Changes in the inflammatory response of the lung during acute respiratory distress syndrome: prognostic indicators.* Am J Respir Crit Care Med, 1996. **154**(1): p. 76-81.
126. Goodman, R.B., et al., *Cytokine-mediated inflammation in acute lung injury.* Cytokine Growth Factor Rev, 2003. **14**(6): p. 523-35.
127. Bertini, R., et al., *Receptor binding mode and pharmacological characterization of a potent and selective dual CXCR1/CXCR2 non-competitive allosteric inhibitor.* Br J Pharmacol, 2012. **165**(2): p. 436-54.
128. Kim, C.H., *Chemokine-chemokine receptor network in immune cell trafficking.* Curr Drug Targets Immune Endocr Metabol Disord, 2004. **4**(4): p. 343-61.

129. Reutershan, J., et al., *Critical role of endothelial CXCR2 in LPS-induced neutrophil migration into the lung.* J Clin Invest, 2006. **116**(3): p. 695-702.
130. Bizzarri, C., et al., *ELR+ CXC chemokines and their receptors (CXC chemokine receptor 1 and CXC chemokine receptor 2) as new therapeutic targets.* Pharmacol Ther, 2006. **112**(1): p. 139-49.
131. Strieter, R.M., et al., *The role of CXCR2/CXCR2 ligands in acute lung injury.* Curr Drug Targets Inflamm Allergy, 2005. **4**(3): p. 299-303.
132. Keane, M.P., et al., *Depletion of CXCR2 inhibits tumor growth and angiogenesis in a murine model of lung cancer.* J Immunol, 2004. **172**(5): p. 2853-60.
133. Podolin, P.L., et al., *A potent and selective nonpeptide antagonist of CXCR2 inhibits acute and chronic models of arthritis in the rabbit.* J Immunol, 2002. **169**(11): p. 6435-44.
134. Romanini, J., et al., *The role of CXCR2 chemokine receptors in the oral squamous cell carcinoma.* Invest New Drugs, 2012. **30**(4): p. 1371-8.
135. Fox, J., J.R. Gordon, and C.K. Haston, *Combined CXCR1/CXCR2 antagonism decreases radiation-induced alveolitis in the mouse.* Radiat Res, 2011. **175**(5): p. 657-64.
136. Russo, R.C., et al., *Role of the chemokine receptor CXCR2 in bleomycin-induced pulmonary inflammation and fibrosis.* Am J Respir Cell Mol Biol, 2009. **40**(4): p. 410-21.
137. Moepps, B., et al., *A homolog of the human chemokine receptor CXCR1 is expressed in the mouse.* Mol Immunol, 2006. **43**(7): p. 897-914.
138. Hartl, D., et al., *Infiltrated neutrophils acquire novel chemokine receptor expression and chemokine responsiveness in chronic inflammatory lung diseases.* J Immunol, 2008. **181**(11): p. 8053-67.
139. Furuichi, K., et al., *Chemokine receptor CCR1 regulates inflammatory cell infiltration after renal ischemia-reperfusion injury.* J Immunol, 2008. **181**(12): p. 8670-6.
140. He, M., R. Horuk, and M. Bhatia, *Treatment with BX471, a nonpeptide CCR1 antagonist, protects mice against acute pancreatitis-associated lung injury by modulating neutrophil recruitment.* Pancreas, 2007. **34**(2): p. 233-41.
141. He, M., et al., *Treatment with BX471, a CC chemokine receptor 1 antagonist, attenuates systemic inflammatory response during sepsis.* Am J Physiol Gastrointest Liver Physiol, 2007. **292**(4): p. G1173-80.
142. Lebre, M.C., et al., *Why CCR2 and CCR5 blockade failed and why CCR1 blockade might still be effective in the treatment of rheumatoid arthritis.* PLoS One, 2011. **6**(7): p. e21772.
143. Nedjai, B., et al., *CXCR3 antagonist VUF10085 binds to an intrahelical site distinct from that of the broad spectrum antagonist TAK-779.* Br J Pharmacol, 2015. **172**(7): p. 1822-33.
144. Neighbour, H., et al., *Safety and efficacy of an oral CCR3 antagonist in patients with asthma and eosinophilic bronchitis: a randomized, placebo-controlled clinical trial.* Clin Exp Allergy, 2014. **44**(4): p. 508-16.
145. Yang, D., et al., *Roles of CC chemokine receptors (CCRs) on lipopolysaccharide-induced acute lung injury.* Respir Physiol Neurobiol, 2010. **170**(3): p. 253-9.
146. Mercer, P.F., et al., *Proteinase-activated receptor-1, CCL2, and CCL7 regulate acute neutrophilic lung inflammation.* Am J Respir Cell Mol Biol, 2014. **50**(1): p. 144-57.
147. Cameron, C.M., et al., *Gene expression analysis of host innate immune responses during Lethal H5N1 infection in ferrets.* J Virol, 2008. **82**(22): p. 11308-17.
148. Neville, L.F., G. Mathiak, and O. Bagasra, *The immunobiology of interferon-gamma inducible protein 10 kD (IP-10): a novel, pleiotropic member of the C-X-C chemokine superfamily.* Cytokine Growth Factor Rev, 1997. **8**(3): p. 207-19.

149. Johnson, M., et al., *Discovery and optimization of a series of quinazolinone-derived antagonists of CXCR3.* Bioorg Med Chem Lett, 2007. **17**(12): p. 3339-43.
150. Jenh, C.H., et al., *A selective and potent CXCR3 antagonist SCH 546738 attenuates the development of autoimmune diseases and delays graft rejection.* BMC Immunol, 2012. **13**: p. 2.
151. Ichikawa, A., et al., *CXCL10-CXCR3 enhances the development of neutrophil-mediated fulminant lung injury of viral and nonviral origin.* Am J Respir Crit Care Med, 2013. **187**(1): p. 65-77.
152. Zhu, G., et al., *CXCR3 as a molecular target in breast cancer metastasis: inhibition of tumor cell migration and promotion of host anti-tumor immunity.* Oncotarget, 2015. **6**(41): p. 43408-19.
153. Du, J., et al., *Pro-Inflammatory CXCR3 Impairs Mitochondrial Function in Experimental Non-Alcoholic Steatohepatitis.* Theranostics, 2017. **7**(17): p. 4192-4203.
154. Yamada, M., et al., *The increase in surface CXCR4 expression on lung extravascular neutrophils and its effects on neutrophils during endotoxin-induced lung injury.* Cell Mol Immunol, 2011. **8**(4): p. 305-14.
155. Lim, K., et al., *Neutrophil trails guide influenza-specific CD8(+) T cells in the airways.* Science, 2015. **349**(6252): p. aaa4352.
156. Liu, Q., et al., *CXCR4 antagonist AMD3100 redistributes leukocytes from primary immune organs to secondary immune organs, lung, and blood in mice.* Eur J Immunol, 2015. **45**(6): p. 1855-67.
157. Muralidharan, R., et al., *HuR-targeted nanotherapy in combination with AMD3100 suppresses CXCR4 expression, cell growth, migration and invasion in lung cancer.* Cancer Gene Ther, 2015. **22**(12): p. 581-90.
158. Eash, K.J., et al., *CXCR2 and CXCR4 antagonistically regulate neutrophil trafficking from murine bone marrow.* J Clin Invest, 2010. **120**(7): p. 2423-31.
159. Gernez, Y., R. Tirouvanziam, and P. Chanez, *Neutrophils in chronic inflammatory airway diseases: can we target them and how?* Eur Respir J, 2010. **35**(3): p. 467-9.
160. Chapman, R.W., et al., *A novel, orally active CXCR1/2 receptor antagonist, Sch527123, inhibits neutrophil recruitment, mucus production, and goblet cell hyperplasia in animal models of pulmonary inflammation.* J Pharmacol Exp Ther, 2007. **322**(2): p. 486-93.
161. Gonsiorek, W., et al., *Pharmacological characterization of Sch527123, a potent allosteric CXCR1/CXCR2 antagonist.* J Pharmacol Exp Ther, 2007. **322**(2): p. 477-85.
162. Holz, O., et al., *SCH527123, a novel CXCR2 antagonist, inhibits ozone-induced neutrophilia in healthy subjects.* Eur Respir J, 2010. **35**(3): p. 564-70.
163. Zhang, S., et al., *Simvastatin regulates CXC chemokine formation in streptococcal M1 protein-induced neutrophil infiltration in the lung.* Am J Physiol Lung Cell Mol Physiol, 2011. **300**(6): p. L930-9.
164. McAuley, D.F., et al., *Simvastatin in the acute respiratory distress syndrome.* N Engl J Med, 2014. **371**(18): p. 1695-703.
165. Fox, J. and C.K. Haston, *CXC receptor 1 and 2 and neutrophil elastase inhibitors alter radiation-induced lung disease in the mouse.* Int J Radiat Oncol Biol Phys, 2013. **85**(1): p. 215-22.
166. Bertini, R., et al., *Noncompetitive allosteric inhibitors of the inflammatory chemokine receptors CXCR1 and CXCR2: prevention of reperfusion injury.* Proc Natl Acad Sci U S A, 2004. **101**(32): p. 11791-6.
167. Zarbock, A., M. Allegretti, and K. Ley, *Therapeutic inhibition of CXCR2 by Reparixin attenuates acute lung injury in mice.* Br J Pharmacol, 2008. **155**(3): p. 357-64.

168. Armstrong, S.M., S. Mubareka, and W.L. Lee, *The lung microvascular endothelium as a therapeutic target in severe influenza.* Antiviral Res, 2013. **99**(2): p. 113-8.
169. Mathieu, C., et al., *Induction of innate immunity in lungs with virus-like nanoparticles leads to protection against influenza and Streptococcus pneumoniae challenge.* Nanomedicine, 2013. **9**(7): p. 839-48.
170. Metzger, D.W., et al., *Limited Efficacy of Antibacterial Vaccination Against Secondary Serotype 3 Pneumococcal Pneumonia Following Influenza Infection.* J Infect Dis, 2015. **212**(3): p. 445-52.
171. Klugman, K.P., Y.W. Chien, and S.A. Madhi, *Pneumococcal pneumonia and influenza: a deadly combination.* Vaccine, 2009. **27 Suppl 3**: p. C9-c14.
172. Huet, O., et al., *Ensuring animal welfare while meeting scientific aims using a murine pneumonia model of septic shock.* Shock, 2013. **39**(6): p. 488-94.
173. Shrum, B., et al., *A robust scoring system to evaluate sepsis severity in an animal model.* BMC Res Notes, 2014. **7**: p. 233.
174. Ashar HK, M.N., Rudd JM, Snider TA, Achanta M, Prasanthi M,, T.P. Pulavendran S, Akhilesh R, Malayer JR, Ritchey JW, Rajasekhar R, Chow VT, Esmon CT,, and T. N, *The role of extracellular histones in influenza virus pathogenesis.* The American Journal of Pathology, 2017.
175. Cepkova, M. and M.A. Matthay, *Pharmacotherapy of acute lung injury and the acute respiratory distress syndrome.* J Intensive Care Med, 2006. **21**(3): p. 119-43.
176. Spragg, R.G., et al., *Effect of recombinant surfactant protein C-based surfactant on the acute respiratory distress syndrome.* N Engl J Med, 2004. **351**(9): p. 884-92.
177. Taylor, R.W., et al., *Low-dose inhaled nitric oxide in patients with acute lung injury: a randomized controlled trial.* Jama, 2004. **291**(13): p. 1603-9.
178. Abraham, E., et al., *Liposomal prostaglandin E1 (TLC C-53) in acute respiratory distress syndrome: a controlled, randomized, double-blind, multicenter clinical trial. TLC C-53 ARDS Study Group.* Crit Care Med, 1999. **27**(8): p. 1478-85.
179. Vincent, J.L., et al., *A multi-centre, double-blind, placebo-controlled study of liposomal prostaglandin E1 (TLC C-53) in patients with acute respiratory distress syndrome.* Intensive Care Med, 2001. **27**(10): p. 1578-83.
180. *Randomized, placebo-controlled trial of lisofylline for early treatment of acute lung injury and acute respiratory distress syndrome.* Crit Care Med, 2002. **30**(1): p. 1-6.
181. Xu, T., et al., *Acute respiratory distress syndrome induced by avian influenza A (H5N1) virus in mice.* Am J Respir Crit Care Med, 2006. **174**(9): p. 1011-7.
182. Traylor, Z.P., F. Aeffner, and I.C. Davis, *Influenza A H1N1 induces declines in alveolar gas exchange in mice consistent with rapid post-infection progression from acute lung injury to ARDS.* Influenza Other Respir Viruses, 2013. **7**(3): p. 472-9.
183. Peiris, J.S., et al., *Innate immune responses to influenza A H5N1: friend or foe?* Trends Immunol, 2009. **30**(12): p. 574-84.
184. Ramos, I. and A. Fernandez-Sesma, *Modulating the Innate Immune Response to Influenza A Virus: Potential Therapeutic Use of Anti-Inflammatory Drugs.* Front Immunol, 2015. **6**: p. 361.
185. Rudd JM, A.H., Chow VTK, Teluguakula N *Lethal Synergism between Influenza and Streptococcus pneumoniae.* J Infect Pulm Dis, 2016. **2**(2).
186. Narasaraju, T. and A. Harshini, *Neutrophils as Possible Therapeutic Targets in Severe Influenza Pneumonia.* J Infect Pulm Dis, 2016. **2**(2).

187. Griffith, J.W., C.L. Sokol, and A.D. Luster, *Chemokines and chemokine receptors: positioning cells for host defense and immunity.* Annu Rev Immunol, 2014. **32**: p. 659-702.
188. Moser, B. and P. Loetscher, *Lymphocyte traffic control by chemokines.* Nat Immunol, 2001. **2**(2): p. 123-8.
189. Pillay, J., et al., *A subset of neutrophils in human systemic inflammation inhibits T cell responses through Mac-1.* J Clin Invest, 2012. **122**(1): p. 327-36.
190. Pauksens, K., et al., *Neutrophil and monocyte receptor expression in uncomplicated and complicated influenza A infection with pneumonia.* Scand J Infect Dis, 2008. **40**(4): p. 326-37.
191. Hazeldine, J., P. Hampson, and J.M. Lord, *The impact of trauma on neutrophil function.* Injury, 2014. **45**(12): p. 1824-33.
192. Beghini, J., et al., *Altered CD16 expression on vaginal neutrophils from women with vaginitis.* Eur J Obstet Gynecol Reprod Biol, 2013. **167**(1): p. 96-9.
193. Relja, B., et al., *Sera from severe trauma patients with pneumonia and without infectious complications have differential effects on neutrophil biology.* BMC Pulm Med, 2016. **16**(1): p. 171.
194. Kim, J.K., et al., *Increased Neutrophil Extracellular Trap Formation in Uremia Is Associated with Chronic Inflammation and Prevalent Coronary Artery Disease.* J Immunol Res, 2017. **2017**: p. 8415179.
195. Droemann, D., et al., *Decreased apoptosis and increased activation of alveolar neutrophils in bacterial pneumonia.* Chest, 2000. **117**(6): p. 1679-84.
196. Bonecchi, R., et al., *Up-regulation of CCR1 and CCR3 and induction of chemotaxis to CC chemokines by IFN-gamma in human neutrophils.* J Immunol, 1999. **162**(1): p. 474-9.
197. Zhang, S., et al., *Differential effects of leukotactin-1 and macrophage inflammatory protein-1 alpha on neutrophils mediated by CCR1.* J Immunol, 1999. **162**(8): p. 4938-42.
198. Yamashiro, S., et al., *Phenotypic and functional change of cytokine-activated neutrophils: inflammatory neutrophils are heterogeneous and enhance adaptive immune responses.* J Leukoc Biol, 2001. **69**(5): p. 698-704.
199. Bless, N.M., et al., *Role of CC chemokines (macrophage inflammatory protein-1 beta, monocyte chemoattractant protein-1, RANTES) in acute lung injury in rats.* J Immunol, 2000. **164**(5): p. 2650-9.
200. Moreland, J.G., et al., *CD11b and intercellular adhesion molecule-1 are involved in pulmonary neutrophil recruitment in lipopolysaccharide-induced airway disease.* Am J Respir Cell Mol Biol, 2002. **27**(4): p. 474-80.
201. Muller Kobold, A.C., et al., *Levels of soluble Fc gammaRIII correlate with disease severity in sepsis.* Clin Exp Immunol, 1998. **114**(2): p. 220-7.
202. Weirich, E., et al., *Neutrophil CD11b expression as a diagnostic marker for early-onset neonatal infection.* J Pediatr, 1998. **132**(3 Pt 1): p. 445-51.
203. Narasaraju, T., et al., *MCP-1 antibody treatment enhances damage and impedes repair of the alveolar epithelium in influenza pneumonitis.* Am J Respir Cell Mol Biol, 2010. **42**(6): p. 732-43.
204. Hartl, D., et al., *Cleavage of CXCR1 on neutrophils disables bacterial killing in cystic fibrosis lung disease.* Nat Med, 2007. **13**(12): p. 1423-30.
205. Asagoe, K., et al., *Down-regulation of CXCR2 expression on human polymorphonuclear leukocytes by TNF-alpha.* J Immunol, 1998. **160**(9): p. 4518-25.
206. Tavares, L.P., et al., *CXCR1/2 Antagonism Is Protective during Influenza and Post-Influenza Pneumococcal Infection.* Front Immunol, 2017. **8**: p. 1799.

207. McMillan, S.J., et al., *Siglec-E is a negative regulator of acute pulmonary neutrophil inflammation and suppresses CD11b beta2-integrin-dependent signaling.* Blood, 2013. **121**(11): p. 2084-94.
208. Chabot, F., et al., *Reactive oxygen species in acute lung injury.* Eur Respir J, 1998. **11**(3): p. 745-57.
209. Doern, G.V., et al., *Antimicrobial resistance among Streptococcus pneumoniae in the United States: have we begun to turn the corner on resistance to certain antimicrobial classes?* Clin Infect Dis, 2005. **41**(2): p. 139-48.
210. Nozoe, K., et al., *Mechanisms of the Macrolide-Induced Inhibition of Superoxide Generation by Neutrophils.* Inflammation, 2016. **39**(3): p. 1039-48.
211. Sun, H.K., et al., *Efficacy of pulsatile amoxicillin and clarithromycin dosing alone and in combination in a murine pneumococcal pneumonia model.* J Antimicrob Chemother, 2005. **56**(3): p. 559-65.
212. Blondeau, J.M., S.D. Shebelski, and C.K. Hesje, *Killing of Streptococcus pneumoniae by azithromycin, clarithromycin, erythromycin, telithromycin and gemifloxacin using drug minimum inhibitory concentrations and mutant prevention concentrations.* Int J Antimicrob Agents, 2015. **45**(6): p. 594-9.
213. Hesje, C.K., G.S. Tillotson, and J.M. Blondeau, *MICs, MPCs and PK/PDs: a match (sometimes) made in hosts.* Expert Rev Respir Med, 2007. **1**(1): p. 7-16.
214. Metzler, K., K. Drlica, and J.M. Blondeau, *Minimal inhibitory and mutant prevention concentrations of azithromycin, clarithromycin and erythromycin for clinical isolates of Streptococcus pneumoniae.* J Antimicrob Chemother, 2013. **68**(3): p. 631-5.
215. Thompson, A.M., et al., *The role of azithromycin in healthcare-associated pneumonia treatment.* J Clin Pharm Ther, 2015.
216. Butler, D., *Tamiflu report comes under fire.* Nature, 2014. **508**(7497): p. 439-40.
217. Kakeya, H., et al., *Efficacy of combination therapy with oseltamivir phosphate and azithromycin for influenza: a multicenter, open-label, randomized study.* PLoS One, 2014. **9**(3): p. e91293.
218. Rennard, S.I., et al., *CXCR2 Antagonist MK-7123. A Phase 2 Proof-of-Concept Trial for Chronic Obstructive Pulmonary Disease.* Am J Respir Crit Care Med, 2015. **191**(9): p. 1001-11.
219. Nicholson, G.C., et al., *A novel flow cytometric assay of human whole blood neutrophil and monocyte CD11b levels: upregulation by chemokines is related to receptor expression, comparison with neutrophil shape change, and effects of a chemokine receptor (CXCR2) antagonist.* Pulm Pharmacol Ther, 2007. **20**(1): p. 52-9.
220. Kirsten, A.M., et al., *The safety and tolerability of oral AZD5069, a selective CXCR2 antagonist, in patients with moderate-to-severe COPD.* Pulm Pharmacol Ther, 2015. **31**: p. 36-41.
221. Kaur, M. and D. Singh, *Neutrophil chemotaxis caused by chronic obstructive pulmonary disease alveolar macrophages: the role of CXCL8 and the receptors CXCR1/CXCR2.* J Pharmacol Exp Ther, 2013. **347**(1): p. 173-80.
222. Semerad, C.L., et al., *G-CSF is an essential regulator of neutrophil trafficking from the bone marrow to the blood.* Immunity, 2002. **17**(4): p. 413-23.
223. Nicholls, D.J., et al., *Pharmacological characterization of AZD5069, a slowly reversible CXC chemokine receptor 2 antagonist.* J Pharmacol Exp Ther, 2015. **353**(2): p. 340-50.
224. Jurcevic, S., et al., *The effect of a selective CXCR2 antagonist (AZD5069) on human blood neutrophil count and innate immune functions.* Br J Clin Pharmacol, 2015. **80**(6): p. 1324-36.

225. Dwyer, M.P., et al., *Discovery of 2-hydroxy-N,N-dimethyl-3-{2-[[(R)-1-(5- methylfuran-2-yl)propyl]amino]-3,4-dioxocyclobut-1-enylamino}benzamide (SCH 527123): a potent, orally bioavailable CXCR2/CXCR1 receptor antagonist.* J Med Chem, 2006. **49**(26): p. 7603-6.
226. Stillie, R., et al., *The functional significance behind expressing two IL-8 receptor types on PMN.* J Leukoc Biol, 2009. **86**(3): p. 529-43.
227. Planaguma, A., et al., *Combined anti CXC receptors 1 and 2 therapy is a promising anti-inflammatory treatment for respiratory diseases by reducing neutrophil migration and activation.* Pulm Pharmacol Ther, 2015. **34**: p. 37-45.
228. Vincent, A., et al., *Review of influenza A virus in swine worldwide: a call for increased surveillance and research.* Zoonoses Public Health, 2014. **61**(1): p. 4-17.
229. Schultz-Cherry, S., C.W. Olsen, and B.C. Easterday, *History of Swine influenza.* Curr Top Microbiol Immunol, 2013. **370**: p. 21-8.
230. Freidl, G.S., et al., *Influenza at the animal-human interface: a review of the literature for virological evidence of human infection with swine or avian influenza viruses other than A(H5N1).* Euro Surveill, 2014. **19**(18).
231. Gray, G.C., et al., *Influenza A(H1N1)pdm09 virus among healthy show pigs, United States.* Emerg Infect Dis, 2012. **18**(9): p. 1519-21.
232. Reperant, L.A., et al., *Companion Animals as a Source of Viruses for Human Beings and Food Production Animals.* J Comp Pathol, 2016. **155**(1 Suppl 1): p. S41-53.
233. Martin, B.E., et al., *US feral swine were exposed to both avian and swine influenza A viruses.* Appl Environ Microbiol, 2017.
234. Sikkema, R.S., et al., *Weighing serological evidence of human exposure to animal influenza viruses - a literature review.* Euro Surveill, 2016. **21**(44).
235. Zhang, J. and K.M. Harmon, *RNA extraction from swine samples and detection of influenza A virus in swine by real-time RT-PCR.* Methods Mol Biol, 2014. **1161**: p. 277-93.
236. Nicholls, J.M., et al., *Sialic acid receptor detection in the human respiratory tract: evidence for widespread distribution of potential binding sites for human and avian influenza viruses.* Respir Res, 2007. **8**: p. 73.
237. Stevens, J., et al., *Glycan microarray analysis of the hemagglutinins from modern and pandemic influenza viruses reveals different receptor specificities.* J Mol Biol, 2006. **355**(5): p. 1143-55.
238. Rogers, G.N. and J.C. Paulson, *Receptor determinants of human and animal influenza virus isolates: differences in receptor specificity of the H3 hemagglutinin based on species of origin.* Virology, 1983. **127**(2): p. 361-73.
239. Nelli, R.K., et al., *Comparative distribution of human and avian type sialic acid influenza receptors in the pig.* BMC Vet Res, 2010. **6**: p. 4.
240. Ma, W., et al., *North American triple reassortant and Eurasian H1N1 swine influenza viruses do not readily reassort to generate a 2009 pandemic H1N1-like virus.* MBio, 2014. **5**(2): p. e00919-13.
241. Urbaniak, K., et al., *Reassortment process after co-infection of pigs with avian H1N1 and swine H3N2 influenza viruses.* BMC Vet Res, 2017. **13**(1): p. 215.
242. Wei, K., et al., *Influenza A virus acquires enhanced pathogenicity and transmissibility after serial passages in swine.* J Virol, 2014. **88**(20): p. 11981-94.
243. Storms, A.D., et al., *Worldwide transmission and seasonal variation of pandemic influenza A(H1N1)2009 virus activity during the 2009-2010 pandemic.* Influenza Other Respir Viruses, 2013. **7**(6): p. 1328-35.

244. Thangavel, R.R. and N.M. Bouvier, *Animal models for influenza virus pathogenesis, transmission, and immunology.* J Immunol Methods, 2014. **410**: p. 60-79.
245. Ibricevic, A., et al., *Influenza virus receptor specificity and cell tropism in mouse and human airway epithelial cells.* J Virol, 2006. **80**(15): p. 7469-80.
246. Bouvier, N.M. and A.C. Lowen, *Animal Models for Influenza Virus Pathogenesis and Transmission.* Viruses, 2010. **2**(8): p. 1530-1563.
247. Herlocher, M.L., et al., *Ferrets as a transmission model for influenza: sequence changes in HA1 of type A (H3N2) virus.* J Infect Dis, 2001. **184**(5): p. 542-6.
248. Lowen, A.C., et al., *The guinea pig as a transmission model for human influenza viruses.* Proc Natl Acad Sci U S A, 2006. **103**(26): p. 9988-92.
249. Judge, E.P., et al., *Anatomy and bronchoscopy of the porcine lung. A model for translational respiratory medicine.* Am J Respir Cell Mol Biol, 2014. **51**(3): p. 334-43.
250. Rajao, D.S. and A.L. Vincent, *Swine as a model for influenza A virus infection and immunity.* Ilar j, 2015. **56**(1): p. 44-52.
251. Khatri, M., et al., *Swine influenza H1N1 virus induces acute inflammatory immune responses in pig lungs: a potential animal model for human H1N1 influenza virus.* J Virol, 2010. **84**(21): p. 11210-8.
252. Van Reeth, K., H. Nauwynck, and M. Pensaert, *Bronchoalveolar interferon-alpha, tumor necrosis factor-alpha, interleukin-1, and inflammation during acute influenza in pigs: a possible model for humans?* J Infect Dis, 1998. **177**(4): p. 1076-9.
253. Groenen, M.A., et al., *Analyses of pig genomes provide insight into porcine demography and evolution.* Nature, 2012. **491**(7424): p. 393-8.
254. Deblanc, C., et al., *Pre-infection of pigs with Mycoplasma hyopneumoniae induces oxidative stress that influences outcomes of a subsequent infection with a swine influenza virus of H1N1 subtype.* Vet Microbiol, 2013. **162**(2-4): p. 643-51.
255. Loving, C.L., et al., *Influenza virus coinfection with Bordetella bronchiseptica enhances bacterial colonization and host responses exacerbating pulmonary lesions.* Microb Pathog, 2010. **49**(5): p. 237-45.
256. Kowalczyk, A., et al., *Cytokine and chemokine mRNA expression profiles in BALF cells isolated from pigs single infected or co-infected with swine influenza virus and Bordetella bronchiseptica.* Vet Microbiol, 2014. **170**(3-4): p. 206-12.
257. Pomorska-Mol, M., et al., *Kinetics of single and dual infection of pigs with swine influenza virus and Actinobacillus pleuropneumoniae.* Vet Microbiol, 2017. **201**: p. 113-120.
258. Tchilian, E. and B. Holzer, *Harnessing Local Immunity for an Effective Universal Swine Influenza Vaccine.* Viruses, 2017. **9**(5).

VITA

Jennifer Margaret Rudd

Candidate for the Degree of

Doctor of Philosophy

Thesis: NEUTROPHIL CHARACTERIZATION FOR THE DEVELPOMENT OF NOVEL COMBINATION THERAPY IN A MURINE MODEL FOR INFLUENZA PNEUMONIA WITH SECONDARY PNEUMOCOCCAL COINFECTION

Major Field: Veterinary Biomedical Sciences

Biographical:

Education:

Completed the requirements for the Doctor of Philosophy in Veterinary Biomedical Sciences at Oklahoma State University, Stillwater, Oklahoma in May, 2018.

Completed the requirements for Doctor of Veterinary Medicine at Oklahoma State University, Stillwater, Oklahoma in 2011.

Completed the requirements for the Bachelor of Science in Biomedical Sciences at Oklahoma State University, Stillwater, Oklahoma in 2008.